Sedimentary DNA-based reconstruction of cyanobacterial communities from Lake Tiefer See, NE Germany, for the last 11,000 years

---

Ebuka Canisius Nwosu

DISSERTATION

zur Erlangung des akademischen Grades

„doctor rerum naturalium“

- Dr. rer. nat. -

in der Wissenschaftsdisziplin „Mikrobiologie“

eingereicht an der

Mathematisch-Naturwissenschaftlichen Fakultät

Institut für Biochemie und Biologie

der Universität Potsdam

und

GFZ Deutsches GeoForschungsZentrum, Helmholtz Zentrum Potsdam

Geomikrobiologie

Potsdam, den 18.04.2022

Tag der Disputation: 14.10.2022

Hauptbetreuerin: Prof. Dr. Susanne Liebner (Universität Potsdam)
Zweitbetreuerin: Prof. Dr. Elke Dittmann (Universität Potsdam)

Gutachter*innen: Prof. Dr. Ulrike Herzschuh (Universität Potsdam)
jr-Prof. Dr. Laura Epp (Universität Konstanz)

Published online on the
Publication Server of the University of Potsdam:
https://doi.org/10.25932/publishup-56359
https://nbn-resolving.org/urn:nbn:de:kobv:517-opus4-563590

Statement of Original Authorship

I herewith assure you that I have developed and written the enclosed PhD-thesis completely by myself and have not used sources or means without declaration in the text. Any thoughts from others or literal quotations are marked. The PhD-thesis was not used in the same or in a similar version to achieve an academic grading or is being published elsewhere.

Ebuka Canisius Nwosu

Preface

This study was supported by the German Federal Environmental Foundation (DBU) through a Doctoral Research Grant Position awarded to Ebuka Canisius Nwosu. This study was also supported by the Helmholtz Association (HGF) in the framework of the Helmholtz Young Investigators Research Group "MicroCene – Microbial Communities of the terrestrial subsurface" by a grant to Susanne Liebner (VH-NG-919). This study was also supported by the Leibniz Association Grant SAW-2017-IOW-2 "BaltRap: The Baltic Sea and its southern Lowlands: proxy—environment interactions in time of rapid change," and the "Climate signal transfer to varved sediments in Lake Tiefer See Klocksin—Monitoring, Transfer functions, Reconstructions" awarded to Achim Brauer. Furthermore, this study is a contribution to the Virtual Institute of Integrated Climate and Landscape Evolution Analyses ICLEA, Grant No. VH-VI-415. The monitoring equipment was funded by the Terrestrial Environmental Observatory Infrastructure Initiative of the Helmholtz Association (TERENO Observatory NE Germany). This thesis focused on the species-level spatiotemporal succession dynamics of cyanobacteria in a deep freshwater lake, the agreement between pelagic and sediment-deposited cyanobacteria populations, and the potential lake environmental factors responsible for changes in their communities since the Holocene. The water column of Lake Tiefer See, NE Germany, was sampled at six depths monthly between January 30 and November 28 in 2019 at the point of maximum depth. In addition, 4-cylinder sediment traps were used to collect suspended particulate matter at 12 and 50 m water depths in the water column, as well as short (115 cm) and long sediment (11 m) cores collected in 2015 and 2019, respectively. The water and sediment samples were used for the analyses in this study. The laboratory work was mainly performed at GFZ German Research Centre for Geosciences, Helmholtz Centre Potsdam. Total dissolved phosphorus and cyanobacteria lipid biomarker analyses were performed at the Leibniz Institute for Baltic Sea Research, Warnemünde.

The thesis is written in English, organized as a publication-based cumulative dissertation, and submitted to the Faculty of Science at the University of Potsdam. It consists of a general introduction comprising the motivation of the study, a scientific background about cyanobacteria in aquatic ecosystems, the consequences of environmental stressors on their dynamics in freshwater ecosystems, and the potential of cyanobacteria sedimentary ancient DNA in lake paleoenvironmental reconstructions. Following the introduction, the aims and

objectives of the study as well as a description of the study site and main methods are described. The results of this work are presented in three manuscripts with first authorship which are published in peer-reviewed scientific journals and one manuscript with first authorship submitted for publication in an international peer-reviewed journal. The thesis finishes with a synthesis including conclusions, critical remarks, and prospects.

To my late parents, Ifeoma Ann and Chukwudi Ephraim Nwosu, for betting and insisting on formal education

Acknowledgments

The popular Nigerian saying “it takes a village to raise a child” perfectly encapsulates my PhD experience. My research quite literally would not have been possible without the help of many people in many institutions, universities, and organizations. My foremost gratitude goes to Prof. Dr. Susanne Liebner, for being the best supervisor anyone could ask for. Thank you for trusting me to foray into this rather new research area for you, for your kind guidance, encouragement, support, and direction during my moments of uncertainty, especially when the COVID-19 pandemic broke out. Most importantly, thank you for enabling a family-friendly working atmosphere, for always being available to patiently listen to me, which altogether further strengthened my enthusiasm for the interesting field of lake paleo cyanobacteria research. My gratitude also goes to Prof. Dr. Ulrike Herzschuh (AWI) and jr-Prof. Dr. Laura Epp (Uni-Konstanz) for evaluating my Dissertation. Special thanks go to Prof. Dr. Elke Dittmann (Uni-Potsdam) for her supervision, support, and guidance since 2016 when I started my Master’s Studies at the Uni-Potsdam. And by extension, I acknowledge the colleagues I met in Dittmann’s Labs for their support and help during my studies and PhD research, especially, Annika Weiz for introducing me to Cyanobacteria. I thank also my mentor Prof. Dr. Achim Brauer for his unwavering support, valuable discussions, and critical evaluation of my work. My gratitude goes to the colleagues at the Climate Dynamics and Landscape Evolution Section of the GFZ, especially to Sylvia Pinkerneil for the sampling campaigns, geochemical data provision, and the exciting field experiences at Lake Tiefer See Klocksin. I also acknowledge Patricia Roeser and Jerome Kaiser at Leibniz Institute for Baltic Sea Research, Warnemünde, as well as Martin Theuerkauf at Uni-Greifswald for data provisions, insightful discussions and fruitful collaborations on my manuscripts. Many thanks also to the co-authors I never met physically who nonetheless played significant roles in the publications of my results. Particularly, Marie-Eve Monchamp at McGill University in Quebec Canada, thank you for the discussions, and critical evaluation of my manuscript. Also, to Dr. Jens-Peter Schmidt at the Landesamt für Kultur und Denkmalpflege Mecklenburg-Vorpommern, thank you for the archaeological data that backed up my findings and for the insightful contributions to my manuscript.

My heartfelt gratitude goes to the DBU for my Doctoral Research Grant which made this work possible. I also thank the Potsdam Graduate School for enabling me to gain graduate

teaching experience through the Junior Teaching Professionals program and for sponsoring my advanced German language classes and exam.

I also acknowledge past and present colleagues at the Geomicrobiology Section of the GFZ for the team spirit, discussions, and willingness to help. Thank you, Lars, Matthias, Patryk, Fabian, Julia, Alex, Steffi, and Sizhong, for the numerous scientific discussions. Many thanks to Anke, Olli, Axel, and Simone, for their excellent laboratory support and for ensuring I got the right experimental materials. Many thanks also to Julia Poloni whose bachelor thesis was of additional value to my work. Thank you, Sybille Hahmann, for your assistance with all the bureaucratic aspects of my PhD research.

My immense gratitude goes to my wonderful friends Loeka and Boris. Loeka thank you for introducing me to the DBU, to Boris, to your lovely family, and to your friends at AWI. Thank you for the many discussions, brainstorming, strategizing, proofreading, and babysitting my kids. I also acknowledge the colleagues I met within the DBU and the Telegrafenberg network, especially Maren and Haruna, thanks for the many insightful conversations and hangouts. Playing football was my escape from research and to this end I thank my friends at Potsdamer Kickers 94 e.V., especially, Stephan Ranz, Pasche, Welskopf, Sören Mühle, Jakob, Sören Geissini, Hakon, Veit, Elsaßer, David Michel, Brunzlow, thank you for making life in Potsdam fun.

I thank my friends in Berlin, Nigeria, and all around for not letting distance come between our friendship, to my siblings Arinze, Kenechi, Chukwunweike, and Uche for their moral support and to my in-laws' Family Lange, Nils, Elke, Swantje, Björn, und Lütje for their unwavering support through the years.

Last but not least, my deepest gratitude goes to my dearest Fenja, Chike and Kaira, you all lovingly had my back covered during this period, and made my life so worth living. Thank you Fenja for your patience with me the last couple of years, for lifting me up whenever I was down, for motivating me, for being my pillar of support, for providing me with new ideas, impulses, perspectives, and countless proofreading. You are the main reason I made it this far, thank you for believing in me.

List of Publications

In the scope of this thesis the following articles and conference contributions were published:

Articles

Nwosu, E. C., Brauer, A., Monchamp, M. E., Pinkerneil, Bartholomäus A., S., Poloni, J., Theuerkauf, M., Schmidt, J-P., Stoof-Leichsenring, K.R., Wietelmann, T., Kaiser, J., Wagner, D., and Liebner, S. (submitted to *Nature Communications*) Bronze Age human-induced increase in cyanobacteria abundance revealed by sedimentary ancient DNA.

Nwosu, E. C., Roeser, P., Yang S., Pinkerneil S., Ganzert L., Dittmann, E., Brauer A., Wagner, D., and Liebner, S. (2021c). Species-Level Spatio-Temporal Dynamics of Cyanobacteria in a Hard-Water Temperate Lake in the Southern Baltics. *Front. Microbiol.* 12:761259. https://https://doi.org//10.3389/fmicb.2021.761259

Nwosu, E. C., Roeser, P., Yang, S., Ganzert, L., Dellwig, O., Pinkerneil, S., Dittmann, E, Brauer, A., Wagner, D., and Liebner, S. (2021b). From Water into sediment—tracing freshwater cyanobacteria via DNA Analyses. *Microorganisms* 2021:9081778. https://https://doi.org//10.3390/microorganisms9081778

Nwosu, E. C., Brauer, A., Kaiser, J., Horn, F., Wagner, D., and Liebner, S. (2021a). Evaluating sedimentary DNA for tracing changes in cyanobacteria dynamics from sediments spanning the last 350 years of Lake Tiefer See, NE Germany. *J. Paleolimnol.* 2021:2069. https://https://doi.org//10.1007/s10933-021-00206-9

Conference contributions

Nwosu, E. C., Brauer, A., Kaiser, J., Horn, F., Wagner, D., and Liebner, S. (2019). Deducing human impact on the environment via sedimentary DNA information Lake Tiefer See, NE Germany *34th International Association of sedimentologists (IAS) Meeting of Sedimentology,* Rome, Italy, 10-13 September 2019 (Abstract, Oral Presentation)

Nwosu, E. C., Roeser, P., Yang, S., Ganzert, L., Dellwig, O., Pinkerneil, S., Dittmann, E, Brauer, A., Wagner, D., and Liebner, S. (2021). From Water into sediment—tracing freshwater cyanobacteria via DNA Analyses. *Annual Meeting of the Association for General and Applied Microbiology (VAAM),* Düsseldorf, Germany, 21-23 February 2022 (Abstract, ePoster Presentation)

Nwosu, E. C., Roeser, P., Yang, S., Ganzert, L., Dellwig, O., Pinkerneil, S., Dittmann, E, Brauer, A., Wagner, D., and Liebner, S. (2021b). From Water into sediment—tracing freshwater cyanobacteria via DNA Analyses. *1st OZCAR-TERENO International Conference,* Strasbourg, France, 4-8 October 2021 (Abstract, Poster)

Nwosu, E. C., Roeser, P., Pinkerneil, S., Yang, S., Bartholomäus, A., Dittmann, E, Brauer, A., Wagner, D., and Liebner, S. (2020). Monitoring seasonal changes in diversity, community structure, and sedimentary deposition of cyanobacteria in Lake Tiefer See, NE Germany. *6th Joint Conference of the DGHM & VAAM – 72nd Annual Meeting of the DGHM & Annual Meeting of the Association for General and Applied Microbiology (VAAM),* Leipzig, Germany, 8-11 March 2020 (Abstract, Poster)

Nwosu, E. C., Brauer, A., Kaiser, J., Horn, F., Wagner, D., and Liebner, S. (2019). Deducing human impact on the environment via sedimentary DNA information Lake Tiefer See, NE Germany *34th International Association of sedimentologists (IAS) Meeting of Sedimentology,* Rome, Italy, 10-13 September 2019 (Abstract, Poster)

Nwosu, E. C., Brauer, A., Kaiser, J., Horn, F., Wagner, D., and Liebner, S. (2019). Deducing human impact on the environment via sedimentary DNA information Lake Tiefer See, NE Germany. *Annual Meeting of the Association for General and Applied Microbiology (VAAM),* Mainz, Germany, 17-20 March 2019 (Abstract, Poster)

Summary

Climate change and human-driven eutrophication promote the spread of harmful cyanobacteria blooms in lakes worldwide, which affects water quality and impairs the aquatic food chain. In recent times, sedimentary ancient DNA-based (sedaDNA) studies were used to probe how centuries of climate and environmental changes have affected cyanobacterial assemblages in temperate lakes. However, there is a lack of information on the consistency between sediment-deposited cyanobacteria communities versus those of the water column, and on the individual role of natural climatic changes versus human pressure on cyanobacteria community dynamics over multi-millennia time scales.

Therefore, this thesis uses sedimentary ancient DNA of Lake Tiefer See in northeastern Germany to trace the deposition of cyanobacteria along the water column into the sediment, and to reconstruct cyanobacteria communities spanning the last 11,000 years using a set of molecular techniques including quantitative PCR, biomarkers, metabarcoding, and metagenome sequence analyses.

The results of this thesis proved that cyanobacterial composition and species richness did not significantly differ among different water depths, sediment traps, and surface sediments. This means that the cyanobacterial community composition from the sediments reflects the water column communities. However, there is a skewed sediment deposition of different cyanobacteria groups because of DNA alteration and/or deterioration during transport along the water column to the sediment. Specifically, single filament taxa, such as *Planktothrix*, are poorly represented in sediments despite being abundant in the water column as shown by an additional study of the thesis on cyanobacteria seasonality. In contrast, aggregate-forming taxa, like *Aphanizomenon*, are relatively overrepresented in sediment although they are not abundant in the water column. These different deposition patterns of cyanobacteria taxa should be considered in future DNA-based paleolimnological investigations. The thesis also reveals a substantial increase in total cyanobacteria abundance during the Bronze Age which is not apparent in prior phases of the early to middle Holocene and is suggested to be caused by human farming, deforestation, and excessive nutrient addition to the lake. Not only cyanobacterial abundance was influenced by human activity but also cyanobacteria community

composition differed significantly between phases of no, moderate, and intense human impact.

The data presented in this thesis are the first on sedimentary cyanobacteria DNA since the early Holocene in a temperate lake. The results bring together archaeological, historical climatic, and limnological data with deep DNA-sequencing and paleoecology to reveal a legacy impact of human pressure on lake cyanobacteria populations dating back to approximately 4000 years.

Zusammenfassung

Der Klimawandel und die vom Menschen verursachte Eutrophierung fördern die Ausbreitung schädlicher Cyanobakterienblüten in Seen weltweit, was die Wasserqualität und die aquatische Nahrungskette beeinträchtigt. In jüngster Zeit wurden sedimentäre DNA (sedaDNA)-Studien verwendet, um zu untersuchen, wie sich klimatische- und menschliche Umweltveränderungen von Jahrhunderten auf Cyanobakteriengemeinschaften in Seen ausgewirkt haben. Jedoch fehlen bislang Informationen, wie repräsentativ die im Sediment abgelagerten Cyanobakterien und deren DNA für die Gemeinschaften der Wassersäule sind, sowie zur individuellen Rolle natürlicher klimatischer Veränderungen gegenüber dem menschlichen Einflusses auf die Dynamik von Cyanobakterien über Zeitskalen von Jahrtausenden.

Daher wurde in dieser Arbeit sedimentäre alte DNA (sedaDNA) des Tiefen Sees in Nordostdeutschland verwendet, um die Ablagerung von Cyanobakterien entlang der Wassersäule in das Sediment zu verfolgen. Ein Hauptteil dieser Arbeit bildete jedoch die Rekonstruktion von Cyanobakteriengemeinschaften der letzten 11.000 Jahre, unter Verwendung einer Reihe von molekularen Techniken, darunter quantitative PCR, Biomarker, Metabarcoding und Metagenom-Sequenzanalysen.

Die Ergebnisse dieser Arbeit beweisen, dass die Cyanobakterien-Zusammensetzung und der Artenreichtum zwischen verschiedenen Wassertiefen, Sedimentfallen und Oberflächensedimenten nicht signifikant unterschiedlich ist. Das bedeutet, dass die Zusammensetzung der Cyanobakteriengemeinschaften aus den Sedimenten die Gemeinschaften der Wassersäule widerspiegelt. Aufgrund von DNA-Veränderungen und/oder -Abbau während des Transports entlang der Wassersäule zum Sediment kommt es jedoch zu einer verzerrten Sedimentablagerung verschiedener Cyanobakterien Arten. Insbesondere sind filamentose Arten wie *Planktothrix* in Sedimenten schlecht vertreten, obwohl sie, laut Ergebnissen einer zusätzlichen Studie dieser Arbeit zur Saisonalität von Cyanobakterien, in der Wassersäule reichlich vorhanden sind. Im Gegensatz dazu sind aggregatbildende Arten wie *Aphanizomenon* in Sedimenten relativ gesehen überrepräsentiert, obwohl sie in der Wassersäule relativ selten vorkommen. Diese unterschiedlichen Muster zur Sedimentablagerung verschiedener Cyanobakterien Arten sollten in zukünftigen DNA-basierten paläolimnologischen Untersuchungen berücksichtigt

werden. Die Dissertation zeigt auch eine deutliche Zunahme der Cyanobakterien Abundanz während der Bronzezeit, die in vorhergehenden Phasen des frühen und mittleren Holozäns nicht erkennbar war. Dies ist wahrscheinlich durch menschliche Landwirtschaft, Entwaldung und übermäßige Nährstoffzufuhr in den See verursacht worden. Nicht nur die Abundanz von Cyanobakterien wurde durch menschliche Aktivitäten beeinflusst, sondern auch die Zusammensetzung von deren Gemeinschaften, die sich signifikant zwischen Phasen unterscheidet, die durch keinen, moderaten, und intensiven menschlichen Einfluss gekennzeichnet sind.

Die in dieser Dissertation präsentierten Daten sind die ersten zu sedimentärer Cyanobakterien-DNA seit dem frühen Holozän eines Sees der gemäßigte Klimazone. Die Ergebnisse vereinen archäologische, historische, klimatische und limnologische Daten mit hochaufgelöster und Hochdurchsatz-DNA-Sequenzierung und belegen, dass der menschliche Einfluss auf Cyanobakteriengemeinschaften in Seen etwa 4000 Jahre zurückreicht.

Table of contents

Abbreviations

Ag	silver
ANOVA	analysis of variance
ASV	amplicon sequence variant
BCE	before common era
Bp	basepair
BLAST	Basic local alignment search tool
Cal. (k)a BP	caliberated (kilo)age before present
C/N	organic carbon to nitrogen ratio
$CaCO_3$	calcium carbonate
CCC	cyanobacteria community composition
CE	common era
Chl*a*	chlorophyll a
CO_2	carbon dioxide
Cond.	conductivity
dbRDA	distance-based redundancy analysis
DBU	Deutsche Bundesstiftung Umwelt
DCM	deep chlorophyl maximum
ddPCR	digital droplet polymerase chain reaction
DNA	deoxyribonucleic acid
dNTP	deoxyribonucleotide triphosphate
DO	dissolved oxygen
F	Forward-Primer
GenBank	International Genetic Database
GFZ	Geoforschungszentrum, German Research Centre for Geosciences
g	gram
gDNA	genomic deoxyribonucleic acid
H_2O	water
HCl	hydrochloric acid
HTS	high-throughput sequencing
ITS	intergenic spacer region
IOW	Leibniz institute for Baltic Sea research
mcy	microcystin gene family
mg	milligram
MOM	metalymnetic oxygen minimum
N	Nitrogen
NCY	non-photosynthetic cyanobacteria
NE	Northeast
NGS	next-generation sequencing
nif	nitrogen fixing gene family
NMDS	Non-Metric multi-dimensional Scaling
NO_3^-	nitrate
*oci*B	non-ribosomal peptide synthetase gene cluster which codes for oligopeptide class cyanopeptolin
OTU	operational taxonomic unit
PC	principal components
PCoA	principal coordinate analysis
PCA	principal component analysis

PC-IGS	intergenic spacer region of the phycocyanin operon
PCR	polymerase chain reaction
PerMANOVA	permutational multivariate analysis of variance
pH	potential of hydrogen, measure of acidity
qPCR	quantitative polymerase chain reaction
R	reverse-Primer
RDA	redundancy analysis
RecVegOpp	reconstructed vegetation openness
rRNA	ribosomal ribonucleic acid
sedaDNA	sedimentary ancient DNA
SIMPER	similarity percentage
TERENO	terrestrial environment observation
TDP	total dissolved phosphorus
TIC	total inorganic carbon content
TN	total nitrogen
TNA	TaqMan nuclease assay
TOC	Total organic carbon
TSK	Tiefer See near Klocksin
TukeyHSD	Tukey's-honestly-significant-difference
UV	ultraviolet
VIF	variance inflation factor
VPDB	Vienna peedee belemnite a standard for measuring δ13C
VPN	variation partitioning analysis
VQ	varve quality
vol%	volume percent
wt%	weight %
$\delta^{15}N$	delta Nitrogen-15
$\delta^{13}C$	isotopic ratio between stable carbon isotopes ^{13}C and ^{12}C

List of Figures

List of Tables

1 Introduction

1.1 Motivation

Cyanobacteria play an important role in the earth's marine and freshwater ecosystems where they contribute significantly to primary production (Garcia-Pichel, 2009). But they can also cause a noticeable intense discoloration of the water known as cyanobacteria blooms (Fig. 1.1) (Huisman et al., 2018). In the affected waters, the resultant cyanobacteria blooms may adversely affect the local food web and quality of such waters for recreational purposes like swimming, fishing, and drinking (Paerl and Huisman, 2008; Sukenik et al., 2015). Since the industrial revolution, the extent, prevalence, and severity of these blooms have continued to increase because of eutrophication (i.e., inordinate nutrient input), global warming, and rising CO_2 levels (Downing et al., 2001; Paerl and Huisman, 2008; Vonlanthen et al., 2012; Sukenik et al., 2015). Because of climate change, especially increasing temperatures, these cyanobacteria blooms pose a global challenge, and their advancements are a growing concern for communities worldwide. Global climate change and anthropogenic activities (e.g., farming) have together sped up nutrient cycling in many aquatic ecosystems thus altering the dynamics and biodiversity of natural communities in favor of cyanobacteria (Steffen et al., 2007; Irfan and Alatawi, 2019). Furthermore, cyanobacteria blooms could contribute to global warming because they emit the greenhouse gas methane during photosynthesis (Bižić et al., 2020). This could establish a positive feedback loop: increasing water temperatures following climate change promote cyanobacterial bloom formation, which in turn produces more methane that contributes to climate change.

Two studies have initially traced the history of cyanobacterial blooms since the beginning of industrialization in temperate lakes across Europe and North America by analyzing sediment cores (Taranu et al., 2015; Monchamp et al., 2018). Their results revealed not only an increase in cyanobacteria populations compared to other phytoplankton (Taranu et al., 2015), but also a decline in cyanobacteria beta diversity, with cyanobacteria populations and their phylogenetic profiles becoming increasingly similar across lakes (Monchamp et al., 2018). Especially with beta diversity loss, lakes become dominated by bloom-forming and toxin-producing cyanobacteria taxa (e.g., *Aphanizomenon* and *Planktothrix*)

(Monchamp et al., 2018). These taxa become abundant because they are able to regulate their buoyancy, which enables them move periodically through the water column to access light and nutrients (Reynolds et al., 1987; Carey et al., 2012). The findings from Monchamp et al., (2018) were made via high-throughput sequencing of cyanobacteria DNA preserved in sediments. Due to the steady improvements in DNA sequencing technology, several studies have used this method since then to reconstruct the effect of global climate change and human impact via eutrophication on cyanobacteria populations in lakes dating back to pre-industrialization (Capo et al., 2019; Pilon et al., 2019; Ibrahim et al., 2021; Zhang et al., 2021b). Despite these advancements, there is a lack of high-resolution studies on changes in cyanobacteria populations within lakes that encompass the present water column communities through to the Holocene. Filling this knowledge gap would reveal if cyanobacteria diversity and composition in a lake are sufficiently reflected in its sediments, and how natural climatic changes without any significant human impact during the Holocene may have led to broad-scale changes in cyanobacteria populations relative to post-industrial rapid climate change and human impact. Therefore, this thesis aims to study the distribution and history of cyanobacteria dynamics in a deep hard-water temperate lake using a combination of molecular biological and geochemical analyses. Furthermore, the thesis offers new insights to how taphonomic processes (i.e., DNA degradation and deterioration) taking place in the water column affect the sediment deposition of different cyanobacteria species.

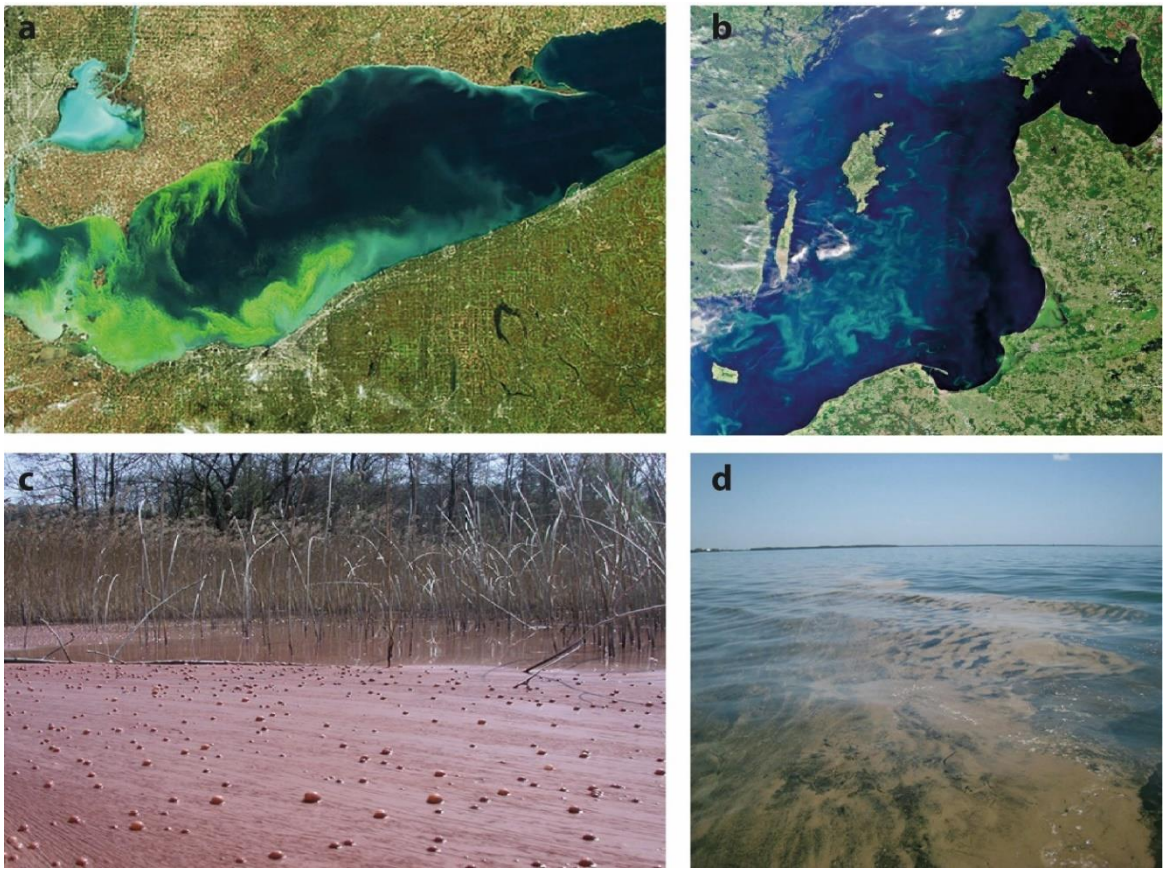

Figure 1.1: Cyanobacteria Blooms. Satellite images of cyanobacteria bloom in (a) Lake Erie (the USA and Canada) and (b) the Baltic Sea, (c) a *Planktothrix rubescence* bloom also known as the Burgundy-blood phenomenon, and (d) a *Trichodesmium* bloom (sea sawdust). [Source: (Huisman et al., 2018)].

1.2 Cyanobacteria

1.2.1 Ecology of cyanobacteria

Cyanobacteria are made up of a morphologically diverse group of evolutionarily ancient bacteria that are thought to have oxidized the earth's atmosphere through their photosynthetic activity (Planavsky et al., 2014; Schirrmeister et al., 2015; Soule and Garcia-Pichel, 2019). Most of the cyanobacteria carry out oxygenic photosynthesis and possess chlorophyll a as the main pigment. Additionally, they use accessory pigment phycobiliproteins (phycoerythrin and phycocyanin) to improve light energy absorption during photosynthesis (Grossman et al., 1993). As the originators of plastid in higher plants and other photosynthetic eukaryotes, cyanobacteria have also played a significant role in the evolution of life (Garcia-Pichel, 2009). They function as the basis of the aquatic food

chain (together with photosynthetic eukaryotes) and are the dominant primary producers even in environments with extreme temperatures (Chrismas et al., 2015; Oren, 2015). Cyanobacteria can also withstand high ultraviolet light and hypersaline environments for several years (Fernandez-Turiel et al., 2005; Pathak et al., 2018). The bacteria classes Melainabacteria and Sericytochromatia, which contain only non-photosynthetic members, were recently discovered and are thought to form a single phylum within cyanobacteria (Di Rienzi et al., 2013a; Soo et al., 2014). Human guts, wastewater treatment facilities, and subsurface groundwater are examples of anoxic environments where their sequences have been found (Soo et al., 2017), but more studies are trying to understand their diversity and composition in lake ecosystems (Monchamp et al., 2019a).

1.2.2 Freshwater cyanobacteria

A large diversity and population of cyanobacteria makeup the phytoplankton in lakes and reservoirs and contribute about 30×10^{12} g to the global biomass (10^{15} g) of cyanobacteria (Soule and Garcia-Pichel, 2019). In temperate climates, most lakes mix at least once a year and are stratified usually beginning in late spring into a warmer upper water column (epilimnion), a dark and cold deep layer (hypolimnion), and a transition zone between the warmer and colder layers (metalimnion). The transition zone acts as a physical barrier between the warmer and colder layers because of rapid changes in temperature and increasing density within it (Boehrer and Schultze, 2008). In temperate freshwater ecosystems, cyanobacteria exhibit a general pattern of seasonal variation. Typically, this variation begins with an abundance of diazotrophic (nitrogen-fixing) taxa (e.g., *Aphanizomenon*) which make use of the sediment-resuspended nutrients made available during mixing of the water column in spring (Cires et al., 2013). The diazotrophic population breakdown in summer, e.g., via fungal parasitism (Gerphagnon et al., 2015), is followed by an increase in the population of non-diazotrophs e.g., *Planktothrix* and *Microcystis* through to late summer and autumn (Walsby and Schanz, 2002; Kardinaal et al., 2007). Cyanobacteria can accumulate in high biomass and dominate the freshwater phytoplankton communities under conditions of nutrient eutrophication and increasing temperature (Paerl and Paul, 2012; Paerl and Otten, 2013).

1.2.3 Harmful cyanobacteria blooms

While a microscope is needed to visualize a single cyanobacterium, the dense colonies and aggregates (blooms) formed by some of their members can even be seen from space (Fig. 1.1). These blooms are often caused by the cyanobacterial genera *Microcystis, Planktothrix, Aphanizomenon*, *Cylindrospermopsis*, *Dolichospermum*, *Nodularia*, and *Trichodesmium* (Fig. 1.2a-c), which thrive in aquatic ecosystems because of three main factors. Firstly, high temperatures may favor the abundance of diazotrophic bloom-forming cyanobacteria groups (e.g., *Aphanizomenon*, *Nodularia*, and *Trichodesmium*; Fig. 1.2b, c) over non-diazotrophic cyanobacteria and eukaryotic phytoplankton in nitrogen limited waters (Breitbarth et al., 2007; Stal, 2009; Kahru and Elmgren, 2014; Huisman et al., 2018). Secondly, to photosynthesize and grow, cyanobacteria need to fix CO_2, however, their blooms can use up the dissolved CO_2 in water (Ibelings and Maberly, 1998; Verspagen et al., 2014). So, to maintain CO_2 fixation, thus preserving their growth and photosynthesis, they evolved carboxysomes which are cellular microcompartments wherein CO_2 is concentrated. Inside the carboxysome, the enzyme carbonic anhydrase raises the local concentration of CO_2 to the level at which Rubisco (carbon-fixing enzyme) functions effectively by converting bicarbonate to CO_2 (Fig. 1.2d) (Price et al., 2008; Burnap et al., 2015). Thirdly, bloom-forming cyanobacteria float upwards owing to hollow gas-filled protein structures in their cells that provide them with buoyancy (Walsby et al., 1995; Pfeifer, 2012). Buoyant cyanobacteria species like *Microcystis spp*., *Trichodesmium spp*., and *Aphanizomenon spp*. that form vast colonies or aggregates can move vertically in the water column (Ibelings et al., 1991; Visser et al., 1997; Villareal and Carpenter, 2003). They do this by actively altering their carbohydrate ballast which offsets buoyancy created by gas vesicles, enabling them to take advantage of the light at the surface and nutrients at the deeper waters (Posch et al., 2012; Salmaso et al., 2015; Huisman et al., 2018). In temperate lakes, climate warming promotes the proliferation of these buoyant cyanobacteria taxa (Monchamp et al., 2019b), because increasing air temperature alters lake thermal regime by extending the period and strength of water column stratification (Posch et al., 2012; Monchamp et al., 2018), Thus, cyanobacteria are able to grow rapidly and adapt eco-physiologically to their changing environment (Carey et al., 2012; Rigosi et al., 2014).

Since the beginning of the industrial revolution, cyanobacteria blooms have caused severe environmental and economic damage. Cyanobacterial blooms in lakes result in unfavorable conditions for other phytoplankton such as low light conditions because of increased turbidity (Scheffer et al., 1993; Sukenik et al., 2015). The microbial breakdown of aging blooms can cause hypoxic and anoxic conditions in waters because of oxygen depletion, which leads to the death of organisms from higher trophic levels like zooplankton and fish (Rabalais et al., 2010; Vonlanthen et al., 2012). In addition, the disintegration of aging blooms produces taste and odors (Kaloudis et al., 2017). Often, cyanobacteria blooms contain toxic taxa that release toxins that are harmful to animals, people and decrease water quality. Moreover, several economic sectors (e.g., agricultural, fishing, tourisms, recreational water treatment plants) have recorded financial losses associated with an impaired water quality caused by cyanobacteria blooms (Saqrane and Oudra, 2009; Silva and Palma, 2010). Furthermore, these potentially toxic bloom-forming cyanobacteria species are now believed to take advantage of climate change and eutrophication to spread geographically (Sinha et al., 2012; Rigosi et al., 2014; Salmaso et al., 2015b), and in some cases irrespective of control measures (Carey et al., 2012; Taranu et al., 2015).

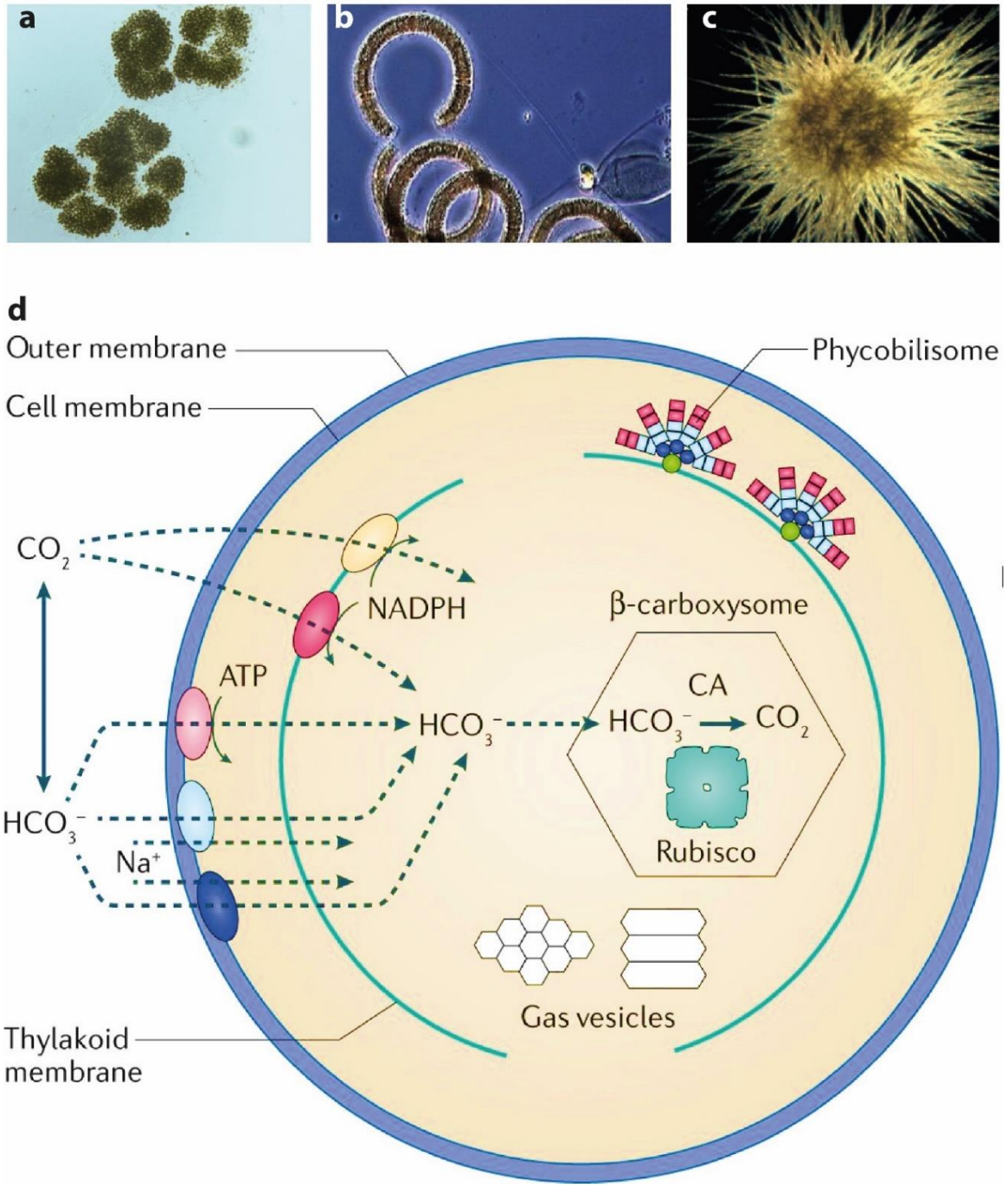

Figure 1.2: Bloom-forming cyanobacteria species and CO2-concentrating mechanism in cyanobacteria (a) colony-forming *Microcystis aeruginosa*, (b) nitrogen-fixing *Nodularia spumigena*, (c) Aggregate forming and nitrogen-fixing *Trichodesmium sp.*, and (d) the microcompartment Carboxysome in cyanobacteria. Figure modified after Huisman et al. (2018).

1.3 Sedimentary DNA as a proxy for past lake ecosystems

1.3.1 Lake sediments as archives of biodiversity changes

Lake sediments are composed of organic and inorganic material that is of autochthonous (from within the lake, e.g., planktonic and plant remains) and allochthonous (from its catchment, e.g., detritus) origins. When lake sediments are annually varved (laminated), they can provide accurate chronologies and seasonally resolved proxy data (e.g., Kemp, 1996). The absence of burrowing organisms due to anoxic conditions at the water-sediment interface promotes the preservation of the varves after deposition (Brauer, 2004). For example, the common calcite varves that form in stratified alkaline temperate lakes are made up of light-dark layers of laminae (Fig. 1.3a), with the light sub-layer originating from endogenic calcite formed during spring–summer in epilimnion waters (e.g., Lotter et al., 1997). Sediment deposits are sometimes homogenous with no identifiable varves (i.e., non-laminated) which likely results from increased lake circulation due to higher wind stress and a more oxic lake bottom (Dräger et al., 2017). Since lake sediments contain autochthonous and allochthonous components (Fig. 1.3b), they can function as biological archives (Moss, 2004).

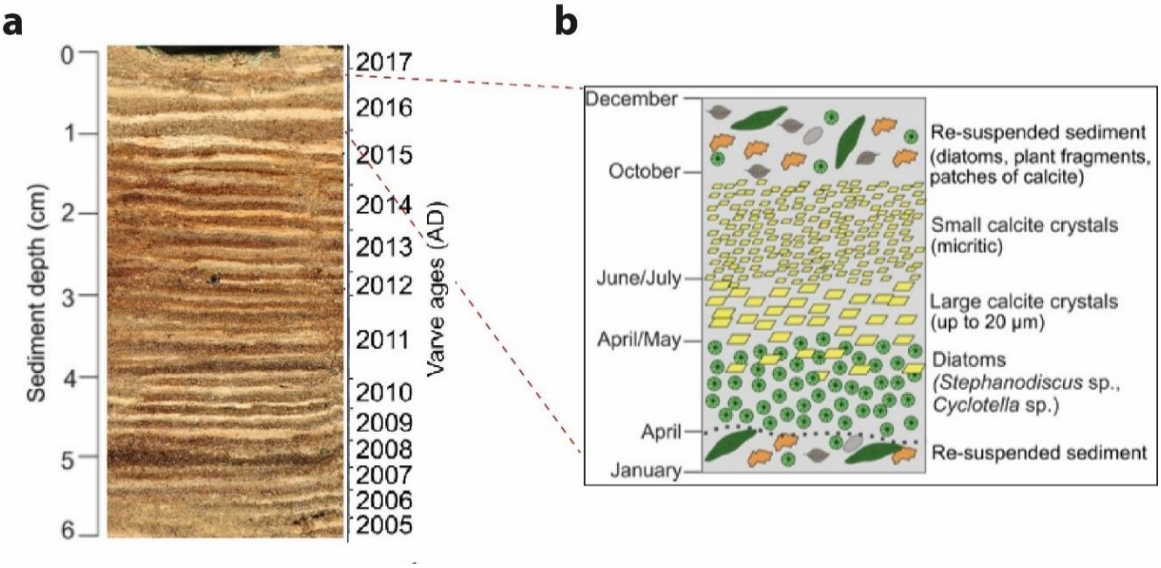

Figure 1.3: Sediment varves and a varve model (a) a sediment core showing light and dark varves (laminae), and (b) a varve model based on microfacies analysis. Dotted gray lines indicate the beginning of a new varve year. Figure modified after Roeser et al. (2021).

Initially, the information in these archives were assessed by analyzing the identifiable fossils of aquatic and terrestrial groups using microscopy, thus, aiding the reconstruction of past ecosystem functioning (Battarbee and Bennion, 2011; Bennion et al., 2011). The fossils from diatoms, Cladocera, dinoflagellates, chironomid, pollen and plants have been the focus of most paleolimnological studies in various environments (Zeeb and Smol, 2005; Castañeda and Schouten, 2011; Väliranta et al., 2015; Herzschuh et al., 2016). The problem with fossil-based studies, however, is that not all morphological remains are well preserved or can be taxonomically identified to the species level. To overcome this limitation, biomarkers (like pigments and lipids) were developed to provide a more detailed and comprehensive understanding of past biological diversity in a broader range of environments (Birks, 1991; Coolen et al., 2013). But even with this approach, the problem of taxonomic assignments persists (Capo et al., 2021a). Recently, targeting the DNA preserved in sediments has emerged as complementary and/or as a more reliable alternative to fossil and biomarker-based paleolimnological investigations (Edwards, 2020). In temperate lakes, the anoxic cold water-sediment interface with no bioturbation are some of the important factors promoting DNA preservation in sediments after deposition (Boere et al., 2011).

1.3.2 Sedimentary DNA as a tool to trace changes in aquatic ecosystems

In sedimentary DNA analysis, in most cases total DNA is extracted from sediments and analyzed. Sequencing sediment archived DNA, either specific gene regions or the whole DNA, has enabled the reconstruction of highly-resolved species diversity over a range of spatio-temporal and ecological time scales (Domaizon et al., 2013; Parducci et al., 2017), as well as revealed additional taxa (Pedersen et al., 2013). Therein lies the foremost advantage of using DNA-based methods in sediment analysis compared to classical paleolimnological tools (Domaizon et al., 2017). The DNA from sediments are typically grouped into sedimentary DNA (sedDNA; younger and better preserved) and sedimentary ancient DNA (sedaDNA; typically, older and less well preserved), based on the extent of degradation caused by environmental factors like age, temperature, and other factors. Thus, sedaDNA refers to nucleic acids buried in subsurface sediments deposited by physiologically inactive organisms (Capo et al., 2021a). Presumably, the first study to use sedaDNA was on the DNA of purple sulfur bacteria in lake sediment which revealed Holocene changes in water column stratification, anoxia, and sulfide contents (Coolen and

Overmann, 1998). Since then, several studies have made substantial progress reconstructing the dynamics of past biological populations within aquatic ecosystems using sedaDNA (e.g., Pedersen et al., 2015; Domaizon et al., 2017; Armbrecht et al., 2019). Usually, a single sedaDNA sample is enough to reflect the dominant bacterial species in a lake (Weisbrod et al., 2020), and identify shifts among them (Pearman et al., 2021b). Furthermore, sedaDNA has also contributed significant insights into the historical impact of climate, environmental and human disturbances on the diversity and composition of different photosynthetic bacteria, phytoplankton, planktonic and Pisces groups in lakes. Recent examples include the organellar genome reconstruction of ancient populations of the algae *Nannochloropsis limnetica* (Lammers et al., 2021), a multi-millennial paleo-diversity of lacustrine eukaryotes (Kisand et al., 2018), centennial changes in daphnia populations (Monchamp et al., 2017), and decadal changes in fish DNA concentration (Kuwae et al., 2020). Beyond the lake, sedaDNA is also reliable in reconstructing the catchment vegetation and landscape development revealing human impacts as well as changes in the terrestrial biota (Niemeyer et al., 2017; Alsos et al., 2020; Liu et al., 2021). A few of the latest insights in past ecosystems functioning based on sedaDNA revealed the past impact of humans and animal husbandry in alpine lake catchments (Bajard et al., 2020; Walsh and Giguet-Covex, 2020), and long-term changes in plant communities caused by climate change and anthropogenic activities in tropical high-altitude locations and the European Alps (Bajard et al., 2017; Dommain et al., 2020).

After DNA extraction from sediments, several analytical approaches are used depending on the research question. In non-specific target studies, the total DNA recovered from the sediment could be sequenced using metagenomic approaches (e.g., shotgun; Pedersen et al., 2016). On the other hand, applications such as the newly emerged droplet digital polymerase chain reaction (ddPCR), quantitative PCR (qPCR), and amplicon high-throughput sequencing (HTS) PCR assays are used to detect or quantify specific target organisms (Belle and Parent, 2019; Pearman et al., 2021a), whole microbial groups or groups with the same functional profiles in a sample (Stoof-Leichsenring et al., 2012; Belle and Parent, 2019). Another method is DNA metabarcoding which combines HTS with PCR amplifications of marker loci known as 'barcodes' (Zimmermann et al., 2017; Taberlet et al., 2018). And finally, in some instances, the DNA fragments of interest can be recovered from sediment metagenomes using hybridization-based enrichment methods (Schulte et al., 2021). Although some limitations do exist with the sedaDNA approach (like incomplete

reference databases for some organismal groups), it is strongly presumed that as DNA sequencing technologies continue to advance and reference databases become more comprehensive and improved, the sedaDNA potential will greatly increase in the future (Capo et al., 2021).

1.3.3 The importance of cyanobacteria sedaDNA as a paleo-proxy

In freshwater ecosystems, early decadal-scale paleolimnology studies used cyanobacteria fossil remains (e.g., akinetes and cysts) and pigments from sediments to reconstruct past lake environmental conditions (Livingstone and Jaworski, 1980; Sanger, 1988; Leavitt and Findlay, 1994). Later studies built on this knowledge by targeting cyanobacteria pigment biomarkers like echinenone, canthaxanthin and zeaxanthin to trace previous eutrophication and bloom periods (e.g., Cook et al., 2016). However, the limitation with these approaches is that only those taxa that leave fossilized remains or produce biomarkers can be detected, revealing no information on other non-fossil/biomarker producing taxa that are equally affected by human and climatic stressors and thus crucial to paleoclimatic studies. Recently, sediment deposited cyanobacteria lipid biomarkers have also been used as tracers of harmful bloom-forming species and their potential drivers (Kaiser et al., 2016, 2020; Bauersachs et al., 2017). For example, recent cyanobacteria bloom reconstructions were done on integrated sediment traps and sediment cores from the Baltic Sea using lipid biomarkers (6- and 7-methylheptadecane lipids). The result from the long-term scale analysis show that blooms caused by *Nodularia spumigena* in the Baltic Sea may be driven by natural processes like temperature variability (Kaiser et al., 2020). With the emergence of sedaDNA however, a complementary and new wealth of knowledge has been gained on the impact of climate change, eutrophication, and environmental change on lake cyanobacteria assemblages across different environments and temporal time scales (Domaizon et al., 2017; Parducci et al., 2017; Capo et al., 2021). This has been shown for instance for the important primary producer *Synechococcus* which does not leave a distinct morphological footprint in sediments, but can reveal information about past climate changes (Ye et al., 2011; Coolen et al., 2013; Domaizon et al., 2013). Furthermore, sedaDNA was used to explore changes in cyanobacteria phylogenetic and functional diversity over decadal to centennial time scales (Monchamp et al., 2016, 2017), as well as regional-scale homogenization of cyanobacteria populations in lakes (Monchamp et al., 2018). A millenia-scale cyanobacteria sedaDNA reconstruction recently showed a

relationship between pre-industrial higher cyanobacterial abundance with higher temperature and lower precipitation (Zhang et al., 2021b). Also, sedaDNA has enabled the investigation into the occurrence and distribution of the non-photosynthetic cyanobacteria sister clades Sericytochromatia and Melainabacteria in several lakes (Monchamp et al., 2019a). The results revealed that their diversity within and between lakes did not alter in the last century. Some studies have used specific primers to reconstruct past dynamics of cyanobacteria groups of interest from sedaDNA archives like *Plankothrix* (Savichtcheva et al., 2011, 2015; Kyle et al., 2014), *Synechococcus* (Domaizon et al., 2013), *Nodularia* (Konkel et al., 2020), *Cylindrospermosis* (Martínez De La Escalera et al., 2014), and even subpopulations within a certain group as was shown for *Planktothrix* (Kyle et al., 2014) and their relationship with chytrid parasite (Kyle et al., 2015). Others have reconstructed the histories of harmful bloom-forming cyanobacteria by targeting several genes controlling toxin synthesis in cyanobacteria. These studies led to the identification of important patterns in potentially toxic cyanobacteria and the genes involved in cyanotoxin synthesis with changes in lake environmental conditions, for example microcystin (Monchamp et al., 2016; Pilon et al., 2019), saxitoxin (Martínez De La Escalera et al., 2014), nodularin (Cegłowska et al., 2018; Wood et al., 2021), anatoxin (Hobbs et al., 2021), and cylindrospermosin (Waters, 2016). Thus far, a variety of analytical methods have been employed in cyanobacteria sedaDNA reconstructions like denaturing gradient gel electrophoresis (e.g., Ye et al., 2011), qPCR (e.g., Savichtcheva et al., 2011), HTS (e.g., Monchamp et al., 2016) or a combination of these methods (e.g., Savichtcheva et al., 2015). The complementarity and agreement between sedaDNA and classical paleolimnology tools in studying cyanobacteria history in lakes have equally been shown e.g., sedaDNA and microscopy (Monchamp et al., 2016), ddPCR and pigment analysis (Picard et al., 2022), as well as the coherence between DNA-based methods (e.g., ddPCR and HTS, Mejbel et al., 2021). The results from these studies underline the usefulness of sedaDNA in unraveling past dynamics of cyanobacteria assemblages in the aquatic ecosystem and their response to changes in local environmental stressors (climate- and human-driven).

1.4 Aims and Objectives

Cyanobacteria can have detrimental ecological effects on aquatic ecosystems via toxic blooms. Sedimentary DNA archives can provide information on their histories and past conditions in a lake (Cronberg, 1986; Huisman et al., 2018), and potentially also lake catchments and entire regions. With the increase in cyanobacteria sedaDNA studies in the last decade, there is a need to examine the consistency between sediment-archived cyanobacteria DNA and those of the water column communities. Furthermore, it is crucial to assess the effect of potential taphonomic processes, i.e., alteration or deterioration of their DNA during transport along the water column to the sediment, at the sediment-water interface and the preservation of deposited DNA under prevailing environmental conditions. This is of utmost importance and particularly useful for aquatic ecosystems where long-term monitoring data is lacking. The main goal of this thesis is to find out whether, and to what extent, natural and/or anthropogenic influences determine the dynamics of cyanobacteria in temprate lakes. Thus, this thesis provides pioneer work in providing evidence of alterations in freshwater cyanobacteria assemblages since the Holocene to the present time driven by a combination of human-mediated local stressors (e.g., land use, eutrophication) with regional to global drivers (e.g., climate).

The work described in this thesis (Fig. 1.4) investigates the seasonal succession dynamics of cyanobacteria populations within the water column of a deep temperate lake concerning potential niche segregation among them. It examines the current understanding on the factors governing the sediment deposition of total cyanobacteria and different cyanobacteria groups in lakes. Furthermore, it reconstructs cyanobacteria Holocene dynamics, covering periods of natural and human impact, and it assesses the potential of sediment reconstructed cyanobacteria populations as proxies for environmental parameters in a lake.

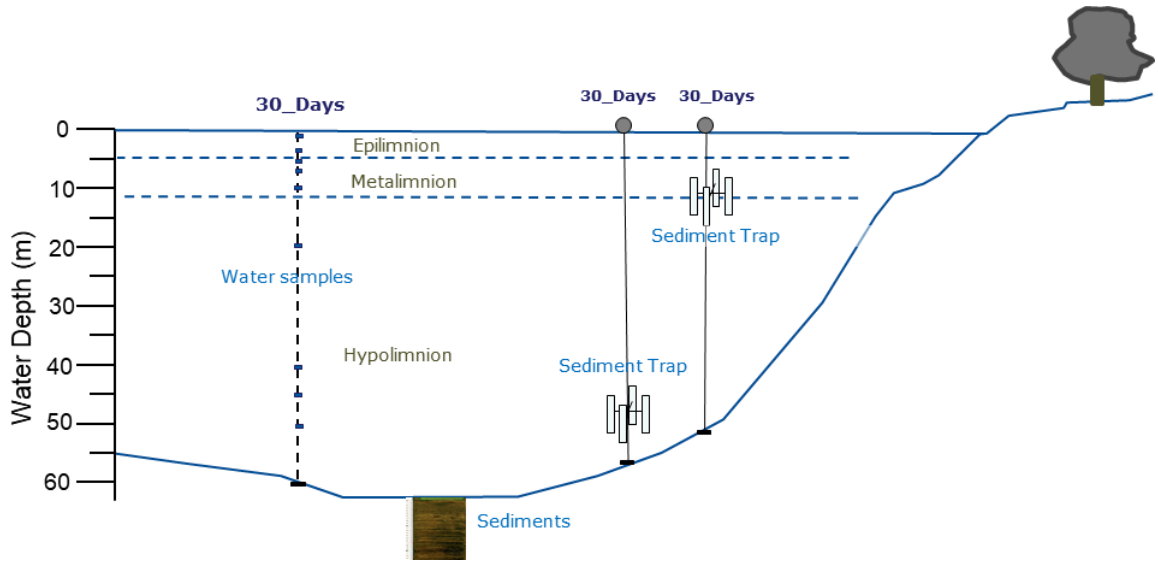

Figure 1.4: Graphical illustration of the work described in this thesis. Highly resolved spatio-temporal monitoring of cyanobacteria assemblages in the water column, their sediment deposition, and long-term dynamics reconstructed from sediments.

The following key questions were addressed in this thesis;

- What are the seasonal dynamics of cyanobacteria populations in deep, hard-water temperate lakes?
- Are the sediment-deposited cyanobacteria assemblages consistent with those in the water column?
- How has cyanobacteria structure (diversity and composition) and abundance changed since the Holocene to present time?

1.5 Study site

Lake Tiefer See is part of the Klocksin-Lake-Chain (latitude 53°35′36″N, longitude 12°31′46″E; Fig. 1.5) located in the natural park „Nossentiner/Schwinzer Heide“. The deep (62 m) and medium-sized lake (~0.75 km^2) resulted from a deep subglacial gully system in a terminal morainic of the Pomeranian Phase of the Weichselian glaciation. Today, the lake is connected to Lake Hofsee in the South while the connection to Lake Flacher See in the North has been channelized in a tunnel after the construction of a railway dam between the two lakes (CE 1884–1886).

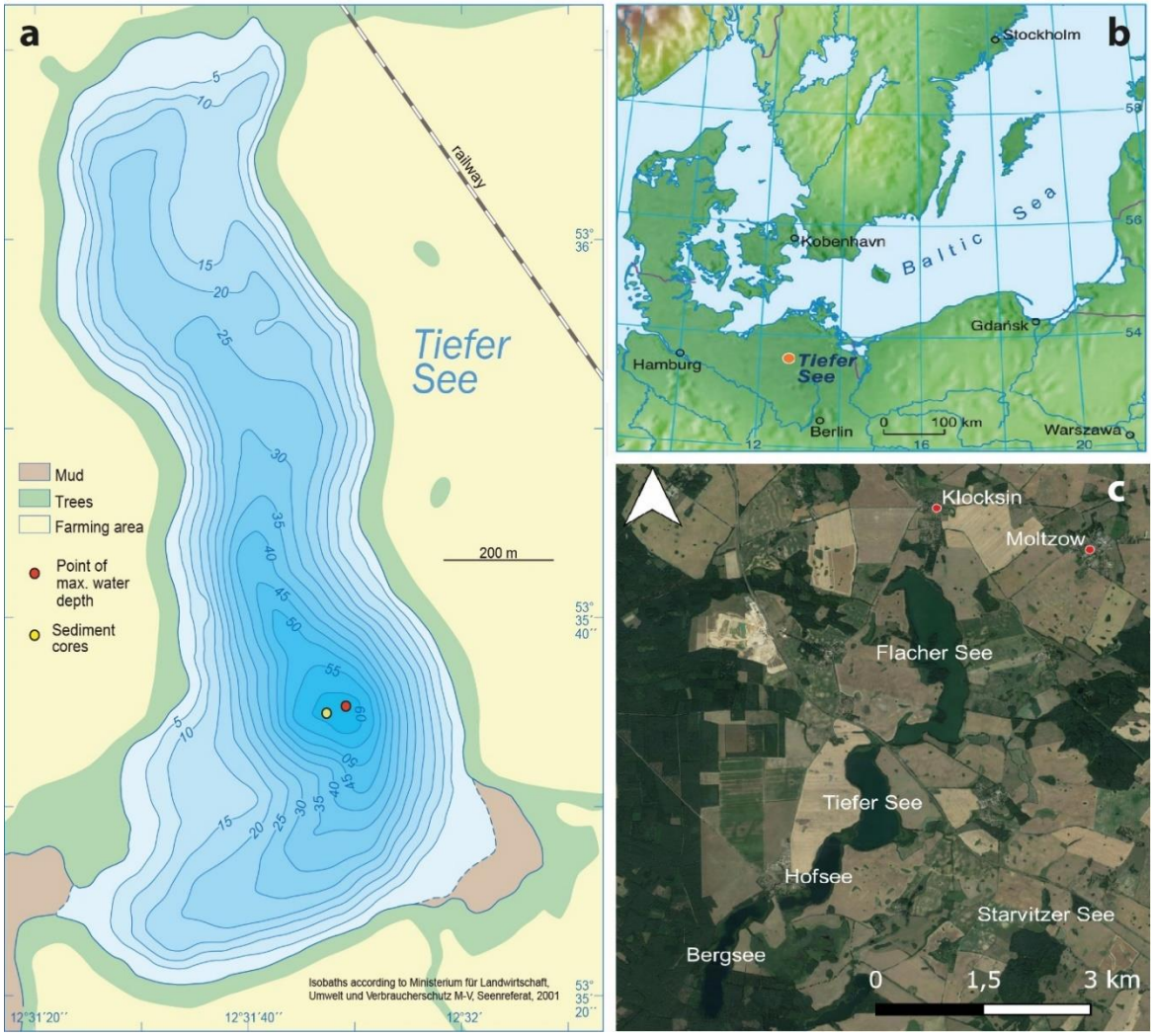

Figure 1.5: Location of study site. (a) Topographic map of Lake Tiefer See showing point of maximum water depth where water samples were collected from (red dot) and point where sediment cores used for the studies in this thesis were collected from (yellow dot), (b) Lake Tiefer See in northeast Germany, and (c) satellite image of Lake Tiefer See in the Klocksin lake chain. Sources: (a) modified after Dräger et al. (2017), (b) Theuerkauf et al. (2021), and (c) Google Earth.

Lake Tiefer See has a surface area of about 0.75 km^2, and the catchment area of about 5.5 km^2 is dominated by glacial till (Kienel et al., 2013). The catchment area is mainly used for agriculture, and dominated by pine forests to the west. The direct shoreline of the lake is covered by a fringe of deciduous trees and there is no anthropogenic infrastructure such as buildings and roads at the lakeshore (Theuerkauf et al., 2015). The lake has a maximum depth of 62–63 m and no major inflow and outflow. The present-day lake water is oligo-mesotrophic and the circulation mode is either mono- or dimictic, depending on the formation of a winter ice cover (Roeser et al., 2021). The study site is characterized by a warm-temperate climate at the transition from oceanic to continental conditions. Mean

monthly temperatures range from 0 °C in January to 18 °C in June, with maxima up to 30 °C and minima down to -5 °C. The weather station Waren (Müritz) close to the lake recorded the mean annual precipitation for the period 1980–2020 to be 591 mm (www.dwd.de).

1.6 History of the study site since the Holocene

1.6.1 Holocene climate history of Central Europe

The Holocene began with a rapid increase in temperature around 11.7 cal. ka BP (calibrated kilo years before present) (Deil, 2000; Walker et al., 2018). Although the climate during the Holocene was relatively warm, there were significant small-scale variations, most notably during the early Holocene (Anderson et al., 2007; Wanner et al., 2015; Florescu et al., 2019). The Holocene climate included periods of gradual as well as so-called Rapid Climate Changes defined by almost centennial-scale cooling (Anderson et al., 2007). Peak Holocene temperatures were recorded in the Northern Hemisphere before 7 cal. ka BP (Fig. 1.6a), followed by a temperature decline with regional differences (Wanner et al., 2015). The Rapid Climate Changes during the early Holocene was related to freshwater pulses in the Nordic and Labrador Sea which led to temperature declines and insulation shifts in the Northern Hemisphere (Wanner et al., 2015). The most notable cooling event during the early Holocene occurred around 8.2 cal. ka BP (Fig. 1.6b) (Kleiven et al., 2008; Renssen et al., 2010), and was as a result of strong meltwater pulses from Norther Hemisphere ice-sheets (Carlson et al., 2008). Although still unexplainable, the most important climate cooling events during the mid-Holocene occurred about 6, 5.3, and 4.2 cal. ka BP (Magny and Haas, 2004; Wanner et al., 2015). In the late Holocene, the most notable cooling events were recorded for 2.8 cal. ka BP (Plunkett and Swindles, 2008), the Migration Period around 1.4 cal. ka BP (Ljungqvist, 2010), and the Little Ice Age between the 13th and 19th century AD (Matthews and Briffa, 2005). These cooling events were interrupted by warmer periods like the Roman Period Warming and the Medieval Warm Period (Wanner et al., 2015). During the entire Holocene, the coldest periods were during the 8.2 cal. ka BP and the Little Ice Age (Wanner et al., 2015).

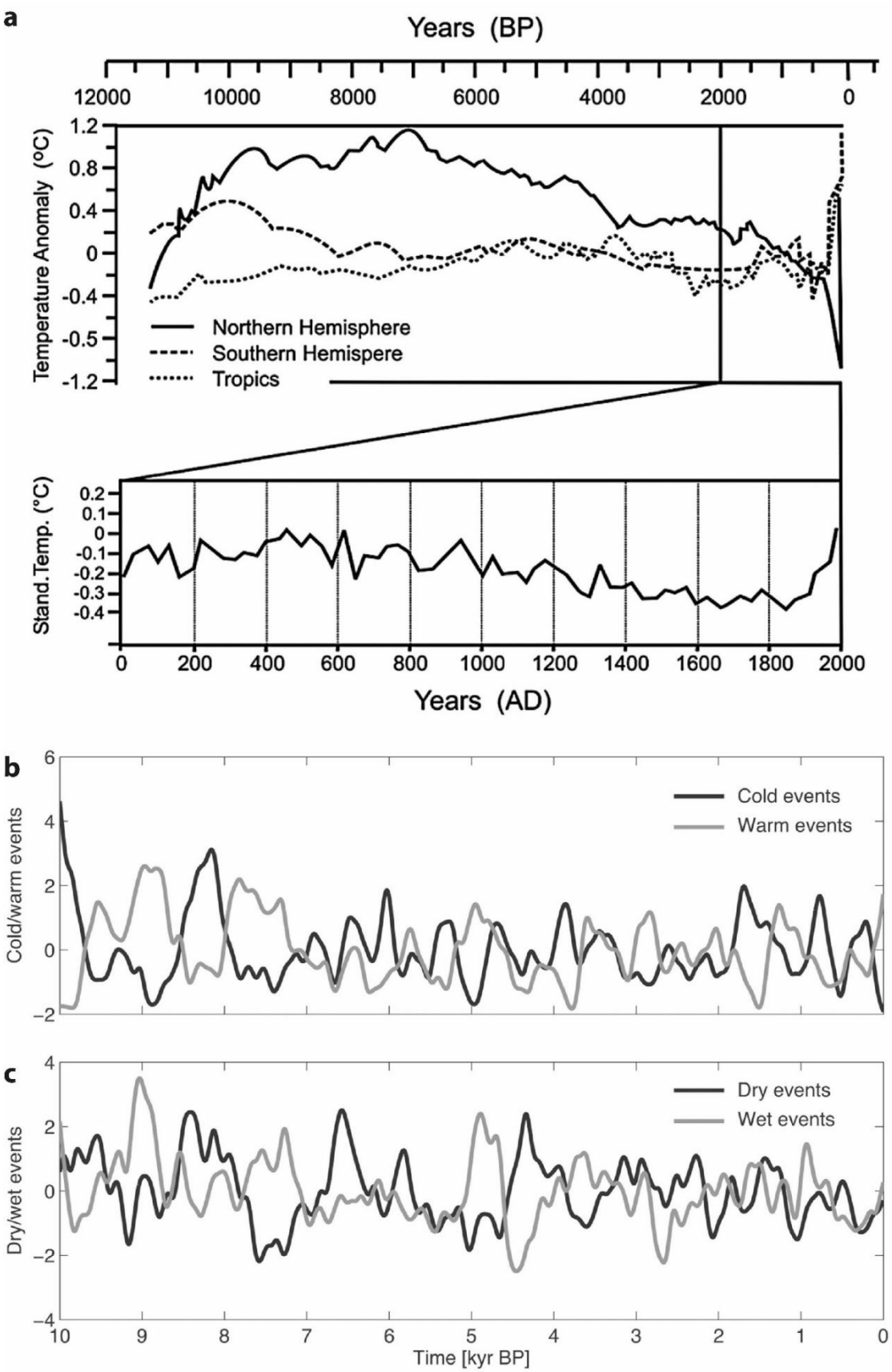

Figure 1.6: Holocene temperature reconstructions and distribution of warm/cold and dry/wet events. (a) Top: Mean Holocene temperature anomalies for the Northern (solid line) and

Southern (dashed line) Hemispheres as well as the Tropics (dotted line) referenced to the Common Era 1961 – 1990 mean (Marcott et al., 2013). Bottom: global temperature anomalies for the last 2000 years: 30-year averages referenced to common era 1200 – 1964 mean (PAGES 2k Consortium, 2013). Distributions of (b) warm and cold events, and (c) dry and wet events. Figure modified after Wanner et al. (2015).

1.6.2 Climate and human impact history in northeastern Germany

The Holocene climatic for northeast Germany was reconstructed from pollen data obtained from Lake Maarfelder Maar in western Germany (Litt et al., 2009). According to the high-resolution data, this region was characterized by a dry-warm early Holocene and a wet-warm mid-Holocene (Fig. 1.6c). Concurrent hydrological events reconstructed for northeast Germany, such as low lake-level in early-Holocene and low groundwater levels in peatlands in mid-Holocene, were therefore thought to have equally resulted from climatic impact (Kaiser et al., 2012). Based on geochronological datasets (radiocarbon dating) obtained from late Quaternary fluvial units, the periods of river flooding activities and stability until 4.2 cal. ka BP in the west and south Germany as well as in the west and central Poland were mainly related to wetter and/or cooler climate periods (Starkel et al., 2006; Hoffmann et al., 2008). Only with increasing human populations combined with accelerated agriculture in these regions during the Bronze Age, between ca. 3.3 and 2.8 cal. ka BP did anthropogenic-influenced river floods became apparent (Hoffmann et al., 2008). Although regional differences caused by human impact likely existed, hydrologic data from northeast Germany mostly concurred with the results from the west and south Germany as well as west and central Poland (Kaiser et al., 2012).

Studies conducted at the German Institute of Regional Studies reported the catchment of Lake Tiefer See to be populated and depopulated during the Bronze Age and Iron Age, respectively (Grundmann, 1999). A pollen-based reconstruction of vegetation revealed human deforestation around Lake Tiefer See exposed it to increased wind stress and was responsible for the non-varved sediment segments corresponding to 4 cal. ka BP (Theuerkauf et al., 2015). A period of Slavic settlements mostly close to and around lakes/rivers followed around 1.5 cal. ka BP. However, from late Medieval periods, intensified anthropogenic deforestation has had a devastating impact on the regional hydrology, e.g., increasing groundwater- and lake levels followed by increasing river

discharge (Bork et al., 1998). From the 18th century AD, the regional peatlands were transformed by hydro-melioration into extensive grasslands (Schultz-Sternberg et al., 2000). The most intensive and widespread land-cover changes and transformations (e.g., into arable land) resulting from human impact between the period 1965 – 1995 (Lenschow, 2001; Kaiser et al., 2012; Kienel et al., 2013).

1.7 Materials and methods

1.7.1 Fieldwork

The data presented in this thesis were from (i) monthly water samples from the water depths 1, 3, 5, 7, 10, 15, 20, 40, 45, and 50 m collected between January 30 and November 28 in 2019, (ii) monthly sediment trap samples collected using four-cylinder traps (KC Denmark A/S, total active area 0.0163 m^2 for the four cylinders) from the metalimnion (12 m water depth) and hypolimnion (50 m water depth) between April and November in 2019, and (iii) 115 cm short and 11 m long sediment cores collected from the point of maximum water depth (62 m) using a 90 mm UWITEC piston corer in 2015 and 2019, respectively, from Lake Tiefer See (Figs. 1.4, 1.7).

Figure 1.7: Images from Lake Tiefer See. (a) Weather monitoring set-up, (b) a freshly retrieved short sediment core, and (c) a platform for long core collection (left) and weather monitoring station (right).

1.7.2 Main laboratory methods

To answer my research questions, an integrated and interdisciplinary approach using microbiological, bioinformatics, physicochemical, geochemical, statistical, and lipid biomarker analyses was used. The microbiological analyses of cyanobacteria abundance and community composition were based on culture-independent methods, and the physicochemical and geochemical analyses were carried out on lake water and sediment samples. Sediment chronology was determined by varve counting, tephrochronology and radiocarbon dating as previously described by Dräger et al., (2017) in the laboratories of

the Climate Dynamics and Landscape Evolution Section at the German Research Centre for Geosciences (GFZ) in Potsdam. Water and sediment samples were analyzed in the laboratories of the Geomicrobiology Section at the German Research Centre for Geosciences (GFZ) in Potsdam. Water samples were filtered less than 24 hours after collection, followed by total DNA extraction and storage at -20 °C pending downstream analyses. Total DNA was also extracted from homogenized trapped sediment samples as well as sediment samples from short (up to 115 cm) and long (up to 11 m) sediment cores. To avoid cross-contamination, water, trapped sediment, and cored sediment samples were processed at different times. For cyanobacteria community composition, the cyanobacteria 16S rRNA were PCR-amplified for barcode HTS sequencing using cyanobacteria-specific primers (Table 1.1; Nübel et al., 1997; Janse et al., 2003). Total cyanobacteria abundance were quantified using primers that amplify the cyanobacteria 16S rRNA gene and intergenic spacer region (ITS) (Janse et al., 2003) based on qPCR assay for absolute gene copy numbers. Total *Planktothrix* and the cyanopeptolin-producing *Planktothrix* subpopulations (*oci*B) were enumerated using a Taq nuclease qPCR assay (TNA; Savichtcheva et al., 2011) and an SYBR-Green qPCR Assay (Kyle et al., 2014), respectively. All qPCR assays were performed in triplicates on a CFX96 real-time thermal cycler (Bio-Rad Laboratories Inc., USA). The 16S rRNA-ITS, PC-IGS, and *oci*B copy numbers were calculated after Savichtcheva et al., (2011) and normalized to extracted DNA (copies ng^{-1} DNA). All amplified PCR and qPCR products were analyzed for unspecific amplification using agarose gel electrophoresis. Assessment of potential DNA fragmentation that could have a negative impact on PCR efficiency was carried out on a few samples selected from the top (200 cm) and bottom (1015 cm) of the long core. Here, the qPCR amplification products from the cyanopeptolin producing *Planktothrix* subpopulation, from total cyanobacteria 16S SYBR Green qPCR assay and from long fragment total cyanobacteria PCR were used to construct clone libraries with a TOPO TA cloning kit (Invitrogen) with PCR vector 2.1 and sequenced. Cyanobacteria-specific primers were used for long fragment PCR (Janse et al., 2003). A subset of samples distributed along the long core was selected for commercial metagenome analysis.

Table 1.1: Oligonucleotide primers. The primer sequences used in high-throughput sequencing (HTS) and TOPO cloning of short and long fragment amplicons for total cyanobacteria, qPCR to target total cyanobacteria, total *Planktothrix*, cyanopeptolin-producing *Planktothrix* subpopulations, and TaqMan probe used for qPCR to target total *Planktothrix* populations. F = forward, R = reverse, Tp = TaqMan probe, FAM = 6-carboxyfluorescein, BHQ-1 = black hole quencher, Ref. = references

Gene	Primers	Primer Sequence (5'-3')	Gene Locus	Amplicon Size (bp)	Ref. ..
Cyanobacteria 16S rRNA (HTS)	CYA106F CYA359F	CGGACGGGTGAGTAACGCGTG CGGACGGGTGAGTAACGCGTG	16S rRNA	ca. 678 ca. 425	a
	CYA784R	ACTACWGGGGTATCTAATCCC			
Cyanobacteria 16S rRNA (Topo Cloning)	CYA371F	CCTACGGGAGGCAGCAGTGGGGAATTTTCC	16S rRNA	ca. 1450	b
	373R	CTAACCACCTGAGCTAAT	ITS1		
SYBR-Green qPCR for total Cyanobacteria	CSIF	G(T/C)CACGCCCGAAGTC(G/A)TTAC	16S rRNA	ca. 350	b
	373R	CTAACCACCTGAGCTAAT	ITS1		b
TaqMan qPCR for total *Planktothrix*	PIPCF	GAGCAGCACTGAAATCCAAG	PC-IGS	ca. 72	c
	PIPCR	GCTTTGGCTGCTTCTAAACC	PC-IGS		
	PIPC Tp	FAM-TTTGGCTTGACGGAAACGACCAA-BHQ	PC-IGS		
SYBR-Green qPCR cyanopeptolin-producing *Planktothrix* ecotypes	*oci*B260F	CCTTTGACTTAGCCCGTGA	*oci*B		d
	*oci*B161R	TTGAATGTATGCGTTATAGAGGT	*oci*B	ca. 161	
	*oci*B247R	AGAATATCTCCCTGTAACCAC	*oci*B	ca. 247	

a = (Nübel et al., 1997), b = (Janse et al., 2003), c = (Schober and Kurmayer, 2006), and d = (Kyle et al., 2014).

Lipid biomarker analysis of 6Me-$C_{17:0}$ and 7Me-$C_{17:0}$ monomethyl branched alkanes (6- and 7-methylheptadecane) that may be representative of cyanobacteria biomass (Kaiser et al., 2020) was carried out on 47 sediment samples dating back to 6183 cal. a BP as

previously described by Kaiser et al., (2020) in the Marine Geology laboratories at the Leibniz Institute for Baltic Sea Research.

1.8 Overview of publications

Manuscript I (*Journal of Paleolimnology. 2021:2069. https://https://doi.org//10.1007/s10933-021-00206-9*)

Evaluating sedimentary DNA for tracing changes in cyanobacteria dynamics from sediments spanning the last 350 years of Lake Tiefer See, NE Germany.

Authors: Ebuka Canisius Nwosu[1], Jérôme Kaiser[2], Fabian Horn[1], Achim Brauer[3,5], Dirk Wagner[1,5], and Susanne Liebner[1,4]

Aims: In this pilot sedaDNA study in Lake Tiefer See, cyanobacteria dynamics was reconstructed from sediments covering the Little Ice Age till present time within the framework of my master thesis. Here the aim was to understand how cyanobacteria assemblages from varved and non-varved sediments differed and how lake environmental conditions at the time of sediment deposition affected cyanobacteria populations reconstructed from sediments.

Summary: In this study, we assessed changes in cyanobacterial community dynamics via sedimentary DNA (sedaDNA) from well-dated lake sediments of Lake Tiefer See spanning the last 350 years. Our diversity and community analysis revealed that cyanobacterial communities form clusters according to the presence or absence of varves. Based on distance-based redundancy and variation partitioning analyses (dbRDA and VPA), we identified that intensified lake circulation inferred from vegetation openness reconstructions, $\delta^{13}C$ data (a proxy for varve preservation) and total nitrogen content were abiotic factors that significantly explained the variation in the reconstructed cyanobacterial community from Lake Tiefer See sediments. Operational taxonomic units (OTUs) assigned to *Microcystis sp.* and *Aphanizomenon sp.* were identified as potential eutrophication-driven taxa of growing importance since circa common era (ca. CE) 1920 till present. This result is corroborated by a cyanobacteria lipid biomarker analysis. Furthermore, we suggest that stronger lake circulation as indicated by non-varved sediments favored the deposition of the non-photosynthetic cyanobacteria sister clade Sericytochromatia, whereas lake bottom anoxia as indicated by subrecent- and recent varves favoured the Melainabacteria in sediments. Our findings highlight the potential of high-resolution amplicon sequencing

in investigating the dynamics of past cyanobacterial communities in lake sediments and show that lake circulation, anoxic conditions, and human-induced eutrophication are main factors explaining variations in the cyanobacteria community in Lake Tiefer See during the last 350 years.

Co-author contributions: *S. Liebner, A. Brauer* and *Ebuka Canisius Nwosu* designed the study. *A. Brauer* conducted field work and provided lake sediment parameter data. *Ebuka Canisius Nwosu* performed sediment sub-sampling, molecular analyses lab work, and initial data analyses and interpretation with focus on bacteria, cyanobacteria, and *Microcystis* for his Master's Thesis. During my doctoral research, I carried out additional sediment sub-sampling for biomarker analysis and amplicon sequencing to generate comparable DNA/Biomarker data for five selected depths, new data analyses, interpretation, and new illustration of the results with sole focus on cyanobacteria, wrote the initial manuscript draft and three rounds of revisions of the manuscript. *J. Kaiser* perfomed cyanobacteria lipid biomarker analysis. *F. Horn* preprocessed the sequence data. All authors contributed to the discussion, interpretation of the data and the writing of the manuscript.

Manuscript II (*Frontiers in Microbiology, Aquatic Microbiology 12:761259. https://https://doi.org//10.3389/fmicb.2021.761259*)

Species-Level Spatio-Temporal Dynamics of Cyanobacteria in a Hard-Water Temperate Lake in the Southern Baltics

Authors: Ebuka Canisius Nwosu[1], Patricia Roeser[2], Sizhong Yang[1], Lars Ganzert[1], Sylvia Pinkerneil[3], Elke Dittmann[4], Achim Brauer[3,5], Dirk Wagner[1,5], and Susanne Liebner[1,4]

Aims: The aim of this study was to assess the seasonal spatial succession of pelagic cyanobacteria assemblages, their abundance and possible niche segregation in the deep hard-water Lake Tiefer See near Klocksin (TSK) in northeastern Germany. Water samples from the lake were collected from different depths representative of the entire water column monthly from January to November 2019. To identify the potential environmental drivers of cyanobacteria dynamics in this lake, cyanobacteria abundance and community composition data were related to lake environmental data.

Summary: Using combined monthly water sampling and monitoring in 2019, amplicon sequence variants analysis (ASVs; a proxy for different species) and quantitative PCR targeting overall cyanobacteria abundance, we observed significant seasonal variation in the cyanobacterial community composition ($p < 0.05$) in the epi and metalimnion layers, but not in the hypolimnion. In winter -when the water column is mixed- picocyanobacteria (*Synechococcus* and *Cyanobium*) were dominant. With the onset of stratification in late spring, we observed potential niche specialization and coexistence among the cyanobacteria taxa driven mainly by light and nutrient dynamics. Specifically, ASVs assigned to picocyanobacteria and the genus *Planktothrix* were the main contributors to the formation of deep chlorophyll maxima along a light gradient. While *Synechococcus* and different *Cyanobium* ASVs were abundant in the epilimnion up to the base of the euphotic zone from spring to fall, *Planktothrix* mainly occurred in the metalimnetic layer below the euphotic zone where also overall cyanobacteria abundance was highest in summer. Our data revealed two potentially psychrotolerant (cold-adapted) *Cyanobium* species that appear to cope well under conditions of lower hypolimnetic water temperature and light as well as increasing sediment-released phosphate in the deeper waters in summer. The potential cold-adapted *Cyanobium* species were also dominant throughout the water column in fall and winter. Furthermore, *Snowella* and Microcystis-related ASVs were abundant in the water column during the onset of fall turnover. Altogether, these findings suggest previously unascertained and considerable spatiotemporal changes in the community of cyanobacteria on the species level especially within the genus *Cyanobium* in deep hard-water temperate lakes.

Co-author's contribution: *S. Liebner, A. Brauer* and *Ebuka Canisius Nwosu* designed the study. *S. Pinkerneil, A. Brauer* and *Ebuka Canisius Nwosu* conducted fieldwork. *Ebuka Canisius Nwosu* carried out laboratory analyses. *S. Pinkerneil* and *P. Roeser* provided lake environmental and sedimentary data. *O. Dellwig* provided total dissolved phosphorus data. *L. Ganzert* and *S. Yang* pre-processed the sequence data. All authors contributed to the discussion and interpretation of the data and the writing of the paper.

Manuscript III (*Microorganisms 2021:9081778. https://https://doi.org//10.3390/microorganisms9081778*)

From Water into Sediment—tracing freshwater cyanobacteria via DNA

Authors: Ebuka Canisius Nwosu[1], Patricia Roeser[2], Sizhong Yang[1], Lars Ganzert[1], Sylvia Pinkerneil[3], Olaf Dellwig[2], Elke Dittmann[4], Achim Brauer[3,5], Dirk Wagner[1,5], and Susanne Liebner[1,4]

Aims: After understanding the diversity and composition of cyanobacteria assemblages in Lake Tiefer See from the previous study, this study aimed to investigate the congruity between pelagic and sediment-deposited cyanobacteria communities in Lake Tiefer See. The special focus was on the possible effects of taphonomic processes on different cyanobacteria groups during transport from the water column to the sediment and thus their suitability as proxies for internal lake physicochemical parameters.

Summary: Sedimentary ancient DNA-based studies have been used to probe centuries of climate and environmental changes and how they affected cyanobacterial assemblages in temperate lakes. As cyanobacteria contain potential bloom-forming and toxin-producing taxa, their reconstruction from sediments is crucial, especially in lakes lacking long-term monitoring data. To extend the resolution of sediment record interpretation, we used high-throughput sequencing, ASV analysis, and quantitative PCR to compare pelagic cyanobacterial composition to that in sediment traps (collected monthly) and surface sediments in Lake Tiefer See. Cyanobacterial composition, species richness, and evenness were not significantly different among the pelagic depths, sediment traps, and surface sediments ($p > 0.05$), indicating that the cyanobacteria in the sediments reflected the cyanobacterial assemblage in the water column. However, total cyanobacterial abundances (qPCR) decreased from the metalimnion down the water column. The aggregate-forming (*Aphanizomenon*) and colony-forming taxa (*Snowella*) showed pronounced sedimentation. In contrast, *Planktothrix* was only very poorly represented in sediment traps (meta and hypolimnion) and surface sediments, despite its highest relative abundance at the thermocline (10 m water depth) during periods of lake stratification (May–October). We conclude that this skewed representation in taxonomic abundances reflects taphonomic processes, which should be considered in future DNA-based paleolimnological investigations.

Co-author's contribution: *S. Liebner, A. Brauer* and *Ebuka Canisius Nwosu* designed the study. *S. Pinkerneil, A. Brauer* and *Ebuka Canisius Nwosu* conducted fieldwork. *Ebuka Canisius Nwosu* carried out laboratory analyses. *S. Pinkerneil* and *P. Roeser* provided lake environmental and sedimentary data. *O. Dellwig* provided total dissolved phosphorus data.

L. Ganzert and *S. Yang* pre-processed the sequence data. All authors contributed to the discussion and interpretation of the data and the writing of the paper.

Manuscript IV (*Submitted for publication at Nature Communications*)

Bronze Age human-induced increase in cyanobacteria abundance revealed by sedimentary ancient DNA

Authors: Ebuka Canisius Nwosu[1], Achim Brauer[3,5], Marie-Eve Monchamp[6], Sylvia Pinkerneil[3], Alexander Bartholomäus[1], Julia Poloni[1], Martin Theuerkauf[7], Jens-Peter Schmidt[8], Kathleen R. Stoof-Leichsenring[9], Theresa Wietelmann[9], Jerome Kaiser[2], Dirk Wagner[1,5], and Susanne Liebner[1,4]

Aims: This study aimed to test the hypothesis of whether cyanobacteria sedaDNA can be used as proxies for anthropogenic disturbance (eutrophication, land-use) during the Holocene. In doing so, the focus was on extending the record of cyanobacteria sedaDNA reconstructions for the entire Holocene period building on the knowledge gained from the pilot short core study.

Summary: Climate change and anthropogenic-influenced eutrophication advance the spread of harmful cyanobacteria blooms in lakes. The rapidly evolving sedimentary ancient DNA-based studies are used to track the effect of centuries of climate and environmental changes on cyanobacterial assemblages in lakes and are particularly useful where long-term monitoring data is lacking. To extend the resolution of sediment record interpretation, we combined quantitative PCR, high throughput, and metagenome sequencing to reconstruct cyanobacteria history since the Holocene in a deep hard-water lake in northeastern Germany. We found a significant increase in total cyanobacteria abundance during the Holocene beginning during the Bronze Age and a peak during the Roman Age. This increase in cyanobacteria abundance is consistent with historical human settlement data in the study area. Furthermore, we show high preservation of cyanobacteria diversity in varved sediments relative to non-varved sediments. Thus, our study reveals that the onset of substantial anthropogenic disturbances initiated the first measurable changes in cyanobacteria assemblages during the Holocene.

Co-author's contribution: *S. Liebner, A. Brauer* and *Ebuka Canisius Nwosu* designed the study. *S. Pinkerneil,* and *Ebuka Canisius Nwosu* conducted fieldwork. *Ebuka Canisius Nwosu* carried out molecular laboratory analyses. *J. Poloni* performed qPCR analysis. *A. Brauer* provided lake sedimentary data and sediment age model data. *M. Theuerkauf*

provided reconstructed vegetation openness data. *J. Kaiser* provided cyanobacteria lipid biomarker data. *K. R. Stoof-Leichsenring* and *T. Wietelmann* performed DNA extraction for metagenome sequencing. *J-P. Schmidt* provided archaeological data. *A. Bartholomäus* preprocessed the amplicon and metagenome sequence data. All authors contributed to the discussion and interpretation of the data and the writing of the paper.

Author affiliations

[1]GFZ German Research Centre for Geosciences, Helmholtz Centre Potsdam, Section Geomicrobiology, 14473 Potsdam, Germany

[2]Leibniz Institute for Baltic Sea Research Warnemünde, Marine Geology, 18119 Rostock, Germany

[3]GFZ German Research Centre for Geosciences, Helmholtz Centre Potsdam, Section Climate Dynamics and Landscape Evolution, 14473 Potsdam, Germany

[4]Institute of Geosciences, University of Potsdam, 14476 Potsdam, Germany

[5]Institute of Biochemistry and Biology, University of Potsdam, 14476 Potsdam, Germany

[6]Department of Biology, University McGill, Montréal, QC H3A 0G4, Canada

[7]Institute of Botany and Landscape Ecology, University of Greifswald, Soldmannstraße 15, 17489 Greifswald, Germany

[8]Landesamt für Kultur und Denkmalpflege Mecklenburg-Vorpommern, Landesarchäologie 19055 Schwerin, Germany

[9]Alfred Wegener Institute für Polar und Meeresforschung, 14473 Potsdam, Germany

2 Manuscript I – Short-term cyanobacteria dynamics

"Evaluating sedimentary DNA for tracing changes in cyanobacteria dynamics from sediments spanning the last 350 years of Lake Tiefer See, NE Germany"

2.1 Abstract

Since the beginning of the Anthropocene, lacustrine biodiversity has been influenced by climate change and human activities. These factors advance the spread of harmful cyanobacteria in lakes around the world, which affects water quality and impairs the aquatic food chain. In this study, we assessed changes in cyanobacterial community dynamics via sedimentary DNA (sedaDNA) from well-dated lake sediments of Lake Tiefer See, which is part of the Klocksin Lake Chain spanning the last 350 years. Our diversity and community analysis revealed that cyanobacterial communities form clusters according to the presence or absence of varves. Based on distance-based redundancy and variation partitioning analyses (dbRDA and VPA) we identified that intensified lake circulation inferred from vegetation openness reconstructions, $\delta^{13}C$ data (a proxy for varve preservation) and total nitrogen content were abiotic factors that significantly explained the variation in the reconstructed cyanobacterial community from Lake Tiefer See sediments. Operational taxonomic units (OTUs) assigned to *Microcystis sp.* and *Aphanizomenon sp.* were identified as potential eutrophication-driven taxa of growing importance since circa common era (ca. CE) 1920 till present. This result is corroborated by a cyanobacteria lipid biomarker analysis. Furthermore, we suggest that stronger lake circulation as indicated by non-varved sediments favored the deposition of the non-photosynthetic cyanobacteria sister clade Sericytochromatia, whereas lake bottom anoxia as indicated by subrecent- and recent varves favored the Melainabacteria in sediments. Our findings highlight the potential of high-resolution amplicon sequencing in investigating the dynamics of past cyanobacterial communities in lake sediments and show that lake circulation, anoxic conditions, and human-induced eutrophication are main factors explaining variations in the cyanobacteria community in Lake Tiefer See during the last 350 years.

2.2 Introduction

The upsurge in human fertilizer and land-use change during the Anthropocene has intensified nutrient cycling. Further acceleration of nutrient cycling by global climate change has consequently resulted in a change in the biodiversity of natural communities in aquatic ecosystems (Steffen et al., 2007; Taranu et al., 2015; Irfan and Alatawi, 2019). Among the most susceptible ecosystems to anthropogenic activities and biodiversity losses is the freshwater ecosystem (Adrian et al., 2009), where cyanobacteria dominance has resulted, amongst others, from intensified land usage and inordinate discharge of nutrients into lakes (Taranu et al., 2015). Perhaps the first direct consequence of cyanobacteria blooms is experienced by diatoms and organisms of higher trophic levels (Dokulil and Teubner, 2000) because cyanobacteria can outcompete the eukaryotic phytoplankton due to their rapid growth and eco-physiological adaptation to low light levels (Carey et al., 2012; Rigosi et al., 2014).

Eutrophic water bodies can be dominated by toxin-producing cyanobacteria like *Microcystis* spp. (Bullerjahn et al., 2016). Some cyanobacteria species like *Aphanizomenon* can fix nitrogen thereby promoting their growth under nitrogen-limited conditions accompanied by high temperatures (Breitbarth et al. 2007). Blooms of cyanobacteria form large clusters and colonies that move vertically in the water column by being able to counteract gas vesicle buoyancy via carbohydrate ballast readjustment (Pfeifer, 2012). Taken together, these attributes coupled with their high susceptibility to human-induced changes make cyanobacteria ideal indicator organisms for investigating long-term changes in lake ecosystems.

Investigating natural archives such as varved (annually laminated) lake sediments has provided us with a better understanding of how aquatic ecosystem communities have responded to anthropogenic changes of the last centuries (Smol 2009). The DNA preserved in sediment records (sedaDNA) has the potential to reconstruct the dynamics of biological communities and, in particular, those taxa that do not leave a distinct morphological footprint (Capo et al., 2017). Information retrieved from varved sedaDNA archives by amplicon sequencing of DNA fragments, i.e., the analysis of specific genes or taxa on a high phylogenetic resolution, have been useful in reconstructing cyanobacterial community from lakes by providing reliable coverage of the entire cyanobacterial phylum as well as historical information on those cyanobacteria group like the picocyanobacteria that do not form resting cysts. Sedimentary DNA has been useful for instance in revealing the

distinctive distribution of *Synechococcus* and *Microcystis* in water and sediment in Lake Taihu (Ye et al., 2011) as well as in revealing the homogenization of cyanobacterial communities in the last century in peri-alpine temperate lakes (Monchamp et al. 2018). Therefore, with the continued advancements in sequencing techniques, sedaDNA is well suited to address knowledge deficits in paleolimnology (Domaizon et al. 2017). Studying the patterns of species diversity across space and time of lake sediments with their seasonally resolved archives opens up the possibility to increase the resolution on past human influences (Brauer and Guilizzoni, 2004), and understanding how such a pattern has the potential to influence how ecosystems can be managed and conserved (Monchamp et al. 2016).

The effects of climate change and eutrophication (Paerl and Huisman 2009), as well as that of environmental changes based on sedaDNA since the beginning of industrialization on cyanobacteria, are well documented (Monchamp et al. 2018). However, much of the history of cyanobacteria before this time point coupled with how the effects of both natural environmental change and human agricultural practices affect their dynamics remains unclear. Also, of increasing interest in recent years are the non-photosynthetic lineages that share a common ancestry with cyanobacteria (NCY): Melainabacteria and Sericytochromatia, and more studies are trying to understand their ecology in lake ecosystems (Di Rienzi et al. 2013a; Soo et al. 2017; Monchamp et al. 2019). To fill these knowledge gaps, the present study focuses on reconstructing cyanobacterial dynamics in three lake sediment segments from present time back to the Little Ice Age (CE 1665 – 2006) using an amplicon sequencing approach, with the aim of understanding changes in their community dynamics during this period as archived in the sediments. We selected Lake Tiefer See within the Klocksin lake chain (Lake TSK) as a study system for several reasons, namely; its detailed record of human impact via land-use intensity (agricultural practices) and deforestation leading to vegetation openness (inferred from pollen data) (Theuerkauf et al., 2015), its varved and non-varved sediment segments (Kienel et al., 2017), and finally, its well-established sediment chronology based on varve counting, radiocarbon dating, tephrochronology as well as reconstructed oxic and anoxic conditions in the water column indicated by organic matter $\delta^{13}C$ (varve preservation proxy; Dräger et al. 2017, 2019). The relevance of an extended reconstruction of cyanobacteria from lake sediments with a reliable age model is that observed community changes can be accurately related to past natural and/or anthropogenic activities potentially responsible for such changes.

2.2.1 Site description

Lake Tiefer See is part of the Klocksin-Lake-Chain (Fig. 2-1), a subglacial gully system in a morainic terrain located in the natural park „Nossentiner/Schwinzer Heide“ (Kienel et al., 2013, 2017; Dräger et al., 2017, 2019). Today, the lake is connected to Lake Hofsee in the South while the connection to Lake Flacher See in the North has been channelized in a tunnel after the construction of a railway dam between the two lakes (CE 1884 – 1886). Lake Tiefer See has a surface area of about 0.75 km^2, and the catchment area of about 5.5 km^2 is dominated by glacial till. Although the catchment is mainly used for agriculture (Theuerkauf et al., 2015), the direct shoreline of the lake is covered by a fringe of trees and there is no anthropogenic infrastructure such as buildings and roads at the lakeshore. The lake has a maximum depth of 62 - 63 m and no major inflow and outflow. The present-day lake water is mesotrophic and the circulation mode is either mono- or dimictic, depending on the formation of a winter ice cover (Kienel et al., 2013). The study site is characterized by a warm-temperate climate at the transition from oceanic to continental conditions. Mean monthly temperatures range from 0 °C in January to 17-18 °C in July with maxima up to 30 °C and minima down to -5 °C. Mean monthly precipitation varies between ~ 40 mm during winter and ~ 60 mm in summer with a mean annual precipitation of 560 -570 mm.

2.3 Materials and methods

2.3.1 Core sampling, chronology, and total nitrogen estimation

A surface sediment core of length 115 cm was obtained in September 2015 from the deepest point of Lake Tiefer See (62.5 m water depth), using a 90-mm UWITEC piston corer. The core was sealed and stored vertically at 4 °C in a dark room. The core was split longitudinally, photographed, and described. For molecular analyses, one half of the core was sub-sampled at 35-time points for continuous 1 cm intervals from three different sediment types (Supplementary Fig. A.1); recent-varved sediments from 9 – 42 cm depth (CE 2006 – 1924), non-varved from 43 – 82 cm and 88 – 99 cm (ca. CE 1920 – 1740 and ca. CE 1715 – 1675) and sub-recent-varved segment from 83 – 87 cm (ca. CE 1735 – 1720). The uppermost 9 cm were excluded from our analyses because of sediment distortion during coring. Molecular analyses were carried out on two subsampled duplicates. The age model was constructed by a multiple dating approach including microscopic varve

counting, radiocarbon dating, and the identification of Askja AD 1875 tephra (Wulf et al., 2016; Dräger et al., 2017).

Total nitrogen (TN) of freeze-dried sediments was measured continuously at 1-cm increments from bulk samples with an elemental analyzer (EA 3000-CHNS Eurovector) as previously described in Dräger et al. 2017.

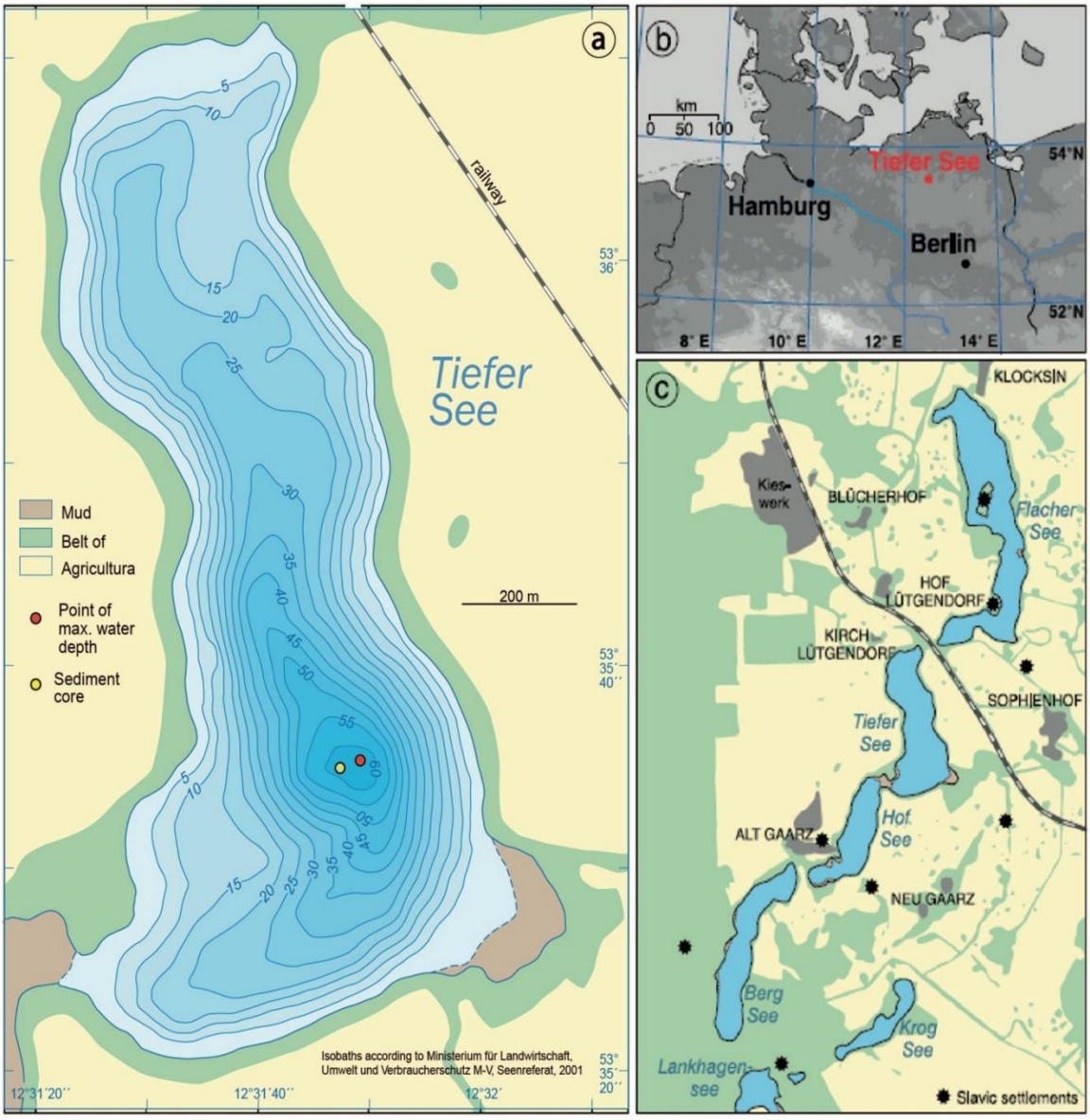

Figure 2.1: Location of study site. (a) Bathymetric map (b) location of Tiefer See in the Klocksin Lake Chain and (c) land cover in the catchment area. Black stars show former Slavic settlements. Modified after Dräger et al. 2017.

2.3.2 Nucleic acids extraction

The top contaminated layers were scraped off with a sterile razor before the uncontaminated anoxic part was put into sterile 15-ml falcon tubes and stored at -80 °C until analysis. Care was taken to prevent cross-contamination of the sediments by processing recent and older samples at different times.

The sediment samples were homogenized following the mortar method described by Herrera and Cockell 2007. All DNA extraction equipment was placed under a UV lamp in a laminar flow hood for a minimum of 25 minutes before use. DNA was then extracted from approximately 300 mg of sediment sample in duplicates, using the PowerSoil DNA Isolation Kit (Qiagen). Briefly, following initial chemical and mechanical lysis steps where DNA is separated from debris via centrifugation, proteins are precipitated and then the DNA is purified with silica spin filters. DNA extractions were done in batches of seven samples with the addition of one negative control each time while avoiding contamination from foreign DNA by following processes described in Monchamp et al. in 2016. Extracted sedaDNA was stored at -20 °C until further downstream analyses.

2.3.3 DNA preparation and amplification

Library preparation for Illumina high-throughput sequencing (HTS) was performed via polymerase chain reaction (PCR) using previously published cyanobacterium-specific primers CYA106F (5’ CGGACGGGTGAGTAACGCGTG 3’) (Nübel et al. 1997), and CYA784R (5’ ACTACWGGGGTATCTAATCCC 3’) (Monchamp et al. 2016). These amplify a 678-nt-long fragment of the V1 - V4 regions of the 16S rRNA gene. Added to the primers were overhanging barcodes for sample differentiation. Being the first study of its kind in this lake, the primer set needed to cover most taxa all over the cyanobacteria phylum. This phylum coverage was tested *in silico* against the ARB-SILVA database v128 (Klindworth et al., 2013).

SedaDNA samples including positive control (*Microcystis aeruginosa* PCC7806) and negative isolation control were amplified in a PCR of 50 µl, containing 10x Pol Buffer C (Roboklon GmbH, Berlin, Germany), 25 mM MgCl, 0.2 mM deoxynucleoside triphosphate (dNTP) mix (ThermoFisher Scientific, Massachusetts, USA), 0.5 mM each primer (TIB Molbiol, Berlin, Germany) and 1.25 U of Optitaq Polymerase (Roboklon). The volume of the template DNA used in each reaction varied between 1 and 4 µl depending on the

sedaDNA concentration. The thermal cycler PCR program included a first denaturation step at 95 °C for 10 min, followed by 35 cycles at 95 °C for 15 s, annealing at 60 °C for 30 s, extension at 72 °C for 45 s and a final extension step at 72 °C for 5 min. PCR products were purified with Agencourt AMPure XP kit (Beckman Coulter, Nyon, Switzerland) and eluted in 30 µl DNA/RNA-free water. The purified product was quantified with a Qubit (2.0) fluorometer. The unique barcoded samples together with the positive and negative controls were pooled in equimolar concentration into one library. The final library was sent to Eurofins Scientific (Constance, Germany) for sequencing using the Illumina MiSeq v3 kit (2x300bp).

2.3.4 Bioinformatics and statistical analyses

Due to the long amplicon lengths, the forward (R1) and reverse read (R2) were not merged during processing but treated separately as R1 and R2. From 35 samples a total of 5,463,680 reads (R1) and 687,801 reads (R2) were obtained. The raw reads were quality checked with FastQC (Andrews et al., 2015). Raw data were demultiplexed using Cutadapt (Martin, 2014). Primer sequences were allowed to have 10% mismatches. Phred-Scores of the barcodes were required to be higher than Q35 and no mismatches were allowed during sorting. Sequences were further processed using Trimmomatic to trim and filter out low-quality sequences (Bolger et al. 2014). USearch (Edgar, 2010) (v6.) was used to identify and remove chimeric sequences. After quality-filtering, chimera removal, and primer trimming 4,505,289 (R1) and 570,095 (R2) reads remained. The negative control had one read in R1 and zero reads in R2 and was therefore removed. The script pick_open_reference.py from the Quantitative Insights into Microbial Ecology (QIIME) pipeline was used for Operational Taxonomic Unit clustering (OTU) with a minimum nucleotide sequence similarity of 97% (Caporaso et al., 2010a) and SILVA database (v128) for taxonomic assignment (Quast et al., 2013).

Before statistical analyses, singletons, OTUs assigned to other bacteria, archaea, chloroplasts, and mitochondria were removed after which 1,134,146 (R1) and 205,775 (R2) cyanobacteria reads remained. The positive control had 250 (R1) and 58 (R2) reads with the OTUs assigned only to *Microcystis spp.*, which did not occur in our samples thus ruling out cross-contamination and was consequently removed. OTUs with less than 0.5% of total read counts and the unclassified cyanobacteria OTUs were filtered out. Cyanobacteria absolute read counts were Hellinger-transformed prior to beta diversity analyses (Legendre

and Gallagher, 2001). We used principal coordinates analysis with Bray-Curtis distance to visualize distances among the investigated sediment segments from R1 and R2. The variance explained by the PCoA axes from R1 and R2 were comparable (Suppl. Fig. A.2A, B). Based on this observation and the low number of reads recovered from the R2 data, we therefore carried out further statistical analyses using only the R1 data. For alpha diversity and richness estimation, we compared both rarefied (using the rtk package in R (Saary et al., 2017)) and unrarefied absolute OTU read counts and found them to be identical (Suppl. Table A.1), thus, we present and discuss data only from the unrarefied read counts. Variation in cyanobacterial OTU composition, diversity among the samples, t-tests for each non-photosynthetic cyanobacteria sister clade separated by varved/non-varved periods, and the different time segments (recent-varved, non-varved and subrecent-varved sediments), as well as relationships with environmental parameters, were determined with PAST3.14 (Hammer et al., 2001), and CANOCO5 (Smilauer and Leps, 2014). A non-parametric permutational multivariate analysis of variance (PerMANOVA) based on the Bray-Curtis dissimilarity index was used to test for significant differences in the overall cyanobacterial communities among the three-time segments. Due to a low number of reads, five samples from the deep non-varved segment ca. CE 1715 – 1675 (88 – 99 cm) were removed before ordination analyses. Environmental data from the different sediment segments were standardized by subtracting the mean and dividing by the standard deviation prior to analyzing their variation in a principal component analysis (PCAs) based on Euclidean distance. Environmental data was then fitted to a distance-based Redundancy Analysis (dbRDA; Bray-Curtis distance) model as explanatory variables with cyanobacteria community data as response variables using the "capscale" function in the vegan package in R (Oksanen et al., 2019). The overall significance of the dbRDA model and its axes were tested by a 999 Monte Carlo permutation test using the "anova.cca" function in vegan. The subset of explanatory variables that contributed significantly to the dbRDA model was further tested by forward selection permutation analysis (999 permutations with pseudo-*F* statistical test) using the "ordiR2step" function in vegan. Canonical variation partitioning analysis (VPA) (Legendre et al., 2005; Ramette and Tiedje, 2007) with redundancy analysis (RDA) was implemented on three categories of environmental variables, that is, eutrophication (TN), lake circulation (reconstructed vegetation openness and $\delta^{13}C$) and other factors (dry density and $CaCO_3$) to identify their unique and combined effects on cyanobacteria community structure. The significance of the fractions of variability

explained by the categories was tested and determined via 999 Monte Carlo permutation in CANOCO5. Trend analysis of absolute read count changes of non-photosynthetic cyanobacteria sister clades during the period investigated was done with Microsoft Excel. Sequencing data and metadata are available at the European Nucleotide Archive (ENA) under BioProject accession number PRJEB33742 and sample accession numbers ERS3606196-ERS3606230.

2.3.5 Phylogenetic analyses of the OTUs

To verify the accuracy of the taxonomic assignment based on SILVA, we used the OTU FASTA sequences from Lake Tiefer See to construct a cyanobacteria phylogenetic tree according to Komárek et al. 2014. Sequences were aligned in the arb software (Ludwig et al., 2004) using the integrated sequence alignment tool under the default setting. *Acidithiobacillus thiooxidans* strain ATCC 19377 was added as an outgroup, and 10 cyanobacteria reference sequences from GenBank and ARB-SILVA database (Quast et al., 2013) were also added. The alignment was used to build a bootstrap tree with 100000 trees based on neighbour-joining. The online tool iTOL was used to visualize and annotate the tree (Letunic and Bork, 2016).

2.3.6 Lipid biomarker analysis

6Me-$C_{17:0}$ and 7Me-$C_{17:0}$ monomethyl branched alkanes (6- and 7-methylheptadecane) are produced mainly by heterocystous, ramified and some filamentous cyanobacteria (Liu et al., 2013; Coates et al., 2014; Bauersachs et al., 2017) and might be representative of cyanobacterial biomass as recently shown for the Baltic Sea (Kaiser et al., 2020). Sediment samples (n = 5) from a parallel core correlated to the reference core based on varve counting (not shown) were analyzed following (Kaiser et al., 2016, 2020). Sediments (0.4 g dry weight) were extracted with a mixture of DCM/MeOH (9:1) and accelerated solvent extraction (Dionex ASE 350). Squalane was added as an internal standard. The apolar lipid fractions containing the hydrocarbons were obtained by column chromatography (SiO2) using hexane as eluent. The fractions were analyzed by gas chromatography-mass spectrometry (GC-MS) using an Agilent Technologies 7890B GC system coupled to a 5977B Mass Selective Detector equipped with an HP-5ms capillary column (30 m * 0.25

mm * 0.25µm). The oven temperature was programmed from 40 to 320 °C at 8 °C/min followed by a 15 min isotherm. GC-MS data were collected in total ion current (TIC) (m/z 50–600). The fractions were also analyzed using a multichannel TraceUltra gas chromatograph (ThermoScientific) equipped with a DB-5ms capillary column (30 m * 0.25 mm * 0.25µm) and a flame ionization detector (FID). The temperature program was identical to that used for analysis by GC-MS and peak identification was made by comparison of retention times using the two methods. For quantification, the GC-FID response of each lipid was normalized to that of the internal standard and the amount of sediment extracted. The detection limit was estimated to ca. 4-5 ng g^{-1}. The data were further normalized to total organic carbon (TOC).

2.4 Results

2.4.1 Cyanobacterial communities reconstructed from Lake Tiefer See sediments

A total of 146 OTUs spanning the entire cyanobacteria phylum was obtained from 35 sedaDNA samples (from ca. CE 1670 – 2006; Fig. 2.2). Almost all the OTUs were assigned to photosynthetic cyanobacteria 89% (130 OTUs) and 5.5% were unclassified (8 OTUs). Of the 130 OTUs assigned to photosynthetic cyanobacteria, 120 could be assigned to the order level, 111 to the family level, and 90 were assigned to the genus level. No OTU was assigned to a species level with high confidence (confidence threshold 0.95).

2.4.2 Richness and diversity

Our study showed that sedaDNA was preserved and concentrations declined from CE 1920 downcore (~40 cm depth) with richness and diversity indices showing a similar trend (Fig. 2.3). High throughput sequencing data revealed cyanobacteria richness to be highest in recent-varved sediments for the period CE 2006 – 1924 (9 – 42 cm depth) and ranged between 69 and 14 (mean richness was 35). Likewise, richness in subrecent-varved sediments for the period ca. CE 1735 – 1720 (83 – 87 cm) was higher and ranged between 21 and 27 (mean richness was 24). In contrast, richness was lower in non-varved sediments for the period ca. CE 1920 – 1740 (43 – 82 cm) compared to both varved sediment segments

and ranged between 10 and 21 (mean 16). Similarly, the Shannon diversity index ranged between 2.5 – 3.3 (mean 2.8) and 2.7 – 2.8 (mean 2.8) in recent- and subrecent-varved sediments, respectively. Lower diversity was recorded in the non-varved sediments and ranged from 2.0 – 2.7 (mean 2.5). Furthermore, a one-way non-parametric permutational multivariate analysis of variance (PerMANOVA) revealed a significant variation in the total cyanobacteria community composition among the three-time segments (p = 0.0001, F = 5.1; Suppl. Table A.2)

2.4.3 Most abundant OTUs

Twenty OTUs predominated the sediments of Lake Tiefer See in the period investigated (1678 – 2006; Fig. 2.4). Out of the total 1,134,146 cyanobacteria read counts, 81.5% (924,329 reads) were assigned to the 20 most abundant OTUs. The remaining 126 OTUs amounted to 18.5% (209,817 reads). The most abundant OTUs were assigned to the picocyanobacteria *Cyanobium* PCC-6307 belonging to the order Synechococcales, and the heterocystous *Aphanizomenon* NIES81 belonging to the order Nostocales.

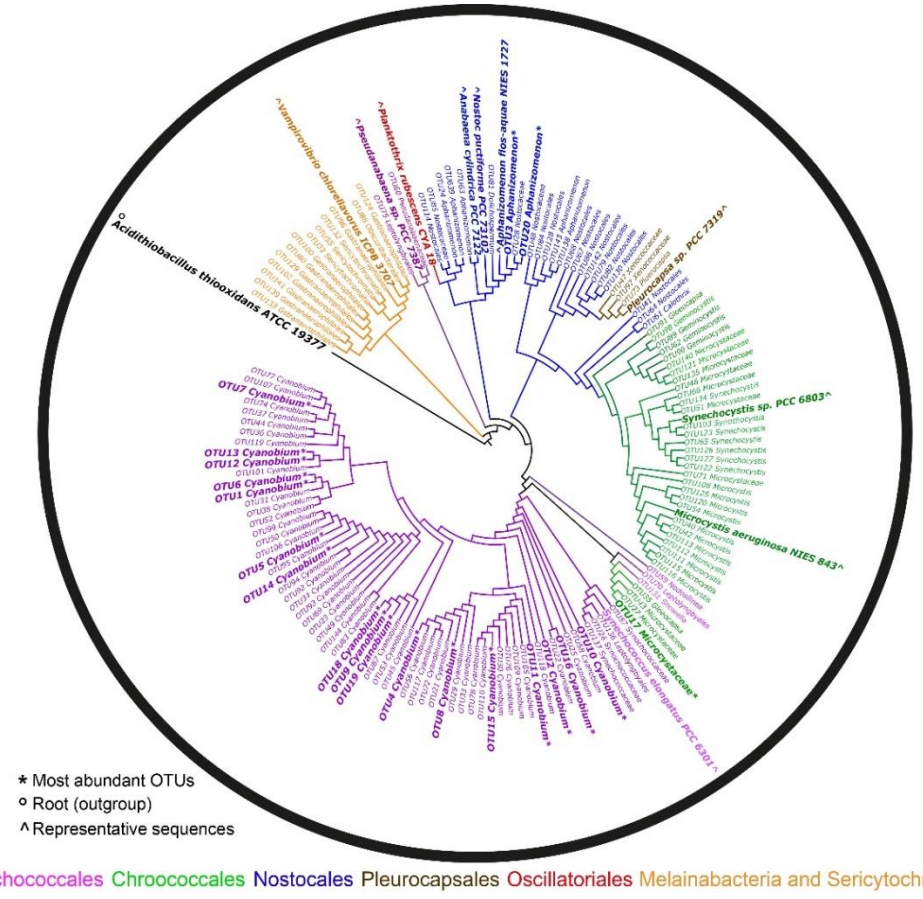

Figure 2.2: Phylogenetic tree constructed from all the 145 OTUs reference sequences from the sediment samples of Lake Tiefer See based on the neighbour-joining method. *Acidothiobacillus*

thiooxidans was used as root with the addition of 10 cyanobacteria reference sequences sourced from the GenBank and ARB-SILVA database. The colors represent the different cyanobacteria orders. The 20 most abundant OTUs are marked with a star, those marked with the '^' symbol are the representative sequences and the reference sequences are in bold fonts.

2.4.4 Non-photosynthetic cyanobacteria sister clades

From all OTUs, 5.5% were assigned to the non-photosynthetic cyanobacteria (NCY) sister lineages the fermentative Melainabacteria and Sericytochromatia (ML635J-21; 8 OTUs in total; Fig. 2.5A). Their occurrence spanned the period CE 1990 – ca. CE 1720 (n = 12 samples; 14 – 87 cm; Suppl. Table. A.1). Melainabacteria represented by 5 OTUs, had higher richness than the Sericytochromatia with 3 OTUs, however, the latter had more sequencing reads than the former. In the Melainabacteria, most OTUs were assigned to the order Gastranaerophilales (4 OTUs) and 1 OTU to Obscuribacterales (Fig. 2.5A). Furthermore, the Sericytochromatia group recorded more reads in the non-varved sediments than the varved sediments (n = 8 samples; p = 0.01; Fig. 2.5B), whereas the Melainabacteria group had significantly more absolute reads in the varved than the non-varved sediments (n = 6 samples; p = 0.001; Fig. 2.5C). Overall, Shannon diversity for the non-photosynthetic cyanobacteria alone was estimated in the 6 samples with more than 1 OTU (Suppl. Table. A.1) and was found, like the richness, to be higher in varved (0.7 to 1.0) than in non-varved sediments (0.3 to 0.5; Fig. 2.5D).

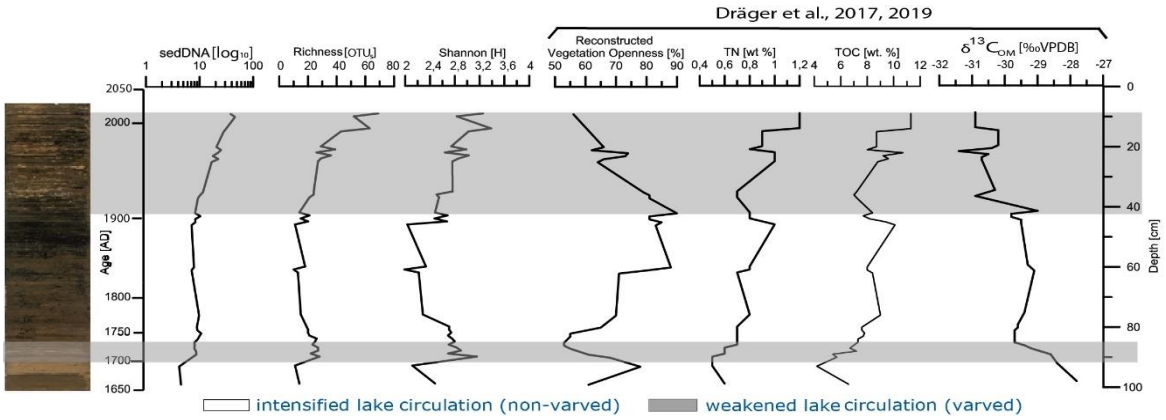

Figure 2.3: Spatio-temporal variation of sediment characteristics, molecular and geochemical analyses. From left to right: $\log_{10}$ transformed sedimentary DNA concentration (sedaDNA), Shannon index (diversity), Richness (no. of OTUs). The TOC content, reconstructed vegetation openness, TN, and $\delta^{13}C$ were published in Dräger et al. 2017, 2019. Dark grey-shaded and non-shaded areas reflect periods of weakened and intensified lake circulation, respectively.

2.4.5 Cyanobacterial community composition in relation to changes in abiotic conditions

Proxies for environmental variables such as reconstructed vegetation openness for lake mixing and circulation, TN for nutrient availability in the lake, and $\delta^{13}C$ for varve preservation in the Lake Tiefer See sediments have been previously published (Dräger et al., 2017, 2019). All environmental data were subject to a principal component analysis (PCAs) to explore variation among the sediment segments; this revealed three distinct, time constrained clusters that contained samples from consecutive depths. The recent-varved sediments CE 2006 – 1924 (9 – 42 cm) were characterized by increased TN, TOC, and $CaCO_3$ whereas the non-varved sediments ca. CE 1920 – 1740 (43 – 82 cm) and the subrecent-varved sediments CE 1735 – 1720 (83 – 87 cm) were defined by elevated values of vegetation openness and $\delta^{13}C$, respectively (Suppl. Fig. A.3). Furthermore, a distance-based redundancy analysis (dbRDA) was used to determine the relationship between cyanobacterial communities from the sediment segments and environmental variables. A forward selection permutation analysis revealed that TN and $CaCO_3$ best explained the cluster of cyanobacterial OTUs from the recent-varved sediments CE 2006 – 1924 (9 – 21 cm), whereas reconstructed vegetation openness and $\delta^{13}C$ best explained the cluster in the non-varved segments ca. CE 1920 – 1740 (43 – 82 cm) and the subrecent-varved segments ca. CE 1735 – 1720 (83 – 87 cm), respectively (all *p*-values < 0.05; Fig. 2.6A; Suppl. Table A.3). As determined by variation partitioning analysis (VPA), eutrophication (represented by TN; 11.9%) and lake circulation (represented by vegetation openness and $\delta^{13}C$; 16.8%) were the groups of factors that significantly explained most of the variability in cyanobacteria composition in Lake Tiefer See, whereas the interaction between them only accounted for 0.6% and a large part of the variation remained unexplained (that is, 71%; Fig. 2.6B; Suppl. Table A.4). Other abiotic factors (that is, dry density and $CaCO_3$) when included in the VPA accounted for an additional 6% and increased the total explained variation to 35.2% (Suppl. Fig. A.4 and Suppl. Table A.5).

2.4.6 Cyanobacterial lipid biomarker reconstructed from sediments

Since the lipid biomarkers 6Me-$C_{17:0}$ and 7Me-$C_{17:0}$ monomethyl branched alkanes representative for cyanobacteria elute very close to each other on a DB-5ms capillary column, their total sum (6+7Me-$C_{17:0}$) was considered hereafter. The TOC normalized

content of 6+7Me-$C_{17:0}$ ranged between ~5 and 13 µg g^{-1}TOC. A maximum content occurred in 1973 (13.3 µg g^{-1} TOC) that correlated with the highest relative abundance of OTUs assigned to *Aphanizomenon* NIES81 (Fig. 2.7).

2.5 Discussion

With our molecular approach, we successfully extracted and sequenced cyanobacterial sedaDNA and reconstructed the cyanobacterial dynamics in Lake Tiefer See sediments spanning the last 350 years. This was made possible due to lake characteristics such as hypoxic to anoxic conditions at the water-sediment interface, the presence of varves, and the absence of burrowing organisms in the sediments which are all conditions known to favor sedaDNA preservation (Coolen et al., 2006; Corinaldesi et al., 2011). We were able to amplify an over 500-nt-long fragment of the cyanobacterial 16S rRNA gene, with a representative coverage of its entire phylum from all samples without enhancements similar to other temperate lakes (Monchamp et al. 2016, 2018; Domaizon et al. 2013). An improved and extended cyanobacteria database (Ramos et al., 2017) was crucial for the phylogenetic analysis of the resulting OTU reference sequences (Fig. 2.2).

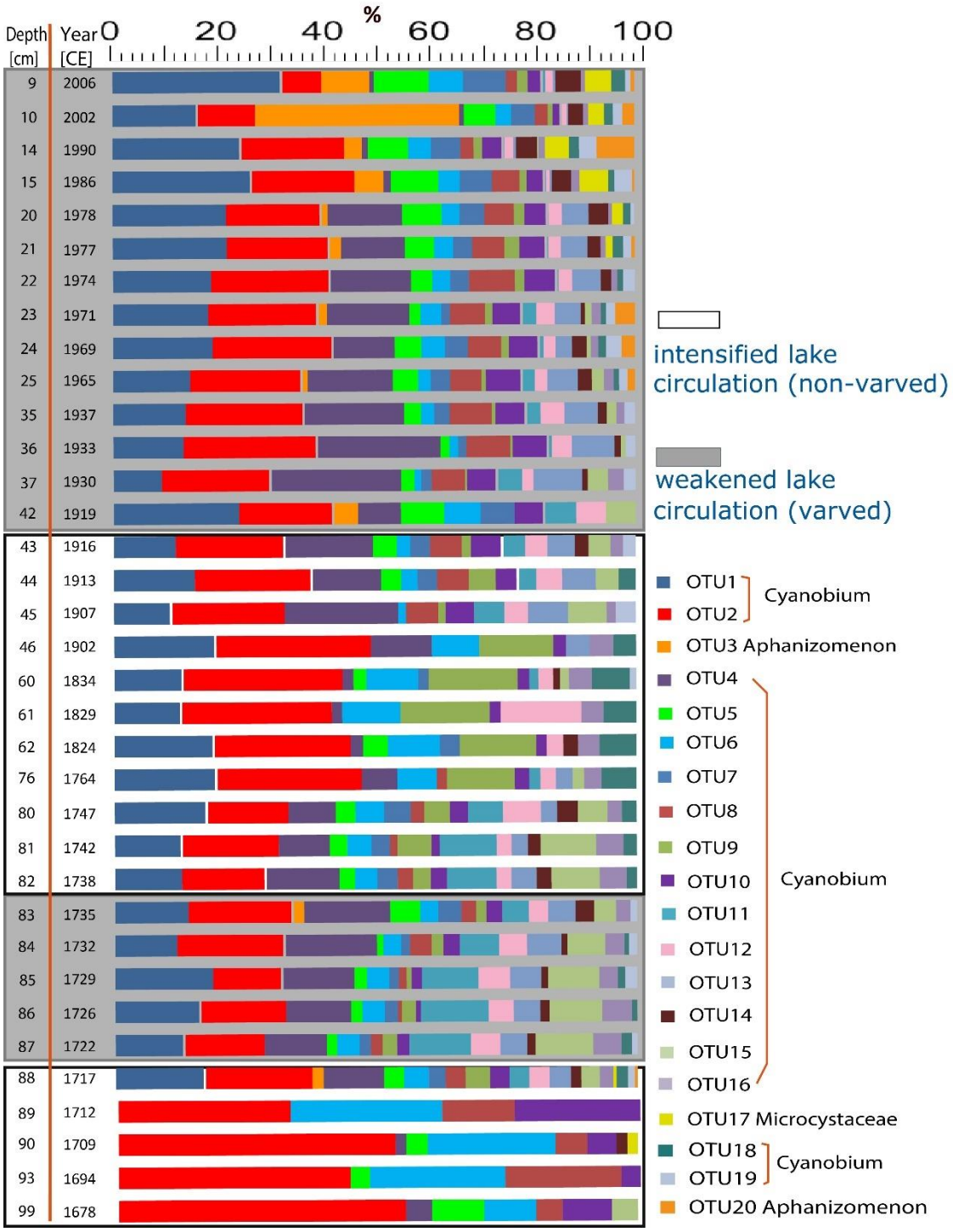

Figure 2.4: Spatio-temporal variation of the relative abundance of the 20 most abundant OTUs. The SILVA database (version128) was utilized for open-reference OTU clustering (97% sequence similarity) and taxonomic assignments. Dark grey-shaded and non-shaded areas reflect periods of weakened and intensified lake circulation, respectively.

Anthropogenic influence in Lake Tiefer See was so far shown via pollen-based vegetation openness reconstruction (Theuerkauf et al., 2015; Dräger et al., 2017). Anthropogenic deforestation within the catchment during settlement periods probably shaped

cyanobacteria dynamics in Lake Tiefer See through the vegetation influence on lake circulation (Dräger et al., 2017). During times of predominant open vegetation, the lake was exposed to stronger wind stress leading to intensified lake circulation and more oxic conditions at the lake bottom which together resulted in the absence of varves (Dräger et al., 2017). Our data revealed a lower diversity in cyanobacteria community composition and a high abundance of OTUs assigned to *Cyanobium spp.* in non-varved sediments (Fig. 2.4). The high abundance of *Cyanobium* concurs with known trends in the water column of temperate lakes where *Cyanobium* together with other picoplankton cyanobacteria (< 0.2 µM in size) make up the most abundant cyanobacteria (Callieri and Stockner, 2000). However, the lower cyanobacteria diversity in non-varved sediments observed herein may be explained by two processes. The increased lake circulation will lead to the disruption of bloom formation by filamentous cyanobacteria species in the water column due to a high water turnover (Visser et al., 2016a). When intensified circulation is coupled with nutrient availability, picocyanobacterial groups are favored over large and buoyant taxa. While on the one hand, an increased water turnover may favor sediment deposition of filamentous cyanobacteria, the DNA preservation of these species at the oxygenated water-sediment interface in this freshwater system will be poor (Domaizon et al., 2017). Therefore, reconstructing filamentous cyanobacteria species DNA in high numbers from non-varved sediments which was shown here for *Cyanobium spp.* becomes less likely. On the other hand, a weaker lake circulation and the resulting anoxic lake bottom favors varve preservation (Kienel et al., 2013, 2017). Constantly lower temperatures at the anoxic lake bottom additionally promote DNA preservation (Coolen et al., 2006). Hence, our results support the hypothesis that the cluster of cyanobacterial OTUs from ca. CE 1720 – 1735 can be explained by the same conditions that result in varve preservation. An anoxic lake bottom favors DNA preservation and decreased water circulation influences the cyanobacterial community composition (Figs. 2.3, 6A).

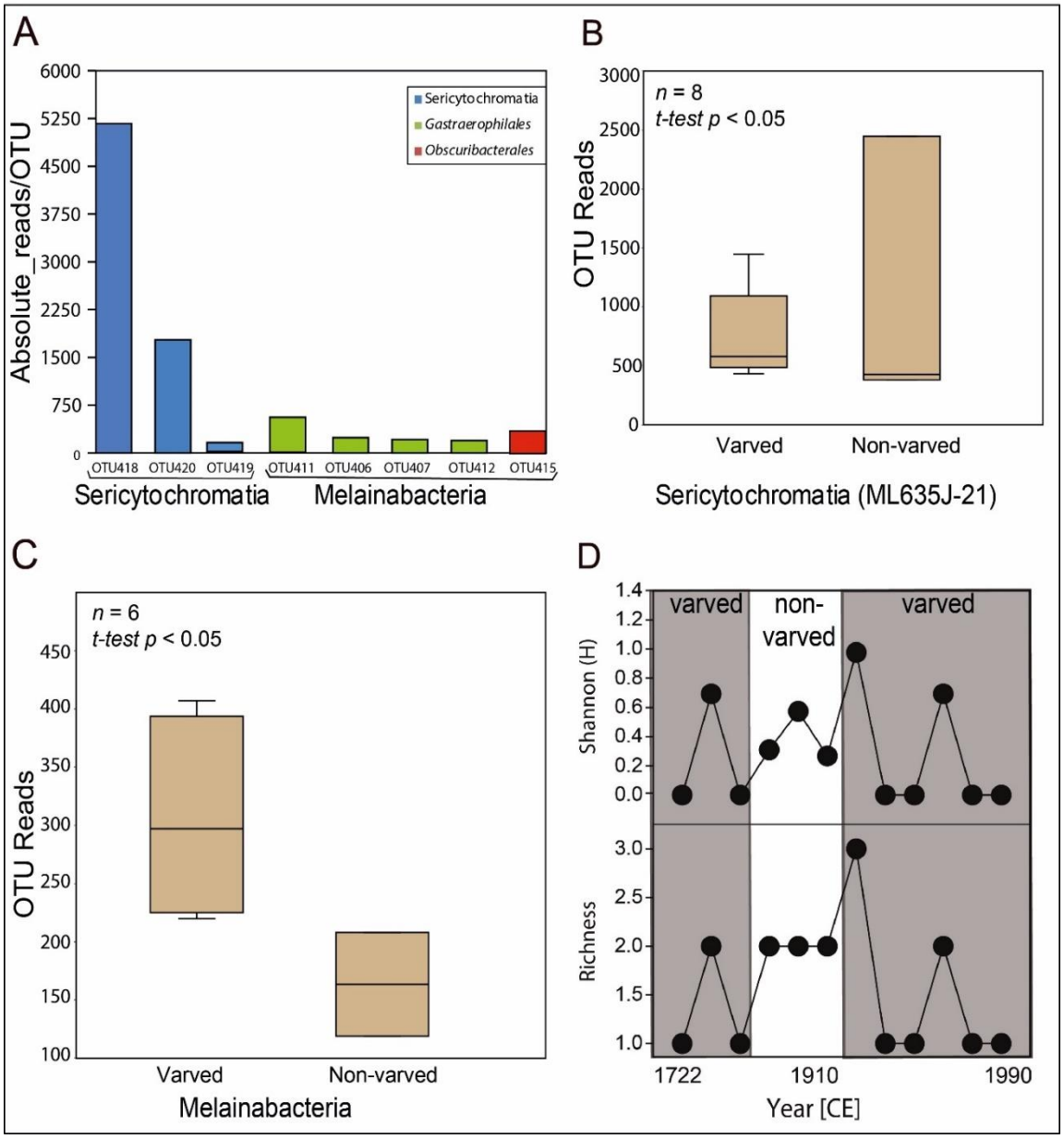

Figure 2.5: Dynamics of non-photosynthetic cyanobacteria (NCY) sister clades observed in Lake Tiefer See. Absolute reads per (A) OTU of the deep branching Sericytochromatia (ML635J-21) (blue) and Melainabacteria orders Gastraerophilaes (green) and the Obscuribacterales (red). Box plots showing OTU reads of (B) Sericytochromatia (ML635J-21) and (C) Melainabacteria across varved and non-varved sediment segments. (D) Alpha diversity indices (richness and Shannon diversity) of all non-photosynthetic clades over the period investigated. Shaded area in D represents varved period, unshaded area is non-varved period.

The relationship between anoxic/oxic conditions is further evident through the different distribution of Sericytochromatia (ML536J-21) and the fermentative Melainabacteria in sediments. The OTUs assigned to Sericytochromatia preferably occur in non-varved sediments while those assigned to the Melainabacteria rather occur in varved sediments (*p*

< 0.05; Figs. 2.5B, C). It has been suggested that members of Sericytochromatia can inhabit both photic and aphotic environments, and since they possess an array of respiratory proteins, they also have members predicted to be capable of aerobic respiration. These members can carry out aerobic respiration under high and low oxygen conditions due to the presence of A- and C- family oxygen reductases in their respiratory mechanisms (Soo et al., 2017). The Melainabacteria have been predicted to adapt to low oxygen and anoxic zones because they possess C-family oxygen reductase and cytochrome bd oxidases (i.e. terminal oxidases that reduces dioxygen to water to avoid the production of reactive oxygen species) in their genomes (Di Rienzi et al., 2013b; Soo et al., 2014, 2017). Since lack of knowledge of their metabolism so far hindered the laboratory growth of the non-photosynthetic sister clades of cyanobacteria and thus also research on their physiology (Wrighton et al., 2014), the current knowledge of their metabolism is so far gained largely from culture-independent metagenome reconstructions from environmental samples (Di Rienzi et al., 2013b; Soo et al., 2014, 2017). Nevertheless, our observations showing a distinct separation of the NCY from the photosynthetic cyanobacteria clades as well as no increasing trend in their richness over the last three centuries covered in this study concur with similar findings from other temperate lake ecosystems (Monchamp et al. 2019). However, the relationship between oxic/anoxic conditions and the dynamics of the NCY clades which we show here for the first time, emphasizes the need for investigations over longer time scales that encompass more intervals of variations in oxic/anoxic conditions at the lake bottom. Furthermore, since Melainabacteria and Sericytochromatia have been predicted to potentially inhabit a variety of environments like photic and aphotic habitats (Soo et al., 2014, 2017), an in-depth spatio-temporal survey of the water column of Lake Tiefer See would be crucial for evidencing their occurrence in this ecosystem, thus, providing more clarity about their existence.

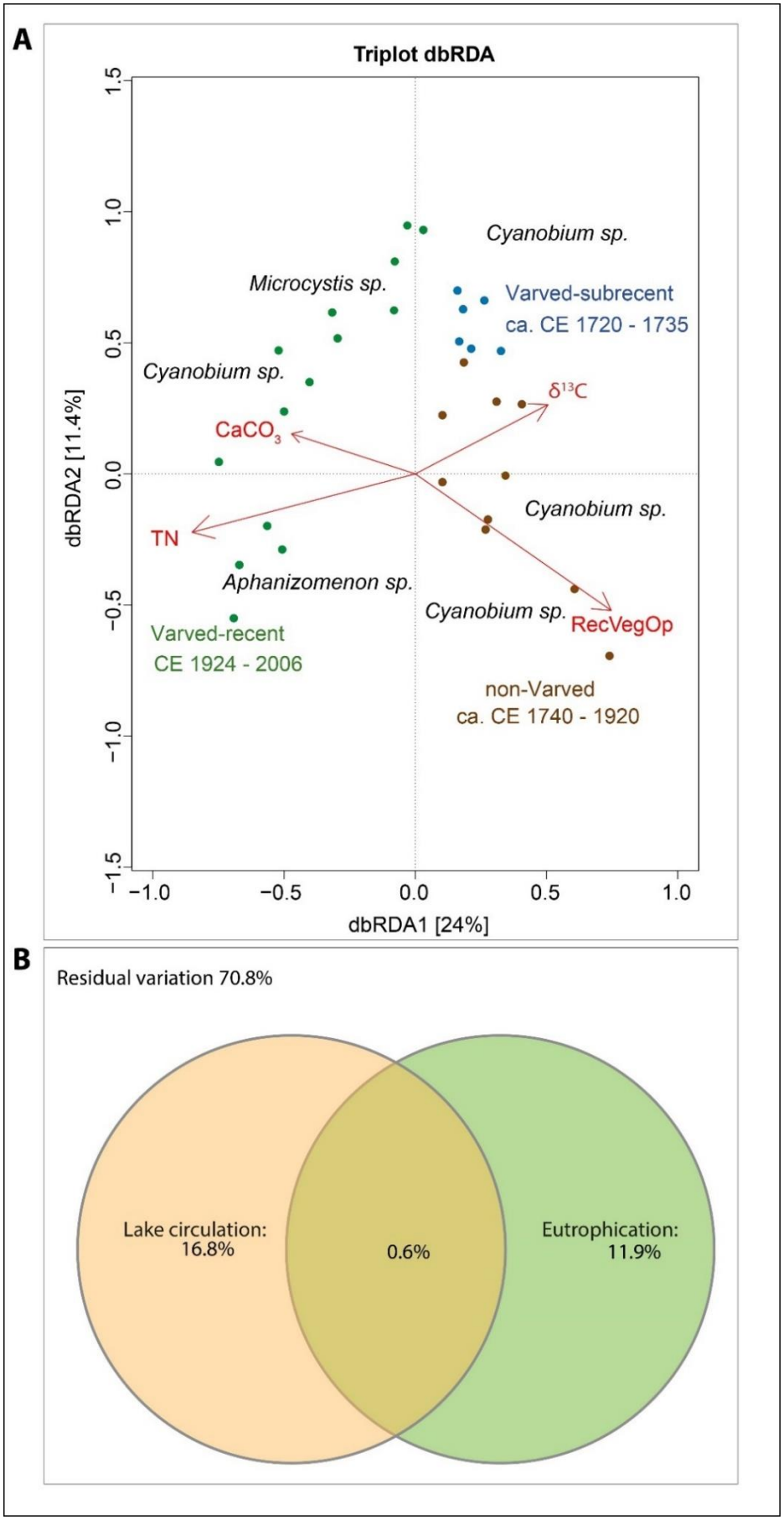
A
Triplot dbRDA
dbRDA2 [11.4%]
dbRDA1 [24%]
1.5
1.0
0.5
0.0
−0.5
−1.0
−1.5
−1.0
−0.5
0.0
0.5
1.0
Cyanobium sp.
Microcystis sp.
Varved-subrecent
ca. CE 1720 - 1735
Cyanobium sp.
δ13C
CaCO3
Cyanobium sp.
TN
Aphanizomenon sp.
Cyanobium sp.
RecVegOp
Varved-recent
CE 1924 - 2006
non-Varved
ca. CE 1740 - 1920
B
Residual variation 70.8%
Lake circulation:
16.8%
0.6%
Eutrophication:
11.9%

Figure 2.6: Multivariate statistics (A) Distance-based Redundancy Analysis (dbRDA) based on Bray-Curtis dissimilarity on the effect of environmental variables on cyanobacteria community composition. The dbRDA axes 1 and 2 together explain 35.4% of the variation, while total variation explained by the dbRDA model was 48.4%. The samples from the different sediment segments are color-coded as follows; green = recent-varved, blue = subrecent-varved and red = non-varved. RecVegOp = reconstructed vegetation openness. The environmental variables explaining the variation in cyanobacteria community were all significant (adjusted R^2 = 0.38) and are projected as red vectors. The response variables are shown at the genus level. (B) Venn diagram displaying the results of variation partitioning analysis (VPA). The two explanatory matrices used contained variables about lake circulation and eutrophication. Each circle represents the portion of variation accounted for by each explanatory matrix or a combination of the explanatory matrices. The bounding rectangle represents the total variation in the response data showing the portion of residual variation not explained by the explanatory matrices.

It has been further shown that agricultural practices in the catchment influenced Lake Tiefer See (Kienel et al., 2013, 2017). Farming in the catchment became intensified with extensive fertilizer application and enhanced transportation of agricultural products after a railway track construction between ca. CE 1884 and 1886. It peaked in the 1970s when pig farming reached 15000 animals with the resulting manure ending up in the lake (Kienel et al., 2017). Typically, runoffs from agricultural wastes ending up in lakes carry nutrients like nitrogen and phosphorus beneficial to cyanobacteria, in worst cases tipping the scale in favor of eutrophication-associated and potential toxin producing taxa like *Aphanizomenon* and *Microcystis* (Preußel et al., 2006; Sukenik et al., 2012). Our reconstruction data show that OTUs assigned to *Microcystis* and *Aphanizomenon*, after only a brief occurrence in the early 18th century, reappear about CE 1920 (*Aphanizomenon*) and CE 1977 (*Microcystis*) and remained part of the lake ecosystem since then (Fig. 2.4). The permanent occurrence of these potential toxins producing taxa is likely a delayed consequence of the intensification of farming within Lake Tiefer See catchment since ca. CE 1880 with the introduction of mechanized farming, mineral fertilizers (organic human and animal manure) and livestock farming (Kienel et al., 2013). This premise is further supported statistically by dbRDA and VPA (Figs. 2.6A, B; Suppl. Table A.4), which show that TN was the best predictor for the cluster of OTUs assigned to *Microcystis* and *Aphanizomenon* and alone explains 11.9% (VPA) of the variability in cyanobacterial community composition. We therefore suggest that anthropogenic farming practices at least partly caused the observed cyanobacteria dynamics reconstructed from recent-varved sediments in Lake Tiefer See. Increased TN values in the sediments (Fig. 2.3) were also related to an increase in livestock farming and field drainage in the catchment (Kienel et

al., 2013, 2017). Our data revealed significant differences in cyanobacteria community composition between the subrecent (ca. CE 1720 – 1735) and recent (CE 1924 – 2005) varved sediments ($p < 0.05$; Suppl. Table A.2). We therefore further posit that while anoxic conditions are partly the reason for higher diversity in subrecent and recent varved sediments, additional intensive farming led to a significantly stronger change in the temporal variation of cyanobacteria communities in recent varved sediments. From CE 1990, following privatization, livestock farming within the catchment of Lake Tiefer See strongly reduced in line with restoration efforts according to EU agricultural policies resulting in decreased nutrient input into the lake (Theuerkauf et al., 2015; Kienel et al., 2017). Studies have shown that eutrophied lake ecosystems tend to recover when subjected to restoration processes (Jeppesen et al., 2005). However, re-establishing the microbial assemblages that existed pre-fertilization is rarely attained (Bennion et al., 2011). This is what we observe here, namely, the persistence of eutrophication associated cyanobacterial OTUs in Lake Tiefer See almost three decades after human farming practices reduced. Our results therefore suggest that cyanobacterial sedaDNA serves as a potential proxy for lake eutrophication in the past.

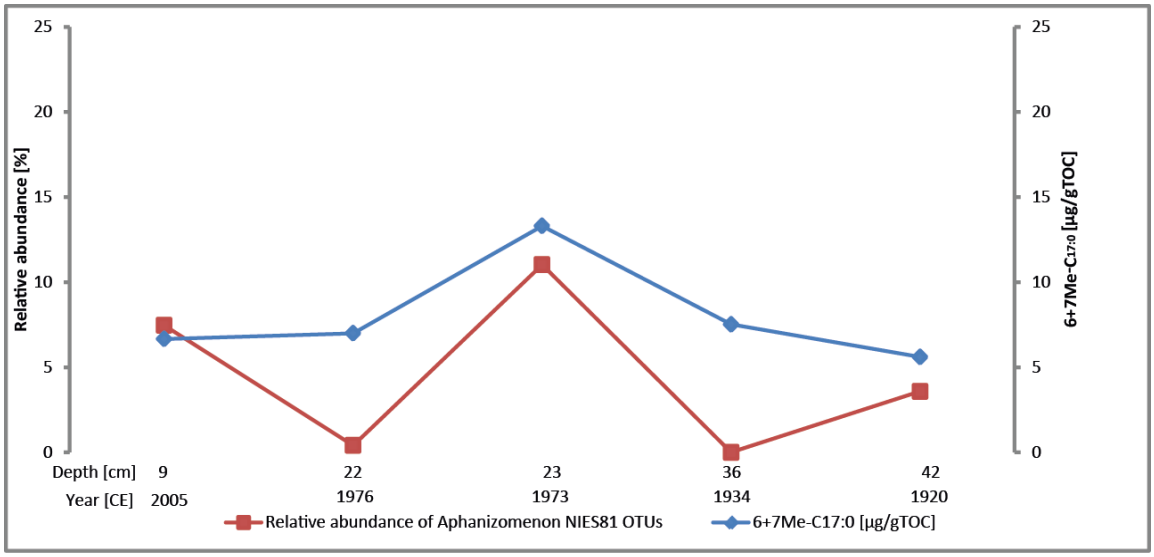

Figure 2.7: Variability of Aphanizomenon NIES81 and cyanobacteria lipid biomarkers. Abundance of OTUs assigned to *Aphanizomenon* NIES81 relative to total cyanobacterial OTUs (in %) based on amplicon sequencing compared to 6+7Me-$C_{17:0}$ methylheptadecane lipid biomarker. Data is shown for selected time points since the onset of increasing eutrophication in Lake Tiefer See (since 1924).

Taken together, oxic/anoxic conditions and human-induced eutrophication are important factors driving cyanobacteria dynamics (abundance and community structure) in Lake Tiefer See although most of the variation in cyanobacteria community structure from our

study remains unexplained (Fig. 2.6B). While eutrophication influences the abundance and diversity of the water column cyanobacteria communities, anoxic conditions in the sediment determine how much of the previous communities gets preserved (Domaizon et al., 2017). This means that the sedaDNA archive deposited under oxic conditions most likely does not reflect the entire spectrum of previous water column cyanobacteria communities. Therefore, cyanobacterial sedaDNA is influenced by both the abundance as well as diversity at a given time in the past and by the preservation conditions in the sediment. Furthermore, our study shows that it is difficult to disentangle between both factors in recent varves because eutrophication in part contributes to anoxia in freshwater systems (Schertzer and Sawchuk, 1990). The occurrence of higher cyanobacteria diversity in varved sediments at times without intensive agriculture points to the preservation of cyanobacteria sedaDNA as a crucial factor in sediments.

Our sedaDNA data is further supported by lipid biomarkers. In detail, 6- and 7-methylheptadecane are considered as cyanobacterial specific biomarkers predominantly observed in clades including heterocystous, ramified, and some filamentous cyanobacteria, and rarely in unicellular cyanobacteria (Liu et al., 2013; Coates et al., 2014). Since *Microcystaceae* hydrocarbon branched alkanes profile are absent (Liu et al., 2013), it is very likely not the source organism of 6+7Me-$C_{17:0.}$ The hydrocarbon profile of *Cyanobium* sp. has not been published to the best of our knowledge, but this unicellular picoplankton cyanobacterium most likely does not produce branched alkanes. Recently, Bauersachs et al. (2017) published the hydrocarbon composition of one strain of the genus *Aphanizomenon* isolated from Baltic Seawater. This strain indeed contained 7Me-$C_{17:0}$, but in small relative amount (ca. 3%). However, it is possible that other lacustrine strains produce relatively more 7Me-$C_{17:0}$, and maybe 6Me-$C_{17:0}$ as well. As records of the TOC normalized content of 6+7Me-$C_{17:0}$ and the relative abundance of OTUs assigned to *Aphanizomenon* present a similar variability over time (Fig. 2.7), we suggest that they may quantitatively reflect the presence of filamentous cyanobacteria such as *Aphanizomenon sp*. in Lake Tiefer See.

2.6 Conclusions

Our study provides the first insights into the community structures of cyanobacteria and their non-photosynthetic sister lineages in Lake Tiefer See as archived in sediments that span the last 350 years. We show that lake circulation, anoxic conditions as indicated by

varve presence and human-induced eutrophication are the main factors explaining variations in the cyanobacterial community in Lake Tiefer See. A relationship between environmental change and cyanobacterial dynamics (e.g.,Sericytochromatia and Melainabacteria) is suggested, thus adding to the cohort of studies making a strong argument for the use of cyanobacterial sedaDNA as a paleo proxy. More importantly, the results from this study add to the growing list of lacustrine ecosystem investigations shedding light on anthropogenic impact on cyanobacterial diversity changes across time and space. We show that eutrophication-associated OTUs were introduced into the lake system mostly as a result of anthropogenic agricultural practices and have since persisted despite restoration efforts. Future investigations will need to focus on exploring the parallels in the dynamics between current water column cyanobacterial communities and those of the sedimentary archive. In addition, reconstructing longer time scales that additionally investigate periods without human influences needs to be done to decipher the role of natural climate variability from anthropogenic effects on cyanobacterial communities.

2.7 Acknowledgements

We thank the German Environmental Foundation (Deutsche Bundesstiftung Umwelt DBU) for funding the research position of EN. This study is a contribution to the Virtual Institute of Integrated Climate and Landscape Evolution Analyses -ICLEA-, grant number VH-VI-415. The monitoring equipment was funded by the Terrestrial Environmental Observatory Infrastructure Initiative of the Helmholtz Association (TERENO Observatory NE Germany). This study was also supported by the Helmholtz Gemeinschaft (HGF) by funding the Helmholtz Young Investigators Group of S.L. (VH-NG-919). JK and AB were supported by the Leibniz Association grant SAW-2017-IOW-2. We thank the coring team of GFZ-section Climate Dynamics and Landscape Evolution who assisted in the fieldwork (B. Brademann, S. Pinkerneil) and B. Plessen for TN analyses. We thank the editors and anonymous reviewers for suggestions that improved the manuscript. We also thank L. Ganzert for help with bioinformatics and result discussions.

3 Manuscript II – Lake cyanobacteria dynamics

"Species-level spatio-temporal dynamics of Cyanobacteria in a hard-water temperate lake in the southern Baltics"

3.1 Abstract

Cyanobacteria are important primary producers in temperate freshwater ecosystems. However, studies on the seasonal and spatial distribution of cyanobacteria in deep lakes based on high-throughput DNA sequencing are still rare. In this study, we combined monthly water sampling and monitoring in 2019, amplicon sequence variants analysis (ASVs; a proxy for different species) and quantitative PCR targeting overall cyanobacteria abundance to describe the seasonal and spatial dynamics of cyanobacteria in the deep hard-water oligo-mesotrophic Lake Tiefer See, NE Germany. We observed significant seasonal variation in the cyanobacterial community composition ($p < 0.05$) in the epi- and metalimnion layers, but not in the hypolimnion. In winter - when the water column is mixed - picocyanobacteria (*Synechococcus* and *Cyanobium*) were dominant. With the onset of stratification in late spring, we observed potential niche specialization and coexistence among the cyanobacteria taxa driven mainly by light and nutrient dynamics. Specifically, ASVs assigned to picocyanobacteria and the genus *Planktothrix* were the main contributors to the formation of deep chlorophyll maxima along a light gradient. While *Synechococcus* and different *Cyanobium* ASVs were abundant in the epilimnion up to the base of the euphotic zone from spring to fall, *Planktothrix* mainly occurred in the metalimnetic layer below the euphotic zone where also overall cyanobacteria abundance was highest in summer. Our data revealed two potentially psychrotolerant (cold-adapted) *Cyanobium* species that appear to cope well under conditions of lower hypolimnetic water temperature and light as well as increasing sediment-released phosphate in the deeper waters in summer. The potential cold-adapted *Cyanobium* species were also dominant throughout the water column in fall and winter. Furthermore, *Snowella* and *Microcystis*-related ASVs were abundant in the water column during the onset of fall turnover. Altogether, these findings suggest previously unascertained and considerable spatiotemporal changes in the

community of cyanobacteria on the species level especially within the genus *Cyanobium* in deep hard-water temperate lakes.

3.2 Introduction

Photosynthetic microorganisms function as the basis of food chains in aquatic environments and are thus of importance to the ecosystem and to humans. Cyanobacteria have been studied extensively as an important contributor to global primary production in oceans and lakes (Garcia-Pichel, 2009; Mazard et al., 2016; Soule and Garcia-Pichel, 2019). In temperate climate, most lakes are stratified usually beginning in late spring into the epilimnion (warmer upper water column), the hypolimnion (dark and cold deep water) and the metalimnion, a transition layer between the warmer and colder layers. Because of the fast changes in temperature and increasing density within the metalimnion, this layer acts as a physical barrier between the epi- and hypolimnion (Boehrer and Schultze, 2008). One of the expected effects of increasing global temperatures and climate change on temperate lakes is that prolonged periods of stratification may extend and thus change the community structure of cyanobacteria (diversity and composition) inhabiting these lakes (Salmaso et al., 2015; Visser et al., 2016; Huisman et al., 2018).

Molecular-based techniques have been employed in studying seasonal changes in lacustrine bacterial communities (e.g., Allgaier and Grossart, 2006; Ivanikova et al., 2007) and the interactions between bacteria and phytoplankton in lakes (Nitin Parulekar et al., 2017; Schweitzer-Natan et al., 2019). Studies on lake bacterioplankton seasonality based on 16S rRNA gene sequencing have for instance brought attention to the sources and dangers of eutrophication via nutrient loading (e.g., Kong et al., 2019). Furthermore, advances in sequencing techniques with improved taxonomic resolution have provided additional understanding to the seasonal succession of bacterioplankton communities in the upper waters of lakes (Okazaki and Nakano, 2016; Diao et al., 2017; Salmaso et al., 2018). For example, in Lake Vechten (The Netherlands; max. depth 11 m), high-throughput sequencing of every meter in the water column revealed changes in bacteria community composition to be driven by lake oxygenation and sulphidic conditions (Diao et al., 2017). Other factors driving cyanobacteria seasonality and niche differentiation include light intensity and differences in cyanobacteria accessory pigments which influence their adaptation to spectral light quality (Pick and Agbeti, 1991; Vörös et al., 1998; Callieri et al., 2012b). Research on seasonality and succession of phytoplankton in lakes either via

cell counts approaches (Butts and Carrick, 2017) or the creation of 16S rRNA sequence clone libraries have helped in the identification of important taxonomic groups within the phylum Cyanobacteria (Albrecht et al., 2017). An advantage of using high-throughput sequencing techniques is the possibility of a more holistic estimation, especially of small (0.2 – 2 µm) picocyanobacteria (e.g., *Synechococcus* sp. and *Cyanobium* sp.). Members of this group are often not reliably identified and differentiated by microscopy (Callieri et al., 2012b; Salmaso et al., 2018). Except for Salmaso et al., (2018) that sequenced bacterial 16S rRNA gene to analyze annual bacterioplankton community composition in the euphotic zone (up to 21 m water depth) of Lake Garda (max. water depth 350 m), there are to the best of our knowledge no spatiotemporal comparative studies of cyanobacterial succession across different water layers and seasons in deep temperate lakes and in combination with cyanobacteria-specific marker gene analysis.

In this study, we integrate highly resolved sampling throughout the year 2019 with high-throughput amplicon sequencing and quantitative PCR to unravel seasonal succession dynamics of pelagic cyanobacteria community composition (CCC) and abundance as well as possible niche segregation in Lake Tiefer See near Klocksin (TSK). We aim to understand the spatiotemporal succession dynamics of cyanobacteria and their potential lake environmental drivers in deep, temperate hard-water lakes. Lake Tiefer See is ideal for this study because with 62 m water depth it belongs to the deepest lakes in northeastern Germany. In addition, since the beginning of the last decade, Lake Tiefer See has been the focus of an extensive and high-resolution climate monitoring program as well as several paleolimnological climate reconstruction investigations (e.g., Dräger et al., 2019; Nwosu et al., 2021a; Roeser et al., 2021)

3.3 Materials and Methods

3.3.1 Study site

The hard-water Lake Tiefer See is located in the natural park „Nossentiner/Schwinzer Heide“ in the southern Baltic lowlands (Fig. 3.1). The lake basin was formed during the last glaciation as part of a subglacial channel system in a morainic terrain and the present lake is part of the Klocksin-Lake-Chain (Dräger et al., 2017). The lake has a maximum depth of 62 m and no major inflow and outflow with a surface area of about 0.75 km^2, and

catchment area of about 5.5 km^2 dominated by glacial till. The area around Lake Tiefer See is characterized by a warm-temperate climate at the transition from oceanic to continental conditions. Mean monthly air temperatures range from 0°C in January to 17 – 18°C in July with maxima up to 30°C and minima down to -5°C. Mean monthly precipitation varies between ~ 40 mm during winter and ~ 60 mm in summer with a mean annual precipitation of 560 -570 mm (Roeser et al., 2021). Although the catchment is mainly used for agriculture (Theuerkauf et al., 2015), the direct shore-line of the lake is covered by a fringe of trees and there is no anthropogenic infrastructure such as buildings and roads at the lakeshore. The present-day lake status is oligo-mesotrophic and the circulation mode is either mono- or dimictic, depending on the formation of a winter ice cover (Dräger et al., 2017).

3.3.2 Collection of water samples

Water samples were taken monthly between 30th January and 28th November 2019 close to the spot of the lake's maximum depth (~62 m; Fig. 3.1A), where also the floating weather monitoring station is installed. The sampled water depths were 1, 3, 5, 7, 10, 15, 20, 40, 45, and 50 m. A sample volume of 250 mL lake water was collected for the upper water depths of 1, 3, 5 m and pooled (750 mL), representing the epilimnion. Likewise, volumes of 375 mL were collected for the lower water depths 45 and 50 m and pooled (750 mL), representing the hypolimnion. For each of the other depths 7, 10, 15, 20 and 40 m, respectively, 750 mL water samples were collected. The samples were collected in sterile glass bottles (Schott Duran®, Germany) were first flushed with lake water from the respective depths before samples were collected and transported in cold dark boxes to the laboratory where they are stored in refrigerators. They are then, along with blank water (autoclaved deionized water), filtered within 24 hours after fieldwork using 0.2 µm cellulose filters (Sartorius AG, Germany) and stored at -20°C until nucleic acid extraction (Kurmayer et al., 2017).

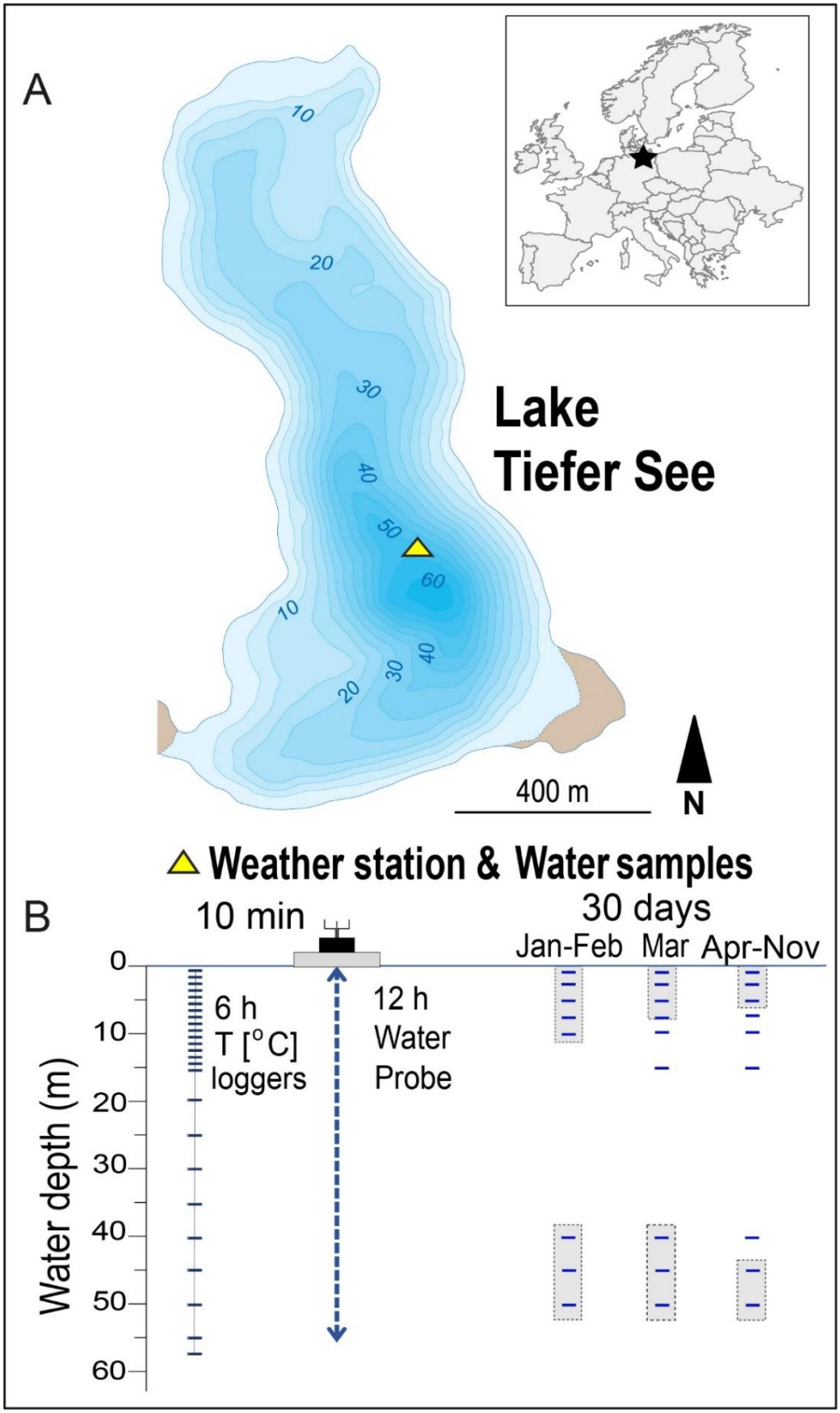

Figure 3.1: Location of the study site and sampling setup. **(**A**)** Location of Lake Tiefer See near Klocksin (TSK, NE Germany). **(**B**)** Scheme of lake monitoring setup showing depths of water column temperature loggers and the depths from which water samples were taken. Shaded sampling points indicate samples that were pooled for genomic DNA extraction.

3.3.3 Lake physicochemical parameters

Measurements of the physicochemical parameters pH, dissolved oxygen (DO), turbidity, conductivity and chlorophyll-a (Chl*a*) in the water column were conducted automatically using a multi-parameter water quality probe (YSI 6600 V2, Yellow Springs USA) in 0.5 to 1-meter steps and 12-hour resolution. The Chl*a* is used here as an indicator of phytoplankton biomass production. Owing to technical problems, data in February were only collected on two days (1st and 28th), and in March no data were recorded between the 2nd and the 10th. Water temperature was measured using 26 depth-stationary data loggers (HOBO Water Temp Pro v2, Onset USA) in one-meter steps from 0 – 15 m and five-meter steps from 15 – 55 m water depth (Fig. 3.1B).

Water samples for molecular analyses, nitrate (NO_3^-) and total dissolved phosphorus (TDP) analyses were collected monthly. Nitrate measurements were done at the German Research Centre for Geosciences (GFZ) while TDP was determined at the Leibniz Institute for Baltic Sea Research Warnemünde (IOW). Nitrate was measured by suppressed ion chromatography using a SeQuant SAMS anion IC suppressor (EMD Millipore, Billerica, Massachusetts), a S5200 sample injector, a 3.0 × 250 mm LCA 14 column and a S3115 conductivity detector (all Sykam, Fürstenfeldbruck, Germany). The eluent was 5 mM Na_2CO_3 with 20 mg L^{-1} 4–hydroxybenzonitrile and 0.2% methanol. The flow rate was set to 1 mL min^{-1} and the column oven temperature to 50°C. Detection and quantification limits were calculated based on signal-to-noise (S/N) ratios of 3 and 10, respectively. All samples were measured in triplicates and every ten injections a standard was measured to check for drift. Reproducibility was always better than 5% and the detection limit ranged between 1 – 4 µM.

For TDP, the water samples were immediately filtered using 0.45 µm syringe filters and acidified with sub-boiled HNO_3 to 2%Vol. The TDP was measured by inductively coupled plasma optical emission spectrometry (ICP-OES; iCAP 7400, Duo, Thermo Fisher Scientific) using external calibration and Sc as internal standard. Precision and trueness were checked with the international reference material SLRS-6 (NRCC) spiked with 20 µg L^{-1} P and were 9.6% and 5.7%, respectively.

3.3.4 Extraction of DNA

Nucleic acid extractions were carried out in a clean laboratory where no polymerase chain reaction (PCR) had been performed prior to the extraction, following established methods and precautions to limit contamination (Nwosu et al., 2021b). Because of the mixed water column in January and February, water samples for molecular analyses from the water depths 1, 3, 5, 7, 10 m were pooled, and reported as the mean depth (5 m; Fig. 3.1B). The water depths 40, 45, 50 m were equally pooled, and reported as the mean depth (45 m). In March, when temperatures began to increase, four depths in the water column were reported as follows: 5 (1, 3, 5 and 7 m pooled), 10, 20 and 45 m (40, 45 and 50 m pooled). Genomic DNA (gDNA) of water samples, blank water filtrations and blank DNA extraction using autoclaved deionized water were extracted from filters using the DNeasy PowerWater Kit (QIAGEN, USA) following the manufacturer's specifications. The extracted gDNA was eluted in 100 µl elution buffer, quantified with the Qubit dsDNA HS Assay Kit (Invitrogn, United States) and stored at -20°C pending downstream analysis.

3.3.5 Quantification of cyanobacteria abundance

Total cyanobacteria were quantified with a SYBRGreen quantitative PCR (qPCR) assay amplifying specifically the cyanobacteria 16S rRNA-ITS (internal transcribed spacer) region ca. 350 bp using the primers CSIF (5'-GYCACGCCCGAAGTCRTTAC-3') and 373R (5'-CTAACCACCTGAGCTAAT-3') (Janse et al., 2003). The final volume of the qPCR reactions was 20 µL containing 10 µL of KAPA SYBR® FAST qPCR Master Mix (Sigma-Aldrich, Germany), 0.2 µL of each forward and reverse primer (100 µM, Biomers), 5.8 µL PCR water and 4 µL of template DNA. The qPCR program consisted of an initial polymerase activation step (95°C for 15 min), followed by 40 cycles of denaturation at 94°C for 60 s, annealing at 60°C for 60 s and extension at 72°C for 60 s. The qPCR program was followed by a melting curve step from 70°C to 95°C at a transition rate of 1°C per 5 s to determine the specificity of the amplification. The amplified products were confirmed with agarose gel electrophoresis. Tenfold dilution standards were prepared from gDNA of *Synechocystis* for each qPCR assay, ranging from 4.7×10^7 to 4.7×10^3 copies ng^{-1} DNA to create the standard curves from which the quantification cycle (*Cq*) values were determined (Bustin et al., 2009). All qPCR assays were performed in triplicates on a CFX96 real-time thermal cycler (Bio-Rad Laboratories Inc., USA). The copy numbers of the 16S

rRNA-ITS region were calculated after Savichtcheva et al., (2011). The obtained values were the mean triplicates of each sample expressed as cyanobacterial abundance normalized to extracted DNA (copies ng^{-1} DNA) with a minimum and maximum quantification efficiency of 91% and 94%, respectively.

3.3.6 Sequence libraries preparation

Cyanobacteria-specific primers CYA359F (5'-CGGACGGGTGAGTAACGCGTG-3') and CYA784R (5'-ACTACWGGGGTATCTAATCCC-3') (Nübel et al., 1997) that amplify a >400-nt-long fragment of the V3 - V4 regions of the 16S rRNA gene were used for preparing two Illumina high-throughput sequencing (HTS) libraries. The primers had unique tags that served to differentiate the samples (Suppl. Table B.1). The samples and negative controls (that is, a reaction with PCR water as template) were amplified in a 50 µL volume PCR reaction, comprising 10x Pol Buffer C (Roboklon GmbH, Berlin, Germany), 25 mM $MgCl_2$, 0.2 mM deoxynucleoside triphosphate (dNTP) mix (ThermoFisher Scientific), 0.5 mM of each primer (TIB Molbiol, Berlin, Germany) and 1.25 U of Optitaq Polymerase (Roboklon). The volume of the template DNA used in each reaction varied between 1 and 4 µL depending on the genomic DNA concentration. The PCR program included a first denaturation step at 95°C for 10 min, followed by 35 cycles at 95°C for 15 s, annealing at 60°C for 30 s, extension at 72°C for 45 s and a final extension step at 72°C for 5 min. To avoid cross-contamination, the PCR reactions were done monthly, after each sampling. Furthermore, to control for reproducibility of the PCR and sequencing results, all samples were amplified in a second PCR run (technical replicates). The tagged PCR products were then purified with the Agencourt AMPure XP kit (Beckman Coulter, Switzerland) and eluted in 30 µL DNA/RNA-free water. The purified product was quantified with a Qubit 2.0 Fluorometer. Equimolar concentrations of all samples and negative purified PCR controls were pooled into a multiplex library (n = 48 samples and 2 negative controls). Similarly, equimolar concentrations of all sample technical replicates including negative controls were pooled into a second multiplex library (n = 48 technical replicates and 2 negative controls). The libraries were paired-end sequenced (2 × 300 bp) on an Illumina MiSeq system at Eurofins Scientific (Constance, Germany).

3.3.7 Bioinformatics

The obtained 10,546,152 sequence reads were quality checked on a raw fastq file with FastQC (Andrews et al., 2015). The reads were demultiplexed, first by using the "make.contigs" function in Mothur (v.1.39.5: pdiff=2, bdiff=1, and default setting for others) (Schloss et al., 2009). Based on the report files generated by "make.contigs" function, the sequence identifiers were retrieved for those sequences with minimum overlap (length > 25), maximum mismatches (< 5), and the maximum number of ambiguous bases of zero (which means there is no base marked with „N"). According to the sequence identifiers from the previous step the sequences were extracted with "filterbyname.sh" function from BBtools (Bushnell et al., 2017) from the raw paired-end fastq file. This step was followed by correcting the sequence orientation and removing sample unique barcodes by using extract_barcodes.py in QIIME1 (Caporaso et al., 2010) and finally, the primers were removed using awk script (Aho et al., 1979). The demultiplexed sequences were fed to DADA2 (Callahan et al., 2016) for filtering, dereplication, chimera check, sequence merge, and ASV (amplicon sequence variants) calling. The output of DADA2 was further fed to QIIME2 (Bolyen et al., 2019) for taxonomic assignment against the SILVA138 database (Quast et al., 2013).

3.3.8 Data availability

Sequencing data and metadata are deposited at the European Nucleotide Archive (ENA) under Bio Project accession number PRJEB40406 as well as sample accession numbers ERS5083566-ERS5083644.

3.3.9 Sequence data processing and statistics

The two libraries were merged together by taking the average of their relative abundances. Bubble plots was used to illustrate differences in seasonal and spatial cyanobacteria assemblage and produced with the free software tool http://shiny.raccoome.de/bubblePlot/. Alpha and beta diversity estimations, Spearman correlation and multivariate permutational analysis of variance (PerMANOVA) were performed using the PAST v4.01 software (Hammer et al., 2001). Two-way analysis of variance (ANOVA) tests, non-metric multidimensional scaling (NMDS) and distance-based redundancy analysis (dbRDA) were

performed in the 'vegan' package in R (Oksanen et al., 2019). Prior to alpha diversity calculation (richness, Shannon diversity and Pielou's evenness) the ASV read counts were rarefied to account for differences in sequencing depth (2,200 read counts per sample) using the "rtk" package in R (Saary et al., 2017). Also, before beta diversity measurements, the ASV cut-off was set to 0.1% to eliminate very rare taxa. The statistical significance level for uni- and multivariate statistical analyses was set to <0.05. To determine which lake factors have a significant impact on cyanobacteria spatiotemporal alpha diversity dynamics a two-way ANOVA (additive and interactive models) test was used to evaluate the effect of seasons and stratification zones (epi-, meta- and hypolimnion) on cyanobacteria species richness and evenness. In the ANOVA models, species richness or evenness was the response variable while season and stratification zones were the predictors. The seasons were defined based on changes in the water column as reveled by multi-parameter probe data. The ANOVA models' assumptions were evaluated with Tukey's-honestly-significant-difference (TukeyHSD) post-hoc tests. An NMDS ordination based on the Bray-Curtis similarity index was used to determine whether the samples at the ASV level showed distinct grouping patterns. To assess whether the grouping patterns of cyanobacterial communities at the ASV level as revealed by the NMDS were significantly different from each other a non-parametric PerMANOVA test based on Bray Curtis using seasons as predictors was conducted. Hellinger-transformed cyanobacteria absolute read counts data were used in the NMDS analysis and PerMANOVA test (Legendre and Gallagher, 2001). To align pooled water samples with depth-specific environmental variables, the averages of the environmental variables from the corresponding water depths were calculated. For example, for the reported mean water depth 5 m (water depths 1, 3, 5, 7, and 10 m) in January, average water temperature from the depths 1, 3, 5, 7, 10 m on the day of sample collection was aligned to the reported mean sample depth 5 m. To assess the correlation of *Cyanobium* ASVs 0005, 0008 and 0014 abundance to environmental parameters a Spearman's correlation coefficient was calculated. Prior to the correlation analysis the environmental data (predictors) were standardized by subtracting the mean and dividing by the standard deviation (Z-Score) and the *Cyanobium* ASVs 0005, 0008 and 0014 (response variables) read counts were Hellinger transformed. Standardized environmental data were also fitted into the dbRDA model. In this model, environmental and cyanobacteria community data were the explanatory and response variables, respectively. The dbRDA analysis was performed using the "capscale" function and Bray-Curtis distance in "vegan". The model and axes significance were tested by a 999 Monte

Carlo permutation test using the "anova.cca" function in vegan. Collinearity in the explanatory variables was tested with a variance inflation factor (VIF) using the "vif.cca" function in "vegan". Explanatory variables were then additively tested until only those with a VIF score <10 remained. The significant subset of explanatory variables that may explain the variability of cyanobacterial community composition was determined via forward selection using the function "ordiR2step" function in "vegan". Variation partitioning analysis (VPA) (Legendre et al., 2005) with redundancy analysis (RDA) was implemented on two categories of explanatory variables, that is, physicochemical parameters (temperature, pH, turbidity, conductivity, and DO) and nutrients (TDP and NO_3^-) to identify their unique and interactive effects on the cyanobacteria population dynamics (response variable). The significance of the fractions of variability explained by the categories was tested and determined via a 999 Monte Carlo permutation test in CANOCO5 (Smilauer and Leps, 2014).

3.4 Results

3.4.1 Water column physicochemical properties

Temperature and dissolved oxygen (DO) in the water column of Lake Tiefer See (Figs. 3.2A, B) showed that in 2019 thermal stratification began in early April and continued beyond late November. Highest epilimnion temperatures (>22°C) were recorded during summer months. In the epilimnion (0 – 6 m) three periods with high temperatures followed by cooling of ~5°C drop occurred. The first lasted the entire month of June (T_{max} = 21.6°C, $T_{average}$ = 20°C) while the second phase covered the last week of July until the first week of August (T_{max} = 20.9°C, $T_{average}$ = 19°C). The last warm period was recorded from late August to the first few days in September (T_{max} = 20.7°C, $T_{average}$ = 17°C). Oxygen depletion in the bottom water started circa three weeks after the onset of thermal stratification and the onset of pelagic productivity. The DO reached minimum values (~0.67 mg L^{-1}) at 40 to 50 m water depth between October and November (Fig. 3.2B). Additionally, Lake Tiefer See developed a zone of metalimnetic oxygen minimum between 10 and 13 m from June to September. Enhanced pH and Chl*a* values (Figs. 3.2C,D) reflect the first algal-blooms in mid-April between 1 and 7 m water depth, shortly before the onset of lake stratification. From late March until mid-July, peak Chl*a* were observed at approximately 7 m water depth, and at 10 m water depth from August to September (Fig.

3.2D). In winter to early spring, conductivity in the mixed water column ranged between 530 and 540 µS cm^{-1} (Fig. 3.2E). During lake stratification, conductivity was lowest in the epilimnion (<480 µS cm^{-1}; 1 – 7 m) and highest in the meta- and hypolimnion (>540 µS cm^{-1}; 10 – 60 m). Nitrate concentrations varied between 1 and 2 µg L^{-1}, except in October and November where they reached only 0.2 µg L^{-1} (Fig. 3.2G). Turbidity peaked between 5 and 6 NTUs in summer in the upper water column (down to 10 m) likely as a combined result of primary productivity and calcite precipitation. TDP values were generally higher in the hypolimnion, gradually increasing from July through November reaching up to ~70 µg L^{-1} in the bottom waters (Fig. 3.2H). In contrast, the TDP in the epilimnion ranged between 10 and 15 µg L^{-1}, except for January and February, when the lake was in an isothermal state and the TDP values were between 20 – 25 µg L^{-1} throughout the mixed water column.

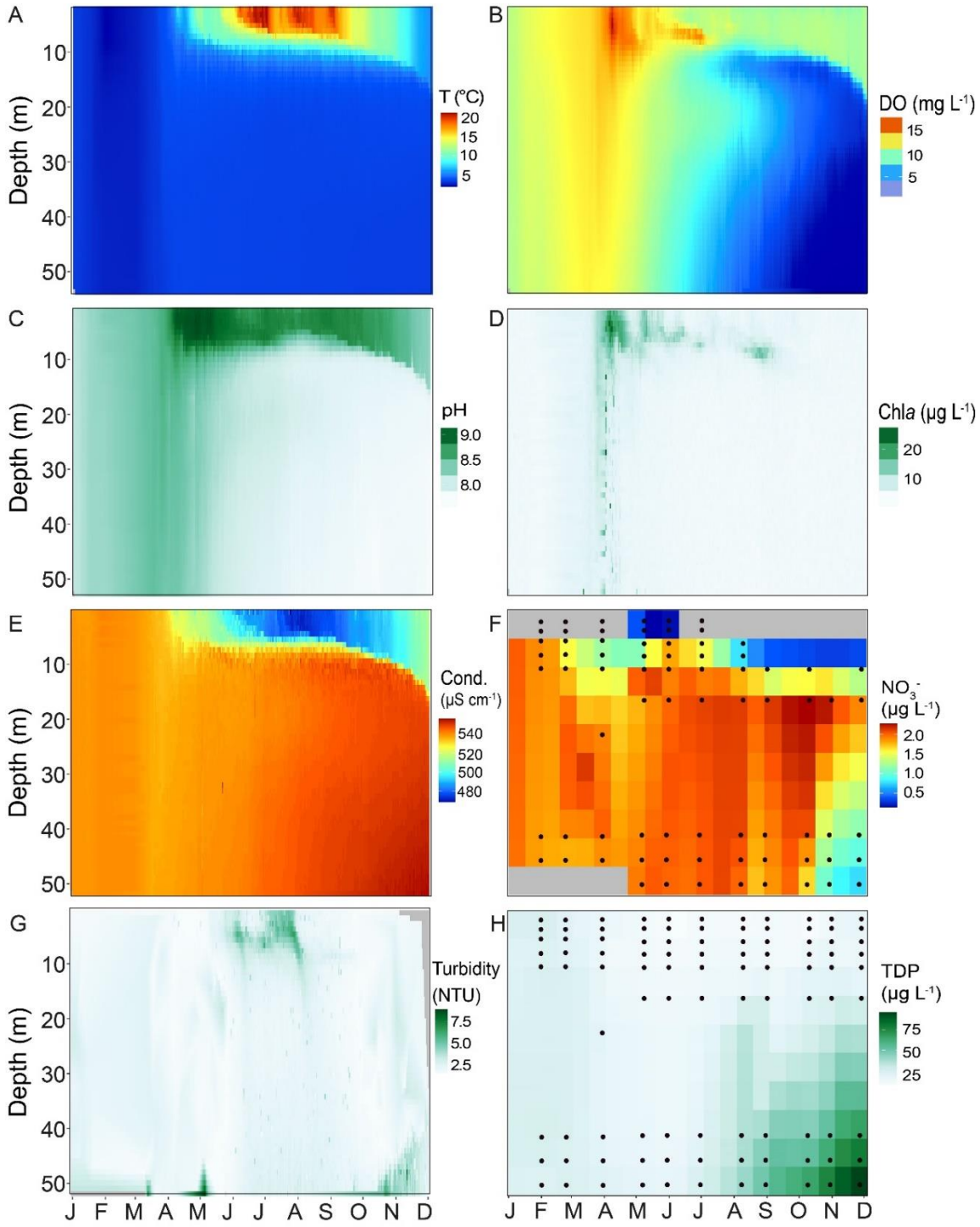

Figure 3.2: Heatmaps of different physicochemical parameters of Lake Tiefer See for the year 2019 measured in the water column using a multi-parameter probe (YSI 6600 V2), showing (A) temperature (T), (B) dissolved oxygen (DO), (C) pH, (D) chlorophyll a (Chl*a*), (E) conductivity (Cond.), (F) nitrate (NO_3^-), (G) turbidity, and (H) total dissolved phosphorus (TDP). Probe data were interpolated for 1 day and 1 m water depth. Black circles in NO_3^- and TDP heatmaps represent the depths from which measurements were taken. The latter were interpolated to 15 days and 5 meters water depth. Gray fields in NO_3^- heatmap are depths with no data.

3.4.2 Cyanobacterial community composition

Sequencing of the water samples resulted in a total of 4,864,912 denoised and error-corrected absolute read counts which DADA2 inferred into 1599 ASVs. The two negative extraction controls that were included in the sequencing run each comprised less than 1% of the reads (17 ASVs) compared with the sample average and were removed. After ASVs assigned to chloroplasts, non-photosynthetic cyanobacteria (the orders Sericytochromatia and Vampirivibrionia) and other bacteria had been removed, 894 ASVs with a total 2,915,251 read counts remained. Next, global singletons and doubletons (492 ASVs) as well as 201 ASVs that occurred in fewer than three samples over the whole dataset were removed to reduce influence from very rare taxa. The filtered dataset comprised 201 ASVs assigned to photosynthetic cyanobacteria with a combined 2,901,116 absolute read counts and distributed across 96 samples (Suppl. Fig. B.1). Of the 201 ASVs, two were assigned to order level (Cyanobacteriales), six were assigned to family level (2x Leptolyngbyaceae, 2x Coleofasciculaceae, Microcystaceae, Cyanobiaceae), and 193 were assigned to genus level. The ASVs of the genera *Planktothrix*, *Cyanobium*, *Synechococcus*, *Snowella*, *Aphanizomenon*, *Microcystis*, *Pseudanabaena* and *Gloeocapsa* were most abundant. Of the cyanobacterial ASVs with 0.1% relative abundance, 65% were assigned to the genus *Cyanobium* (Fig. 3.3).

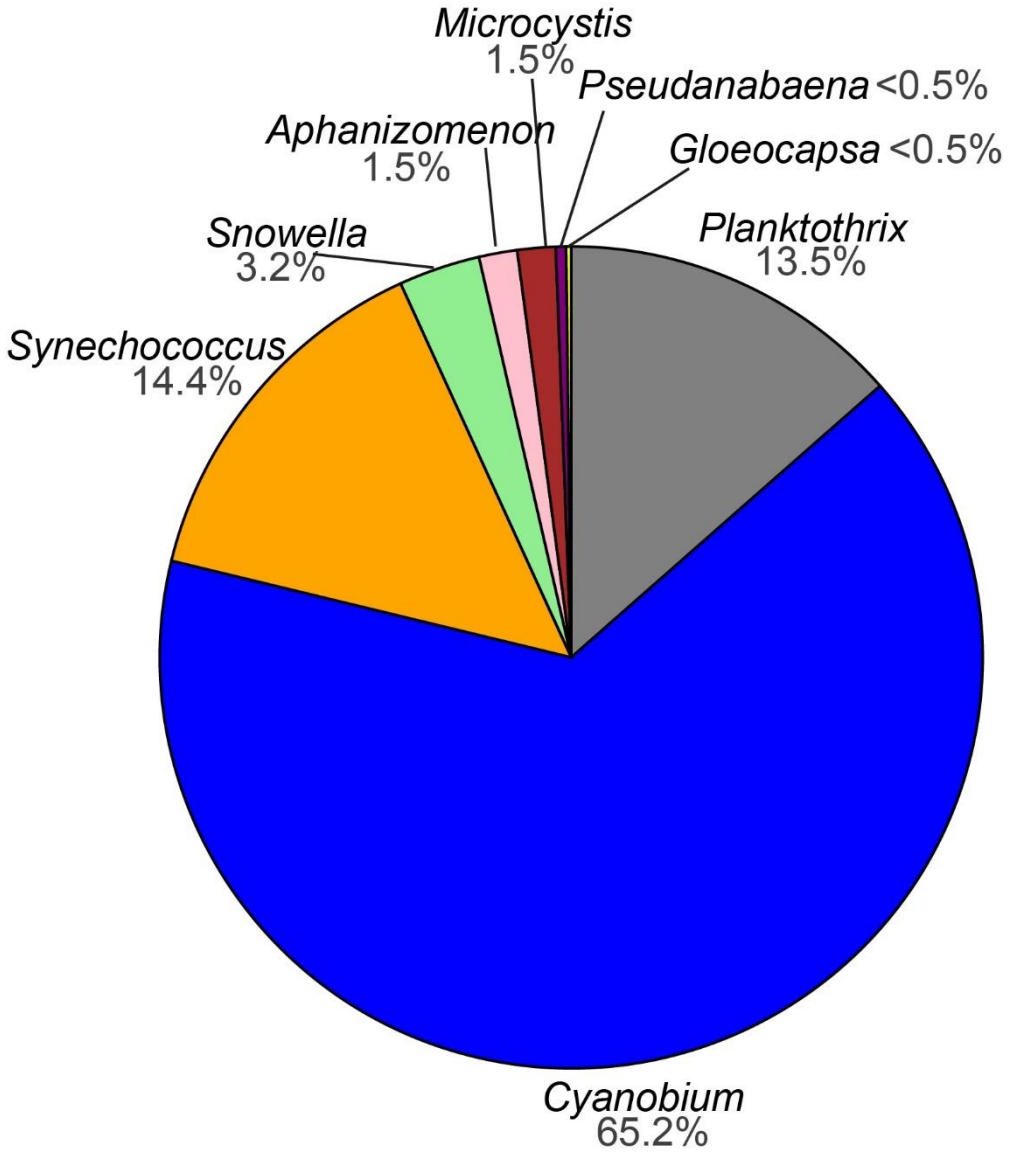

Figure 3.3: Pie chart showing the percentage of amplicon sequence variants (ASVs) assigned to cyanobacteria (>0.1% relative abundance) from this study.

3.4.3 Cyanobacterial seasonal variation

A general trend in cyanobacterial 16S rRNA-ITS gene copy numbers was observed with highest mean cyanobacteria abundances in summer (1.2×10^6 copies ng^{-1} DNA, $n = 18$) and fall (6.7×10^5 copies ng^{-1} DNA, $n = 18$) throughout the water column. In contrast, lower mean cyanobacteria abundances were observed in spring (3.2×10^5 copies ng^{-1} DNA, $n = 16$) and winter (9.4×10^4 copies ng^{-1} DNA, $n = 4$), respectively, throughout the water column. The highest average numbers of cyanobacterial 16S rRNA-ITS gene copies were measured in the epi- and metalimnion in summer (2.2×10^6 copies ng^{-1} DNA, 1 – 10 m, *n*

= 9) and fall (1.1×10^6 copies ng^{-1} DNA, 1 – 10 m, n = 9), while the hypolimnion had the lowest numbers throughout the different seasons, except for winter (Fig. 3.4A).

The spatiotemporal variation was mainly driven by the ASVs belonging to the cyanobacterial orders Synechococcales (*Cyanobium*, *Snowella* and *Synechococcus*), Nostocales (*Aphanizomenon*), Chroococcales (*Microcystis*) and Oscillatoriales (*Planktothrix*)(Fig. 3.4B). The seasonal and spatial dynamics of the ASVs assigned to the most dominant taxa (>1% relative abundance) in Lake Tiefer See during the study period were as follows. In Winter (January - February), ASV0008 (*Cyanobium*) and ASV0007 (*Synechococcus*) were the most abundant (≥30%) cyanobacteria species throughout the water column. In Spring (March – May), *Cyanobium* ASV0008 bloomed in the epi- and metalimnion exceeding a relative abundance of 40%. At the same time, in the metalimnion the abundance of *Planktothrix* ASV0006 increased more than five-fold to ≥ 30% and was maintained high until late autumn. In the hypolimnion, ASV0004 (*Aphanizomenon*) and ASV0009 (*Microcystis*) increased only slightly (≥5%) in spring. In summer, *Aphanizomenon* ASV0004 (June) and the two *Snowella* ASVs 0016 and 0022 (August) behaved similarly with increase in abundance from ~2% to 11% in the epilimnion. *Synechococcus* ASV0007 abundance increased to more than 30% throughout the water column in June. Starting in August, ASVs 0006 and 0014 assigned to *Planktothrix* and *Cyanobium*, respectively, subsequently became the most dominant ASVs (≥40%) in the meta- and hypolimnion, respectively. In fall (October), *Cyanobium* ASV0005 was the most abundant (≥40%) in the epi- and hypolimnion. In the metalimnion (10 m), *Planktothrix* ASV0006 abundance was higher (≥40%) than that of *Cyanobium* ASV005 (~30%). Also, the *Microcystis* abundance increased throughout the water column from 2% to 6% whereas the *Snowella* ASVs 0016 and 0022 increased by more than 20% in the hypolimnion only.

The cyanobacteria community composition at the ASV level showed distinct spatial and temporal clustering patterns as shown by NMDS (Suppl. Fig. B.2), and confirmed by a one-way PerMANOVA test to be significantly different from each other ($p < 0.05$; $F = 10.72$; Suppl. Table B.2).

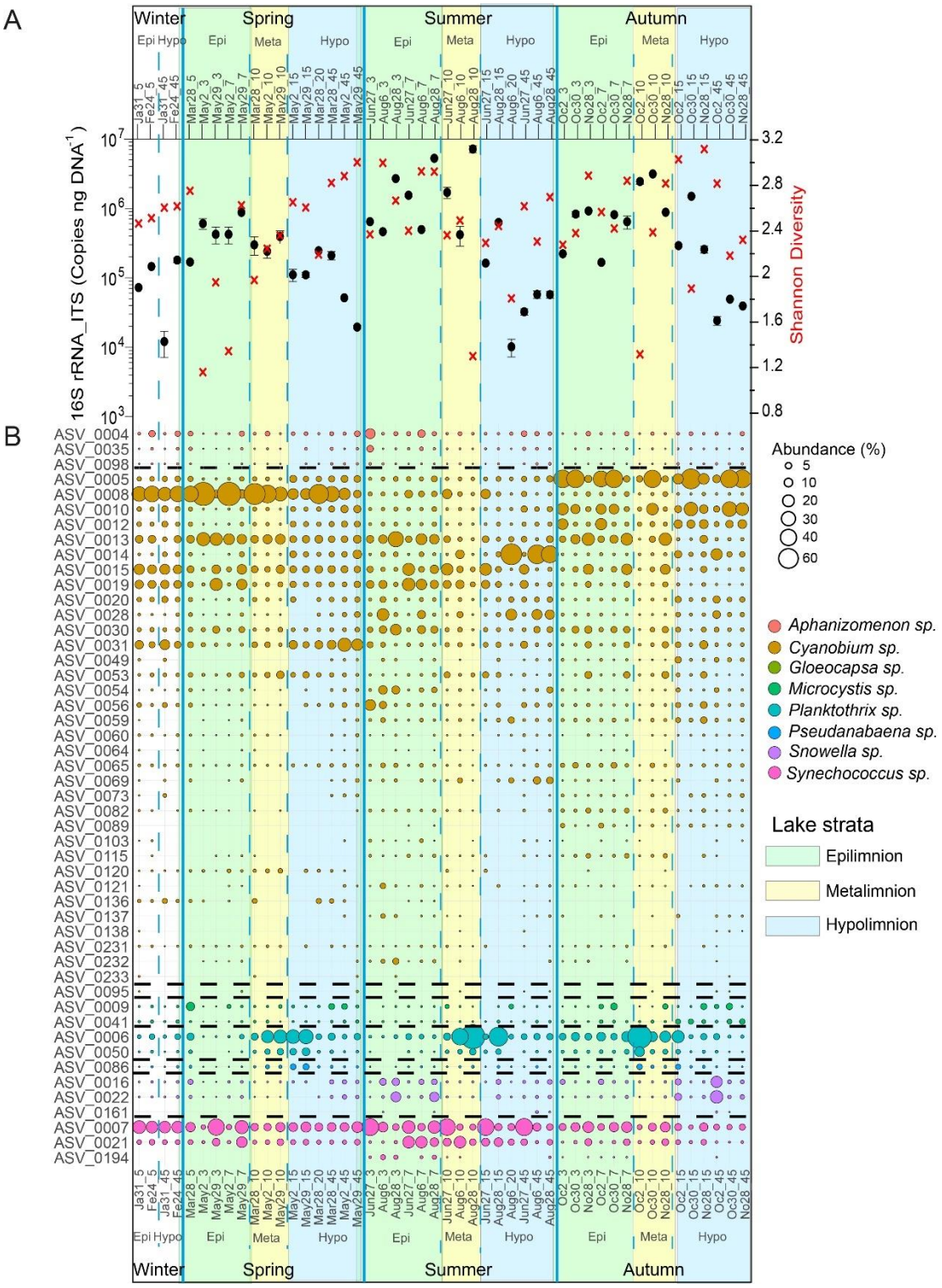

Figure 3.4: Cyanobacteria community structure, abundance and diversity in Lake Tiefer See throughout the year 2019. (A) cyanobacterial abundance quantified via qPCR (black dots; Error bars, which are hidden by the dots in some cases, give the standard deviations for three independent amplifications.) and Shannon diversity (red crosses). (B) bubble plot showing the spatiotemporal variation of cyanobacteria community composition at the amplicon sequence variant level (cutoff > 0.1% abundance). Numbers beside months refer to sampling date while number after the underscore refers to water depth, e.g., May2_10 refers to a sample collected at 10 m water depth on 2nd May. Epi = epilimnion, Meta = metalimnion, Hypo = hypolimnion. Taxa follow the same

order as in the legend and broken lines indicates where the bubbles of one taxon end and the next begins.

3.4.4 Cyanobacterial alpha diversity indices

A two-way ANOVA was used to determine if possible differences in cyanobacteria species richness were driven by seasonality, lake stratification (epi-, meta-, and hypolimnion) and/or an interaction effect of both factors. Species richness was found to be significantly impacted by season ($f(3) = 8.046$, $p < 0.05$; Fig. 3.4), but not by depth nor an interaction between both terms. A Tukey post-hoc test revealed significant pairwise differences in cyanobacteria species richness between spring and summer (+ 5.8 species richness; Suppl. Table B.3), spring and autumn (- 8.6 species richness), and between epi- and hypolimnion depths (- 3.7 species richness). Cyanobacteria species evenness was not significantly impacted by the seasonal and lake stratification factors (Suppl. Fig. B.3).

In general, mean cyanobacterial species diversity across the seasons as revealed by Shannon index was lowest in the metalimnion compared to the epi- and hypolimnion (Figs. 3.5,3.4A). In the epilimnion, diversity was highest in summer (2.7) and lowest in spring (2.0). Conversely, diversity decreased slightly from spring to summer from 2.2 to 2 in the metalimnion and 2.7 to 2.3 in the hypolimnion. Cyanobacteria diversity in the metalimnion from March to November was between 2.1 and 2.2.

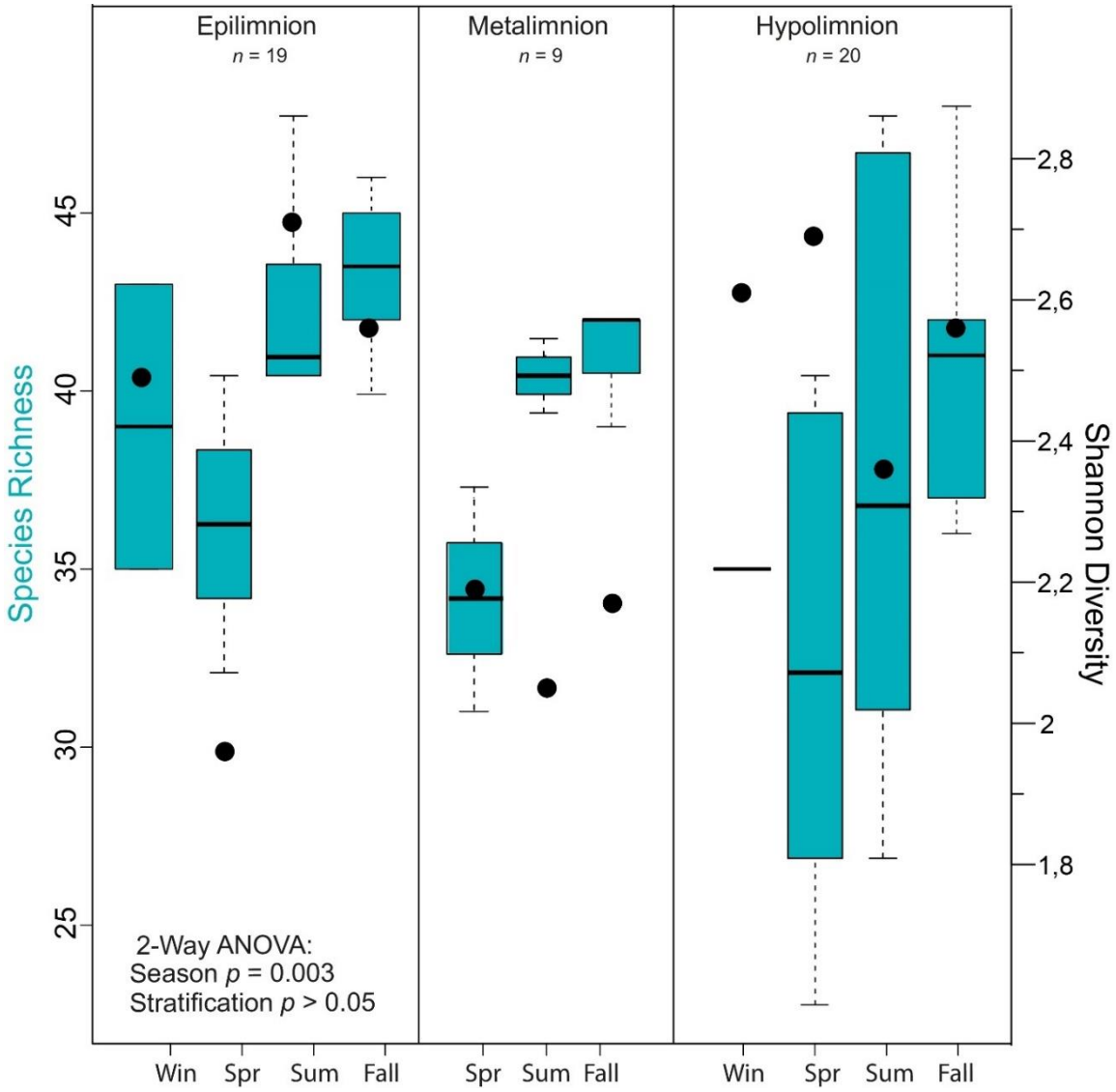

Figure 3.5: Alpha diversity of cyanobacteria communities in Lake Tiefer See. Box plots showing the results of seasonal and stratification effects on cyanobacteria richness in Lake Tiefer See via a two-way analysis of variance (ANOVA) analysis and Shannon diversity indices shown by black dots. Significant seasonal variation in cyanobacterial species richness within the epi-, meta- and hypolimnion layers was tested via a one-way ANOVA. Win = winter, Spr = spring, Sum = summer.

3.4.5 Relationship between certain *Cyanobium* ASVs and environmental variables

We observed a potential niche separation among the three most abundant ASVs 0005, 0008 and 0014 assigned to *Cyanobium* (Figs. 3.4B,3.6A). Because of the different seasonal relative abundances among the *Cyanobium* ASVs 0005, 0008 and 0014, we used a rank-based Spearman's correlation coefficient to check potential correlations of these ASVs with

environmental parameters (Figs. 3.6A,B). The ASV0005 which was dominant in fall had a significant positive correlation with TDP (R_S = 0.52), and negatively correlated to temperature, pH, turbidity and DO although insignificant (R_S > -0.4). ASV0008 which was most abundant in winter and spring correlated positively with pH (R_S = 0.48) and DO (R_S = 0.76). Lastly, the ASV0014 which dominated the hypolimnion in summer correlated positively with TDP and conductivity (R_S > 0.52) and negatively with temperature and pH (R_S > -0.47).

A dbRDA was used to ascertain the environmental parameters responsible for the variation in the general cyanobacterial seasonal communities (Fig. 3.6). The dbRDA model explained 48% of the total observed community variation and identified temperature, turbidity, TDP, NO_3^-, pH, conductivity and DO as environmental variables that significantly shaped cyanobacterial communities in Lake Tiefer See over the investigated seasons. Furthermore, canonical VPA (Fig. 3.8) was used to determine the percentage of variation explained by nutrients, physicochemical parameters as well as their combined effect on cyanobacterial population. The physicochemical parameters (23%; temperature, DO, turbidity, conductivity, and pH) and nutrients (11.2%; TDP and NO_3^-) were the groups of factors that significantly explained most of the variability in cyanobacteria composition in Lake Tiefer See. The interaction between both groups accounted for 6.1% of community variation, while 60% of the variation remained unexplained. Turbidity was not included in the VPA model because it has been shown to be triggered by both abiotic sediment-resuspension in the bottom waters and biotic biomass production in the upper waters. However, when turbidity is included as part of the physicochemical parameters, total amount of variation explained by the VPA model increases to 45% (accounting for an additional 5%).

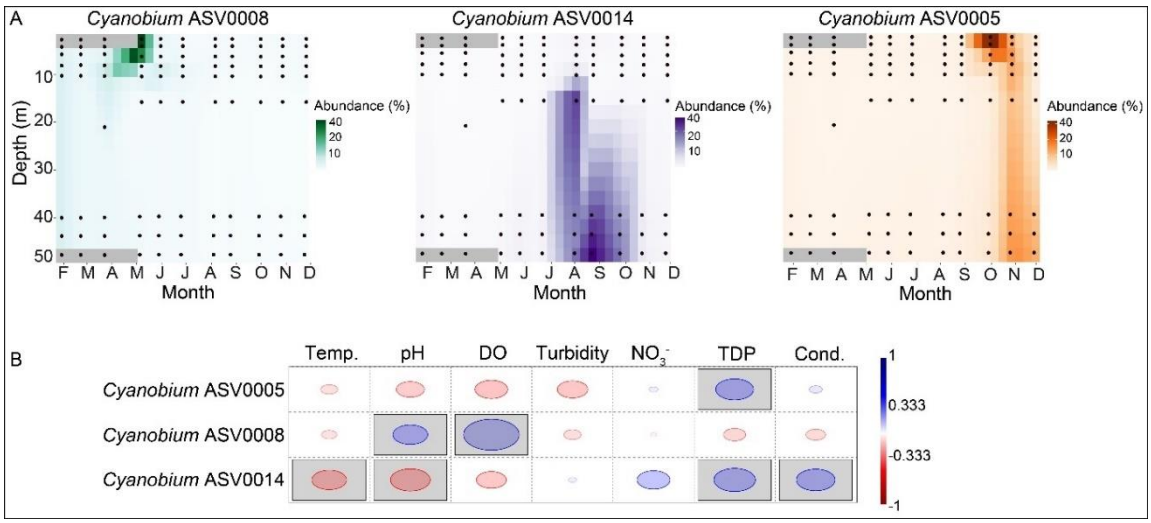

Figure 3.6: Dynamics of the three most abundant Cyanobium ASVs and correlation with environmental parameters. (A) Heatmaps show the spatiotemporal distribution across the water column of Lake Tiefer See. Data were interpolated for 10 days and 3 m water depth. Black circles represent the depths of water sample collection. (B) Rank-based Spearman correlation of the most abundant *Cyanobium* ASVs with lake physicochemical properties in Lake Tiefer See. Gray-shaded squares are significant at $p < 0.05$ with Bonferroni *p*-value correction. Blue circles show positive while red circles show negative correlation. Temp. = Temperature, DO = dissolved oxygen, NO_3^- = nitrate, TDP = total dissolved phosphorus, Cond. = conductivity.

3.5 Discussion

Altogether the cyanobacteria community in Lake Tiefer See is dominated by the orders Synechococcales and Oscillatoriales indicative of its oligo-mesotrophic status (Callieri et al., 2012a; Soule and Garcia-Pichel, 2019). This aligns with observations in several natural and artificial lakes e.g., peri-Alpine lakes (Monchamp et al., 2018), sub-Alpine deep and shallow lakes as well as reservoirs and fish ponds (Vörös et al., 1998). However, our study shows a previously unknown cyanobacteria inter-species spatio-temporal variation in a temperate hard-water lake. Although this study spanned a monomictic circulation mode, its results can be extrapolated to years with similar circulation modes provided other lake environmental parameters remain the same. This is based on the premise that despite the potential annual variability in inter-species relative abundances which are mainly influenced by fluctuations in lake environmental parameters, a general pattern would still be observed. That is, cyanobacteria seasonal variation would typically begin with an increase in abundance of nitrogen-fixing taxa which utilize sediment resuspended nutrients made available during water turnover in spring (e.g., *Aphanizomenon*), then a breakdown in their population in summer e.g., by fungal parasitism (Gerphagnon et al., 2015), and followed by an increase in abundance of non-nitrogen fixers e.g., *Planktothrix* sp. at the base of the euphotic zone or in the epilimnion (Walsby and Schanz, 2002).

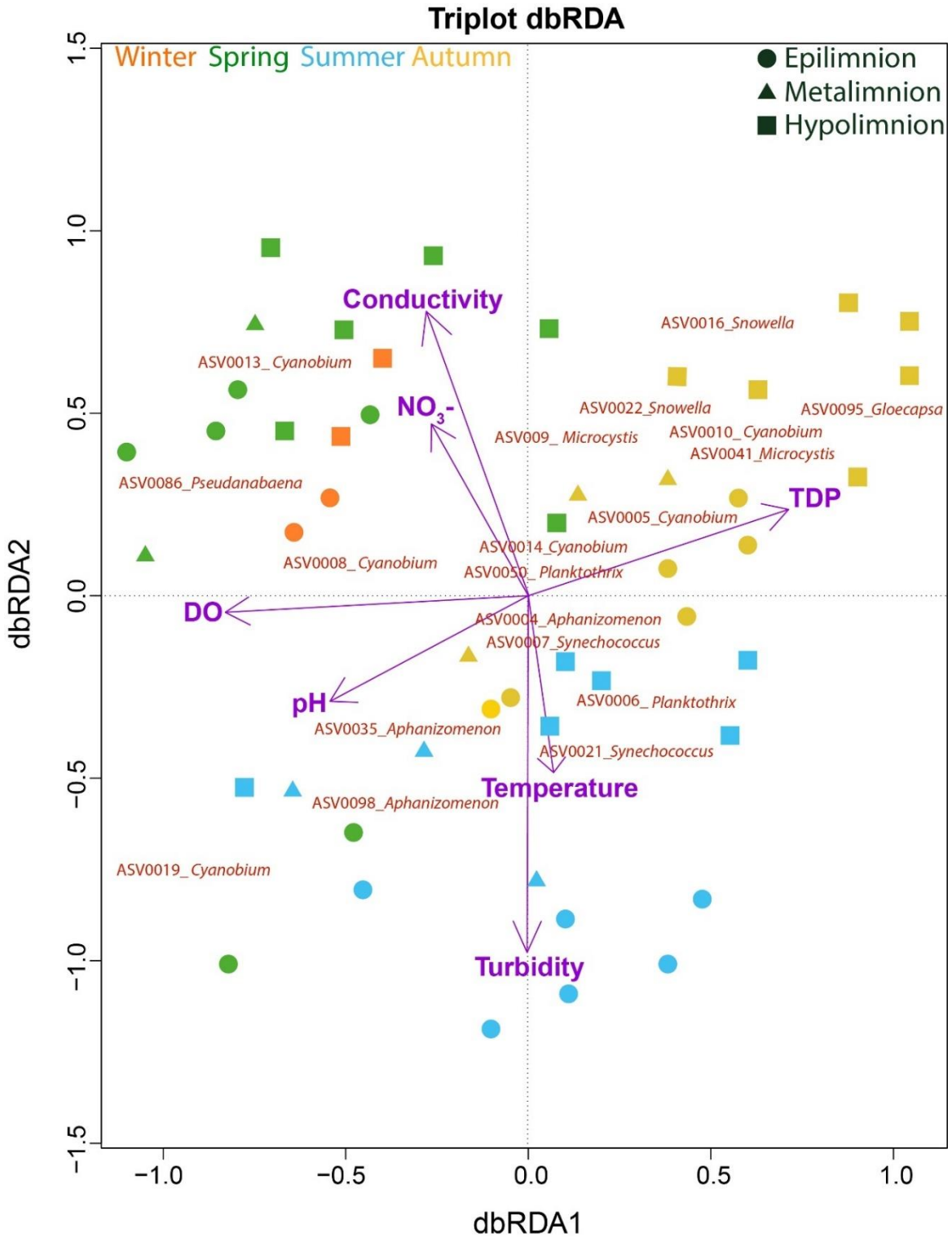

Figure 3.7: Cyanobacterial composition in relation to environmental variables. Distance-based Redundancy Analysis (dbRDA) on the effect of environmental variables on cyanobacteria community composition. The total variation explained by the dbRDA model was 48%. The samples are color-coded according to seasons. The environmental variables explaining the variation in cyanobacteria community were all significant (adjusted R^2 = 0.34) and are projected as purple vectors. The response variables are shown at the ASV level.

3.5.1 Succession and seasonal variation of cyanobacterial communities

The observed seasonal variation of the CCC suggests the formation of distinct subpopulations in Lake Tiefer See dominated by a few taxa belonging to Synechococcales (*Cyanobium, Snowella* and *Synechococcus*), Nostocales (*Aphanizomenon*- spring to summer), Chroococcales (*Microcystis*- fall) and Oscillatoriales (*Planktothrix*- late spring to fall). The interplay of abiotic factors and nutrients such as temperature, turbidity, DO, pH, conductivity, NO_3^- and TDP were likely responsible for shifting the CCC and the abundance of the dominant taxa (Fig. 3.8). This observation adds to previous amplicon-based CCC studies in shallow and deep temperate lakes (Diao et al., 2017; Salmaso et al., 2018). Unlike in the nearby Lake Stechlin, where *Dolichospermum circinale* and *Aphanizomenon flosaquae* were the dominant cyanobacteria taxa (Dadheech et al., 2014), *Cyanobium*, *Synechococcus* and *Planktothrix* were most abundant in Lake Tiefer See (Figs. 3.3,3.4B). The dominance of these taxa in Lake Tiefer See may be attributed to physiological advantages like rapid growth (*Cyanobium, Synechococcus*), colony formation (*Cyanobium*) and cell buoyancy regulation (*Planktothrix*, (Carey et al., 2012). Consequently, these taxa are able to better adapt to the seasonally changing in-lake conditions (Reynolds et al., 1987; Callieri and Stockner, 2000; Carey et al., 2012). Our observation of higher abundance of potential toxin-producing taxa (*Planktothrix, Aphanizomenon* and *Microcystis*) accompanied by a lower picocyanobacterial abundance (*Cyanobium* and *Synechococcus*) is in line with that from other temperate lakes with varying depths and trophic status (Callieri et al., 2012b). *Planktothrix, Aphanizomenon* and *Microcystis* were shown to cause surface blooms either directly because of anthropogenic nutrient loading e.g., via agriculture (Paerl and Huisman, 2008; Sukenik et al., 2015) or indirectly by continuous warming (Wagner and Adrian, 2009; Winder et al., 2009).

The seasonality of cyanobacteria observed in Lake Tiefer See is similar to known succession patterns in various temperate lakes which typically begins in spring when picocyanobacteria and nitrogen-fixing taxa (e.g., *Aphanizomenon* that survived the winter in sediments) become dominant by taking advantage of increasing temperature, light intensity, and the nutrients made available during spring mixing of the lake (Walsby, 2005; Hense and Beckmann, 2006; Kaiblinger et al., 2007). This leads to a cyanobacterial bloom evidenced by an increase in the total cyanobacteria abundance in the upper waters (epi- and metalimnion) in early spring likely associated with increase in bio-productivity, oxygen

concentrations and the higher pH of the epilimnion (Figs. 3.2B,D,3.4B; Roeser et al., 2021). The onset of stratification in Lake Tiefer See as seen from the temperature, DO and other parameters in the upper water column (i.e., mid-April, Fig. 3.2B), follows an increase in bio-productivity from the aforementioned cyanobacteria groups that grow optimally as temperature begins to increase. The breakdown of fall cyanobacteria populations (e.g., picocyanobacteria and *Aphanizomenon*) is likely due to factors such as viral lysis (Personnic et al., 2009), increased epilimnion turbidity resulting from biomass production in spring, subsequent lower light intensity, nutrient depletion, predation and grazing by zooplankton communities like rhizopods, ciliates, rotifers (Gerphagnon et al., 2015), *Daphnia* (Urrutia-Cordero et al., 2016), copepods (Ger et al., 2016) and/or parasitic fungi (Jia et al., 2010). In fall, the concurrent resuspension of shallow-water sediments together with the release of phosphorus into the water column favored a second cyanobacteria bloom (Fig. 3.2H). Our data show that this bloom comprises mainly cyanobacterial ASVs assigned to *Microcystis*, *Snowella*, *Planktothrix* and *Cyanobium*.

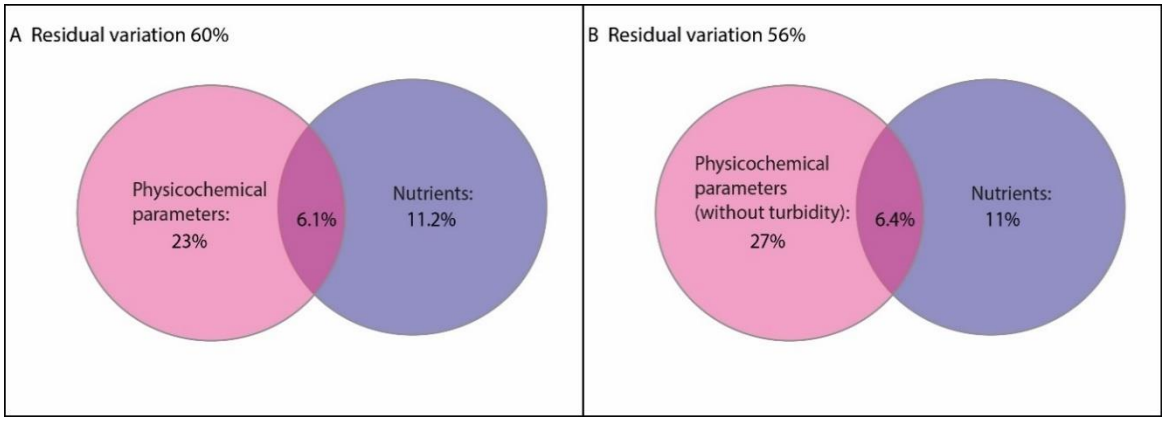

Figure 3.8: Venn diagrams displaying the results of the variation partitioning analysis (VPA). The two explanatory matrices used contained variables on lake internal physicochemical parameters (A) (temperature, dissolved oxygen, turbidity, conductivity and pH) and nutrients (total dissolved phosphorus and nitrate). (B) (temperature, dissolved oxygen, conductivity and pH) and nutrients (total dissolved phosphorus and nitrate). Each circle represents the portion of variation accounted for by each explanatory matrix or a combination of them. The significance of the fractions of variability explained by the categories was determined via a 999 Monte Carlo permutation test.

The peak in total cyanobacteria abundance in late August in the metalimnion (10 m; Fig. 3.4A) may have resulted from the presence of a density gradient zone during lake stratification that prevent complete downward transport of the CCC from the water column to the sediments, especially of buoyant and filamentous taxa like *Planktothrix* (Halstvedt et al., 2007; Boehrer and Schultze, 2008). Also, the peak in summer cyanobacteria

abundance in upper waters aligns with previous findings which identified temperature as an important factor leading to increase of cyanobacteria populations in lakes in central and northern European regions (Richardson et al., 2018). Considering that the copy numbers of the 16S rRNA gene among cyanobacteria genera have a low range in variability (2.7 ± 1.0 copies; Větrovský and Baldrian, 2013), we do not think the abundance and sequencing data from our study are skewed.

We further observed that seasonal changes significantly altered species richness especially in the epi- and metalimnion in Lake Tiefer See (Fig. 3.4). The increase in water temperature, light and nutrient availability likely explains the significant increase in species richness between spring and summer in the epi- and the metalimnion. In addition, the Shannon species diversity minima in spring (epilimnion) and summer (meta- and hypolimnion) are attributed to the dominance of a few ASVs assigned to *Cyanobium* and *Planktothrix* and supported by the uneven species distribution during these seasons (Suppl. Fig. B.3). An environmental factor that likely affects the CCC in Lake Tiefer See is the lake circulation mode which depends on the formation of a winter ice cover. Thus, our results show that the lake mixing regime is an important environmental factor that affects the CCC in Lake Tiefer See. Further investigation of the CCC covering longer periods with potentially different lake mixing regimes would be necessary to compare and trace possible changes in cyanobacteria dynamics driven by water circulation mode.

3.5.2 Picocyanobacterial dynamics

The abundance of the picocyanobacterial *Cyanobium* and *Synechococcus* observed in Lake Tiefer See followed a bimodal pattern common in most temperate lakes, it means, a spring or early summer peak and a second peak in late summer or fall (Stockner et al., 2000). The bimodal picocyanobacterial abundance observed in Lake Tiefer See concurs with previous observations in the nearby oligo-mesotrophic Lake Stechlin (Padisák et al., 2003) and/or in large subalpine lakes such as Lake Constance (Gaedke and Weisse, 1998) and Lake Maggiore (Callieri and Piscia, 2002). The peak abundance of ASVs assigned to *Synechococcus* (in June) and *Cyanobium* (in October; see Fig. 2.4B) at different water depths throughout the year may be explained by their ability to tolerate and adapt to a variety of light conditions (Gervais et al., 1997; Callieri and Piscia, 2002). Other abiotic factors driving picocyanobacterial variability include nutrient availability (Bell and Kalff, 2001), lake morphometry and thermal regime (i.e., deep lakes with a stable vertical

structure promote picocyanobacterial development, Camacho et al., 2009), changes in lake physicochemical factors that promote the coexistence of phycoerythrin- and phycocyanin-rich picocyanobacterial groups (Postius and Ernst, 1999; Stomp et al., 2007), and the interplay between ultraviolet and photosynthetically active radiation (Callieri et al., 2001, 2012b). Additionally, variations in picocyanobacterial dynamics could be driven by biotic factors such as grazing by ciliates and protists (Callieri et al., 2002; Jezberová and Komárková, 2007) as well as viral lysis (Personnic et al., 2009). Based on the low Chl*a* values (<20 µg L^{-1} in 2019; Fig. 3.2E) from Lake Tiefer See and thus its oligo-mesotrophic status, we suggest that there is likely an enrichment of phycoerythrin picocyanobacteria population in Lake Tiefer See. This would be in line with a European multi-lake series investigation comprising deep and shallow lakes which revealed that phycoerythrin-rich picocyanobacteria dominated the water column at low Chl*a* levels (Vörös et al., 1998).

The seasonal and spatial (i.e., water depth) differences in the relative abundances of the *Cyanobium* ASVs 0005, 0008 and 0014 suggests niche specialisation within this genus. The spring epilimnetic peak abundance (>40%) of *Cyanobium* ASV0008 suggests that it copes well at 10 – 15°C and it may also contribute substantially to the increase in pH values (up to 9). This is in line with monitoring reports from Lake Tiefer See that showed the increase in phytoplankton bio-productivity in spring increases the pH value of the water up to 8.6 (Roeser et al., 2021).

Table 3.1: Summary of significant explanatory parameters used in the distance-based redundancy analysis (dbRDA) model. The model explained 48% of the total variation (p = 0.001). The significance of the environmental variables was tested by 999 Monte Carlo permutations and were selected by forward selection (Adjusted R^2 = 0.34). AIC = Akaike information criterion.

Explanatory variable	AIC	Pseudo-*F*	*p*
DO	159.73	8.77	0.001
Conductivity	156.75	4.92	0.002
Turbidity	157.26	4.92	0.002
TDP	154.76	4.56	0.002
pH	153.98	4.42	0.005
NO_3^-	152.98	3.56	0.004
Temperature	150.95	3.07	0.008

In Lake Tiefer See, the thermal stratification in summer seems to establish a niche for *Cyanobium* ASV0014 in the hypolimnion (~15 – 50 m) because of a high relative abundance (40%) of this ASV, compared to the upper waters or other seasons where it was generally ≤15%. While it has been suggested that temperature plays a key role in initiating picocyanobacterial abundance and growth in freshwater ecosystems (Weisse, 1993; Vörös et al., 2009), its effect on regulating picocyanobacterial dynamics is still unclear (Callieri et al., 2012a). The negative correlation of ASV0014 with temperature suggests that this taxon copes better with lower temperatures in the hypolimnion than other groups. In addition, ASV0014 might utilize the most penetrating green and blue lights in the lower meta- to upper hypolimnion to outcompete other autotrophs and promote its success in the low-light reaching deeper waters in summer (Pick and Agbeti, 1991; Vörös et al., 1998; Callieri et al., 2007). Elsewhere, higher picocyanobacterial abundances have also been reported in the lower meta- to upper hypolimnion in Lake Stechlin (Padisák et al., 2003) and Lakes Huron and Michigan (Fahnenstiel and Carrick, 1992). In October, when thermal gradient diminishes caused by lower temperatures in the water column, ASV0005 became the most abundant *Cyanobium* ASV. Similar to ASV0014 it is also negatively correlated to temperature albeit insignificant. This means the *Cyanobium* ASVs 0014 and 0005 may be psychrotolerant (cold-adapted) in nature able to tolerate lower temperatures better than other cyanobacteria groups. Their generally lower relative abundances during periods of warmer water temperature (11 – 20°C) poses the assumption that they may be "cold-water-preference" species. Psychrophilic picocyanobacterial taxa have been reported in various

aquatic environments ranging from the temperate East China sea (Choi et al., 2013) to polar seas (Tang et al., 1997) and most recently in freshwater Lake Biwa, Japan (Cai et al., 2021). While the psychrotolerant picocyanobacteria observed in other freshwater ecosystems were either from surface water samples (Xu et al., 2015) or in the deeper epilimnion (5 m, Lake Biwa Japan), the *Cyanobium* ASVs 0014 and 0005 from Lake Tiefer See were also abundant in the meta- and hypolimnion. In addition, a further factor that possibly contributed to the increase in abundance of the *Cyanobium* ASVs 0014 and 0005, is the increase in TDP availability beginning in summer in the hypolimnion with a peak in fall. Also, the sediment re-suspension in the shallower parts of the lake may facilitate the release of phosphorus (Nuhfer et al., 1993). Our data suggest that *Cyanobium* ASVs 0005 and 0014 may be main utilizers of this nutrient. Since the cyanobacteria community data from our study are based on relative abundances, the observed hypolimnetic abundance of *Cyanobium* ASV0014 in summer could also result from a decrease of other ASVs. Nevertheless, even if the other ASVs were only reduced while ASV0014 was "maintained/stable", it still indicates that it is able to cope well with the prevailing ambient conditions in deeper waters.

Altogether, the observed fine-scale spatiotemporal dynamic of the picocyanobacteria is a clear indication for niche separation in the water column of deep temperate hard-water lakes especially of individual taxa within *Synechococcus* and *Cyanobium*. Future studies could combine isolation, cultivation and physiological tests as well as metagenomics to get a more complete insight on the picocyanobacterial dynamics we observed here.

3.5.3 Planktothrix dynamics

The *Planktothrix* ASV0006 in Lake Tiefer See showed a peak abundance in the zone of low light intensity (0.1%) in the metalimnion which concurs with observations in a number of European lakes such as Lake Pusiano (Legnani et al., 2005), Lake Zürich (Posch et al., 2012), Lake Bourget (Jacquet et al., 2005) Lake Stechlin (Dadheech et al., 2014), and Lake Steinsfjorden (Halstvedt et al., 2007). The results from our molecular approach are also substantiated by similar findings based on microscopic (Posch et al., 2012; Selmeczy et al., 2016) and cell count studies (Jacquet et al., 2005; Wentzky et al., 2019). The late summer to fall peak in the relative abundance of *Planktothrix* in the metalimnion of Lake Tiefer See may be explained by factors such as low light intensity (0.1%) sufficient for photosynthesis (Walsby and Schanz, 2002; Walsby et al., 2006), lower temperatures (<10°C) and

buoyancy adjustments in the face of changing light dynamics (Konopka, 1982; Teubner et al., 2003; Walsby et al., 2004). The presence of *Planktothrix* at all investigated depths, even at 45 m depth both during and after thermal stratification, indicates an acclimation to water temperatures as low as 5°C, thus ensuring their winter survival (Walsby, 2005; Holland and Walsby, 2008; Dokulil and Teubner, 2012).

3.5.4 Deep chlorophyll maxima and metalimnetic oxygen minimum

In Lake Tiefer See, the deep chlorophyll maxima (DCM) formed by *Cyanobium* ASV0008/*Synechococcus* (7 m; spring), *Cyanobium* ASV0005 (7 m; fall) and *Planktothrix* (10 – 15 m; spring to fall) probably result from the adaptation of these taxa to both low nutrients and light intensity in the thermocline (Walsby et al., 2004; Callieri et al., 2007). This suggests ecotype and niche specialization as well as coexistence among the DCM-forming taxa in Lake Tiefer See. The coexistence may be explained by their different responses to environmental factors such as light and nutrient (NO_3^- and TDP) availability (Selmeczy et al., 2016). For example, the requirements for different degrees of light intensity might explain the *Planktothrix* and *Synechococcus* summer peak relative abundances at 10 m and 7 m water depths, respectively. In the nearby Lake Stechlin spatial segregation and coexistence of DCM forming cyanobacteria was reported with *Aphanizomenon* as a main contributor (Selmeczy et al., 2016). Similar observations of the coexistence and niche specialization among cyanobacterial taxa with red and green pigments along the light gradient were reported for several aquatic ecosystems (Pick and Agbeti, 1991; Vörös et al., 1998; Stomp et al., 2007). The heterotrophic decomposition of the DCM-forming taxa as indicated by the qPCR results would explain consumption of dissolved oxygen (11 and 13 m; Fig. 3.2B) between August and November (Gerphagnon et al., 2015). The development of a metalimnetic oxygen minimum indicates that enhanced particle retention time in this relatively denser region, favors heterotrophic decomposition of organic matter (Wentzky et al., 2019; Mi et al., 2020).

3.6 Conclusion

This study provides the first detailed seasonal survey of the dynamics of cyanobacteria community composition, spatial distribution and abundance in the deep hard-water Lake Tiefer See. Combining high-throughput sequencing and ASV analysis enables to reveal freshwater cyanobacteria dynamics on a high taxonomic resolution and suggests niche separation and coexistence of individual cyanobacterial species. At the same time, the study underlines limitations of purely DNA-based pelagic surveys in providing evidence for potentially novel, cold-adapted cyanobacterial species whose occurrence is suggested here.

3.7 Acknowledgements

We thank the German Environmental Foundation (Deutsche Bundesstiftung Umwelt DBU) for funding the research position of EN. The monitoring equipment was funded by the Terrestrial Environmental Observatory Infrastructure Initiative of the Helmholtz Association (TERENO Observatory NE Germany). This study was also supported by the Leibniz Association grant SAW-2017-IOW-2 649 „BaltRap: The Baltic Sea and its southern Lowlands: proxy – environment interactions in time of rapid change“, and the „Climate signal transfer to varved sediments in Lake Tiefer See Klocksin – Monitoring, Transfer functions, Reconstructions“ awarded to AB. We thank the technical team of GFZ-section Climate Dynamics and Landscape Evolution who assisted in the fieldwork, especially Brian Brademann. We thank Jens Kallmeyer (GFZ-section Geomicrobiology) for assisting with nitrate measurements, Olaf Dellwig (IOW- Marine Geology) for assisting with TDP measurements, and Anne Köhler for support in the ICP lab at the IOW. We also want to thank Alexander Bartholomäus (GFZ-section Geomicrobiology) for additional help with bioinformatics and insightful result interpretation that improved the manuscript. The authors have declared no conflicts of interest.

4 Manuscript III – Cyanobacteria sediment deposition

"From Water into Sediment—Tracing Freshwater Cyanobacteria via DNA Analyses"

4.1 Abstract

Sedimentary ancient DNA-based studies have been used to probe centuries of climate and environmental changes and how they affected cyanobacterial assemblages in temperate lakes. Due to Cyanobacteria containing potential bloom-forming and toxin-producing taxa, their approximate reconstruction from sediments is crucial, especially in lakes lacking long-term monitoring data. To extend the resolution of sediment record interpretation, we used high-throughput sequencing, amplicon sequence variant (ASV) analysis, and quantitative PCR to compare pelagic cyano-bacterial composition to that in sediment traps (collected monthly) and surface sediments in Lake Tiefer See. Cyanobacterial composition, species richness, and evenness was not significantly different among the pelagic depths, sediment traps and surface sediments ($p > 0.05$), indicating that the Cyanobacteria in the sediments reflected the cyanobacterial assemblage in the water column. However, total cyanobacterial abundances (qPCR) decreased from the metalimnion down the water column. The aggregate-forming (*Aphanizomenon*) and colony-forming taxa (*Snowella*) showed pronounced sedimentation. In contrast, *Planktothrix* was only very poorly represented in sediment traps (meta- and hypolimnion) and surface sediments, despite its highest relative abundance at the thermocline (10 m water depth) during periods of lake stratification (May–October). We conclude that this skewed representation in taxonomic abundances reflects taphonomic processes, which should be considered in future DNA-based paleolimnological investigations.

4.2 Introduction

Anthropogenic environmental changes continue to affect the community dynamics of the ancient and widespread bacterial phylum cyanobacteria (Vitousek et al., 1997; Fischer et al., 2016). In some temperate oligo-mesotrophic lakes, warming and prolonged stratification have led to the dominance of toxin-producing species belonging to *Planktothrix*, *Dolichospermum*, and *Microcystis*, despite a reduction in nutrient inputs

(Dokulil and Teubner, 2012; Posch et al., 2012). Due to the ecological impact of cyanobacteria in aquatic ecosystems, such as toxic bloom formation (Huisman et al., 2018), their reconstruction from aquatic sediments serving as environmental archives could provide vital information regarding their history and earlier conditions in a water body (Cronberg, 1986).

Early paleolimnology studies reconstructed the occurrence of cyanobacteria in freshwater sediments by targeting their remains, e.g., the akinetes of *Aphanizomenon* and *Anabaena* (Livingstone and Jaworski, 1980; van Geel et al., 1994) or pigments (Hertzberg et al., 1971; Sanger, 1988; Leavitt and Findlay, 1994). Findings from these earlier studies established our understanding of the long-term survival of cyanobacteria remains in sediments and how they could be used to track pelagic dominance of cyanobacteria in lakes (Swain, 1985; Sanger, 1988), thus establishing a basis upon which molecular-based paleolimnology studies began (Coolen and Overmann, 1998).

Combining (paleo)limnology with DNA-based tools has gained popularity in recent times because of the high taxonomic resolution they provide (Domaizon et al., 2013). For example, targeting the 16S rRNA gene revealed a novel pico-cyanobacteria clade in the sediments of a glacial lake (Jasser et al., 2011), and resulted in the identification of higher diatom species diversity in a tropical lake (Stoof-Leichsenring et al., 2012). Targeting of methane-oxidizing genes in bacteria revealed possible methanotrophy in lake sediments (Belle and Parent, 2019). As DNA-based techniques available for paleolimnology studies continue to advance, the amount of new information on ancient organisms has increased (Leavitt, 1993; Domaizon et al., 2013), as has the demand for paleolimnological studies on past abiotic–biotic relationships (Domaizon et al., 2017).

With the increase in sedimentary ancient DNA (sedaDNA) studies in the last decade, there is a need to verify the congruence between sediment-archived DNA and the pelagic communities that acted as seeds, as well as to assess potential taphonomic processes, i.e., alteration or deterioration of DNA during transport and at the sediment–water interface under prevailing environmental conditions (Capo et al., 2015, 2021; Domaizon et al., 2017). There is a need to verify congruence, in particular, because taphonomic processes could lead to the underrepresentation of certain groups in sedimentary records (Pedersen et al., 2015; Giguet-Covex et al., 2019; Ellegaard et al., 2020). A common approach used to substantiate sedaDNA information has focused on comparing molecular data obtained from

the water column and short sediment cores (up to 30 cm) for planktonic protists (Capo et al., 2015). Recently, Gauthier et al. used DNA-based methods on sediment trap and water samples to trace eukaryotic communities that deposit in sediment traps from the water column (Gauthier et al., 2021). For cyanobacteria, consistency between historical microscopic data and sedimentary DNA have been shown (Monchamp et al., 2016).

To date, our understanding of how representative sediment-deposited cyanobacteria are for those in the water column is, however, still restricted to a few studies. Among these, lakes whose sediments serve as highly resolved paleo-archives are not well represented. Therefore, this study investigated the congruity between pelagic and sediment-deposited cyanobacteria communities in Lake Tiefer See, a well-studied climate archive and monitoring site located in northeastern Germany. Specifically, we tracked changes in cyanobacterial sedimentation by generating monthly DNA-based high-throughput sequence and abundance data from the water column (covering the epi-, meta-, and hypolimnion), sediment traps (meta- and hypolimnion), and surface sediments (0–2 cm). We used a highly resolved dataset to assess the suitability of sediment-deposited cyanobacterial assemblages as proxies for lake internal physicochemical parameters by correlating cyanobacteria dynamics with daily to monthly resolved water column temperature, pH, dissolved oxygen (DO), turbidity, nitrates, and total dissolved phosphorus (TDP).

4.3 Materials and Methods

4.3.1 Study site

The hard-water oligo-mesotrophic Lake Tiefer See (near Klocksin; 53°35.5′N, 12°31.8′E; 62 m a.s.l.) is part of the southern Baltic Lake District and was formed during the final stage of the last glacial period (~13,000 years ago; Figs 4.1a,b; Suppl. Information. C.1). Lake Tiefer See is part of a subglacial gully system in a morainic terrain located in Nature Park „Nossentiner/Schwinzer Heide“. Lake Tiefer See has a surface area of approximately 0.75 km^2, a catchment area of approximately 5.5 km^2 dominated by glacial till and a maximum depth of 62 m with no major inflows or outflow. Lake Tiefer See has been the focus of an extensive and high-resolution climate monitoring program since the beginning of the last decade (Roeser et al., 2021). The lake is well-preserved and seasonally laminated

sediments have aided climate reconstructions spanning the last 6000 years (Dräger et al., 2019).

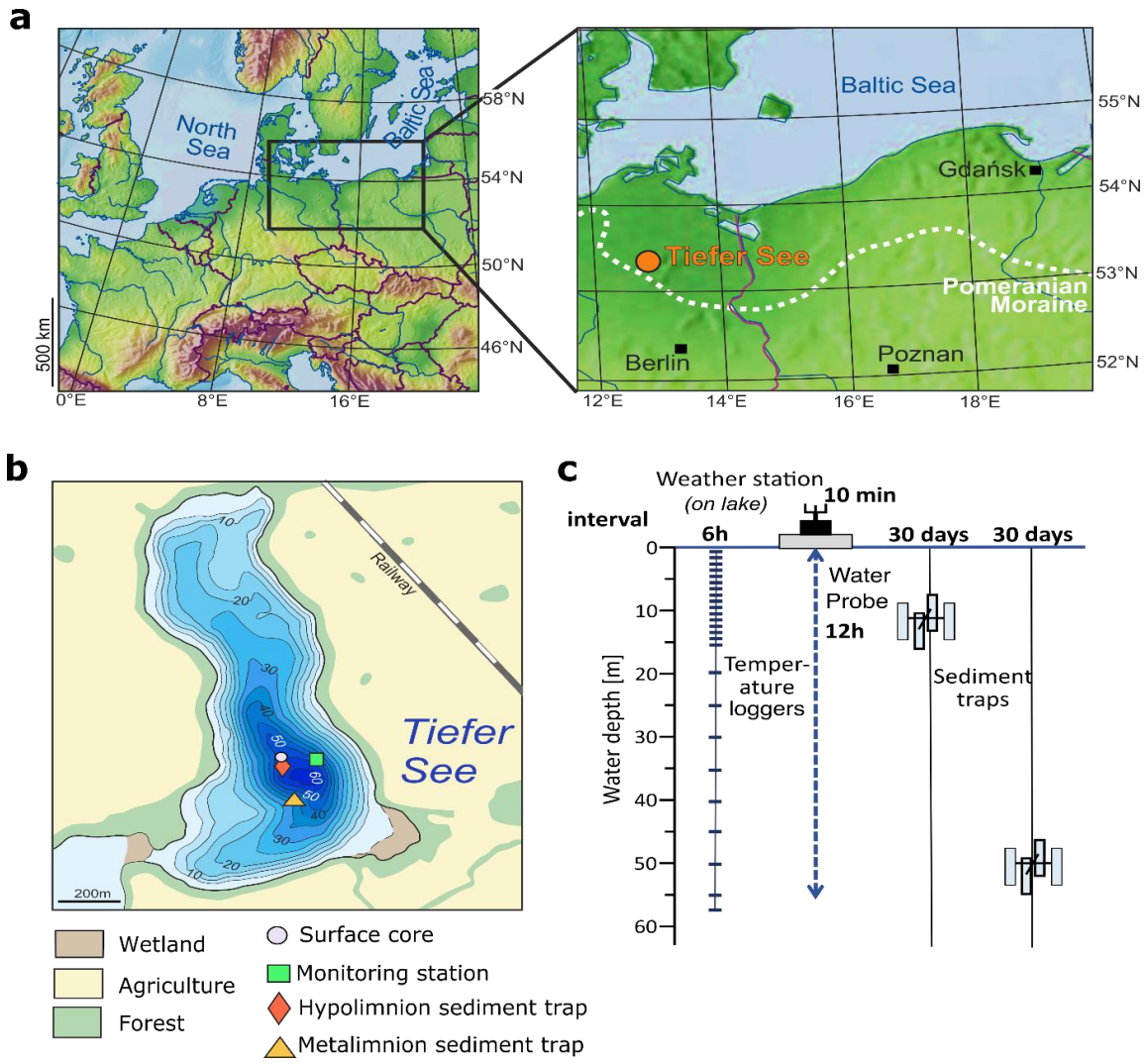

Figure 4.1: Location of the study site and information on the monitoring setup. (**a**) The location of Lake Tiefer See near Klocksin (TSK, northeastern Germany); (**b**) A bathymetric map of Lake Tiefer See showing the sites of climate monitoring stations, water sampling, sediment traps, and surface core extraction, and (**c**) A scheme of lake monitoring setup showing depths of water column, temperature loggers, and depths at which the sediment traps are anchored.

4.3.2 Collection of Water, Sediment Trap Material, and Sediment Cores

Water samples were collected monthly between January 30 and November 28 in 2019 at the floating weather monitoring station, located at the maximum depth of the lake (62 m; Fig. 4.1b). The sampled water depths were 1, 3, 5, 7, 10, 15, 20, 40, 45, and 50 m. A sample

volume of 250 mL of lake water was collected for the upper 1, 3, and 5 m water depths and pooled (750 mL), representing the epilimnion. Likewise, 375 mL volumes were collected for the lower 45 and 50 m water depths and pooled (750 mL), representing the bottom waters. For each of the other 7, 10, 15, 20, and 40 m water depths, 750 mL water samples were collected. Samples were collected in sterile glass bottles (Schott Duran®, Mitterteich, Germany), filtered within 24 h after fieldwork using 0.2 µm cellulose filters (Sartorius AG, Göttingen, Germany). Filters were stored at −20 °C until nucleic acid extraction.

Suspended particulate matter was collected using four-cylinder traps (KC Denmark A/S, total active area 0.0163 m^2 for the four cylinders) at two depths in the water column (Fig. 4.1c). One trap was anchored in the metalimnion (12 m water depth), and the second trap was secured in the hypolimnion (55 m water depth). For both depths, the traps were emptied monthly between April and November 2019, i.e., the annual interval of increased lake productivity. The trapped material was transferred into 2 L plastic bottles, which were allowed to settle overnight at 4 °C. About 1200 mL of water was discarded from the bottles, and the remaining suspension was transferred into sterile 50 mL Falcon tubes (Fischer Scientific GmbH, Schwerte, Germany). Tubes containing suspended particulate matter were then centrifuged at 4000×*g* for 5 min. Subsequently, the supernatant was discarded, and the pellet was stored in 50 mL Falcon tubes at −20 °C until nucleic acid extraction.

A surface sediment core (TSK19-SC6; 115 cm length) was collected on August 29, 2019, from the point of maximum water depth (62 m) using a 90 mm UWITEC piston corer. The temperature of the upright positioned core was maintained at 4 °C during transportation and short-term storage at the facilities of the GFZ Potsdam. To preserve the uppermost varves, the core was allowed to dry in a vertical position at 4 °C for approximately 2 weeks before longitudinal splitting. After splitting the core, one half was lithologically described. A triplicate 0–2 cm subsample of the other core half was stored in sterile 15 mL Falcon tubes at −20 °C until nucleic acid extraction. All core handling was performed under clean conditions in a room where no molecular biological work had been previously conducted to avoid contamination.

4.3.3 Lake Physicochemical Properties

Water column temperature, pH, DO, turbidity, and chlorophyll-a (Chl*a* which we used as an indicator of phytoplankton biomass production) were measured using a multi-parameter water quality probe (YSI 6600 V2, Yellow Springs, Greene, OH, USA), in 1 m steps and 12 h resolution. Owing to technical problems, in February data were only collected on 2 d (1st and 28th), and in March no data were recorded between the 2nd and 10th. Water temperature was additionally measured using 26 stationary data loggers (HOBO Water Temp Pro v2, Onset USA) in 1 m steps from 0 to 15 m and 5 m steps from 15 to 55 m water depth (Fig. 4.1c). Water samples for nitrate (NO_3^-) and total dissolved phosphorus (TDP) analyses were also collected monthly, in parallel with those for molecular analysis. Water samples for total sulfide were collected from the hypolimnion in October and November. Nitrate was measured by suppressed ion chromatography using a SeQuant SAMS anion IC suppressor (EMD Millipore, Billerica, MA, USA), an S5200 sample injector, a 3.0 × 250 mm LCA 14 column, and an S3115 conductivity detector (all Sykam, Fürstenfeldbruck, Germany). The TDP was measured by inductively coupled plasma optical emission spectrometry (ICP-OES; iCAP 7400, Duo, Thermo Fisher Scientific, Berlin, Germany) using external calibration and Sc as the internal standard.

Sediment fluxes (in g m^{-2} d^{-1}) were determined from the weighted and freeze-dried trapped sediment material. Total carbon (TC), total organic carbon (TOC, and total nitrogen (TN) contents were measured continuously at 1 cm increments from bulk samples as described by Dräger et al. (2019) using the elemental analyzers NC2500 and EA3000-CHS Eurovectors, respectively. Briefly, TIC and TN were measured from 5 mg of sediment in tin capsules, while TOC was examined by decalcifying 3 mg of sediment in Ag capsules by treating with 3% HCl, 20% HCl, and drying at 75 °C. The TOC and TN values were used to calculate the atomic C:N ratio. Calcium carbonate ($CaCO_3$) was estimated after obtaining the total inorganic carbon content (TIC = TC–TOC) and multiplying by a factor of 8.33, which is the percentage of molecular weight in inorganic carbon in the calcium carbonate structure.

4.3.4 Molecular Analyses

All monthly water samples plus two depths of sediment traps in four biological replicates and the surface sediments were processed independently from each other and at different times to avoid cross-contamination. Due to a mixed water column in January and February, water samples for molecular analyses from 1, 3, 5, 7, and 10 m water depths were pooled and reported as the mean depth (5 m). Water depths of 40, 45, and 50 m were equally pooled and reported as the mean depth (45 m). In March, when temperatures began to increase, four depths in the water column were reported as follows: 5 (1, 3, 5, and 7 m pooled), 10, 20, and 45 m (40, 45, and 50 m pooled). Genomic DNA, PCR amplification, library preparation and bioinformatics were carried out as described in supplementary information. Briefly, DNA from water samples was extracted from the filters using the DNeasy PowerWater Kit (QIAGEN, Hilden, Germany) following the manufacturer's specifications. The DNA from the homogenized sediment trap samples and surface sediment samples was extracted from approximately 0.75 g using the DNeasy PowerSoil Kit (QIAGEN, Hilden, Germany). DNA concentrations for both water, sediment trap, and surface sediment samples were measured using a Qubit (2.0) Fluorometer (Invitrogen, Carlsbad, CAL, USA) highly selective for double-stranded DNA following the manufacturer's instructions (Qubit ds-DNA HS Assays, Invitrogen, Carlsbad, CAL, USA). Total cyanobacteria were quantified with a SYBR Green quantitative PCR (qPCR) assay that specifically amplified the cyanobacterial 16S rRNA-ITS (internal transcribed spacer) region. Each water sample was quantified in triplicates and the four biological replicates (i.e., four cylinders) from the monthly meta- and hypolimnion sediment trap samples were each quantified separately in triplicates. The values were calculated following Savichtcheva et al. (Savichtcheva et al., 2011), and expressed as cyanobacterial abundance normalized to extracted DNA (copies ng^{-1} DNA).

The PCR for the Illumina high-throughput sequence libraries was conducted using the cyanobacteria-specific primers CYA359F (5′-CGGACGGGTGAGTAACGCGTG-3′) and CYA784R (5′-ACTACWGGGGTATCTAATCCC-3′) (Nübel et al., 1997) which amplify a >400 nt long fragment of the V3–V4 regions of the 16S rRNA gene. The primers had unique tags (Suppl. Table C.1) that served to differentiate the samples. The PCR products were purified with the Agencourt AMPure XP kit (Beckman Coulter, Brea, CA, USA) and quantified using a Qubit (2.0) fluorometer (Invitrogen). Equimolar concentrations of all

samples, including two negative purified PCR controls, were pooled into two multiplex libraries (*n* = 160 samples, including 78 samples and 2 controls per library), which were paired-end sequenced (2 × 300 bp) on an Illumina MiSeq system (Eurofins Scientific; Constance, Germany).

4.3.5 Bioinformatics and sequence processing

Sequencing data and metadata are deposited in the European Nucleotide Archive (ENA) under BioProject accession number PRJEB40406 and sample accession numbers ERS5083533—ERS5083564 (trap material and surface sediment samples) and ERS5083566—ERS5083644 (water samples) and processed as described in Figure S1. Briefly, the obtained 14,649,824 sequence reads were quality checked on a raw FASTQ file with FastQC v0.11.8 (Andrews et al., 2015)**,** on a local machine. The reads were then demultiplexed using the make.contigs function in Mothur (v.1.39.5) (Schloss et al., 2009). Based on the report files, the sequence identifiers were retrieved for those sequences with minimum overlap (length >25), maximum mismatches (<5), and the maximum number of ambiguous bases of zero (which means there was no base marked with N′). The 160 samples resulted in a total of 7,297,946 denoised and error-corrected sequences that DADA2 (Callahan et al., 2016) inferred in 2538 ASVs. We filtered out non-cyanobacteria ASVs, chloroplasts, rare taxa, and negative controls. In total, the filtered dataset comprised 2,031,142 sequence reads in 559 ASVs assigned to photosynthetic cyanobacteria and distributed across 64 samples (Suppl. Table C.1). Of the 559 ASVs, 19 were assigned to the order level, 61 to the family level, and 479 to the genus level (86% of all cyanobacteria ASVs; 2,025,258 read counts). We presented the distribution of shared and unique ASVs among the sample types in a Venn diagram (Suppl. Fig. C.1).

4.3.6 Data Treatment and Statistics

To compare differences in cyanobacteria assemblage from water, sediment traps, and surface sediments, we transformed ASV absolute read counts into relative abundances. To simplify the presentation of the cyanobacteria assemblage data, the mean relative abundances for each water (3, 5, 7, 10, 15, 20, and 45 m) and sediment trap sampled (meta- and hypolimnion) depths were merged as shown in bubble plot in Figure 4.3a. In Suppl. Fig. C.2a, we present the highly-resolved cyanobacteria composition from all sample

matrices. Bubble plots were plotted using the free software tool (http://shiny.raccoome.de/bubblePlot/). To compare the differences in cyanobacteria abundance (qPCR) between the sample matrices, the mean copies ng DNA^{-1} for each sampled water depth (3, 5, 7, 10, 15, 20, and 45 m) was calculated. For the sediment traps, the mean of the four biological replicates of each monthly meta- and hypolimnion trap was calculated, followed by calculating the mean of all months (8 months) for the meta- and hypolimnion trap as shown in Figure 3b. In Suppl. Fig. C.2b, we present the highly-resolved cyanobacteria abundance data from all sample matrices.

Alpha and beta diversity estimations, ANOVA, and Tukey's pairwise test for alpha diversity boxplots, correlations of the ASV composition with physicochemical parameters, and similarity percentage (SIMPER) analysis, as well as multivariate permutational analysis of variance (PerMANOVA) were performed using the PAST v4.01 software (Hammer et al., 2001). Prior to alpha diversity (richness, Shannon diversity and Pielou's evenness), the ASV read counts were rarefied to account for differences in sequencing depth (2200 read counts per sample) using the "rtk" package in R (Saary et al., 2017). Since the biological triplicates of the surface sediment samples are from one core, we pooled them into the mean of one sample before calculating alpha and beta diversity. The water column samples were further grouped into thermal stratification zones, that is, epi-, meta-, and hypolimnion, whereas sediment trap samples were grouped into meta- and hypolimnion, and the surface 0–2 cm of the sediment. A one-way ANOVA was used to test for significant seasonal change in species richness and evenness within each stratification zone followed by a Tukey's test. Cyanobacteria absolute read counts were Hellinger-transformed prior to beta diversity analysis and the subsequent PerMANOVA test (Legendre and Gallagher, 2001). Clustering patterns of the cyanobacteria community from all sample matrices were assessed using Bray–Curtis dissimilarity in a non-metric multidimensional scaling analysis (NMDS). The PerMANOVA analysis was then used to test for significant community differences within and among the samples. SIMPER analysis, also based on Bray–Curtis dissimilarity, was used to calculate the taxa similarity contributions among the sample types. The environmental data from water and sediment traps were standardized by subtracting the mean and dividing by the standard deviation (z-score) prior to principal component analyses (PCAs) based on the Euclidean distance. Due to the very distinct density and resolution data, PCAs were performed for all physicochemical water parameters and trapped material composition data to assess

similarities within the sample types (Suppl. Fig. C.3). To control for the effect of confounders in the explanatory variables dataset, collinearity was tested with a variance inflation factor (VIF) using the "vif.cca" function in vegan in R (Oksanen et al., 2019). Explanatory variables were then additively tested until only those with a VIF score <10 remained. The significant subset of the explanatory variables for community composition was determined via forward selection using the function "ordiR2step" function in vegan. A rank-based Spearman correlation coefficient was used to calculate the correlations of cyanobacterial community data from the water column and hypolimnion sediment trap (relative abundances of total and most abundant ASVs from all samples, 16S rRNA-ITS gene abundance, and Shannon diversity indices) to a significant subset of physicochemical parameters (temperature, pH, DO, turbidity, NO_3^-, and TDP) with the Bonferroni *p*-value correction. The physicochemical parameters and cyanobacterial community data were the explanatory and response variables, respectively.

4.4 Results

4.4.1 Physicochemical Properties of Pelagic Water and Trap Material

Temperature and DO in the water column of Lake Tiefer See showed that thermal stratification began in early April 2019 and ended in late November, with a thermocline between 7 and 13 m water depth (Figs. 4.2a,b). Oxygen depletion in the bottom water began 3 weeks after thermal stratification and the onset of pelagic productivity, as revealed by Chl*a* and DO (Figs. 4.2b,e). The DO reached minimum values (~0.67 mg L^{-1}) at 40–50 m water depth between October and December (Fig. 4.2b). In October and November 2019, total sulfide concentrations were found to gradually increase below 53 m water depth, from ~2 µmol L^{-1} to ~45 µmol L^{-1}, respectively (Suppl. Table C.2). Lake Tiefer See developed a zone of a metalimnetic oxygen minimum between 10 and 12 m from June to September. Turbidity reached higher values between 5 and 6 NTUs in summer in the upper water column (down to 10 m) because of bio-productivity and calcite formation (Fig. 4.2c). In the hypolimnion, turbidity values reached 6 NTUs, because of resuspension in spring and autumn (April and September). Pelagic nitrate values ranged between 1 and 2 µg L^{-1}, except in October and November, when they only reached 0.2 µg L^{-1} (Suppl. Table C.3). The values of TDP (Fig. 4.2f) were generally higher in the hypolimnion, gradually

increasing from July through November, reaching up to 67 µg L^{-1} in the bottom waters. In contrast, the TDP values in the epilimnion ranged between 8 and 15 µg L^{-1}, except in January and February, when the lake was in an isothermal state and the TDP values were between 20 and 25 µg L^{-1} throughout the mixed water column. The overall pattern of seasonal physicochemical changes and the TDP distribution in Lake Tiefer See throughout the year agrees with the behavior in the previous 5 years (Roeser et al., 2021).

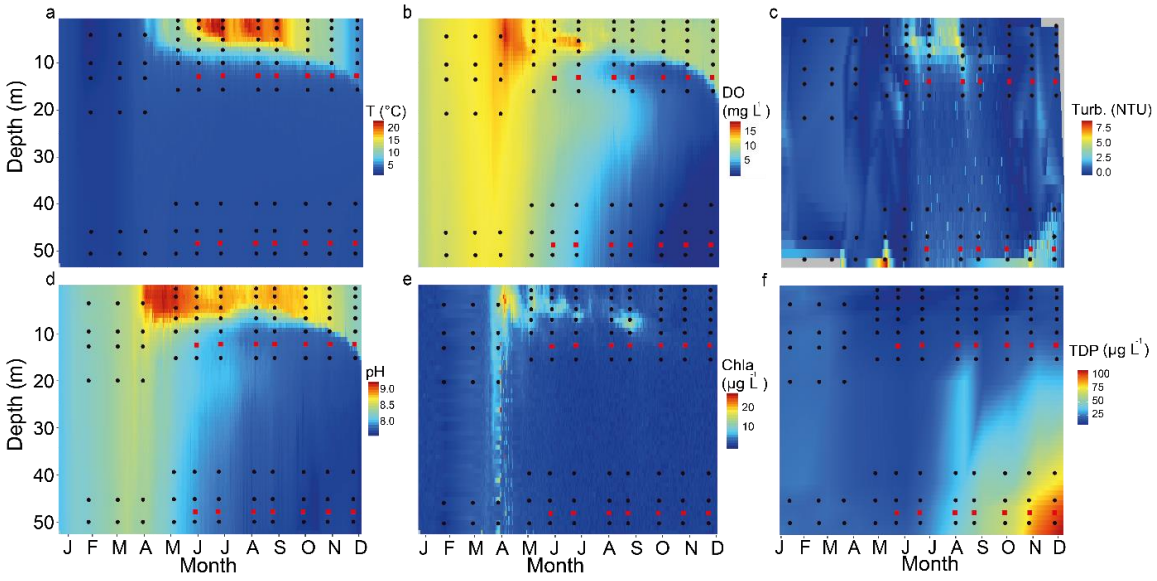

Figure 4.2: Physicochemical parameters from Lake Tiefer See. Heatmaps of physicochemical parameters for 2019 measured using a multi-parameter water quality probe in the water column of Lake Tiefer See showing (**a**) Temperature (T); (**b**) Dissolved oxygen (DO); (**c**) Turbidity (Turb.); (**d**) pH; (**e**) Chlorophyll-a (Chl*a*), and (**f**) Total dissolved phosphorus (TDP). Data are interpolated for 1 d and 1 m water depth. Black circles and red squares represent the depths and timing of sampling of water and sediment traps, respectively.

During the 1-year cycle, the overall suspended matter accumulation in the metalimnion sediment trap peaked from May to June at 3 g m^{-2} d^{-1}. From October to November, particulate deposition at a water depth of 12 m decreased to ~1 g m^{-2} d^{-1} (Fig. 4.3). In the hypolimnion, maximum particulate deposition was reached between June and July, with 4 g m^{-2} d^{-1} (Fig. 4.3). The composition of the trapped material showed an overall contrasting value in the atomic C:N ratio during summer between the meta- (mean 7.5) and hypolimnion (mean 8.4), except in July when the ratio in both meta- and hypolimnion traps was 7.6 (Fig. 4.3). In October and November, TOC, and TN fluxes at the bottom waters (hypolimnion traps) were practically absent, although fluxes of 0.2 g m^{-2} d^{-1} TOC and 0.02 g m^{-2} d^{-1} TN were measured in the metalimnion trap (Fig. 4.3).

Principal component analyses (PCAs) showed that in the water column, the variance was mostly explained by Chl*a*, DO, temperature, and turbidity, with 64% of the variance distributed along the two main principal components, PC1 (44%) and PC2 (20%; Suppl. Fig. C.3a). From the trapped sediment composition data, the two main principal components together explained 77% of the total variance, and PC1 accounted for 59% of the variance (Suppl. Fig. C.3b). The variables TN, TOC, and sediment deposition rate mainly explained the variance among these samples.

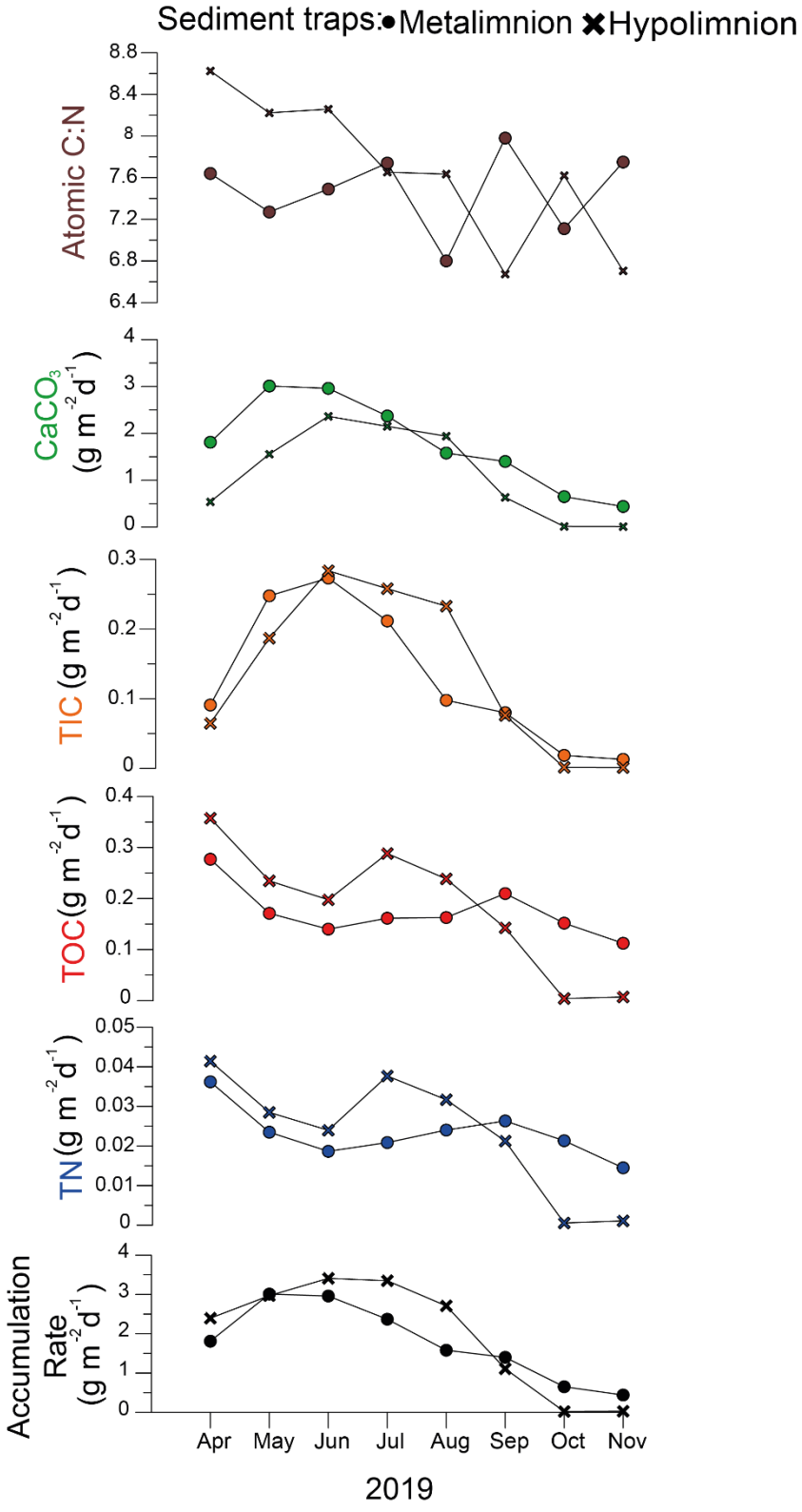

Figure 4.3: The results of geochemical analysis carried out on sediment trap samples from Lake Tiefer See showing sediment accumulation rate, total nitrogen (TN), total organic carbon (TOC), total inorganic carbon (TIC), calcium carbonate (CaCO3), and atomic TOC and TN ratio (atomic C:N).

4.4.2 Cyanobacteria Community Structure

Of the 559 total photosynthetic cyanobacteria ASVs in this study, only 26 had a relative abundance of ≥1% in the water column, sediment trap material, and surface sediment samples (Fig. 4.4a; Suppl. Fig. C.2a). They included 16 ASVs assigned to the unicellular pico-*Cyanobium* (order Synechococcales), two ASVs assigned to *Aphanizomenon* (Nostocales), *Planktothrix* (Oscillatoriales), *Snowella*, *Synechococcus* (Synechococcales), and *Microcystis* (Chroococcales). The abundance of the 26 ASVs varied among the sample types. The ASVs 0010 and 0012 assigned to *Cyanobium* and all ASVs assigned to *Aphanizomenon* were more abundant in trapped material (≥10%) than in the corresponding zone in the water column (≤5%). Within this group of ASVs, ASV0004 assigned to *Aphanizomenon* was the most dominant, with ≥30% relative abundance. Conversely, ASVs assigned to *Planktothrix*, ASV0021 assigned to *Synechococcus*, and ASVs 0008, 0013, 0015, 0019, and 0031 assigned to *Cyanobium* were more abundant in the water column (≥ 10%) but not commensurate in the sediment traps. In this group of ASVs, ASV0006 assigned to *Planktothrix* was the most prominent, but despite having a maximum abundance (>40%) in the water column in August and October (10 and 15 m), its relative abundance was low (<2%), even in the metalimnion trap at ~12 m water depth (Fig. 4.4a; Suppl. Fig. C.2a). Additionally, we observed some taxa with comparable abundances across the different water and sediment matrices, including ASVs assigned to *Microcystis*, *Snowella*, ASVs 0028, 0054 (<10%), and ASVs 0005 and 0014, assigned to *Cyanobium* (Suppl. Fig. C.2a).

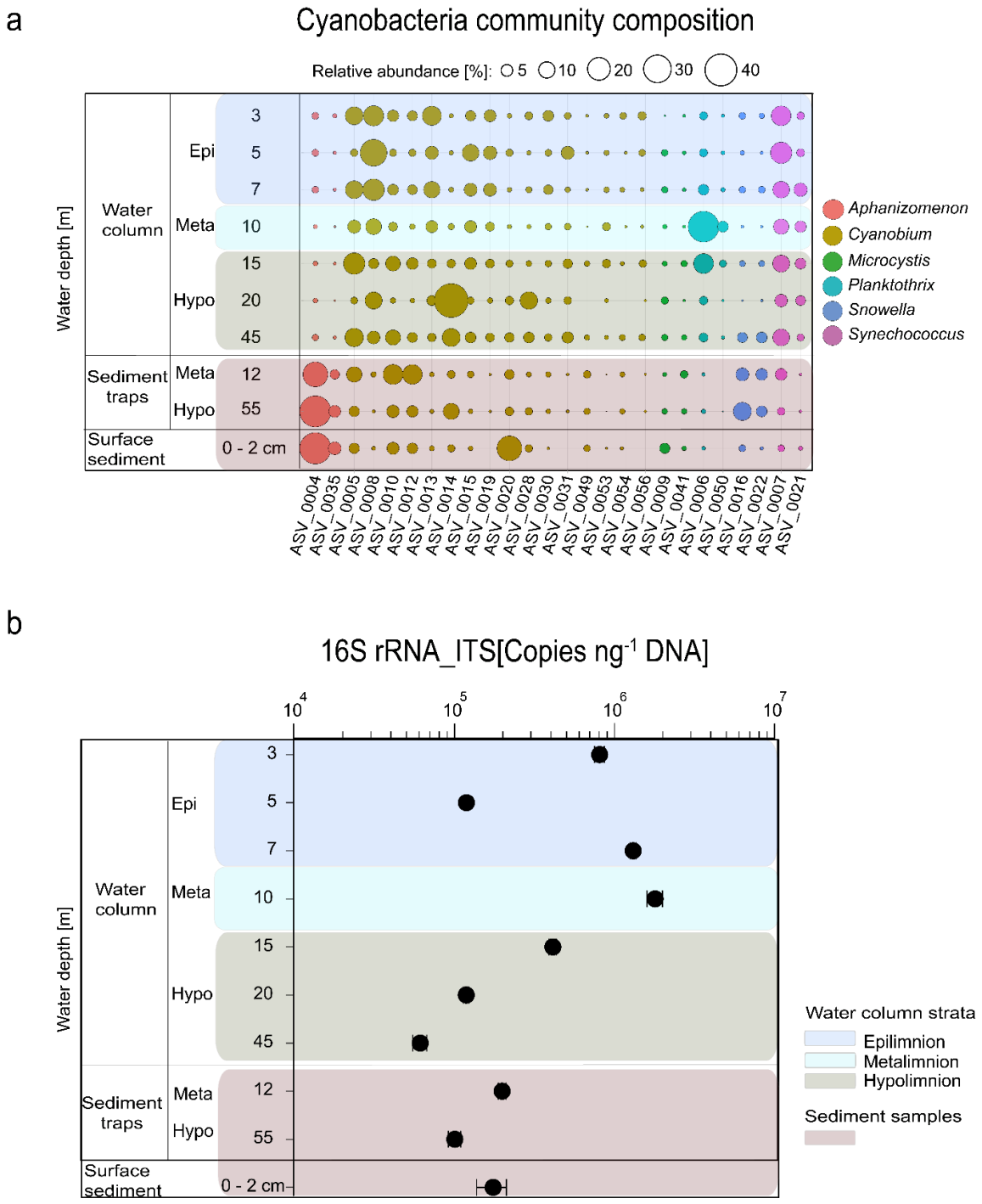

Figure 4.4: Cyanobacteria community composition and abundance in Lake Tiefer See water, trapped material, and sediments. (**a**) Bubble plot showing mean relative abundances for 2019 of the most abundant cyanobacteria amplicon sequence variants (>1% reads) in the water column, sediment traps and surface sediments, and (**b**) Mean cyanobacterial abundance for 2019 in the water column, sediment traps, and surface sediments quantified via qPCR with primers that amplified part of the 16S rRNA internal transcriber spacer (ITS) region of cyanobacteria (data were normalized to ng DNA extracted). Epi = epilimnion, meta = metalimnion, and hypo = hypolimnion.

Cyanobacteria Abundance

In the water column, the highest mean abundance of the cyanobacterial 16S rRNA-ITS gene copy numbers was recorded in the metalimnion (10 m, $n = 9$, 1.8×10^6 copies ng^{-1} DNA; Fig. 4.4b). The mean abundances in the epi- and hypolimnion of the water column were 9.8×10^5 ($n = 19$) and 2.3×10^5 ($n = 19$) copies ng^{-1} DNA, respectively. The mean abundance of the cyanobacterial 16S rRNA-ITS gene copy numbers in the water column was higher (7.9×10^5 copies ng^{-1} DNA) than those of the trapped (1.49×10^5 copies ng^{-1} DNA) and surface (6.94×10^5 copies ng^{-1} DNA) sediments, respectively. The mean abundance of cyanobacterial 16S rRNA-ITS gene copy numbers was 2.2×10^5 and 1.4×10^5 copies ng^{-1} DNA in the meta- and the hypolimnion sediment traps, respectively.

4.4.3 Alpha and Beta Diversity

Mean cyanobacteria species richness was higher in the sediments (trapped and topmost $n = 17$, mean = 50) than in the water column ($n = 47$, mean = 41; Fig. 4.5a). A one-way analysis of variance (ANOVA) test revealed significant variation in cyanobacteria species richness between the water (epi-, meta-, and hypolimnion) and sediment traps (meta- and hypolimnion; $p = 0.006$; Fig. 4.5a, Suppl. Table C.4). A subsequent Tukey's pairwise test showed that richness did not significantly differ between the meta- and hypolimnion traps, as well as among the distinct lake strata in the water column ($p > 0.05$). The difference in richness between the hypolimnion sediment trap and metalimnion of the water column was marginal ($p = 0.04$). The cyanobacteria subpopulations among the sample types did not significantly vary in evenness ($p > 0.05$; Fig. 4.5b).

Bray–Curtis dissimilarity in non-metric multidimensional scaling (NMDS) was used to visualize the beta diversity patterns among the sample types (Fig. 4.5c). The NMDS revealed cyanobacterial community clusters of trap material and surface sediments that were distinct from those of the water column. Within the water column, the overlapping water samples likely resulted from homogenous water when the water column was mixed (Fig. 4.5c). The solitary samples separated from the overlap represent the summer months where a stronger difference in community and environmental parameters occurred because of thermal stratification. A one-way permutational analysis of variance (PerMANOVA) test revealed that there was no significant difference between the meta- and hypolimnion subpopulations of the sediment traps ($p = 1$). The epi- and hypolimnion subpopulations of

the water column also did not differ from each other (p = 0.08). Similarly, the relative abundance of the cyanobacterial subpopulation from the surface sediment (0–2 cm) was not different from those of the water column (p > 0.7) and from those of the sediment traps (p = 1; Table 4.1). A similarity percentage analysis (SIMPER; Suppl. Table C.5) on the ASVs >1% revealed that ASV0004 assigned to *Aphanizomenon* was the strongest (9.34%) contributor to community similarity across pelagic, trapped, and surface sediments.

Table 4.1: One-way PerMANOVA on cyanobacterial communities grouped into epi-, meta-, and hypolimnion in the water column, meta-, and hypolimnion of the sediment traps and surface sediments. Summary presents overall test statistics. Pairwise analysis shows Bonferroni corrected *p*-values (values in bold are significant at p < 0.05) above the diagonal and corresponding *F*-values below. Where „W“ indicates water column samples from the epi-, meta- and hypolimnion. The „ST“ indicates sediment trap material from the meta- and hypolimnion and „Sed“ represents the surface sediment samples.

PERMANOVA		**Pairwise**	**Epi**	**Meta**	**Hypo**	**TrapM**	**TrapH**	**Sed**
Summary		**Epi**		**0.012**	0.0775	**0.0015**	**0.0015**	0.786
Permutation N:	9999	**Meta**	3.962		**0.027**	**0.0015**	**0.0015**	0.8835
Total sum of squares:	8.29	**Hypo**	3.244	4.66		**0.0015**	**0.0015**	1
Within-group sum of squares:	5.438	**TrapM**	8.943	10.24	5.544		1	1
F:	6.085	**TrapH**	11.15	12.78	6.638	0.4568		1
p (same):	**0.0001**	**Sed**	4.397	5.151	4.244	0.7717	1.116	

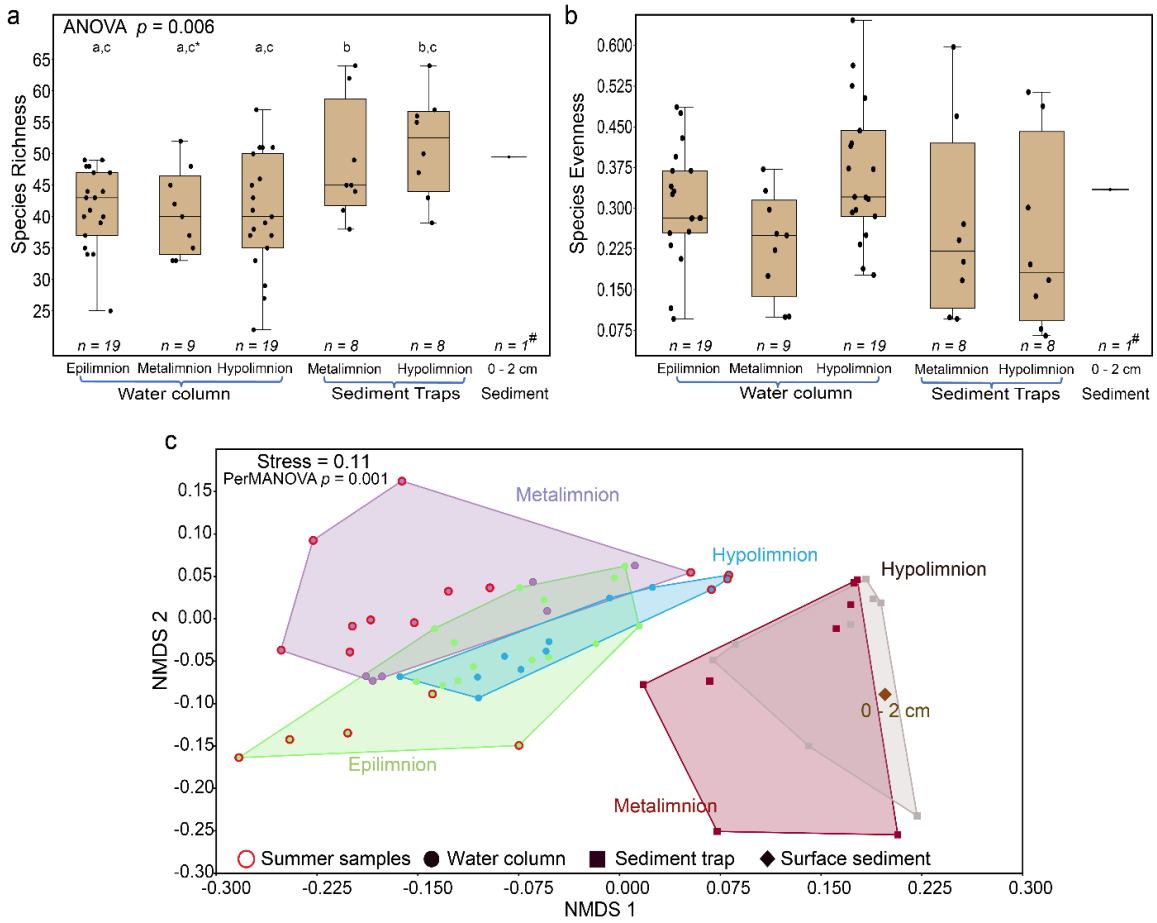

Figure 4.5: Alpha and beta diversity of cyanobacteria communities in Lake Tiefer See. Alpha diversity of cyanobacteria community composition in the water column, trap, and surface sediments where (**a**) ANOVA test for equal means on species richness followed by Tukey's pairwise tests; a = non-significant zones in water column, b = non-significant zones in sediment traps, c = significance in hypolimnion traps, and * = marginal significance. # = one sample representing the mean of biological triplicates; (**b**) ANOVA test for equal means on Pielou's species evenness among the groups was not significant p = 0.07, and (**c**) Visualization of beta diversity via a non-metric multidimensional scaling (NMDS) of cyanobacteria community composition in the water column, trap material, and surface sediments based on Bray–Curtis dissimilarity.

4.4.4 Correlation of Biotic with Physicochemical Properties

A rank-based correlation analysis between cyanobacteria ASVs and a significant subset of lake environmental variables revealed pelagic cyanobacterial abundance measures; cyanobacteria composition and 16S rRNA-ITS gene copy numbers to be positively correlated with temperature (n = 47, $p < 0.05$, R_S = 0.5, and 0.75, respectively; Fig. 4.6; Suppl. Table C.6,7; Suppl. Fig. 4), and negatively correlated with NO_3^- ($p < 0.05$, $R_S = -0.4$ and −0.4, respectively). Additionally, 16S rRNA gene copy numbers were negatively correlated with TDP ($p < 0.05$, R_S = 0.5). Among the most abundant taxa, ASV0004

assigned to *Aphanizomenon* and ASV0014 assigned to *Cyanobium* were positively correlated with turbidity ($p < 0.05$, $R_S = 0.41$, and 0.31, respectively), whereas ASV0014 was the only taxon that correlated positively with TDP ($p < 0.05$, $R_S = 0.5$). Furthermore, positive correlations with pH ($p < 0.05$, $R_S = 0.46$) and DO ($p < 0.05$, $R_S = 0.68$) occurred for ASV0008 assigned to *Cyanobium*. In contrast, ASVs 0005 and 0014 also assigned to *Cyanobium* were negatively correlated with pH ($p < 0.05$, $R_S = -0.4$ and -0.51, respectively) and DO ($p < 0.05$, $R_S = -0.63$, and -0.64, respectively). Additionally, ASVs 0006 and 0016 assigned to *Planktothrix* and *Snowella*, respectively, were negatively correlated with DO ($p < 0.05$, $R_S = -0.31$ and -0.38, respectively). Among all ASVs, only ASV0007 assigned to *Synechococcus* showed a positive correlation with temperature ($p < 0.05$, $R_S = 0.33$).

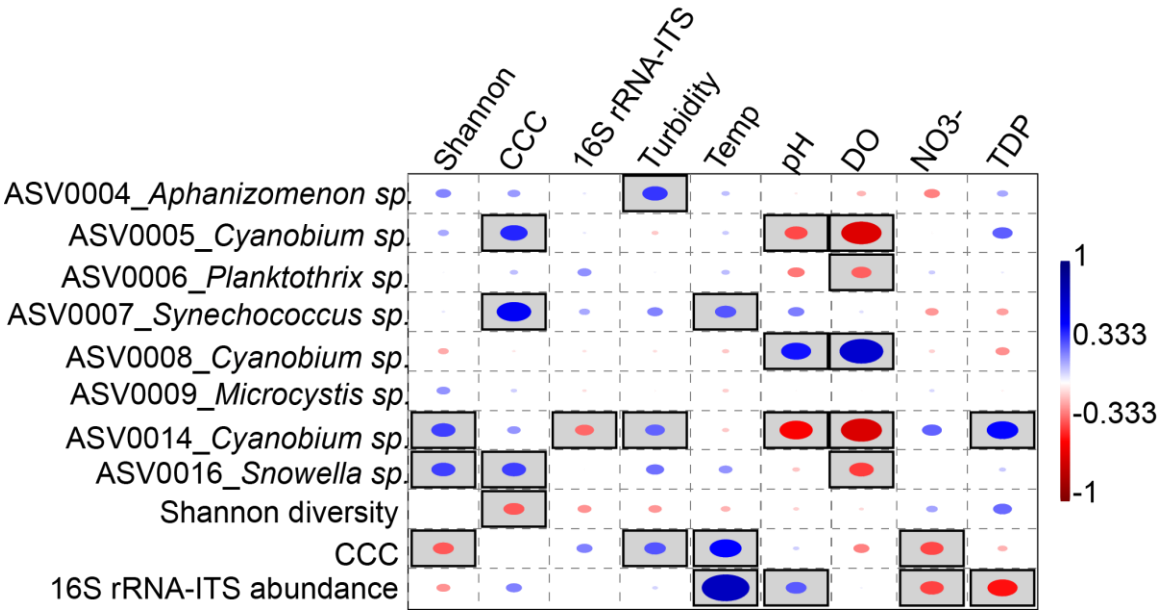

Figure 4.6: Correlation of pelagic cyanobacteria communities with environmental parameters. Rank-based Spearman correlation coefficients of the most abundant cyanobacteria ASVs, total cyanobacteria composition, and cyanobacteria 16S rRNA-ITS gene abundance with internal physicochemical properties in Lake Tiefer See. Gray-shaded squares are significant at $p < 0.05$ with Bonferroni p-value correction. Blue circles show positive, whereas red circles show negative correlations. Shannon diversity = cyanobacteria diversity, Temp. = temperature, DO = dissolved oxygen, NO_3^- = nitrate, TDP = total dissolved phosphorus, and 16S rRNA-ITS = 16S rRNA gene internal transcriber spacer (ITS) region of cyanobacteria.

4.5 Discussion

4.5.1 Tracing Cyanobacteria from the Water Column into the Sediment

This study used high throughput sequencing and lake monitoring to trace the deposition of pelagic cyanobacterial taxa in the sediments of Lake Tiefer See. We correlated pelagic cyanobacterial community data with in-lake physicochemical parameters to identify taxa, whose sedimentary records have future research prospects as potential paleolimnological proxies. Our comparative analysis of pelagic and deposited cyanobacteria revealed that the deposited community is representative of pelagic communities. This observation adds to previous DNA-based and traditional paleolimnological findings (Livingstone and Jaworski, 1980; Leavitt et al., 1989; Weisbrod et al., 2020). However, unlike these previous studies, differences were observed in the relative abundances of individual cyanobacteria taxa, such as *Planktothrix* and *Aphanizomenon*, between the water column, sediment trap material, and surface sediments. These differences may be explained by different deposition patterns of these taxa because of ecology, physiology, and spatiotemporal dynamics (Heiskanen and Olli, 1996; Halstvedt et al., 2007), as well as taphonomic processes, such as alteration or deterioration of DNA along the water column during transport to the sediments.

We further observed that alpha diversity indices (richness and evenness) did not change significantly throughout the water column, and between the sediment traps and surface sediments, indicating that the changes in the relative abundances of individual taxa had no significant effect on the overall cyanobacteria species richness and the distribution of single species (evenness) throughout the water column. This supports our finding that sediment-deposited cyanobacteria composition is significantly representative of those in the water column and is important for paleolimnological reconstruction of microbial groups from aquatic sediments. Our observations are consistent with a study on the vertical distribution of protistan taxa (at 2 and 130 m water depth) in Lake Bourget, which also revealed that richness (number of phylogenetic units) within the different phyla at both sampled depths were comparable (Capo et al., 2015).

In contrast, the decline in cyanobacteria abundance (qPCR) from the meta- to hypolimnion sediment traps and from 10 m water depth downwards (Fig. 4.4b) could be attributed to

taphonomic processes, such as decomposition and the effect of zooplankton grazing communities, such as rhizopods, ciliates, rotifers, and crustaceans (Gerphagnon et al., 2015). A minimum of dissolved oxygen between 11 and 13 m water depth, e.g., for August (Suppl. Fig. C.5), points to the formation of a metalimnetic oxygen minimum (MOM) resulting from the heterotrophic decomposition of the deep chlorophyll maximum-forming taxa such as *Planktothrix*, *Cyanobium*, and *Synechococcus*. This is supported by the decrease in cyanobacterial abundance by one order of magnitude between 10 m (1.8×10^6) and 15 m (4.1×10^5) water depths, respectively (Fig. 4.4b).

Altogether, our data suggest that although taphonomic processes may lead to a decrease in the number of quantifiable cyanobacteria at deeper depths, the composition and alpha diversities of deposited cyanobacterial communities are statistically comparable to those of the water column. Additionally, conditions in Lake Tiefer See, such as its hard water with calcite production that facilitates rapid sedimentation in spring and summer (Roeser et al., 2021), bottom water anoxia, and low bottom water temperatures coupled with intact laminated sediments (Dräger et al., 2019), are all likely to promote DNA preservation in the sediments (Ellegaard et al., 2020; Capo et al., 2021). Sediment-deposited cyanobacteria in Lake Tiefer See are thus promising candidates for reconstructing pelagic cyanobacterial dynamics of the past **(**Nwosu et al., 2021a).

4.5.2 Taxa with High Deposition

Unfavorable limnological conditions, such as a decrease in light intensity and nutrient depletion, especially nitrogen, can result in a breakdown of *Aphanizomenon* summer blooms followed by their sedimentation (Klemer et al., 1982; Hense and Beckmann, 2006), likely explaining their high abundance in sediments (Fig. 4.4a, Suppl. Fig. C.2a). Under the aforementioned unfavorable conditions, senescent *Aphanizomenon* cells lose the ability to regulate their own buoyancy, thus sinking or producing akinetes that equally settle in sediments (Kromkamp et al., 1986). Furthermore, physiological features, such as higher biomass production, larger cell sizes (e.g., for akinetes 40–220 × 6–10.8 μm (Komárek et al., 2013)) and cluster formation in *Aphanizomenon* promote their sedimentation compared to non-colonial unicellular and filamentous cyanobacteria taxa (Tallberg and Heiskanen, 1998). The high abundance of *Aphanizomenon* in the sediment traps in fall when the stratification of the water column weakened (Suppl. Fig. C.6a), may be because of wind-

induced downward transport of senescent cells and akinetes (Hansson et al., 1994; Tallberg and Heiskanen, 1998). It is unlikely that deposited *Aphanizomenon* either actively (via buoyancy regulation) or passively (via remobilization) reinvaded the water column from surface sediments in fall. This is based on the premise that senescent cells, though still alive, cannot regulate their buoyancy, and any remobilized akinetes will not grow into vegetative cells because of unfavorable conditions (see above) (Heiskanen and Olli, 1996; Hense and Beckmann, 2006).

The higher abundance of *Snowella* especially in the hypolimnion trap, and sediment relative to the water column could be attributed to their ability to form colonies (Rajaniemi-Wacklin et al., 2006), similar to the aggregate formation of *Aphanizomenon*. Currently, there is sparse literature on *Snowella* sediment deposition and its occurrence in deep temperate lakes. To date, they are known to be common in lakes of varying trophic states in central Europe and the Baltic Sea (Komárek and Komárková-Legnerová, 1992). A GenBank analysis of the *Snowella* sequences obtained from this study showed that the main ASV was 100% similar to the sequences of the *Snowella litoralis* strain OTU35S07 isolated from the eutrophic Lake Tuusulanjärvi, Finland (Rajaniemi-Wacklin et al., 2006). However, unlike that in Lake Tuusulanjärvi, where *Snowella* was recorded in samples from the upper waters (0–2 m), we showed a previously unknown bottom water peak in their population and a high sedimentation in the deep hard-water temperate Lake Tiefer See.

Overwintering communities of *Microcystis* in sediments may explain their high abundance in traps and surface sediments compared to the water column (Figure 4a; Suppl. Fig. C.6b) (Preston et al., 1980). *Microcystis* communities in temperate lakes are known to escape unfavorable conditions, such as poor nutrients, lower temperature, and insufficient light in the water column by forming „dormant“ colonies (resting stages), which settle on sediments (overwintering). The density gradient in the thermocline during stratification serves as a barrier hindering the migration of *Microcystis* from deeper waters into the euphotic zone (Hansson et al., 1994). The physiological barrier caused by the gradient could contribute to the very low (<1%) relative abundance of *Microcystis* in the upper water column during its usual bloom season in late summer to fall (McDonald and Lehman, 2013). This assumption is supported by the fact that thermal stratification in Lake Tiefer See (2019) ended in late November (Figs. 4.2a,b).

4.5.3 Taxa with Poor Deposition

Considering the all-year presence and abundance of *Planktothrix* in the metalimnion of the water column, their high abundance in sediment traps, especially in the metalimnion trap, and the sediment was expected (Figure 4a). The observed disproportionate abundance between the water column and sediment trap samples is possibly because of *Planktothrix* occurrence as single filaments containing gas vesicles, which hinder their rapid sedimentation (Halstvedt et al., 2007). Taphonomic processes, such as heterotrophic decomposition and DNA degradation during transport along the water column, as well as grazing by zooplankton, e.g., Daphnia and Cyclops (Kurmayer, 1999), could be other factors explaining the low abundance of *Planktothrix* in sediments. As discussed earlier, the formation of a temperature gradient (7–13 m water depth; Figure 2a) during lake stratification appears to favor the dominance of *Planktothrix* in the low-light metalimnion (10 m; Fig. 4.4a). In this layer, *Planktothrix* abundance contributes to deep chlorophyll maximum (DCM) formation, as shown by the peak in Chl*a* (Fig. 4.2e; Suppl. Fig. C.5). The temperature gradient also likely acts as a physical barrier preventing rapid sedimentation; thus, promoting heterotrophic decomposition of *Planktothrix* in the water column (Halstvedt et al., 2007). The observed DO-minimum at 11–13 m water depth suggests that DCM-forming taxa, such as *Planktothrix*, are decomposed at this water depth, leading to the formation of the metalimnetic oxygen minimum (MOM) zone (Suppl. Fig. C.5). This is supported by a reduction in the relative abundance of *Planktothrix* between 10 (>40% of all cyanobacteria) and 15 m (<20%) water depths (Fig. 4.4a). Wentzky et al. (2019) equally observed a connection between the increased decomposition of dead organic material resulting from *Planktothrix* and the development of the MOM (Wentzky et al., 2019). The development of the MOM zone indicates that as particulate organic matter sinks from the epilimnion into a zone of lower temperatures and higher water density (metalimnion), particle retention time increases, favoring heterotrophic decomposition in the metalimnion (Wentzky et al., 2019). It is not likely that the *Planktothrix* abundance disparity is caused by methodological limitations, such as primer amplification bias, because the same primer set was used to amplify the cyanobacteria 16S rRNA gene in the water and sediment samples. Additionally, complete degradation and/or fragmentation of *Planktothrix* DNA seems unlikely, because Kyle et al. (Kyle et al., 2014) used qPCR assay to amplify and quantify 383 bp fragments of this taxon from up to 50-year-old sediments from the dimictic

Lake Gjersjøen (max. depth = 64 m) (Rohrlack et al., 2008). Thus, while data from the spatio-temporal integrated sediment traps (~1 month) reveal extremely low abundance of the potential toxin-producing *Planktothrix*, single-point sampling of the water column, however, show they are the most abundant metalimnetic taxa in Lake Tiefer See. This means that relying on sedimentary DNA sequencing based on universal cyanobacteria marker alone would be insufficient to reveal previous pelagic *Planktothrix* importance. Therefore, future paleolimnological reconstructions based on sedaDNA may require an additional molecular approach (e.g., via qPCR assay (Rohrlack et al., 2008; Savichtcheva et al., 2011)) specifically targeting *Planktothrix* to reveal the history of their past pelagic importance in Lake Tiefer See.

Factors, such as rapid DNA degradation because of their small size (<0.2 µm; (Callieri and Stockner, 2000)), grazing by nano-flagellates, e.g., *Ochromonas* sp. (Jezberová and Komárková, 2007), and/or the presence of a density gradient, which impedes their sedimentation (Callieri, 2008), might explain the low abundance of *Cyanobium* ASV0008 in sediments (Fig. 4.4a, Suppl. Fig. C.2a). However, *Cyanobium* ASV0020 with high sediment deposition may be colony-forming in nature. Although studies on the ecology and physiology of colonial *Cyanobium* in freshwater ecosystems are still sparse, most are thought to be part of a metaphyton community associated with littoral and benthic sediments (Callieri et al., 2012b). While our data suggest the identification of possible *Cyanobium* ecotypes based on conserved small subunit ribosomal ribonucleic acid (SSU rRNA) genetic markers, future research should focus on isolating and obtaining full genome sequences that could provide information on the factors influencing the sedimentation of individual *Cyanobium* ecotypes.

4.5.4 Linking Cyanobacteria Community Dynamics with Environmental Data

Comparison of cyanobacteria assemblages from water and sediment matrices revealed that overall cyanobacteria composition as well as ASVs assigned to *Synechococcus*, *Aphanizomenon*, and *Snowella* are potential proxies for paleoclimate reconstruction (Fig. 4.6). This is because of their high sediment representation and significant correlation of their pelagic fraction with lake internal physicochemical parameter(s). Their suitability as proxies is based on the assumption that with high sedimentation, coupled with optimal DNA preservation conditions at the time of deposition, e.g., bottom water anoxia, and

absence of burrowing organisms (Domaizon et al., 2017), their DNA could be reconstructed from long-term sediment records. The overall pelagic cyanobacteria composition and that of *Synechococcus* were positively correlated with water temperature. Since the overall sediment-deposited cyanobacteria composition is representative of the water column ($p < 0.05$; Table 4.1), and *Synchococcus* had a high abundance in the sediment matrices (its DNA is also known to be well preserved in sediments (Coolen et al., 2008; Domaizon et al., 2013)), coupled with positive correlations to temperature, they could be useful as proxies for temperature in paleolimnological reconstructions. In temperate lakes, temperature has been shown to be a major factor leading to an increase in total cyanobacteria and, in particular, *Synechococcus* biomass (Joint et al., 1986). Furthermore, reconstructing a taxon in high abundance from late Holocene sediments could point to a bloom and potential toxin production in the water column at the time of deposition (Ballot et al., 2010). This was illustrated recently in Lake Tiefer See, where previous eutrophication was inferred from the increased abundance of operational taxonomic units assigned to *Aphanizomenon* which positively correlated with increased TN values in sediments (Nwosu et al., 2021a). In summary, our study provides information for establishing cyanobacteria as proxies for long-term paleoclimate reconstructions. This could be further approached using structural equation modeling (SEM or path analysis) to evaluate directed relationships between dependent and independent variables and not just sheer correlations (Chen and Ficetola, 2020).

4.6 Conclusions

Our study assesses the deposition of freshwater cyanobacteria based on high resolution taxonomic profiling of both pelagic and sedimented taxa using DNA-based techniques. It is the first study providing strong arguments for a skewed representation in taxonomic abundances of sediment-deposited cyanobacteria composition in a temperate hard-water lake with annual mixing. It reveals two critical findings regarding cyanobacterial sedaDNA reconstructions using universal gene markers. First, taphonomic processes occurring along the water column during sedimentation as well as post-sedimentary processes challenge an approximate estimation of some taxa from sediments, such as those occurring as single filaments (e.g., *Planktothrix*). Second, aggregate- (e.g., *Aphanizomenon*) and colony- (e.g., *Snowella*) forming taxa seem to be less impaired by these taphonomic processes. That is, while factors, such as predation, heterotrophic decomposition, and DNA degradation in the

water column, may lead to a poor representation of solitary or single filamentous cells, the ability to form aggregates or colonies in *Aphanizomenon* and *Snowella*, respectively, could be responsible for their overrepresentation in sediments. Our study thus reveals limitations of using high-throughput sequencing analysis based on sediments alone to infer pelagic cyanobacteria dynamics. Therefore, applying additional qPCR assay targeting specific taxa may potentially overcome the amplification biases observed in high-throughput sequence-based analyses. This is valuable knowledge for future DNA-based paleolimnological studies, especially in lakes without available long-term monitoring data, because obtaining reliable information about past limnological conditions using cyanobacteria sedaDNA as indicators will depend on an accurate estimation of species abundance. This means that complementing pelagic surveys of cyanobacteria with in situ sediment traps is crucial for optimally tracking their sediment deposition in lakes. Hereafter, results from such a combined survey will reveal relevant pelagic taxa that may require special targeting during sedaDNA reconstruction.

4.7 Acknowledgments

We thank the German Environmental Foundation (Deutsche Bundesstiftung Umwelt DBU) for funding the research position of E.C.N. We thank the coring team of GFZ-section Climate Dynamics and Landscape Evolution who assisted in the fieldwork (Brian Brademann). We thank Jens Kallmeyer (GFZ-section Geomicrobiology) for assisting with nitrate measurements and Anne Köhler for support in the ICP lab (IOW). We also want to thank Alexander Bartholomäus (GFZ-section Geomicrobiology) for additional help with bioinformatics.

5 Manuscript IV – Long-term cyanobacteria dynamics

"Bronze Age human-induced increase in cyanobacteria abundance revealed by sedimentary ancient DNA"

5.1 Abstract

Sedimentary ancient DNA-based studies have contributed to reveal effects of eutrophication on lake cyanobacterial communities in the last centuries, yet we are still lacking information over longer timescales (millennia). Here, we apply quantitative PCR, amplicon, and shotgun sequence analyses on sedimentary ancient DNA to reconstruct cyanobacteria history for the entire Holocene from a deep hard-water lake in northeastern Germany. Based on qPCR we find a substantial increase in total cyanobacteria abundance coinciding with deforestation during the early Bronze Age around 4000 years ago, suggesting increased nutrient supply to the lake by local communities settling on the lakeshore. Moreover, cyanobacterial community composition since then significantly differ from that of the seven millennia under natural conditions before. The next anthropogenic-induced significant shift in cyanobacterial communities only occurred about a century ago related to intensified agricultural fertilization. Our study reveals that humans began to impact lake ecology earlier than previously thought even in rather remote areas.

5.2 Introduction

Climate and anthropogenic activities are known to have shaped aquatic communities, but the role of climate change versus human pressure over lake biodiversity remains hard to disentangle. In the last century anthropogenic drivers have strongly influenced the abundance and diversity of cyanobacteria (Taranu et al., 2015; Huisman et al., 2018; Monchamp et al., 2018), causing massive blooms that hinder water quality (Chorus, Ingrid & Bartram, 1999) and ecosystem function (Rabalais et al., 2010; Huisman et al., 2018). In worst cases, cyanobacteria blooms are dominated by taxa which produce toxins that are harmful to zooplankton, birds, and mammals, including humans (Carmichael, 2001; Whitton, 2012). However, due to the paucity of long-term data, the dynamics of cyanobacteria in previous centuries and millennia remains only poorly determined.

Lake sediments are a repository for organic and inorganic material produced within the lake and transported from its catchment and act as natural archives for regional climate and environmental history (Smol et al., 2002). Lake sedimentary archives thus provide evidence of natural and anthropogenic driven ecosystem changes (Domaizon et al., 2017) recorded in various types of proxy data. Early cyanobacteria paleolimnological studies commonly used fossilized remains (akinetes, cysts) (Livingstone and Jaworski, 1980; van Geel et al., 1994), pigments (Hertzberg et al., 1971; Leavitt and Findlay, 1994) and biomarkers (Kaiser et al., 2016; Bauersachs et al., 2017) preserved in sediments as proxies to infer past changes. However, not all cyanobacteria leave sufficient identifiable remains in sediments that allow a high degree of taxonomic differentiation as distinctive species (e.g., picocyanobacterial (Domaizon et al., 2013)), and the presence of highly labile conjugated double bonds make some of their biomarkers unstable (e.g., the carotenoids zeaxanthin and echinenone) (Britton et al., 2008). Therefore, the potential of reconstruction based on classical fossil-based proxies is limited. In the last decade, a variety of DNA-based paleolimnological methods have emerged as novel and complementary proxies to reconstruct past cyanobacteria variability at improved accuracy (Domaizon et al., 2017) including physiologically dormant, active and inactive organisms buried in sediments (Capo et al., 2021). A major advantage of DNA-based approaches are the high phylogenetic resolution and the reliable coverage of the entire cyanobacteria phylum preserved in sediment archives (Domaizon et al., 2013; Monchamp et al., 2016; Nwosu et al., 2021a). Recent sedaDNA reconstruction studies have successfully linked changes in freshwater cyanobacteria structure and diversity to variations in temperature, precipitation, eutrophication as well as increased lake circulation and dust input (Monchamp et al., 2016; Nwosu et al., 2021b; Zhang et al., 2021b). However, most studies report changes only for the last two millennia (Nwosu et al., 2021a; Zhang et al., 2021b), a period which is influenced by both climatic changes and human impact on the environment, while large parts of the Holocene remain largely unknown. This knowledge deficit limits our understanding of how natural climatic changes devoid of any significant human impact during the Holocene may have led to broad scale changes in cyanobacteria dynamics compared to the last century of extensive anthropogenic disturbance.

The objective of this study is to reconstruct the dynamics of cyanobacteria throughout the entire Holocene in a well-studied, deep temperate lake and to discuss how far back in time climatic and anthropogenic factors have influenced cyanobacterial community composition, abundance and diversity. We combined shotgun (metagenome) sequencing,

amplicon sequence variants analysis (ASVs; a proxy for different species and variants within the same species), quantitative polymerase chain reaction (qPCR) assays, cyanobacteria lipid biomarker (7-methylheptadecane) analyses with reconstruction of vegetation openness (Theuerkauf et al., 2015) to investigate changes in cyanobacteria during the last 11,000 years in Lake Tiefer See, northeastern Germany. A special emphasis of this study was on multi-millennia records of total *Planktothrix* populations and the cyanopeptolin-producing *Planktothrix* subpopulations which were recently shown via 16S ASV analysis to be the most abundant potential toxin-producing cyanobacteria in the study site (Nwosu et al., 2021c). This site is selected for our study because lake sedimentation is monitored since 2012 (Roeser et al., 2021) and the processes of cyanobacterial DNA from water to the burial in sediments have been studied in detail (Nwosu et al., 2021b) providing a great validity of our data interpretation.

Lake Tiefer See, located in northeastern Germany (Fig. 5.1) and formed at the end of the last glaciation as part of the Klocksin lake chain, and its sediment record has been studied under various aspects (Brauer et al., 2019). Previous studies of the sediments of this 62 m deep lake focused on focused on climatic and environmental history of the last 6000 years based on sedimentological and geochemical proxies (Dräger et al., 2017, 2019) as well as vegetation and lake level reconstructions (Theuerkauf et al., 2021). The main characteristic of the sediment record is the succession of varved (annually laminated) and non-varved intervals proving that the lake is sensitive to climate and environment changes (Dräger et al., 2017). The lake is integrated part of the TERENO long-term monitoring program and seasonal sedimentation processes and their drives are well-known (Roeser et al., 2021). Furthermore, excellent sedaDNA preservation has been demonsrated (Nwosu et al., 2021a) and it has been proven that cyanobacteria communities found in the sediments well reflect their composition in the water column (Nwosu et al., 2021b).

5.3 Materials and methods

5.3.1 Core sampling and chronology

A total of 11 sediment cores (TSK19H1-H6 and TSK19K1-K5) were collected in parallel in May 2019 from the deepest part of Lake Tiefer See (latitude 53°35′36″N, longitude 12°31′46″E; Fig. 5.1), using a 90-mm UWITEC piston corer. Transportation of the cores, treatment in the laboratory and sediment subsampling were carried out as previously

described (Nwosu et al., 2021c). The age model of the sediment composite profile (Suppl. Table D.1) was ascertained based on varve counting, tephrochronology and radiocarbon dating as previously described (Dräger et al., 2017). Sediment sample ages are given either as calibrated years before present CE 1950 (cal. a BP) and/or CE. The following epochal boundaries and durations have been defined for the Lake Tiefer See region: (i) Bronze Age 3950 – 2500 cal. a BP, (ii) Pre-Roman iron age 2500 – 1950 cal. a BP, (iii) Roman Age 1950 – 1575 cal. a BP, (iv) The Migration Period (Dark Ages) 1575 – 1300 cal. a BP, and (v) The Slavic settlement period 1300-700 cal. a BP. Evidence of human settlement in the vicinity of Lake Tiefer See during the Bronze Age, Pre-Roman Iron Age and Roman Age are based on archaeological finds (Suppl. Fig. D.1).

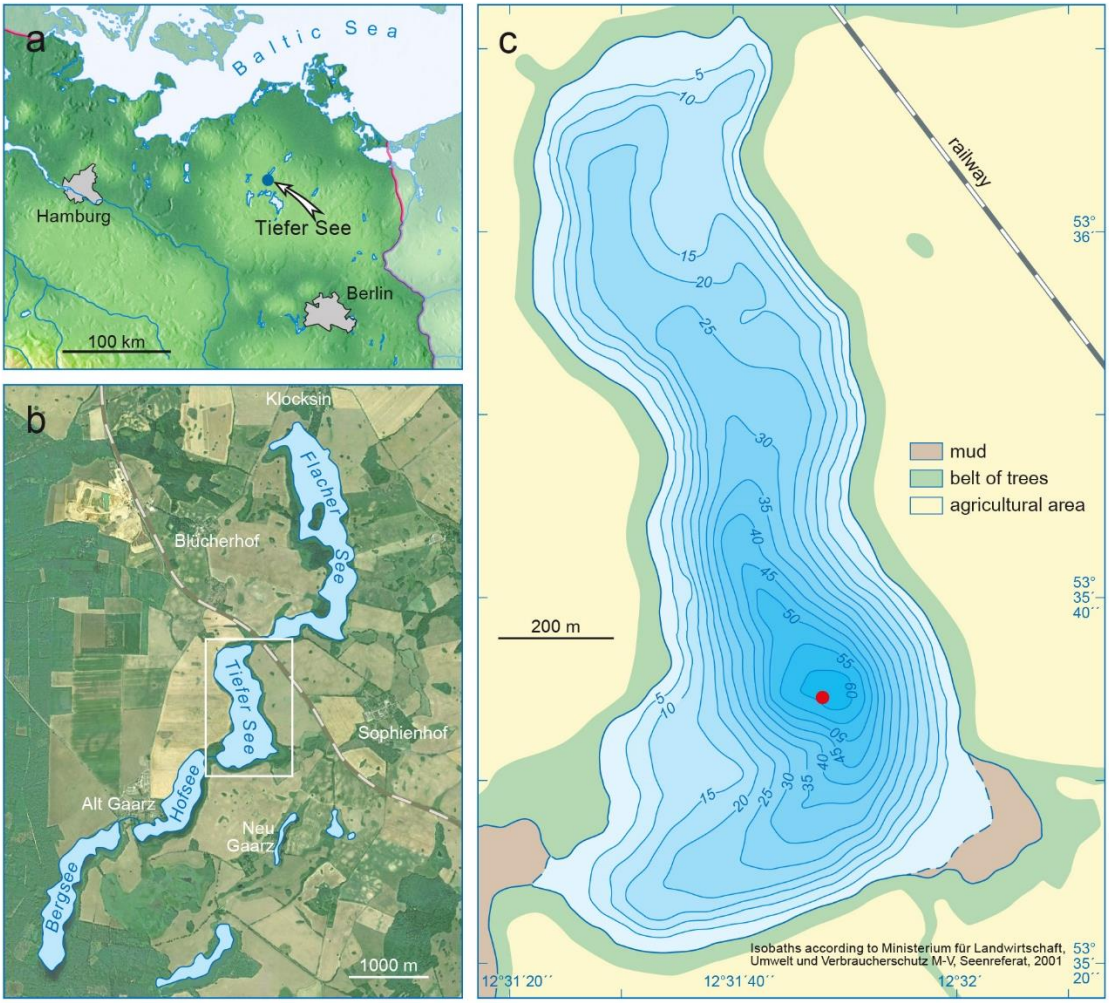

Figure 5.1: (a) location of Lake Tiefer See in the southern Baltic lowlands (blue dot), (b) Lake Tiefer See within the Klocksin lake chain, and (c) topographic map of Lake Tiefer See showing the coring site (red dot).

5.3.2 Total organic carbon analysis

Total organic carbon (TOC) contents for the last 6000 years have been previously published (Dräger et al., 2017). For this study, we measured also the additional samples covering the lower part of the record using the same methods like the previous samples: 1-cm bulk samples were freeze-dried, grinded and homogenized and analyzed with the NC2500 Eurovectors. Total carbon was measured from 5 mg of sediment in tin capsules, and TOC was examined by decalcifying 3 mg of sediment in Ag capsules by treating with 3% HCl, 20% HCl, and drying at 75 ◦C. The TOC content is expressed as percent of dry weight (wt.%).

5.3.3 Sedimentary ancient DNA analysis

The top sediment layers were scraped off with a sterile razor before the uncontaminated anoxic part was put into sterile 15-ml falcon tubes and stored at -80 °C until analysis. Care was taken to prevent cross contamination of the sediments by processing recent and older samples at different times. Total DNA used for the qPCR assay and amplicon sequencing was extracted from sediment samples using the PowerSoil DNA Isolation Kit (Qiagen) as described in (Nwosu et al., 2021b), in the laboratories at the German Research Centre for Geosciences (GFZ) Potsdam. DNA extractions were done in batches of seven samples with the addition of one negative control each time while avoiding contamination from foreign DNA by following processes described in (Monchamp et al., 2016). The sedaDNA extracts were stored at -20 °C until further downstream analyses. The DNA for shotgun sequencing was extracted using DNeasy PowerMax Soil DNA and the DNeasy Power Soil DNA 100 DNA isolation kits (Qiagen) from 14 sediment samples distributed from top to bottom of the long core (Suppl. Table D.2, Suppl. Information-Methods). The extraction protocols were modified as previously described (Epp et al., 2019). Briefly, prior to adding the sediment sample, solution C1, 400 µL of proteinase K (2 mg ml^{-1}) and 100 µL of Dithiothreitol (DTT) (5M) were added when using the PowerMax Kit, and vortexed for 10 min. For the PowerSoil kit, 20 µL of proteinase K (2 mg ml^{-1}) and 5 µL of Dithiothreitol (DTT) (5M) was used and two extractions per sample were performed and combined after the extractions, to compensate for lower amount of substrate compared to the PowerMax kit.

5.3.4 Quantification of cyanobacteria and *Planktothrix* abundance

Total cyanobacteria were quantified with the nonselective fluorescent dye SYBR Green quantitative PCR (qPCR) assay amplifying specifically the cyanobacteria 16S rRNA-ITS (internal transcribed spacer) region using the primers CSIF (5'-GYCACGCCCGAAGTCRTTAC-3') and 373R (5'-CTAACCACCTGAGCTAAT-3')(Janse et al., 2003) as described previously (Nwosu et al., 2021d).

Two types of qPCR chemistries were applied to enumerate total *Planktothrix* populations and sub-populations of *Planktothrix* producing the non-ribosomal peptide synthetase cyanopeptolin (most dominant in the Lake Tiefer See (Nwosu et al., 2021d)) in sediments. A Taq nuclease assay (TNA) was used to quantify total *Planktothrix* by amplifying the intergenic spacer region of the phycocyanin operon (PC-IGS; c. 72 bp) region in *Planktothrix* with the primers PIPC fw (5'-GAGCAGCACTGAAATCCAAG-3') and PIPC rev (5'-GCTTTGGCTGCTTCTAAACC-3')(Schober and Kurmayer, 2006). The TaqMan probe (FAM-TTTGGCTTGACGGAAACGACCAA-BHQ) (Schober and Kurmayer, 2006) had a fluorescent reporter dye (6-carboxyfluorescein [FAM]) and black hole quencher 1 (BHQ-1) attached covalently to the 5' and 3' ends, respectively. The final volume of the qPCR reactions was 25 µL containing 12.5 µL of KAPA SYBR® FAST qPCR Master Mix (Roboklon, Germany), 0.8 µL of each forward and reverse primer (100 µM, Biomers), 5.5 µL PCR water and 5 µL of template DNA. The two-step qPCR program consisted of an initial polymerase activation step (95°C for 10 min), followed by 40 cycles of denaturation at 95°C for 15 s, annealing and extension at 60°C for 60 s. The SYBR Green qPCR (SG) assay was used to quantify the total population of cyanopeptolin producing *Planktothrix* chemotype by amplifying the non-ribosomal peptide synthetase cyanopeptolin gene cluster (*oci*B gene fragments) using two different primer lengths (161 and 247 bp) (Kyle et al., 2014). The final volume of the qPCR reactions was 20 µL containing 10 µL of KAPA SYBR® FAST qPCR Master Mix (Sigma-Aldrich, Germany), 0.2 µL of each forward and reverse primer (100 µM, Biomers), 4.8 µL PCR water and 5 µL of template DNA. The qPCR program consisted of an initial polymerase activation step (98°C for 2 min), followed by 40 cycles of denaturation at 98°C for 15 s, annealing at 30°C for 58 s and extension at 72°C for 30 s. No-template controls made up of PCR water were included in all runs. Positive controls comprising genomic DNA from a non-axenic culture of *Planktothrix rubescens* DSM 109804 sourced from the German Collection of Microorganisms and Cell Cultures (DSMZ GmbH, Germany) were also included in all runs. Any amplification beyond 40 cycles was treated as a non-detect.

All qPCR programs were followed by a melting curve step from 70°C to 95°C at a transition rate of 1°C per 5 s to determine the amplification specificities. Five- and sixfold dilution standards were prepared from cultured gDNA of *Planktothrix rubescens* DSM 109804 (DSMZ GmbH, Germany) for each qPCR assay. The dilution standards ranged from 1×10^5 to 4.7×10^0 and 6.29×10^3 to 4.7×10^{-2} copies ng^{-1} DNA and used to create the standard curves from which the quantification cycle (*Cq*) values were determined (Bustin et al., 2009) for total *Plankothrix* and cyanopeptolin producing *Planktothrix* chemotype, respectively. All qPCR assays were performed in triplicates on a CFX96 real-time thermal cycler (Bio-Rad Laboratories Inc., USA). The 16S rRNA-ITS, PC-IGS and oci*B* copy numbers were calculated after Savichtcheva et al., (2011). The obtained values were at least mean duplicates of each sample expressed as total cyanobacterial, total *Planktothrix* and cyanopeptolin-producing *Planktothrix* chemotype abundances normalized to extracted DNA (copies ng^{-1} DNA). The amplified products were confirmed and analyzed for unspecific PCR amplification with agarose gel electrophoresis.

5.3.5 Analysis of cyanobacterial and cyanopeptolin producing *Planktothrix* DNA preservation.

To assess whether DNA fragmentation occurred after deposition and whether this could have negatively influenced the PCR efficiency (Coolen et al., 2006), we compared the cyanobacterial composition of the long (~ 1500 bp) amplicons with short to medium (~ 350 bp) amplicons on three different samples from the sediment depths 210, 410 and 985 cm. The PCR amplification of the long fragments was done by targeting the 16S rRNA-ITS genomic region (PCR targeting the entire cyanobacterial community) using the primers CYA371F (5'-CCTACGGGAGGCAGCATGTGGGGAATTTTCC-3') and 373R (5'-CTAACCACCTGAGC-3') as described in (Savichtcheva et al., 2011). The sequencing of short cyanobacteria fragments was performed on the amplification products from total cyanobacteria 16S rRNA-ITS qPCR assays. The *Planktothrix oci*B (cyanopeptolin) gene amplification products (fragments 161 bp and 247 bp) from the sediment depths 210 (CE 1137) and 1015 (11,058 cal. a BP) cm were also sequenced to assess the specificity of the products. The qPCR amplification products from the cyanopeptolin producing *Planktothrix* subpopulation and those from total cyanobacteria 16S rRNA-ITS qPCR assays were used to construct clone libraries using a TOPO TA cloning kit (Invitrogen) with PCR vector 2.1 according to the manufacturer's instructions. A total of 38 long fragments and 58 short

fragments cyanobacterial clones were sequenced for samples from the sediment depths 210, 410 and 985 cm. The cyanopeptolin *Planktothrix* clones from *oci*B247 (29 fragments) and *oci*B161 (34 fragments) were also sequenced for the samples from the sediment depths 210 and 1015 cm (Beckman Coulter Genomics, Hertfordshire, UK).

5.3.6 DNA preparation for amplicon sequence library

The PCR for the Illumina high-throughput sequence libraries was conducted using the cyanobacteria-specific primers CYA359F (5′-GGGGAATYTTCCGCAATGGG-3′) and CYA784R (5′-GACTACWGGGGTATCTAATCCC-3′) (Monchamp et al., 2016) which amplify a >400-nt-long fragment of the V3–V4 regions of the 16S rRNA gene. The primers had unique tags that served to differentiate the samples. The samples and negative controls (that is, a reaction with PCR water as template) were amplified in a 50 µL volume PCR reaction, comprising 5x Platinum™ II PCR Buffer (Invitrogen, ThermoFischer Scientific), 25 mM $MgCl_2$, 0.2 mM deoxynucleoside triphosphate (dNTP) mix (ThermoFisher Scientific), 0.5 mM of each primer (TIB Molbiol, Berlin, Germany) and 2 U of Platinum™ II *Taq* Hot-Start DNA Polymerase (Invitrogen, ThermoFischer Scientific). The volume of the template DNA used in each reaction varied between 1 and 4 µL depending on the genomic DNA concentration. The PCR program included a first denaturation step at 94°C for 2 min, followed by 35 cycles at 94°C for 15 s, annealing at 60°C for 15 s, and extension at 68°C for 15 s. To avoid cross-contamination, older sedaDNA samples were amplified at different times than younger ones. Furthermore, to control for reproducibility of the PCR and sequencing results, all samples were amplified in a second PCR run (technical replicates). The tagged PCR products were then purified with the Agencourt AMPure XP kit (Beckman Coulter, Switzerland) and eluted in 30 µL DNA/RNA-free water. The purified product was quantified with a Qubit 2.0 Fluorometer. Equimolar concentrations of all samples, their technical replicates and purified negative PCR controls were pooled into 2 separate multiplex libraries (á n = 74 samples and 2 negative controls). The libraries were pair-end sequenced (2 × 300 bp) on an Illumina MiSeq system at Eurofins Scientific (Constance, Germany).

5.3.7 Amplicon sequence data processing

Sequencing raw reads were demultiplexed and adapter and quality trimmed using cutadapt v3.4 using the pair-end mode and the following parameters: -e 0.2 -q 15,15 -m 150 --discard-untrimmed. The ASVs were generated using trimmed reads and DADA2 package v1.20 (Callahan et al., 2016) using the pseudo-pooled approach with the following parameters: truncLen=c(240,200), maxN=0, rm.phix=TRUE, compress=TRUE, multithread=TRUE, minLen = 150 with R v4.1. Taxonomic assignment was done using DADA2 and SILVA database v138. At Genus level there was 98% agreement between 50s and 80s minBoot and 95% at the family level. The number of inputs, processed and final reads of the DADA2 pipeline is shown in Suppl. Table. D.2. Subsequently, ASVs representing chloroplasts, mitochondria, singletons, doubletons, other bacteria, rare taxa and negative controls were removed. The 74 sedaDNA samples resulted in a total of 9,770,821 denoised, nonchimeric and error-corrected sequences that DADA2 (Callahan et al., 2016) inferred in 9,548 ASVs. In total, the filtered dataset comprised 441,045 sequence reads in 433 ASVs assigned to photosynthetic cyanobacteria and distributed across 74 samples. Of the 433 ASVs, 9 were assigned to the order level, 45 to the family level, and 393 to the genus level (91% of all cyanobacteria ASVs; 436,981 read counts).

5.3.8 Shotgun sequencing and bioinformatics

The 13 sedaDNA samples for shotgun sequence analysis were sequenced at Eurofins Scientific (Constance, Germany) on an Illumina NovaSeq6000 machine aiming for 35 million pair-end reads of length 150 nt. Sequencing depth differed between samples because of input DNA concentration with deepest sediment samples having the lowest DNA concentrations (Suppl. Table D.1). The raw reads were processed using the ATLAS metagenome pipeline (Kieser et al., 2020) to obtain dereplicated, quality controlled, and trimmed reads. These reads were mapped to the SILVA 16S SSU database v138 (Yilmaz et al., 2014) to obtain taxonomy and calculate species abundance. Mapping was performed using bowtie2 v2.4.2 (Langmead and Salzberg, 2012). To obtain nitrogen fixation (*nif* gene family) and microcystin synthesis (*mcy* gene family) gene abundances, quality-controlled reads were assembled into contigs using the ATLAS metagenome pipeline (Kieser et al., 2020). The genes were predicted using prodigal v2.6.3 (Hyatt et al., 2010) and annotated using the eggNog emapper v2.0.1 (Huerta-Cepas et al., 2019) with a database from October 2020 (Cantalapiedra et al., 2021). TaxonKit v0.8.0 was used to obtain lineage information from taxon IDs of annotated genes (Shen and Ren, 2021). To obtain the final gene

abundances, quality-controlled reads were mapped against all assembled contigs using bowtie2 v2.4.2 (Langmead and Salzberg, 2012). The obtained counts were normalized as follows: First, gene counts were corrected for sequencing depth by normalizing to the total sequencing reads of each sample. Second, to correct for different gene length, counts were normalized by kilobases of gene length. These normalized gene counts represent gene abundance that is comparable between different genes within and between samples. Taxon abundance was finally obtained by summing up gene counts by taxonomic level of interest.

5.3.9 Statistical analyses

The two amplicon sequence libraries were merged by taking the average of their relative abundances. Bubble plots were used to illustrate differences in seasonal and spatial cyanobacteria assemblage and were produced with the open source software http://shiny.raccoome.de/bubblePlot/. Alpha and beta diversity estimations, and multivariate permutational analysis of variance (PerMANOVA) based on amplicon data were performed using the PAST v4.01 software (Hammer et al., 2001). Non-metric multidimensional scaling (NMDS) was performed in the „vegan“ package in R (Oksanen et al., 2019). Also, before beta diversity estimations, the ASV cut-off was set to 0.1% to eliminate very rare taxa. Statistical analysis on shotgun sequence data was done using R v3.6.2 with the package clusterProfile 3.14.3 (Wu et al., 2021) and the package ggplot2 v3.3.2 was used for visualization.

To assess whether the cyanobacterial communities at the ASV level showed clustering patterns related to three major time periods in the last 11,000 years, an NMDS analysis using Hellinger-transformed cyanobacteria absolute read counts data as dependent variables was performed(Legendre and Gallagher, 2001). The time periods were defined based on changes in climate as revealed by regional paleoclimate data (Kaiser et al., 2012) and human-impact data in the study site derived from archaeological finds (Jantzen et al., 2011; Schmidt, 2019, 2020), Holocene hydrological evolution (Theuerkauf et al., 2021) and vegetation reconstruction studies (Theuerkauf et al., 2015). The three defined time periods were thus; (I) climate variability with no human impact (early to mid-Holocene 11,058 – 5067 cal. a BP), (II) climate variability and moderate human impact (Bronze Age to the Little Ice Age 4067 – 96 cal. a BP), and (III) climate warming and intense human impact (CE 1870 – 2000). The significance of the clusters was analyzed with a non-parametric PerMANOVA based on Bray-Curtis using the time periods as predictors and

Hellinger-transformed cyanobacteria absolute read counts data as response variables (Legendre and Gallagher, 2001). A subsequent pairwise post-hoc Monte Carlo permutation test (n = 9999) was used to assess significant differences among the clusters. To assess the correlation of cyanobacteria richness and abundance to environmental parameters, a Spearman's rank-based correlation coefficient was calculated. Prior to the correlation analysis the environmental data (predictors) were standardized by subtracting the mean and dividing by the standard deviation (Z-Score), while cyanobacteria richness and abundance were used as response variables. Collinearity in the explanatory variables was tested with a variance inflation factor (VIF) using the "vif.cca" function in "vegan" (Oksanen et al., 2019). Explanatory variables were then additively tested until only those with a VIF score < 10 remained (Suppl. Table D.3). The significant subset of explanatory variables that may explain the variability of cyanobacterial community composition was determined via forward selection using the function "ordiR2step" function in "vegan".

5.3.10 Data availability

The amplicon and shotgun sequencing raw reads have been uploaded to the European Nucleotide Archive (ENA) under BioProject accession number PRJEB51951. The filtered sedaDNA datasets analyzed during this study are available in Supplementary Tables D1 and 2. The cyanobacteria lipid biomarker 7-Methylheptadecane data analyzed for this study are available in Supplementary Table 2. The sediment age chronology up to 6000 cal. a BP for Lake Tiefer See have been published at https://doi.org/10.1177/0959683616660173. The pollen-based reconstructed vegetation openness data for Lake Tiefer See up to 6000 cal. a BP have been published at https://doi.org/10.1177/0959683614567881. Lake-level changes for Lake Tiefer See for the entire Holocene have been published at https://doi.org/10.1111/bor.12561.

5.4 Results

5.4.1 Lake environmental parameters

The total organic carbon (TOC) contents reached highest values in sediment samples from mid-Holocene (mean 17.5 wt.%; ca. 8470 - 4070 cal. a BP) and lowest value in the basal early-Holocene sediment sample (1.4 wt.%; ca. 11,060 cal. a BP) and in samples from the Little Ice Age (mean 7.2 wt.%; 717 – 96 cal. a BP; ca. CE 1230 – 1850). A correspondence between TOC contents and varve preservation was observed (Dräger et al., 2017). The pollen-based vegetation openness reconstruction displayed repeated changes in vegetation openness in the pollen source area of Lake Tiefer See over the past 11,000 years (Fig. 5.2). The lowest values (<20%) were observed from ca. 11,060 – 4070 cal. a BP and during short periods between ca. 3970 and 810 cal. a BP. The highest openness values (>35 %) was reconstructed in the samples spanning the time periods ca. 3960 – 3360, ca. 2800 – 2100, and since ca. 880 cal. a BP (ca. CE 1070) that reflect periods of enhanced human settlement (Theuerkauf et al., 2015, 2021).

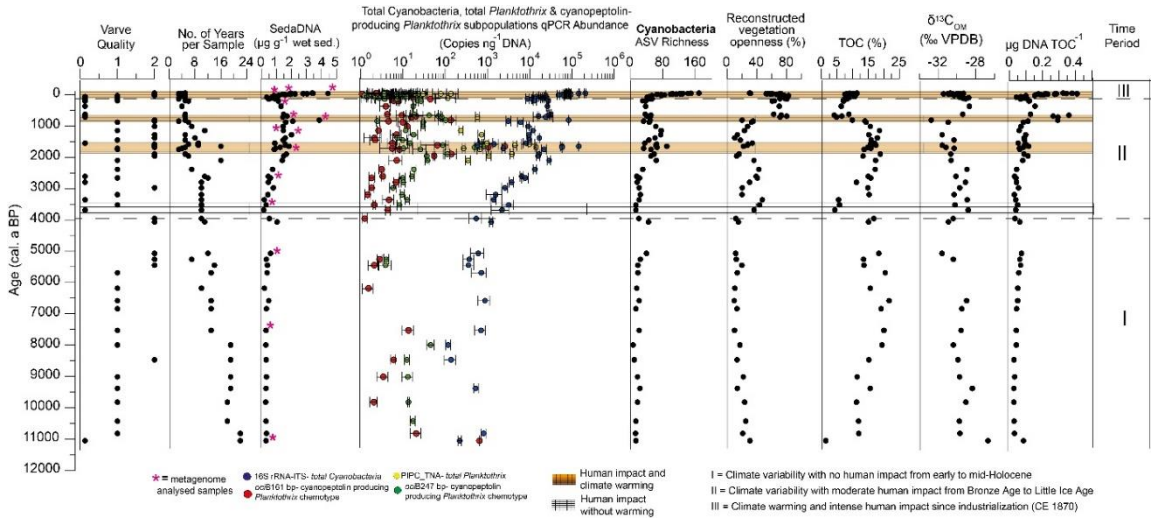

Figure 5.2: Sediment composite profile with sedimentological parameters, sedaDNA and cyanobacteria data, and selected lake paleoenvironmental records. Sedimentological analysis: varve quality and number of years in each analyzed sediment sample. Microbiological analysis: sedaDNA concentration normalized to sediment weight (µg DNA g^{-1} sed; magenta colored stars indicate metagenome analyzed samples) and total organic carbon content (µg DNA TOC^{-1}), abundances of total cyanobacteria, *Planktothrix* and cyanopeptolin-producing *Planktothrix* subpopulations (determined via quantitative PCR; error bars give the standard deviations for three independent amplifications), cyanobacteria taxonomic richness from amplicon sequencing. Geochemical analysis: TOC content and stable carbon isotope value of sediment organic matter (δ^{13}COM) values (Dräger et al., 2019). Pollen-based reconstructed vegetation openness data (Theuerkauf et al., 2015, 2021). Broken black lines demarcate the three significantly different temporal clusters identified by non-metric multidimensional scaling (I) ca. 11,060 to 4070 cal. a BP, (II) ca. 3960 to 100 cal. a BP, and (III) ca. CE 1870 to 2000, (see Fig. 5.4). Orange colored grids highlight peaks in cyanobacteria abundance with warming periods while uncolored grid highlight human impact without climate warming.

5.4.2 Cyanobacteria and *Planktothrix* abundance determined by qPCR

Overall, the sedaDNA concentration normalized over sediment wet weight and total organic carbon shows similar long-term trends (Fig. 5.2, Suppl. Table D.1). The main finding is a distinctly higher concentration in sedaDNA concentrations since ca. 3960 cal. a BP (n = 57, *mean*: 1.4 µg g^{-1} wet sediment and 0.14 µg TOC^{-1} %) than between ca 11,060 – 4070 cal. a BP (n = 17, *mean*: 0.2 µg $\%^{-1}$ wet sediment and 0.02 µg TOC^{-1}%). Cyanobacterial gene copies were most abundant in the topmost sediment sample (CE 2000; 2.3×10^5 copies ng^{-1} DNA). Other peaks in cyanobacteria gene copies were detected in samples dated at ca. 810 cal. a BP (8.4×10^4 copies ng^{-1} DNA) and ca. 1900 cal. a BP (2.1×10^5 copies ng^{-1} DNA) following a progressive increase since ca. 3970 cal. a BP. The

lowest cyanobacteria gene copies was detected from ca. 11,060 – 4070 cal. a BP, where values ranged between 10^2 and 10^3 gene copies ng^{-1} DNA.

The highest *Planktothrix* abundance was quantified from two samples at ca. 1630 and 1690 cal. a BP (5.8×10^4 and 1.4×10^4 copies ng^{-1} DNA, respectively). In contrast, the lowest *Planktothrix* abundance was measured in a recently deposited sediment layer (CE 1990; 3.2×10^1 copies ng^{-1} DNA). The quantification of the sub-populations of *Planktothrix* that produce the non-ribosomal peptide synthetase cyanopeptolin was based on two alternative targets: 161 bp-long and 247 bp-long fragments of the *oci*B gene. Based on both targets it was possible to quantify the *Planktotrix* subpopulations in all samples except in 8 samples from early Holocene with results close to or lower than the detection limit (Fig. 5.2; Suppl. Table D.2). The results from both gene targets were consistent except for a slight overestimation by the *oci*B247 target. The abundance of the cyanopeptolin-producing *Planktothrix* chemotype peaked in the samples dated to ca. 1580 and 1650 cal. a BP (*oci*B161: 2.6×10^3 and 1.1×10^3 copies ng^{-1} DNA; *oci*B247: 8.3×10^2 and 5×10^2 copies ng^{-1} DNA, respectively) and in the sample at ca. 11,060 cal. a BP (*oci*B161 6.5×10^2 copies ng^{-1} DNA). The lowest abundance ($< 10^1$ copies ng^{-1} DNA) of *oci*B161 and *oci*B247 were measured in recent sediment layers (CE 1970 – 1977) and in two samples from ca. 9830 and 6180 cal. a BP.

Robustness and quality of sedaDNA was validated with cyanobacteria lipid biomarker analysis (7-methylheptadecane, Suppl. Table D.2) and clone libraries created from selected qPCR amplification products for total cyanobacteria (~350 bp), *oci*B (161 and 247 bp) and long cyanobacteria amplicons using long-fragment primers (see "Suppl. Information-Methods" section, Suppl. Information-Results, Suppl. Table D.4). The results confirm both cyanobacterial and cyanopeptolin-producing *Planktothrix* subpopulation DNA fragments are well preserved along the entire sediment core (11 m).

5.4.3 Cyanobacteria ASV analysis

The cyanobacteria sedaDNA analysis of the 100 most abundant ASV's revealed that *Cyanobium* is the most abundant (>50%) cyanobacterial genus (Fig. 5.3). Potential bloom-forming and toxin-producing genera like *Aphanizomenon, Microcystis, Dolichospermum* and *Planktothrix* did not only become abundant in Lake Tiefer See in the last century, but also already since ca. 10,830 cal. a BP. After CE 1952 *Aphanizomenon* was the most abundant (25 – 50%) potentially toxin producing genus. In sediment samples spanning ca.

3960 and 100 cal. a BP, *Planktothrix* was the most abundant (~25%) potentially toxin producing genus. Specifically, *Planktothrix* abundance peaked in samples from ca. 1650 and 1580 cal. a BP. Further peaks in *Planktothrix* abundance were measured in samples dated at 10,820 and 5450 cal. a BP. These peaks in *Planktothrix* abundance were further confirmed by calculating ratios of relative abundance of *Planktothrix* from amplicon sequencing to total cyanobacteria abundance (qPCR). The proportion of *Planktothrix* in the cyanobacterial population confirmed the above described observations. This finding is consistent with the results from the ASV and qPCR analyses (Suppl. Fig. D.5). Altogether, cyanobacteria ASV (taxonomic) richness is generally higher in recent sediment layers (42 – 169; since CE 1870; Fig. 2; Suppl. Table D.2) compared to sediment from ca. 11,060 – 5070 cal. a BP (7 – 40). Between 4070 – 100 cal. a BP, cyanobacteria ASV richness varied between 14 and 90.

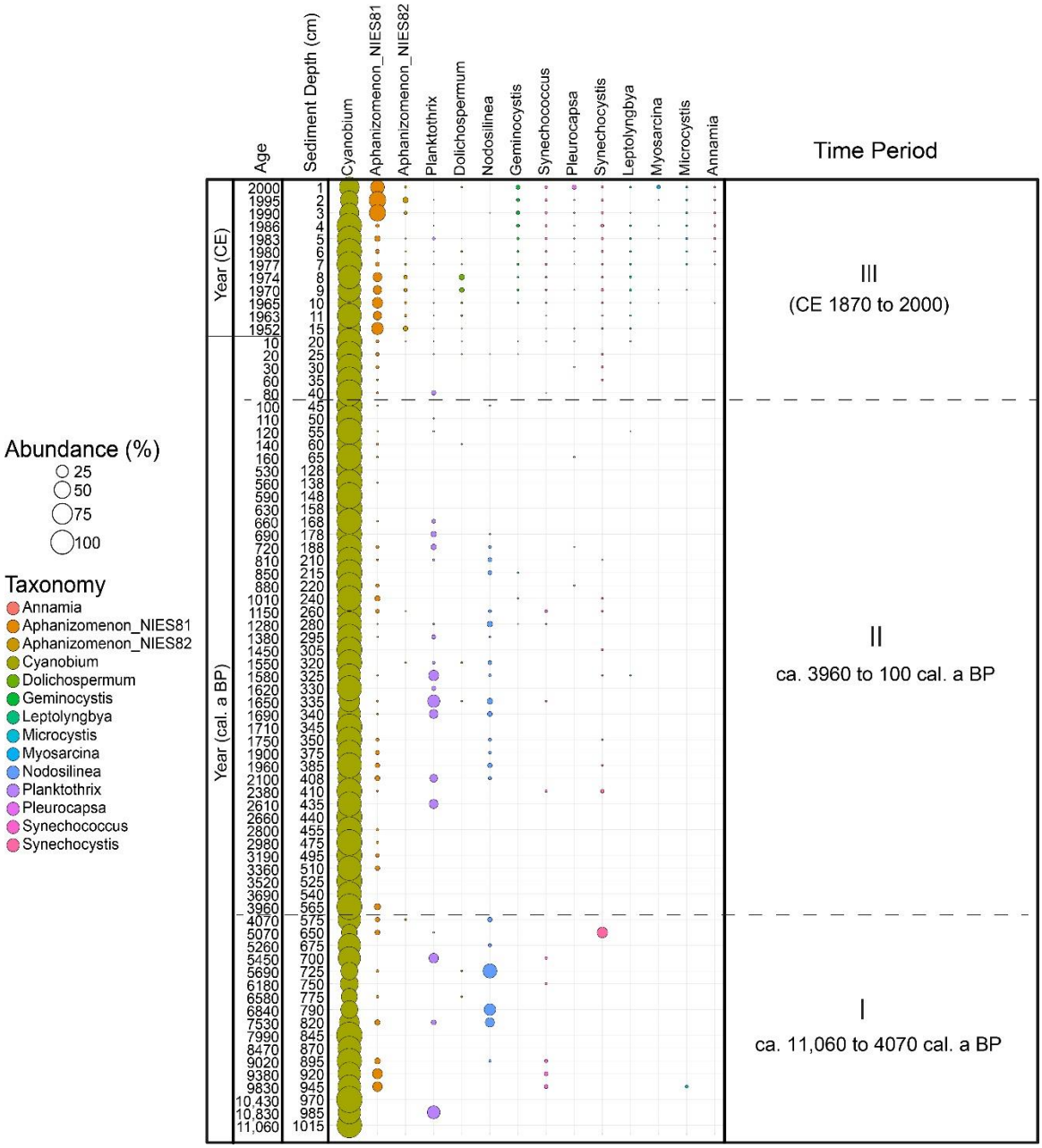

Figure 5.3: Cyanobacteria taxonomic distribution. Bubble plot showing the variation of cyanobacteria community composition at the amplicon sequence variant level (cutoff > 0.1% relative abundance) spanning over 11,000 years. Broken black lines demarcate the three significantly different temporal clusters identified by non-metric multidimensional scaling (see Fig. 5.4).

A non-metric multidimensional scaling (NMDS) revealed the cyanobacteria community dynamics at the ASV level showed three significantly different temporal clusters of which the youngest only covers 150 years compared to the two older ones which comprise several millennia (Fig. 5.4). A conservative one-way permutational analysis of variance (PerMANOVA) and a subsequent pairwise test shows that the three clusters are significantly different (p-value = 0.0001; F = 7; Table 1). A Spearman rank-based

correlation confirms a significant positive correlation between cyanobacterial abundance (qPCR) and vegetation openness (n = 74, p-value = 0.003, R_S = 0.5; Suppl. Table D.5), while there is no significant correlation between vegetation openness and cyanobacteria ASV richness (n = 74, p-value = 0.1, R_S = 0.26). Both sediment weight and organic carbon normalized DNA contents are significantly positively correlated to cyanobacteria ASV richness (n = 74, p-value = 0.003, R_S > 0.8) and cyanobacteria abundance (n = 74, p-value = 0.003, R_S = 0.7). Moreover, VQ and species richness are significantly correlated (n = 74, p-value = 0.003, R_S = 0.5) while VQ and cyanobacteria abundance are not significantly correlated (n = 74, p-value = 0.1, R_S = 0.2).

Table 5.1: Overall test statistics of the one-way PerMANOVA on cyanobacterial assemblage from amplicon sequencing grouped into the time periods: (I) ca. 11,060 to 4070 cal. a BP, (II) ca. 3960 to 100 cal. a BP, and (III) CE 1870 to 2000. Pairwise analysis shows Bonferroni corrected significant p-values (in bold) above the diagonal and corresponding F-values below.

Permutation N:	9999				
Total sum of squares:	27.39	**Pairwise**	**III**	**II**	**I**
Within-group sum of squares:	22.74	**III**		**0.0003**	**0.0003**
F:	6.952	**II**	9.412		**0.0003**
p (same):	0.0001	**I**	7.246	4.52	

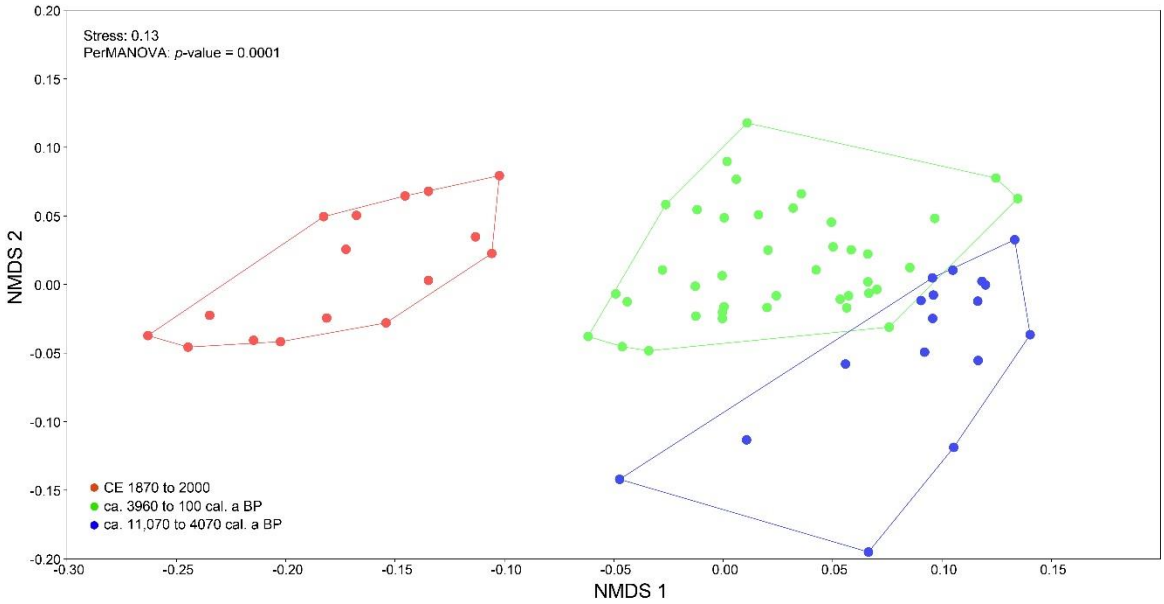

Figure 5.4: A non-metric multidimensional scaling (NMDS) visualization of Holocene beta diversity of cyanobacteria community dynamics based on amplicon sequence data using Bray–Curtis dissimilarity.

5.4.4 Metagenomic analysis

A shotgun sequence analysis was used to assess the presence of the cyanobacteria functional genes responsible for nitrogen fixation (*nif gene family)* and microcystin synthesis (*mcy gene family)* in 13 selected samples (Fig. 5.5), as well as to verify the taxonomic assignment from amplicon sequencing (Suppl. Fig. D.3). From samples dated to ca. 3520 and 530 cal. a BP, the abundance of *nif* genes distinctly increased for the first time and ranged between 0.012 – 0.02% of total cyanobacteria. The *nif* abundance was highest (0.05 – 0.20%) in samples from CE 1940, 1970 and 1990. In samples where *nif* abundance was recorded, a relatively high abundance of the diazotroph *Aphanizomenon* was also observed via amplicon sequencing (Fig. 5.3). The *mcy* genes were recorded for the first time in sample dated to ca. 1900 cal. a BP. Also, like *nif*, *mcy* was most abundant in recent sediment strata CE 1940 and 1990.

Regarding the taxonomic distribution, 16S rRNA taxonomic mapping from shotgun sequences confirmed the observed changes based on amplicon sequence data, with minor differences in the relative abundance of cyanobacteria groups (Suppl. Fig. D.4). For example, the family *Cyanobiaceae* was the most abundant in all the shotgun-analyzed samples, similar to amplicon sequencing for the same samples with *Cyanobium* as the most abundant. Other abundant families based on shotgun data were *Phormidiaceae, Nostocaceae, Microcystaceae* and *Synechococcaceae*. The low overall number of shotgun sequence reads for cyanobacteria in samples dated to ca. 5070, 7530 and 11,060 cal. a BP (< 8,00,000 reads) compared to the other samples (> 22,000,000) may explain the absence of *nif* and *mcy* functional genes in these samples.

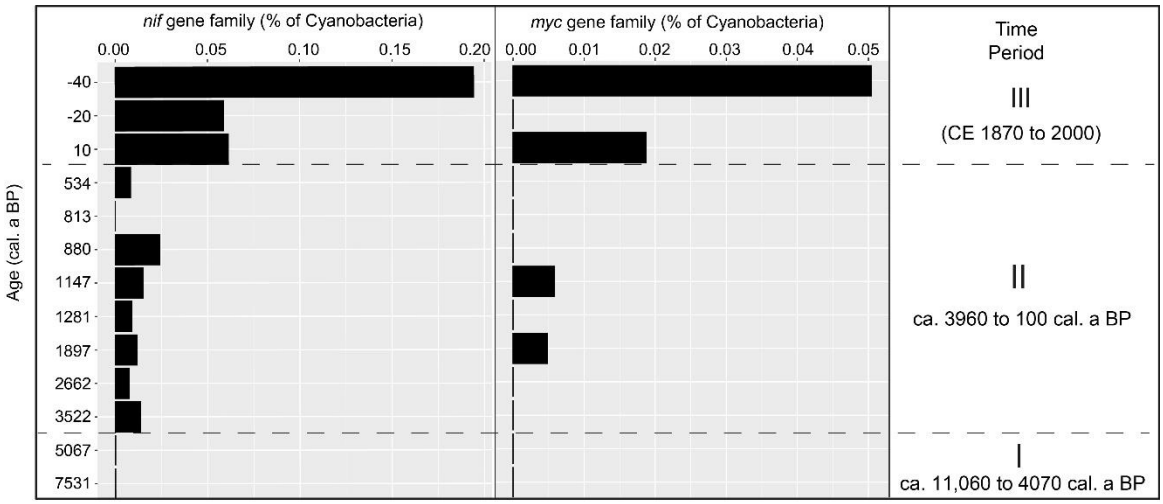

Figure 5.5: Barplots of key gene families involved in (a) nitrogen fixation (*nif*) and (b) microcystin (*mcy*) biosynthesis. The counts are normalized gene counts relative to all cyanobacteria counts in percentage for the selected sediment layers spanning over 11,000 years ago. Broken black lines demarcate the three significantly different temporal clusters identified by non-metric multidimensional scaling (see Fig. 5.4).

5.5 Discussion

5.5.1 Influence of sedimentation processes on cyanobacteria sedaDNA reconstruction

First, our results provide robust evidence of the long-term preservation of lake cyanobacteria DNA in ancient sediments dating back to 11,000 years. They confirm the high potential of combining sedaDNA analytical methods (qPCR, amplicon and shotgun sequencing) with biomarker analysis in providing a more detailed insight into past cyanobacteria community dynamics than using a single approach (Nwosu et al., 2021a, 2021b). Cyanobacteria communities are ideal indicator organisms for climate change and human impact (Huisman et al., 2018; Monchamp et al., 2018), however, until now to our knowledge they have been reconstructed only dating back to two millennia from lake sediments (Zhang et al., 2021b). Our data show that sediment characteristics like VQ (varve quality) did not have an impact on reconstructed cyanobacteria abundance (qPCR; *p*-value = 0.1; Fig. 5.2; Suppl. Table D.5) and cyanobacteria species composition (beta diversity; Fig. 4) from sedaDNA since the early Holocene. However, VQ significantly affected the number of reconstructed cyanobacteria ASV richness (alpha diversity; *p*-value = 0.003;

Fig. 2). Therefore, while VQ can have an impact on the number of reconstructed cyanobacteria taxa, their significant community compositional clustering patterns (*p*-value = 0.0001; Table 5.1) is not impacted by this factor. In addition, VQ had no impact on the increased cyanobacteria abundances caused by first human impact 4000 years ago and intensively in the last 150 years. One foremost challenge of sedaDNA data interpretation is the current limited knowledge on taphonomic processes during transport to and preservation of DNA in sediments under prevailing environmental conditions (Capo et al., 2021a). Here, we show the continuous increase in cyanobacteria abundance despite consistently low sedaDNA concentration (e.g., in Bronze Age samples, Fig. 5.2), suggests a true signal and not an artefact because the copy numbers were normalized to the amount of DNA in these samples (Suppl. Fig. D.4). We have previously shown that cyanobacteria sedaDNA reconstructions from Lake Tiefer See are robust and the mainly anoxic cold water–sediment interface promote DNA preservation after incorporation (Nwosu et al., 2021a, 2021b). Here we demonstrate further that the reconstruction of cyanobacterial dynamics, both at the phylum- and at the (sub)species-level (*Planktothrix*), were not related to nor dependent on changes in sedaDNA concentration over time (based on qPCR and amplicon sequencing; Suppl. Figs. D.4, D.5). Additionally, the trend observed in the cyanobacteria lipid biomarker 7-methylheptadecane reconstructed for the last 6000 years from Lake Tiefer See supports the DNA-based results from this study, suggesting there was likely no degradation of cyanobacteria ancient DNA (Suppl. Fig. D.6). The biomarker results confirm the human impact on cyanobacteria in Lake Tiefer See about 4000 years ago by showing a slight increase in 7-methylheptadecane quantity like the increase in total cyanobacteria abundance. Even at the species-level, the relative abundance of *Aphanizomenon*, also known to produce 7-methylheptadecane (Liu et al., 2013; Coates et al., 2014; Bauersachs et al., 2017), shows similar variability to 7-methylheptadecane quantities over time in some samples (Suppl. Fig. D.6), in line with previous evidence(Nwosu et al., 2021a). In samples where similar variations are not evident, it suggests the 7-methylheptadecane quantities may have originated from other cyanobacteria producers (Liu et al., 2013; Coates et al., 2014).

5.5.2 Human impact on cyanobacteria abundance and species richness

Our results show a first substantial increase in cyanobacteria abundance dating back to the Bronze Ages between ca. 3960 and 3690 cal. a BP (Fig. 5.2) which coincided with archaeological findings of settlements around Lake Tiefer See (Jantzen et al., 2011; Küster et al., 2015; Schmidt, 2019, 2020) (Suppl. Fig. D.1). Presumably, the increase in cyanobacteria abundance was driven by the impact of intensified human activities like deforestation and land-use (Theuerkauf et al., 2015) for farming within the catchment, and consistent with fluvial paleorecords (Kaiser et al., 2012; Theuerkauf et al., 2021). The archeological evidence is clearly seen in reconstructed vegetation openness from pollen data showing first increase of human-induced clearcutting and land openness from 12 to 36% between ca. 3960 and 3690 cal. a BP (Fig. 5.2). The coincidence of the first intensive land use in the lake catchment and increase in cyanobacteria abundance during the Bronze Age suggests a causal relation. We assume that the agricultural activity and use of lake water by the Bronze Age communities (Curry, 2016), for the first time, via excessive nutrient input impacted on the abundance of lake cyanobacteria. Human settlement activities in the region is further buttressed by the Bronze Age Tollense Battle ~74 km from Lake Tiefer See (Jantzen et al., 2011). Peaks in cyanobacteria abundance during Holocene warmer phases like the Roman Climate Optimum (ca. 1960 – 1740 cal. a BP) and the Medieval Warm Period (ca. 1010 – 810 cal. a BP; Fig. 2; Suppl. Fig. D.2) may have resulted from cyanobacteria blooms during these periods. Increasing water temperature as result of climate warming has been shown to stimulate cyanobacterial growth, especially bloom-forming cyanobacteria taxa (Visser et al., 2016b; Ullah et al., 2018).

Interestingly, the observed shift in cyanobacteria structure and abundance, marking the onset of cluster II (Figs. 5.2, 5.3, 5.4), did not reverse even when the population density decreased again (e.g., in four Bronze Age sediment samples spanning a ca. 600-year period; Suppl. Table D.1). This suggests a long-lasting legacy effect of anthropogenic eutrophication on Lake Tiefer See cyanobacteria community dynamics, probably because nutrients remained in the lake after inundation due to little outflow (Brauer et al., 2019).

Additionally, our data from a variety of sedaDNA analytical methods confirm the pattern of cyanobacteria community changes to be consistent up to sub-species levels, and shows increased cyanobacteria diversity between ca. 2400 and 820 cal. a BP (Figs. 5.2, 5.3; Suppl. Fig. D.5). This period spans the archaeological pre-Roman Iron Age (ca. 2500 – 1960 cal.

BP), and two rather warmer climatic phases in the Northern Hemisphere (Marcott et al., 2013; Wanner et al., 2015): Roman Optimum (ca. CE 1960 – 1740 cal. a BP) and Medieval Period (ca. 1010 – 820 cal. a BP). There is archeological evidence of human settlement around the vicinity of Lake Tiefer See during the pre-Roman and Roman Iron Ages (Suppl. Fig. D.1). Also, the Medieval Warm Period coincided with the Slavic Settlement Period ca. 1300 – 700 cal. a BP (Schmidt, 2012; Küster et al., 2015).

At the genus and sub-species level we found a first long-term relevance of lake *Planktothrix* populations with peaks during the Roman Iron Age and Slavic Settlement Period that likely resulted from past intense blooms (Figs. 5.2, 5.3). We have shown previously that *Planktothrix*, most especially the cyanopeptolin-producing ecotypes, are the most abundant potentially toxic taxa in Lake Tiefer See (Nwosu et al., 2021c). At the functional level, the first abundances of nitrogen-fixing (*nif*) and microcystin synthesis (*mcy*) genes were from Bronze Age and Roman Iron Age, respectively, (shotgun data; Fig. 5.5). Especially for the possibly toxic *mcy* gene which increased first in samples with equally corresponding peaks in *Planktothrix* abundances (qPCR and amplicon; Figs. 5.2, 5.3), that may have been the potential *mcy* producers (Meissner et al., 2013). These changes in cyanobacteria dynamics between the pre-Roman Iron Age and Slavic Settlement Period points foremost to a distinct human influence during settlement periods. This assumption is supported by reconstructions which showed lake level maxima in Lake Tiefer See (ca. 4000 – 3000, 2500, 1800, 1200, 1000 and 600 cal. a BP) were due partly to land-cover changes (deforestation) occurring during settlement periods (Theuerkauf et al., 2021). Furthermore, since there was an overlap between settlement and rather warmer climatic phases, it is possible that climate variability also had an additional impact on cyanobacteria dynamics during these periods. This suggests human impact and possibly climate warming as the main drivers of *Planktothrix* populations in the lake, as observed in other deep hard-water peri-Alpine lakes (Posch et al., 2012; Savichtcheva et al., 2015; Monchamp et al., 2019b). It is well documented that the ability to regulate buoyancy promotes *Planktothrix* proliferation under lake warming and a stable water column (reduced water turnover) (Walsby et al., 2006; Carey et al., 2012; Posch et al., 2012; Rigosi et al., 2014). Under such conditions they can move vertically within the water column to gain optimum nutrient and light conditions necessary for growth (Walsby et al., 2006; Posch et al., 2012). In contrast, the relatively low abundance of *Planktothrix* in the last 150 years of intense human impact and climate warming is probably because of taphonomic processes. We have shown

previously that the sediment deposition of *Planktothrix* may be impaired by heterotrophic decomposition, zooplankton grazing and DNA degradation during transport along the water column in Lake Tiefer See (Nwosu et al., 2021b). Furthermore, total *Planktothrix* abundance was only detected prior to the pre-Roman Iron Age (ca. 2100 cal. a BP, qPCR), even though amplicon sequencing show *Planktothrix* relative abundances several millennia earlier (Figs. 5.2, 5.3). This is perhaps an indication of *Planktothrix* lineage differences between ca. 2100 cal. a BP to CE 2000 and the mainly natural climate-influenced early to mid-Holocene period. Therefore, combining molecular approaches have helped identify for the first time changes in *Planktothrix* populations dating back to 11,000 years from sedaDNA.

If we would define the Anthropocene in Lake Tiefer See based on our DNA data this would be with the onset of industrialization from ca. CE 1870 (Figs. 5.2, 5.3). Since this period intensified human impact via farming (Kienel et al., 2013), and deforestation (Theuerkauf et al., 2015) resulted in an unprecedented change in cyanobacteria dynamics that clearly differs from that of the 11 millennia before. Specifically, our data clearly shows that the high cyanobacteria abundance and richness during the last 150 years in Lake Tiefer See never existed before since the early Holocene and strongly suggests human impact as the major driver. It is also probable that the current climate warming contributes to these observed changes in cyanobacteria community structure. Decades of research have shown that eutrophication (nutrient enrichment via anthropogenic farming) (Paerl and Otten, 2013; Ibrahim et al., 2021) and climate change (high temperatures) (Paerl and Huisman, 2008; Paerl and Otten, 2013) are the foremost environmental drivers that promote cyanobacteria dominance in a wide range of aquatic environments(Paerl and Paul, 2012; Paerl and Otten, 2013; Huisman et al., 2018). Taken together, cyanobacteria taxa were always present in the more than 11,000 years sediment record but with distinct phases of human-induced and possibly climate related variations in their dynamics.

5.6 Conclusion

We provide the first record of cyanobacteria sedaDNA for the entire Holocene that allows us to compare cyanobacteria abundance and species composition in times influenced by humans to pristine natural conditions in the first millennia of the Holocene. Particularly, combining amplicon and shotgun sequencing with qPCR on sedaDNA samples led to an enhanced understanding of the Holocene evolution of cyanobacterial assemblages in a lake formed during the Lateglacial. We find evidence for a distinct shift mainly in the abundance of cyanobacteria at around 4000 years ago, coinciding with first human settlements and increased agricultural activity on the lake shore during the Bronze Age. This shift marks a tipping point since the cyanobacterial abundance and assemblages never again reversed to the pre-settlement state, even in times when human impact in the lake catchment decreased. The second major cyanobacteria shift occurred 150 years ago coinciding with the industrial revolution and intensive use of fertilizers in agriculture. These last 150 years are unprecedented than the eleven millennia before, emphasizing the strong impact of our modern societies on natural environments. Nevertheless, it is also evident that human activity already impacted on the lake ecology much earlier than previously known. This must be taken into consideration when the role of humans on their local environments is evaluated.

5.7 Acknowledgments

We thank the German Environmental Foundation (Deutsche Bundesstiftung Umwelt DBU) for funding the research position of E.C.N. We thank the coring team of GFZ-section Climate Dynamics and Landscape Evolution who assisted in the fieldwork (Brian Brademann). We thank Anke Saborowski for laboratory support with TOPO Cloning analysis.

6 Synthesis

6.1 Introduction

Cyanobacteria play a key role in aquatic ecosystems where they contribute significantly to the global primary production and their community composition is driven by climate change and human impacts (Garcia-Pichel, 2009; Huisman et al., 2018). The combined effects of climate warming and anthropogenic eutrophication (excessive discharge of nutrients) on freshwater cyanobacteria assemblage have been studied in various lakes and reservoirs, but mostly at decadal to centennial time scales (e.g., Monchamp et al., 2016, 2019b; Cao et al., 2020; Erratt et al., 2021). Disentangling the distinct effects of climate and/or human stressors in shaping cyanobacteria assemblages is central to aquatic ecology and management. In light of the impacts these stressors exert on biodiversity and ecosystem functions (Cardinale et al., 2012; Grimm et al., 2013), it is crucial to understand how they distinctively shaped cyanobacteria community structure, composition and abundance over large spatial and temporal scales. This thesis contributes to our understanding of cyanobacteria and their distribution patterns in a deep temperate lake, and provides valuable information in predicting their response to future climate change and human impact.

In this thesis, a site-specific long-term cyanobacteria sedaDNA analysis was conducted to understand how cyanobacteria populations have changed since the early Holocene, and to investigate alterations in their dynamics caused by climate and/or human stressors during this time period. To my knowledge it is the first study to explicitly describe the Holocene history of cyanobacteria in a temperate lake spanning the last 11,058 years. Chapters 3 to 5 build on the results of Chapter 2, which evaluates the dynamics of cyanobacteria from the Little Ice Age to present time. The work described in this thesis combines a higher number of biological replicates and more extensive analyses to assess changes in cyanobacteria assemblages and abundance over ten millennia. Furthermore, the lake environmental parameters driving cyanobacteria community composition across geographical and spatial scales were also determined. In the following synthesis the main outcomes of this study (chapters 2 to 5) are put into a broader sense by elaborating on the dynamics of present-day cyanobacteria in the deep hard-water Lake Tiefer See (Chapter 6.2), the factors influencing cyanobacteria sediment deposition (6.3), and the drivers of

cyanobacteria community dynamics since the early Holocene (Chapter 6.4). The knowledge gaps filled by this study are outlined in the conclusions and possible focus of future research are recommended in the outlook.

6.2 Present day cyanobacteria dynamics

The analysis of the current and ancient cyanobacteria populations in Lake Tiefer See show the dominant taxa in the water column have always been present in the system since the early Holocene, with phases of climate- and/or human-related community variations (Chapters 2, 3 and 5). For example, the dominance of *Cyanobium* in sediments, and occasionally *Planktothrix*, reflects the spatio-temporal dynamics of their potential ecotypes in the water column (Figs. 5.3, 3.4b). Furthermore, the results from my research suggest an adaptation of a potential *Cyanobium* ecotype to the cold and dark deeper waters in Lake Tiefer See (ASV0014; Fig. 3.4b). This finding is substantiated by similar observations made in other aquatic environments like in temperate (Choi et al., 2013) and polar (Tang et al., 1997) seas, as well as in a shallow temperate lake (max. depth 5 m; Cai et al., 2021). Additionally, the results from this study show community shifts, niche specialization and coexistence of pelagic cyanobacteria populations in Lake Tiefer See, which is influenced mainly by their different responses to lake environmental factors (temperature, turbidity, dissolved oxygen, pH, conductivity and light) and nutrient (nitrate and dissolved phosphorus) availability (Fig. 3.7). This result concurs with previous observations made in the nearby Lake Stechlin (Selmeczy et al., 2016).

6.3 Taphonomy and cyanobacteria sedaDNA reconstruction

I found that irrespective of taphonomic processes sediment deposited cyanobacteria communities from Lake Tiefer See are representative of those in the water column ($p < 0.05$; Chapter 4). Taphonomic processes taking place along the water column which together may hinder sediment deposition of cyanobacteria assemblages include: the presence of a physical barrier in the metalimnion which favors heterotrophic decomposition (Halstvedt et al., 2007), zooplankton grazing (Kurmayer and Jüttner, 1999; Jezberová and Komárková, 2007), and DNA degradation (Callieri et al., 2012b). However, the main difference between the water column and sediment-reconstructed communities is that taphonomic processes occurring along the water column, and at the sediment-water

interface, impact individual taxa differently which may misrepresent their true pelagic relevance (Chapter 4). Perhaps the most glaring example of this finding is the disproportionate relative abundances of the potential toxin producing *Aphanizomenon* and *Planktothrix* in water and sediments (Fig. 4.3a). On the one hand, the solitary nature of the filamentous *Planktothrix* make them more susceptible to factors like predation, heterotrophic decomposition, and DNA degradation which likely cause their low abundance in sediments (Sønstebø and Rohrlack, 2011; Gerphagnon et al., 2015). On the other hand, aggregate formation in *Aphanizomenon* may make them less affected by the same taphonomic processes, and likely result to their overrepresentation in sediments (Heiskanen and Olli, 1996; Tallberg and Heiskanen, 1998). Nevertheless, *Aphanizomenon* populations appear to bloom in the epilimnion during late spring and early summer in Lake Tiefer See (Fig. 3.4b). This suggests that the steady increase in their relative abundances in the last century and peak relative abundances at other times during the early Holocene (Figs. 2.3, 5.3), were probably previous bloom events driven by anthropogenic eutrophication and/or climate warming (Fig. 2.6). Together, these results highlight the importance of combining sediment and water column community analysis in monitoring aquatic ecosystems threatened by the spread of potentially toxic cyanobacteria species.

6.3.1 Cyanobacteria sedaDNA as a paleo-proxy

I showed that cyanobacteria sedaDNA is an ideal paleolimnological proxy for lake-environmental factors and anthropogenic activity due to the long-term persistence of the DNA in sediments (Chapters 2, 4 and 5). Although uncertainties remain on how DNA is preserved in lake sediments over long periods, my findings support previous evidence (Domaizon et al., 2013; Mejbel et al., 2022) that a cold and anoxic lake bottom is crucial for the long-term preservation of cyanobacteria DNA after sediment deposition. Nevertheless, it has been shown that, irrespective of ideal preservation conditions, inter-strand crosslinks and strand breakages may critically affect the quality of sedaDNA molecules older than 10,000 years (Willerslev and Cooper, 2005; Hansen et al., 2006; Dabney et al., 2013). Therefore, in my research, I examined the long-term preservation of cyanobacteria sedaDNA in over 10,000-year-old sediments by HTS and clone libraries of short fragment qPCR assay products, as well as long fragment cyanobacteria PCR amplicons. The results confirmed the amplified sedaDNA products were indeed those of cyanobacteria (Figs. 5.2, 5.3, Suppl. Table D.4). In these ancient sediments, the community

composition showed the presence of taxa that form resting stages like *Aphanizomenon* (akinetes), which are better protected against taphonomic processes in sediments (Cires et al., 2013), as well as taxa that do not form resting stages such as *Planktothrix*, *Cyanobium* and *Synechococcus* (Fig. 5.3), meaning that cyanobacteria populations were generally well-preserved. Furthermore, the positive correlations of cyanobacteria taxa (both those that form and those that do not form resting stages) to lake physicochemical parameters such as temperature and turbidity ($p < 0.05$; Fig. 4.6), as well as that of total cyanobacteria abundance to human-influenced vegetation openness ($p < 0.05$; Suppl. Table D.5), strongly suggest cyanobacteria sedaDNA are suitable proxies for tracing changes in lake environmental parameters and human impact over longer geographical time scales.

6.3.2 Recommended approach to reconstruct cyanobacteria sedaDNA

With my work I showed the importance of using a combination of molecular analytical methods to optimally track changes in cyanobacteria assemblages reconstructed from lacustrine sediments (Chapters 4 and 5). Specifically, the data show that a universal molecular marker alone is insufficient to trace poorly sediment-depositing species (e.g., *Planktothrix*; Chapter 4; Fig. 4.3a), and consequently targeted approaches are necessary to optimally reconstruct their populations from sediments (Wood et al., 2019). To my knowledge for the first time, changes in cyanobacteria structure and abundance during the Holocene were revealed using (i) universal marker-based HTS to reveal community variations, (ii) targeted qPCR assays to show changes in the abundances of total cyanobacteria, total *Planktothrix* and cyanopeptolin-producing *Planktothrix* ecotypes, and (iii) metagenomic sequencing to confirm the results from HTS and qPCR (Suppl.Fig. D.3). Also, my work identifies concurrent increase in abundances of nitrogen fixing (*nif*) and microcystin (*mcy*) synthesis genes with their potential source organisms *Aphanizomenon* and *Planktothrix*, respectively (Fig 5.3, 5.5). This means the DNA-based data generated in my research are complementary and consistent with each other, as well as in line with previous evidence (Mejbel et al., 2021), thus underlining their suitability for historical cyanobacteria community analysis from sedaDNA. Although for HTS, it should be noted that the choice of cyanobacteria universal marker substantially impacts the resolution of cyanobacteria community analysis obtainable from sedaDNA. The longer (670 bp) cyanobacteria universal primer (Chapter 2), for example, did not reveal any information on the poor sediment-depositing potentially toxic *Planktothrix* (Fig. 2.3), despite being one of

the dominant taxa in Lake Tiefer See (Figs. 3.4b, 4.3a). In contrast, the shorter (359 bp) universal cyanobacterial marker (Chapters 4 and 5) successfully amplified *Planktothrix* (Figs. 3.4b, 4.3a, 5.3). In both analyses, the same SILVA version 138 database (Yilmaz et al., 2014) was used for taxonomic assignment. This means it is unlikely that the discrepancy is linked to the database but it rather is due to primer bias (i.e., different PCR amplicon sizes), which impacted the diversity of cyanobacteria populations obtained from the same sediment records (Lee et al., 2012). My research thus suggests PCR amplicon length plays a crucial role in the amplification of cyanobacteria populations from sediments. This is because compared to longer fragments, PCRs with shorter fragment lengths are generally more efficient with low artefact formation (Huber et al., 2009). This observation is supported by a recent finding which showed shorter fragment ddPCR better quantified cyanobacteria absolute abundances from sediments compared to HTS approach due to the high tolerance of ddPCR to PCR inhibitors (Mejbel et al., 2021) Therefore, as DNA-based analytical methods continue to advance, taxonomic databases continue to expand and costs of running these analyses reduce, it becomes more advantageous to simultaneously implement these approaches in sedaDNA studies (Mejbel et al., 2021). This will improve the robustness and effectiveness of using cyanobacteria sedaDNA as proxy for lake physicochemical factors and historical human impact. Overall, the results from my research emphasize the relevance of combining universal and targeted approaches in reconstructing cyanobacteria assemblages from sedaDNA.

6.4 Cyanobacteria dynamics since the early Holocene

I used sedaDNA to reconstruct the history of cyanobacteria spanning the entire Holocene period (Chapter 5) which enabled a differentiation among phases of climate variability with no, moderate, and intense human impact on freshwater cyanobacteria community dynamics (Figs. 5.2, 5.3, 5.4). Thus, providing clarity on one of the current challenges facing cyanobacteria sedaDNA research, namely, untangling the specific effect of climate variability and human impact on freshwater cyanobacteria dynamics. Differentiating between these factors until now has been difficult because most cyanobacteria sedaDNA reconstructions extend back only to the beginning of industrialization (e.g., Domaizon et al., 2013; Monchamp et al., 2018; Cao et al., 2020). During this period, the combined effect of climate warming and anthropogenic eutrophication has led to the expansion of cyanobacteria blooms in lakes worldwide (Rigosi et al., 2014; Huisman et al., 2018).

Previous studies have reported, for example, the invasion and colonization of *Dolichospermum* in many oligo-mesotrophic temperate lakes because of increasing water temperatures and human nutrient input (nitrogen and phosphorus) during the last century (Salmaso et al., 2015b, 2015a; Monchamp et al., 2018). The results from my research, however, show the abundance of *Dolichospermum* (and other bloom-forming taxa like *Microcystis*) in Lake Tiefer See at some intervals during the early to mid-Holocene, a period marked with a variable climate with no human impact (Fig. 5.3). This suggests a long-term prevalence of potentially toxin-producing and bloom-forming cyanobacterial taxa, and broadens our knowledge on their dynamics since the early Holocene unknown before now in the Lake Tiefer See region. Furthermore, cyanobacteria abundance during the early to mid-Holocene was relatively stable and only increased substantially during the otherwise relatively cooler Bronze Age climate as shown by qPCR (Figs. 1.6, Suppl. Fig. D.2). This steady increase in cyanobacteria abundance by more than one order of magnitude coincided with historical human impact (deforestation and eutrophication) in the region derived from pollen data, and is supported by archaeological findings as well as war records (Suppl. Fig. D.1) (Jantzen et al., 2011; Schmidt, 2012; Theuerkauf et al., 2021). Also, sedaDNA concentrations did not increase in the four Bronze Age sediment samples, meaning that the observed increase in cyanobacteria abundance measured in them is a true signal and not an artefact, because the cyanobacteria copy numbers were normalized to DNA quantities extracted from these samples (Suppl. Fig. D.4). Also, the Bronze Age samples together span a 600-year period (3950 – 3350 cal. a BP; Suppl. Table D.1) which illustrates the long-lasting legacy impact of human eutrophication in promoting lake cyanobacteria abundance. Even at the species-level, as shown by HTS data, the eutrophication-associated *Aphanizomenon* was dominant in the Bronze Age samples (Fig. 5.3). This supports the assumption that human nutrient input into the lake likely promoted their growth during the Bronze Age.

Furthermore, my research shows pre-industrial revolution maxima in cyanobacteria abundance during periods of climate warming (Roman Climate Optimum and Medieval Warm Period), that also coincided with moderate human impact (Fig. 5.2, Suppl. Fig. D.2). This suggests combined climate warming and human impact are the strongest drivers of lake cyanobacteria abundance, which is in line with evidence from several recent sedaDNA studies spanning the last century (e.g., Savichtcheva et al., 2015; Capo et al., 2019; Erratt et al., 2021; Zhang et al., 2021b). To my knowledge, the only other millennia-scale

freshwater reconstruction of cyanobacteria was from Lake Moon, China (max. depth 6.5 m) which spanned the last 2000 years (Roman Iron Age; Zhang et al., 2021). Pre-industrial cyanobacteria abundance in Lake Moon was mainly influenced by increased nutrient availability recycled from sediment due to low lake levels, variations in temperature and precipitation (Qin et al., 2020; Zhang et al., 2021b). In contrast, cyanobacteria dynamics in the deep hard-water Lake Tiefer See has been mostly driven by external human impact (farming and deforestation) and climate warming since the early Holocene (Chapters 2 and 5). Additionally, during the cooler Little Ice Age marked with increased human activity around Lake Tiefer See (Theuerkauf et al., 2021), cyanobacteria abundance reduced by one order of magnitude (Suppl. Fig. D.2). However, during phases of warm temperature anomalies from early to mid-Holocene with no human impact cyanobacteria abundance did not comparably increase. Together these findings suggest that periods with both human impact and climate warming had the strongest impact on lake cyanobacteria abundance and composition, compared to the effect of either signal.

Recently, several decadal to centennial-scale sedaDNA studies have targeted cyanobacteria as a group (e.g., Pal et al., 2015; Monchamp et al., 2018; Zhang et al., 2021a), or the toxins produced by harmful cyanobacteria (e.g., Zastepa et al., 2017; Tse et al., 2018; Pilon et al., 2019), to show climate change and human eutrophication promote increased bloom formations and toxin concentrations in lakes since the industrial revolution. The results from this thesis concur with these previous studies by showing a high abundance of the *mcy* (microcystin gene family) in recent sediments. Furthermore, they also extend the temporal scale record of *mcy* reconstructed from sediments to two millennia (Fig. 5.5). Particularly, I found concurrent high abundances in *mcy* gene and total *Planktothrix* (also known to produce *mcy*, Meissner et al., 2013), during the Roman Climate Optimum and Medieval Warm Period (Fig. 5.5b), which also coincide with human presence in the Lake Tiefer See region (Suppl. Fig. D.1). These observations suggest that both human influence and climate warming promoted the proliferation of *Planktothrix* populations during these periods, which consequently resulted in the abundance of potentially toxic *mcy* genes in Lake Tiefer See.

Furthermore, the molecular data from my research is supported by the results of cyanobacteria biomarker reconstructed for the last 6000 years from Lake Tiefer See in this study (Chapters 2 and 5). Specifically, the lipid biomarker 7-methylheptadecane show the same variation with *Aphanizomenon* relative abundance from metabarcoding and total

cyanobacteria abundance from qPCR over time (Figs. 2.7, 5.3, Suppl. Fig. D.6). Therefore, these data from three different cyanobacteria proxies showing similar trends over time illustrate the preservation of cyanobacteria DNA in ancient sediments. This is consistent with previous observations in the Baltic Sea where cyanobacteria biomarkers were reconstructed from up to 7200 cal. a BP ancient sediments (Sollai et al., 2017).

6.5 Conclusions

The results from this thesis extend our understanding of long-term cyanobacteria assemblage and abundance in a deep temperate lake since the early Holocene. Specifically, it reveals first insights into the separate and combined effects of climate warming and anthropogenic disturbances on cyanobacteria structure and abundance and through this on a lake ecosystem along the Holocene. The thesis additionally investigates the distribution of cyanobacteria populations at the species level in the deep oligo-mesotrophic lake, as well as identifies possible processes in the water column and at the sediment-water interface that affect their sediment deposition. Furthermore, it underlines the benefit of pelagic monitoring prior to ancient DNA paleo reconstructions, as it identified specific groups that require a targeted approach during sedaDNA investigation. The answers to the key questions addressed in this thesis can thus be summarized as follows:

- **What are the seasonal dynamics of cyanobacteria populations in deep, hard-water temperate lakes?**

I. There is seasonal variability in cyanobacteria populations with the dominant taxa belonging to the cyanobacteria orders Synechococcales (*Snowella*- summer to autumn), Nostocales (*Aphanizomenon*- spring to summer), Chroococcales (*Microcystis*- autumn), and Oscillatoriales (*Planktothrix*- late spring to fall). However, some of the dominant taxa (*Cyanobium* and *Synechococcus*) were abundant throughout the year

II. The community dynamic is significantly influenced by the interplay between lake physicochemical factors and nutrients.

III. There is evidence that suggests niche specialization and coexistence of cyanobacteria species in the water column of the deep hard-water Lake Tiefer See.

IV. The high-resolution cyanobacteria community data analysis also implies the adaptation of a potential *Cyanobium* ecotype to the cold and dark environment of deeper waters.

- **Are the sediment-deposited cyanobacteria assemblages consistent with those in the water column?**

I. Cyanobacterial DNA in the sediment significantly reflects cyanobacteria communities of the water column.

II. The only difference between sediment and water sample matrices is in the relative abundances of cyanobacteria species, which is related to the different ways taphonomic processes affect the sediment deposition of various cyanobacteria taxa due to their eco-physiological differences, e.g., single-filament and aggregate-forming taxa, and their spatiotemporal dynamics.

III. Consequently, utilizing both universal and targeted marker approaches is central to robustly capture changes in cyanobacteria assemblages in sediment records.

- **How has cyanobacteria structure (diversity and composition) and abundance changed since the Holocene to present time?**

I. Cyanobacteria abundance during the early to mid-Holocene was relatively stable despite moderate climatic changes.

II. A first significant steady increase in cyanobacteria abundance coincided with increasing human acivity and settlement in the study region during the Bronze Age. The effects of both climate variability and moderate human impact during the Roman Iron Age, Medieval Warm Period, as well as climate warming and intense human impact since industrialization (CE 1870) were main factors responsible for peaks in cyanobacteria abundance. The reduction in cyanobacteria abundance during the Little Ice Age despite a constantly high human impact in the study region demonstrates that besides human activity climatic changes are also also drivers for lake cyanobacteria dynamics.

III. The current dominant cyanobacteria taxa in Lake Tiefer See have been in the lake since the early Holocene. However, there have been periods with climate- and/or human-driven community shifts.

IV. The positive correlations of various cyanobacteria sedaDNA data to selected lake environmental parameters and reconstructed vegetation openness via anthropogenic deforestation strongly suggests cyanobacteria sedaDNA are ideal paleolimnological proxies.

6.6 Outlook

This thesis investigated changes in cyanobacteria assemblages since the Holocene. The sediment samples from which the long-term data presented in this study were generated were however not continuous for the entire Holocene but rather represent snapshots of different points during this time period. Further studies could attempt a high-resolution sampling of periods where the results from this study showed peaks in cyanobacteria abundance and periods of climate variability with moderate human impact. Combining high resolution sampling with multiple sedaDNA and lake environmental analyses may identify additional factors which have impacted Holocene cyanobacteria dynamics. This might contribute more clarity to the ongoing discussion of how climate and human stressors separately affect lake cyanobacteria populations. Especially, it would be helpful if future studies could target more data points for the mainly climate-driven early to mid-Holocene. This could reveal additional information on the impact of climate warming anomalies (10 and 7.5 cal. ka BP) on cyanobacteria assemblages.

The results shown in this thesis were site-specific, so future studies should reconstruct cyanobacteria populations from sediments in other regional lakes. This may offer insights into previous human impact in the region, since the data shown in this thesis strongly demonstrates the suitability of cyanobacteria sedaDNA as a paleo-environmental proxy. Moreover, such a comparative study would also serve to validate the observations made in the present study. Furthermore, in addition to sheer correlations, advanced statistical analysis like structural equation modeling (Chen and Ficetola, 2020) can be used to examine the directed relationships between dependent (cyanobacteria sedaDNA) and independent (lake environmental factors) variables.

A detailed analysis of the dynamics of the non-photosynthetic cyanobacteria (NCY) sister clades- Sericytochromatia and Melainabacteria- since the Holocene was not the objective of this thesis. The preliminary results spanning the last 350 years show that they are clearly separated from photosynthetic cyanobacteria clades and their species richness did not increase during this time period (Chapter 2). Furthermore, there seems to be a link between anoxic/oxic conditions at the lake bottom during sediment deposition and distribution of their assemblages from sedaDNA. Particularly, Sericytochromatia preferably occurred in non-varved (more oxic) sediments while Melainabacteria occurred in varved (more anoxic)

sediments (Fig. 2.5). These results are in agreement with previous evidence (Monchamp et al., 2019a) and suggest their community dynamics are not driven by the typical factors like climate warming and anthropogenic eutrophication that affect photosynthetic cyanobacteria. Also, current knowledge on their occurrence from mainly culture-independent metagenome reconstructions suggest they are adapted to photic and aphotic habitats (Di Rienzi et al., 2013; Soo et al., 2014, 2017). Therefore, future research could combine high-resolution sampling with molecular analytical methods to study in more detail the dynamics of the NCY over longer geographical time- (Holocene) and spatial- (water column) scales. This might improve the understanding of their occurrence in this ecosystem and provide more clarity on the lake environmental stressors shaping their dynamics.

In this thesis, estimates of total *Planktothrix* could only be obtained in sediments dating bak to the late Bronze Age, which may be because of a change in *Planktothrix* lineage from this time point. A valuable area of focus in future research may be a detailed investigation of this potential lineage change by increasing the sample resolution (more data points) used for metagenome analysis especially during early to mid-Holocene. In addition, quantification of total *Planktothrix* abundance in these sediments using targeted approaches like the new digital droplet PCR, which has been shown to have a high tolerance to PCR inhibitors (Mejbel et al., 2022) or optimized qPCR markers.

References

Adrian, R., O'Reilly, C. M., Zagarese, H., Baines, S. B., Hessen, D. O., Keller, W., et al. (2009). Lakes as sentinels of climate change. *Limnol. Oceanogr.* **54**, 2283–2297. https://doi.org/10.4319/lo.2009.54.6_part_2.2283

Aho, A. V., Kernighan, B. W., and Weinberger, P. J. (1979). Awk — a pattern scanning and processing language. *Softw. Pract. Exp.* **9**, 267–279. https://doi.org/10.1002/spe.4380090403

Albrecht, M., Pröschold, T., and Schumann, R. (2017). Identification of Cyanobacteria in a eutrophic coastal lagoon on the Southern Baltic Coast. *Front. Microbiol.* **8**, 293. https://doi.org/10.3389/fmicb.2017.00923

Allgaier, M., and Grossart, H. P. (2006). Seasonal dynamics and phylogenetic diversity of free-living and particle-associated bacterial communities in four lakes in northeastern Germany. *Aquat. Microb. Ecol.* **45**, 115–128. https://doi.org/10.3354/ame045115

Alsos, I. G., Sjögren, P., Brown, A. G., Gielly, L., Merkel, M. K. F., Paus, A., et al. (2020). Last Glacial Maximum environmental conditions at Andøya, northern Norway; evidence for a northern ice-edge ecological "hotspot." *Quat. Sci. Rev.* **239**, 106364. https://doi.org/10.1016/j.quascirev.2020.106364

Anderson, D. G., Maasch, K. A., Sandweiss, D. H., and Mayewski, P. A. (2007). "Climate and culture change: Exploring Holocene transitions," in Climate Change and Cultural Dynamics 2007, pp 1-23, ISBN 9780120883905, https://doi.org/10.1016/B978-012088390-5.50006-6

Andrews, S., Krueger, F., Seconds-Pichon, A., Biggins, F., and Wingett, S. (2015). FastQC. *A quality control tool for high throughput sequence data.* Babraham Bioinformatics. Babraham Inst.

Armbrecht, L. H., Coolen, M. J. L., Lejzerowicz, F., George, S. C., Negandhi, K., Suzuki, Y., et al. (2019). Ancient DNA from marine sediments: Precautions and considerations for seafloor coring, sample handling and data generation. *Earth-Science Rev.* **196**, 102887. https://doi.org/10.1016/j.earscirev.2019.102887

Bajard, M., Poulenard, J., Sabatier, P., Bertrand, Y., Crouzet, C., Ficetola, G. F., et al. (2020). Pastoralism increased vulnerability of a subalpine catchment to flood hazard through changing soil properties. *Palaeogeogr. Palaeoclimatol. Palaeoecol.* **538**, 109462, https://doi.org/10.1016/j.palaeo.2019.109462

Bajard, M., Poulenard, J., Sabatier, P., Develle, A. L., Giguet-Covex, C., Jacob, J., et al. (2017). Progressive and regressive soil evolution phases in the Anthropocene. *Catena*. Vol. 150, 2017, pp 39-52 https://doi.org/10.1016/j.catena.2016.11.001

Ballot, A., Fastner, J., and Wiedner, C. (2010). Paralytic shellfish poisoning toxin-producing cyanobacterium Aphanizomenon gracile in Northeast Germany. *Appl. Environ. Microbiol.* **76**, 1173-1180, https://doi.org/10.1128/AEM.02285-09

Battarbee, R. W., and Bennion, H. (2011). Palaeolimnology and its developing role in assessing the history and extent of human impact on lake ecosystems. *J. Paleolimnol.* **45**, 399–404. https://doi.org/10.1007/s10933-010-9423-7

Bauersachs, T., Talbot, H. M., Sidgwick, F., Sivonen, K., and Schwark, L. (2017). Lipid biomarker signatures as tracers for harmful cyanobacterial blooms in the Baltic Sea. *PLoS One.* **12**, e0186360. https://doi.org/10.1371/journal.pone.0186360

Bell, T., and Kalff, J. (2001). The contribution of picophytoplankton in marine and freshwater systems of different trophic status and depth. *Limnol. Oceanogr.* **46**, 1243–1248. https://doi.org/10.4319/lo.2001.46.5.1243

Belle, S., and Parent, C. (2019). Reconstruction of Past Dynamics of Methane-Oxidizing Bacteria in Lake Sediments Using a Quantitative PCR Method: Connecting Past Environmental Changes and Microbial Community. *Geomicrobiol. J.* **36**, 570–579. https://doi.org/10.1080/01490451.2019.1583698

Bennion, H., Battarbee, R. W., Sayer, C. D., Simpson, G. L., and Davidson, T. A. (2011). Defining reference conditions and restoration targets for lake ecosystems using palaeolimnology: A synthesis. *J. Paleolimnol.* **45**, 533–544. https://doi.org/10.1007/s10933-010-9419-3

Birks, H. H. (1991). Holocene vegetational history and climatic change in west Spitsbergen - plant macrofossils from Skardtjørna, an Arctic lake. *The Holocene.* **1**, 209-218. https://doi.org/10.1177/095968369100100303

Bižić, M., Klintzsch, T., Ionescu, D., Hindiyeh, M. Y., Günthel, M., Muro-Pastor, A. M., et al. (2020). Aquatic and terrestrial cyanobacteria produce methane. *Sci. Adv.* **6**, eaax5343. https://doi.org/10.1126/sciadv.aax5343

Boehrer, B., and Schultze, M. (2008). Stratification of lakes. *Rev. Geophys.* **46**, 210. https://doi.org/10.1029/2006RG000210

Boere, A. C., Rijpstra, W. I. C., De Lange, G. J., Sinninghe Damsté, J. S., and Coolen, M. J. L. (2011). Preservation potential of ancient plankton DNA in Pleistocene marine sediments. *Geobiology.* **9**, 377-393. https://doi.org/10.1111/j.14724669.2011.00290.x

Bolger, A. M., Lohse, M., and Usadel, B. (2014). Trimmomatic: A flexible trimmer for Illumina sequence data. *Bioinformatics.* **30**, 2114–2120. https://doi.org/10.1093/bioinformatics/btu170

Bork et al. (1998). Landschaftsentwicklung in Mitteleuropa. Gotha (Klett- Perthes). 328.

Brauer, A. (2004). "Annually Laminated Lake Sediments and Their Palaeoclimatic Relevance," in: H. Fischer et al. (eds.), The Climate in Historical Times. GKSS School of Environmental Research. Springer, Berlin, Heidelberg. Pp 109-127, https://doi.org/10.1007/978-3-662-10313-5_7

Brauer, A., and Guilizzoni, P. (2004). The record of human/climate interactions in lake sediments. *Quat. Int.* **113**, 1–3. https://doi.org/10.1016/s1040-6182(03)00076-4

Brauer, A., Schwab, M. J., Brademann, B., Pinkerneil, S., and Theuerkauf, M. (2019). Tiefer See – a key site for lake sediment research in NE Germany. *DEUQUA Spec. Publ.* **2**, 89–93. https://doi.org/10.5194/deuquasp-2-89-2019

Breitbarth, E., Oschlies, A., and LaRoche, J. (2007). Physiological constraints on the global distribution of *Trichodesmium* - Effect of temperature on diazotrophy. *Biogeosciences.* **4**, 53–61. https://doi.org/10.5194/bg-4-53-2007

Britton, G., Liaaen-Jensen, S., and Pfander, H. (2008). "Special Molecules, Special Properties," in Britton, G., Liaaen-Jensen, S., Pfander, H. (eds) Carotenoids. Carotenoids vol 4. Birkhäuser Basel. Pp 1-6, https://doi.org/10.1007/978-3-76437499-0_1

Bullerjahn, G. S., McKay, R. M., Davis, T. W., Baker, D. B., Boyer, G. L., D'Anglada, L. V., et al. (2016). Global solutions to regional problems: Collecting global expertise to address the problem of harmful cyanobacterial blooms. A Lake Erie case study. *Harmful Algae.* **54**, 223–238. https://doi.org/10.1016/j.hal.2016.01.003

Burnap, R. L., Hagemann, M., and Kaplan, A. (2015). Regulation of CO2concentrating mechanism in cyanobacteria. *Life.* **5**, 348-371. https://doi.org/10.3390/life5010348

Bushnell, B., Rood, J., and Singer, E. (2017). BBTools Software Package. *PLoS One*. **12**, e0185056. https://doi.org/10.1371/journal.pone.0185056

Bustin, S. A., Benes, V., Garson, J. A., Hellemans, J., Huggett, J., Kubista, M., et al. (2009). The MIQE guidelines: Minimum information for publication of quantitative real-

time PCR experiments. *Clin. Chem.* **55**, 611–622. https://doi.org/10.1373/clinchem.2008.112797

Butts, E., and Carrick, H. J. (2017). Phytoplankton Seasonality along a Trophic Gradient of Temperate Lakes: Convergence in Taxonomic Compostion during Winter Ice-Cover. *Northeast. Nat.* **24**, B167–B187. https://doi.org/10.1656/045.024.s719

Cai, J., Hodoki, Y., and Nakano, S. ichi (2021). Phylogenetic diversity of the picocyanobacterial community from a novel winter bloom in Lake Biwa. *Limnology*. **22**, 161–167. https://doi.org/10.1007/s10201-020-00649-5

Callahan, B. J., McMurdie, P. J., Rosen, M. J., Han, A. W., Johnson, A. J. A., and Holmes, S. P. (2016). DADA2: High-resolution sample inference from Illumina amplicon data. *Nat. Methods*. **13**, 581-583. https://doi.org/10.1038/nmeth.3869

Callieri, C. (2008). Picophytoplankton in Freshwater Ecosystems: The Importance of Small-Sized Phototrophs. *Freshw. Rev.* **1**, 1-28. https://doi.org/10.1608/frj-1.1.1

Callieri, C., Caravati, E., Corno, G., and Bertoni, R. (2012a). Picocyanobacterial community structure and space-time dynamics in the subalpine Lake Maggiore (N. Italy). *J. Limnol.* **63**, 244–249. https://doi.org/10.4081/jlimnol.2012.e9

Callieri, C., Corno, G., Caravati, E., Galafassi, S., Bottinelli, M., and Bertoni, R. (2007). Photosynthetic characteristics and diversity of freshwater Synechococcus at two depths during different mixing conditions in a deep oligotrophic lake. *J. Limnol.* **66**, 81–89. https://doi.org/10.4081/jlimnol.2007.81

Callieri, C., Cronberg, G., and Stockner, J. G. (2012b). "Freshwater picocyanobacteria: Single cells, microcolonies and colonial forms," *in Ecology of Cyanobacteria II: Their Diversity in Space and Time*, ed. B. Whitton (Dordrecht: Springer), 229–269 https://doi.org/10.1007/978-94-007-3855-3_8

Callieri, C., Karjalainen, S. M., and Passoni, S. (2002). Grazing by ciliates and heterotrophic nanoflagellates on picocyanobacteria in Lago Maggiore, Italy. *J. Plankton Res.* **24**, 785–796. https://doi.org/10.1093/plankt/24.8.785

Callieri, C., Morabito, G., Huot, Y., Neale, P. J., and Litchman, E. (2001). Photosynthetic response of pico- and nanoplanktonic algae to UVB, UVA and PAR in a high mountain lake. in *Aquatic Sciences* **63**, 286–293. https://doi.org/10.1007/PL00001355

Callieri, C., and Piscia, R. (2002). Photosynthetic efficiency and seasonality of autotrophic picoplankton in Lago Maggiore after its recovery. *Freshw. Biol.* **47**, 947-956. https://doi.org/10.1046/j.1365-2427.2002.00821.x

Callieri, C., and Stockner, J. (2000). Picocyanobacteria success in oligotrophic lakes: Fact or fiction? *J. Limnol*. **59**, 72–76. https://doi.org/10.4081/jlimnol.2000.72

Camacho, A., Picazo, A., Miracle, M. R., and Vicente, E. (2009). Spatial distribution and temporal dynamics of picocyanobacteria in a meromictic karstic lake. Arch. Hydrobiol. *Suppl. Algol. Stud.* **109**, 171–184. https://doi.org/10.1127/18641318/2003/0109-0171

Cantalapiedra, C. P., Hernández-Plaza, A., Letunic, I., Bork, P., and Huerta-Cepas, J. (2021). eggNOG-mapper v2: Functional Annotation, Orthology Assignments, and Domain Prediction at the Metagenomic Scale. *Mol. Biol. Evol.* https://doi.org/10.1093/molbev/msab293

Cao, X., Xu, X., Bian, R., Wang, Y., Yu, H., Xu, Y., et al. (2020). Sedimentary ancient DNA metabarcoding delineates the contrastingly temporal change of lake cyanobacterial communities. *Water Res.* **15**, 183:116077. https://doi.org/10.1016/j.watres.2020.116077

Capo, E., Debroas, D., Arnaud, F., and Domaizon, I. (2015). Is Planktonic Diversity Well Recorded in Sedimentary DNA? Toward the Reconstruction of Past Protistan Diversity. *Microb. Ecol*. **70**, 865–875. https://doi.org/10.1007/s00248-015-0627-2

Capo, E., Domaizon, I., Maier, D., Debroas, D., and Bigler, C. (2017). To what extent is the DNA of microbial eukaryotes modified during burying into lake sediments? A repeat-coring approach on annually laminated sediments. *J. Paleolimnol*., **58**, 479-495. https://doi.org/10.1007/s10933-017-0005-9

Capo, E., Giguet-Covex, C., Rouillard, A., Nota, K., Heintzman, P. D., Vuillemin, A., et al. (2021). Lake sedimentary DNA research on past terrestrial and aquatic biodiversity: Overview and recommendations. *Quaternary*. **4**, 6. https://doi.org/10.3390/quat4010006

Capo, E., Rydberg, J., Tolu, J., Domaizon, I., Debroas, D., Bindler, R., et al. (2019). How Does Environmental Inter-annual Variability Shape Aquatic Microbial Communities? A 40-Year Annual Record of Sedimentary DNA From a Boreal Lake (Nylandssjön, Sweden). *Front. Ecol. Evol*. **7**, 245. https://doi.org/10.3389/fevo.2019.00245

Caporaso, J. G., Kuczynski, J., and et al (2010). QIIME allows high throughput community sequencing data. *Nat. Methods*. **7**, 335–336. https://doi.org/10.1038/nmeth0510335

Cardinale, B. J., Duffy, J. E., Gonzalez, A., Hooper, D. U., Perrings, C., Venail, P., et al. (2012). Biodiversity loss and its impact on humanity. *Nature* 486, 59–67. https://doi.org/10.1038/nature11148

Carey, C. C., Ibelings, B. W., Hoffmann, E. P., Hamilton, D. P., and Brookes, J. D. (2012). Eco-physiological adaptations that favour freshwater cyanobacteria in a changing climate. *Water Res*. **46,** 1394–1407. https://doi.org/10.1016/j.watres.2011.12.016

Carlson, A. E., Legrande, A. N., Oppo, D. W., Came, R. E., Schmidt, G. A., Anslow, F. S., et al. (2008). Rapid early Holocene deglaciation of the Laurentide ice sheet. *Nat. Geosci*. **1**, 620–624. https://doi.org/10.1038/ngeo285

Carmichael, W. W. (2001). Health Effects of Toxin-Producing Cyanobacteria: "The CyanoHABs." *Hum. Ecol. Risk Assess. An Int. J.* **7**, 1393–1407. https://doi.org/10.1080/20018091095087

Castañeda, I. S., and Schouten, S. (2011). A review of molecular organic proxies for examining modern and ancient lacustrine environments. *Quat. Sci. Rev.* **30**, 2851-2891. https://doi.org/10.1016/j.quascirev.2011.07.009

Cegłowska, M., nska-Sitarz, A. T., Kowalewska, G., and Mazur-Marzec, H. (2018). Specific chemical and genetic markers revealed a thousands-year presence of toxic *nodularia spumigena* in the baltic sea. *Mar. Drugs*. **16**, 116. https://doi.org/10.3390/md16040116

Chen, W., and Ficetola, G. F. (2020). Numerical methods for sedimentary-ancient-DNA-based study on past biodiversity and ecosystem functioning. *Environ. DNA*. **2**, 115–129. https://doi.org/10.1002/edn3.79

Choi, D. H., Noh, J. H., and Shim, J. (2013). Seasonal changes in picocyanobacterial diversity as revealed by pyrosequencing in temperate waters of the East China Sea and the East Sea. *Aquat. Microb.* **71**, 75–90. Ecol. https://doi.org/10.3354/ame01669

Chorus, Ingrid & Bartram, J. (1999). Toxic cyanobacteria in water. A guide to their public health consequences, monitoring, and management / edited by Ingrid Chorus and Jamie Bertram. World Heal. Organ. (1st ed.). *CRC Press*. https://doi.org/10.1201/9781482295061

Chrismas, N. A. M., Anesio, A. M., and Sánchez-Baracaldo, P. (2015). Multiple adaptations to polar and alpine environments within cyanobacteria: A

phylogenomic and Bayesian approach. *Front. Microbiol*. 6:1070 https://doi.org/10.3389/fmicb.2015.01070

Cires, S., Wörmer, L., Agha, R., and Quesada, A. (2013). Overwintering populations of *Anabaena*, *Aphanizomenon* and *Microcystis* as potentia inocula for summer blooms. *J. Plankton Res*. **35**, 1254-1266. https://doi.org/10.1093/plankt/fbt081.

Cline, J. D. (1969). Spectrophotometric Determination of Hydrogen Sulfide In Natural Waters. *Limnol. Oceanogr*. **14**, 454-458. https://doi.org/10.4319/lo.1969.14.3.0454

Coates, R. C., Podell, S., Korobeynikov, A., Lapidus, A., Pevzner, P., Sherman, D. H., et al. (2014). Characterization of cyanobacterial hydrocarbon composition and distribution of biosynthetic pathways. *PLoS One*. **9**, e85140. https://doi.org/10.1371/journal.pone.0085140

Consortium, P. 2k (2013). Continental-scale temperature variability during the last two millennia. *Nat. Geosci.* **6**, 339–346.

Cook, P. L. M., Jennings, M., Holland, D. P., Beardall, J., Briles, C., Zawadzki, A., et al. (2016). Blooms of cyanobacteria in a temperate Australian lagoon system post and prior to European settlement. *Biogeosciences*. **13**, 3677–3686. https://doi.org/10.5194/bg-13-3677-2016

Coolen, M. J. L., Boere, A., Abbas, B., Baas, M., Wakenham, S. G., and Sinninghe Damsté, J. S. (2006). Ancient DNA derived from alkenone-biosynthesizing haptophytes and other algae in Holocene sediments from the Black Sea. *Paleoceanography*. **21**, PA1005. https://doi.org/10.1029/2005PA001188

Coolen, M. J. L., Orsi, W. D., Balkema, C., Quince, C., Harris, K., Sylva, S. P., et al. (2013). Evolution of the plankton paleome in the Black Sea from the Deglacial to Anthropocene. *Proc. Natl. Acad. Sci. U. S. A.* **110**, 8609-8614. https://doi.org/10.1073/pnas.1219283110

Coolen, M. J. L., and Overmann, J. (1998). Analysis of subfossil molecular remains of purple sulfur bacteria in a lake sediment. *Appl. Environ. Microbiol.* **64**, 4513–4521. https://doi.org/10.1128/aem.64.11.4513-4521.1998

Coolen, M. J. L., Talbot, H. M., Abbas, B. A., Ward, C., Schouten, S., Volkman, J. K., et al. (2008). Sources for sedimentary bacteriohopanepolyols as revealed by 16S rDNA stratigraphy. *Environ. Microbiol*. **10**, 1783-1803. https://doi.org/10.1111/j.1462-2920.2008.01601.x

Corinaldesi, C., Barucca, M., Luna, G. M., and Dell'Anno, A. (2011). Preservation, origin and genetic imprint of extracellular DNA in permanently anoxic deep-sea sediments. *Mol. Ecol*. **20**, 642–654. https://doi.org/10.1111/j.1365294X.2010.04958.x

Cronberg, G. (1986). "Blue-green algae, green algae and chrysophyceae in sediments," in *Handbook of Holocene Palaeoecology and Palaeohydrology*, Berglund, B., Ed.; John Wiley and Sons: Chichester, UK, 1986; pp. 507–526

Curry, A. (2016). Slaughter at the bridge. *Science* **351**, 1384-1389. https://doi.org/10.1126/science.351.6280.1384

Czymzik, M., Muscheler, R., Adolphi, F., Mekhaldi, F., Dräger, N., Ott, F., et al. (2018). Synchronizing ^{10}Be in two varved lake sediment records to IntCal$_{13}$ ^{14}C during three grand solar minima. *Clim. Past.* **14**, 687–696. https://doi.org/10.5194/cp-14-6872018

Dabney, J., Meyer, M., and Pääbo, S. (2013). Ancient DNA damage. Cold Spring *Harb. Perspect. Biol.* **5**, a012567. https://doi.org/10.1101/cshperspect.a012567

Dadheech, P. K., Selmeczy, G. B., Vasas, G., Pádisak, J., Arp, W., Tapolczai, K., et al. (2014). Presence of potential toxin-producing cyanobacteria in an oligo-mesotrophic lake in Baltic lake district, Germany: An ecological, Genetic and

toxicological survey. *Toxins (Basel).* **6**, 2912-2931. https://doi.org/10.3390/toxins6102912

Deil, U. (2000). Frey & R Losch: Lehrbuch der Geobotanik. Pflanze und Vegetation in *Raum und Zeit*. 436 S. Gustav Fischer Verlag. Stuttgart, 1998. ISBN 3-437-25940-7. Feddes Repert. https://doi.org/10.1002/fedr.20001110110

Dellwig, O., Wegwerth, A., Schnetger, B., Schulz, H., and Arz, H. W. (2019). Dissimilar behaviors of the geochemical twins W and Mo in hypoxic-euxinic marine basins. *Earth-Science Rev*. **193**, 1-23. https://doi.org/10.1016/j.earscirev.2019.03.017

Di Rienzi, S. C., Sharon, I., Wrighton, K. C., Koren, O., Hug, L. A., Thomas, B. C., et al. (2013). The human gut and groundwater harbor non-photosynthetic bacteria belonging to a new candidate phylum sibling to Cyanobacteria. *Elife*. **2**, e01102. https://doi.org/10.7554/elife.01102

Diao, M., Sinnige, R., Kalbitz, K., Huisman, J., and Muyzer, G. (2017). Succession of bacterial communities in a seasonally stratified lake with an anoxic and sulfidic hypolimnion. *Front. Microbiol*. **8**, 2511. https://doi.org/10.3389/fmicb.2017.02511

Dokulil, M. T., and Teubner, K. (2000). Cyanobacterial dominance in lakes. *Hydrobiologia*. **698**, 29–46 https://doi.org/10.1023/A:1004155810302

Dokulil, M. T., and Teubner, K. (2012). Deep living Planktothrix rubescens modulated by environmental constraints and climate forcing. *Hydrobiologia*. **161**, 185-201. https://doi.org/10.1007/s10750-012-1020-5

Domaizon, I., Savichtcheva, O., Debroas, D., Arnaud, F., Villar, C., Pignol, C., et al. (2013). DNA from lake sediments reveals the long-term dynamics and diversity of *Synechococcus* assemblages. *Biogeosciences Discuss*. **10**, 2515–2564. https://doi.org/10.5194/bgd-10-2515-2013

Domaizon, I., Winegardner, A., Capo, E., Gauthier, J., and Gregory-Eaves, I. (2017). DNA-based methods in paleolimnology: new opportunities for investigating long-term dynamics of lacustrine biodiversity. *J. Paleolimnol.* **52**, 1–21. https://doi.org/10.1007/s10933-017-9958-y

Dommain, R., Andama, M., McDonough, M. M., Prado, N. A., Goldhammer, T., Potts, R., et al. (2020). The Challenges of Reconstructing Tropical Biodiversity With Sedimentary Ancient DNA: A 2200-Year-Long Metagenomic Record From Bwindi Impenetrable Forest, Uganda. *Front. Ecol. Evol.* **8**, 218. https://doi.org/10.3389/fevo.2020.00218

Downing, J. A., Watson, S. B., and McCauley, E. (2001). Predicting Cyanobacteria dominance in lakes. *Can. J. Fish. Aquat. Sci*. **58**, 1905–1908. https://doi.org/10.1139/f01-143

Dräger, N., Plessen, B., Kienel, U., Słowiński, M., Ramisch, A., Tjallingii, R., et al. (2019). Hypolimnetic oxygen conditions influence varve preservation and δ13C of sediment organic matter in Lake Tiefer See, NE Germany. *J. Paleolimnol*. **62**, 181–194. https://doi.org/10.1007/s10933-019-00084-2

Dräger, N., Theuerkauf, M., Szeroczyńska, K., Wulf, S., Tjallingii, R., Plessen, B., et al. (2017). Varve microfacies and varve preservation record of climate change and human impact for the last 6000 years at Lake Tiefer See (NE Germany). *The Holocene* **27**. 450–464, https://doi.org/10.1177/0959683616660173

Edgar, R. C. (2010). Search and clustering hundreds of times faster than BLAST. *Bioinformatics*. **6(19)**, 2460–2461. https://doi.org/10.1093/bioinformatics/btq461

Edwards, M. E. (2020). The maturing relationship between Quaternary paleoecology and ancient sedimentary DNA. *Quat. Res. (United States)*. **96**, 39-47. https://doi.org/10.1017/qua.2020.52

Ellegaard, M., Clokie, M. R. J., Czypionka, T., Frisch, D., Godhe, A., Kremp, A., et al. (2020). Dead or alive: sediment DNA archives as tools for tracking aquatic evolution and adaptation. *Commun. Biol.* **3**, 169. https://doi.org/10.1038/s42003020-0899-z

Epp, L. S., Zimmermann, H. H., and Stoof-Leichsenring, K. R. (2019). "Sampling and extraction of ancient DNA from sediments," In: Shapiro B., Barlow A., Heintzman P., Hofreiter M., Paijmans J., Soares A. (eds) *Ancient DNA. Methods in Molecular Biology*, vol 1963. Humana Press, New York, NY. pp 31-44. https://doi.org/10.1007/978-1-4939-9176-1_5

Erratt, K., Creed, I. F., Favot, E. J., Todoran, I., Tai, V., Smol, J. P., et al. (2021). Paleolimnological evidence reveals climate-related preeminence of cyanobacteria in a temperate meromictic lake. *Can. J. Fish. Aquat. Sci.* **79(4)**, 558-565. https://doi.org/10.1139/cjfas-2021-0095

Fahnenstiel, G. L., and Carrick, H. J. (1992). Phototrophic picoplankton in Lakes Huron and Michigan: abundance, distribution, composition, and contribution to biomass and production. *Can. J. Fish. Aquat. Sci.* **43**, 235–240. https://doi.org/10.1139/f92043

Fernandez-Turiel, J. L., Garcia-Valles, M., Gimeno-Torrente, D., Saavedra-Alonso, J., and Martinez-Manent, S. (2005). The hot spring and geyser sinters of El Tatio, northern Chile. Sediment. Geol. **180**, 125-147. https://doi.org/10.1016/j.sedgeo.2005.07.005

Fischer, W. W., Hemp, J., and Johnson, J. E. (2016). Evolution of Oxygenic Photosynthesis. *Annu. Rev. Earth Planet. Sci.* **44**, 647–683. https://doi.org/10.1146/annurev-earth-060313-054810

Florescu, G., Brown, K. J., Carter, V. A., Kuneš, P., Veski, S., and Feurdean, A. (2019). Holocene rapid climate changes and ice-rafting debris events reflected in high-resolution European charcoal records. *Quat. Sci. Rev.* **222**, 105877. https://doi.org/10.1016/j.quascirev.2019.105877

Gaedke, U., and Weisse, T. (1998). Seasonal and interannual variability of picocyanobacteria in Lake Constance (1987 - 1996). *Lake Constance Charact. an Ecosyst*. Transit. **53**, 143–158.

Garcia-Pichel, F. (2009). "Cyanobacteria," in *Encyclopedia of Microbiology*. Elsevier Inc.. pp 107-124. https://doi.org/10.1016/B978-012373944-5.00250-9

Gauthier, J., Walsh, D., Selbie, D. T., Bourgeois, A., Griffiths, K., Domaizon, I., et al. (2021). Evaluating the congruence between DNA-based and morphological taxonomic approaches in water and sediment trap samples: Analyses of a 36-month time series from a temperate monomictic lake. *Limnol. Oceanogr*. **66**, n. pag. https://doi.org/10.1002/lno.11856

Ger, K. A., Urrutia-Cordero, P., Frost, P. C., Hansson, L. A., Sarnelle, O., Wilson, A. E., et al. (2016). The interaction between cyanobacteria and zooplankton in a more eutrophic world. *Harmful Algae*. **54**, 128–144. https://doi.org/10.1016/j.hal.2015.12.005

Gerphagnon, M., Macarthur, D. J., Latour, D., Gachon, C. M. M., Van Ogtrop, F., Gleason, F. H., et al. (2015). Microbial players involved in the decline of filamentous and colonial cyanobacterial blooms with a focus on fungal parasitism. *Environ. Microbiol*. **8**, 2573–2587. https://doi.org/10.1111/1462-2920.12860

Gervais, F., Padisák, J., and Koschel, R. (1997). Do light quality and low nutrient concentration favour picocyanobacteria below the thermocline of the oligotrophic Lake Stechlin? *J. Plankton Res.* **19**, 771–781. https://doi.org/10.1093/plankt/19.6.771

Giguet-Covex, C., Ficetola, G. F., Walsh, K., Poulenard, J., Bajard, M., Fouinat, L., et al. (2019). New insights on lake sediment DNA from the catchment: importance of taphonomic and analytical issues on the record quality. *Sci. Rep.* **9**, 14676. https://doi.org/10.1038/s41598-019-50339-1

Grimm, N. B., Staudinger, M. D., Staudt, A., Carter, S. L., Chapin, F. S., Kareiva, P., et al. (2013). Climate-change impacts on ecological systems: Introduction to a US assessment. *Front. Ecol. Environ*. **11(9)**, 456-464. https://doi.org/10.1890/120310

Grossman, A. R., Schaefer, M. R., Chiang, G. G., and Collier, J. L. (1993). The phycobilisome, a light-harvesting complex responsive to environmental conditions. *Microbiol. Rev*. **57**, 725-749. https://doi.org/10.1128/mmbr.57.3.725-749.1993

Grundmann, L. (1999). Das Müritzgebiet: Ergebnisse der landeskundlichen Bestandsaufnahme im Raum Waren, Klink, Federow und Rechlin. H. Böhlaus Nachfolger, Inst. für Landerkd. Leipzig - Bereich Dtsch. Landeskd.

Guerrini, C. J., Botkin, J. R., and McGuire, A. L. (2019). QIIME2. Nat. Biotechnol. https://doi.org/10.1038/s41587-019-0190-3

Halstvedt, C. B., Rohrlack, T., Andersen, T., Skulberg, O., and Edvardsen, B. (2007). Seasonal dynamics and depth distribution of Planktothrix spp. in Lake Steinsfjorden (Norway) related to environmental factors. *J. Plankton Res*. **29**,471–482. https://doi.org/10.1093/plankt/fbm036

Hammer, Ø., Harper, D. A. T. a. T., and Ryan, P. D. (2001). PAST: Paleontological Statistics Software Package for Education and Data Analysis. *Palaeontol. Electron*. **29**, 471–482. https://doi.org/10.1016/j.bcp.2008.05.025

Hansen, A. J., Mitchell, D. L., Wiuf, C., Paniker, L., Brand, T. B., Binladen, J., et al. (2006). Crosslinks rather than strand breaks determine access to ancient DNA sequences from frozen sediments. *Genetics* **173**, 1175–1179. https://doi.org/10.1534/genetics.106.057349

Hansson, L. A., Rudstam, L. G., Johnson, T. B., Soranno, P., and Allen, Y. (1994). Patterns in algal recruitment from sediment to water in a dimictic, eutrophic lake. *Can. J. Fish. Aquat. Sci*. **51**, 2825-2833. https://doi.org/10.1139/f94-281

Heiskanen, A. S., and Olli, K. (1996). Sedimentation and buoyancy of Aphanizomenon cf. flos-aquae (Nostocales, Cyanophyta) in a nutrient-replete and nutrient-depleted coastal area of the Baltic Sea. *Phycologia*. **35**, 94–101. https://doi.org/10.2216/i0031-8884-35-6s-94.1

Hense, I., and Beckmann, A. (2006). Towards a model of cyanobacteria life cycle-effects of growing and resting stages on bloom formation of N2-fixing species. *Ecol. Modell*. **195**, 205–218. https://doi.org/10.1016/j.ecolmodel.2005.11.018

Herrera, A., and Cockell, C. S. (2007). Exploring microbial diversity in volcanic environments: A review of methods in DNA extraction. *J. Microbiol. Methods* **70**, 1–12. https://doi.org/10.1016/j.mimet.2007.04.005

Hertzberg, S., Liaaen-Jensen, S., and Siegelman, H. W. (1971). The carotenoids of blue-green algae. *Phytochemistry*. **10(12)**, 3121-3127. https://doi.org/10.1016/S00319422(00)97362-X

Herzschuh, U., Birks, H. J. B., Laepple, T., Andreev, A., Melles, M., and Brigham-Grette, J. (2016). Glacial legacies on interglacial vegetation at the Pliocene-Pleistocene transition in NE Asia. *Nat. Commun*. **7**, 11967. https://doi.org/10.1038/ncomms11967

Hobbs, W. O., Dreher, T. W., Davis, E. W., Vinebrooke, R. D., Wong, S., Weissman, T., et al. (2021). Using a lake sediment record to infer the long-term history of cyanobacteria and the recent rise of an anatoxin producing Dolichospermum sp. *Harmful Algae*. **101**, 101971. https://doi.org/10.1016/j.hal.2020.101971

Hoffmann, T., Lang, A., and Dikau, R. (2008). Holocene river activity: analysing 14C-dated fluvial and colluvial sediments from Germany. *Quat. Sci. Rev*. **27**, 2031-2040. https://doi.org/10.1016/j.quascirev.2008.06.014

Holland, D. P., and Walsby, A. E. (2008). Viability of the cyanobacterium Planktothrix rubescens in the cold and dark, related to over-winter survival and summer recruitment in Lake Zürich. *Eur. J. Phycol*. **43**, 179–184. https://doi.org/10.1080/09670260801904822

Huber, J. A., Morrison, H. G., Huse, S. M., Neal, P. R., Sogin, M. L., and Mark Welch, D. B. (2009). Effect of PCR amplicon size on assessments of clone library microbial diversity and community structure. *Environ. Microbiol*. **11(5)**, 1292-1302. https://doi.org/10.1111/j.1462-2920.2008.01857.x

Huerta-Cepas, J., Szklarczyk, D., Heller, D., Hernández-Plaza, A., Forslund, S. K., Cook, H., et al. (2019). EggNOG 5.0: A hierarchical, functionally and phylogenetically annotated orthology resource based on 5090 organisms and 2502 viruses. *Nucleic Acids Res*. **47(D1)**, D309-D314. https://doi.org/10.1093/nar/gky1085

Huisman, J., Codd, G. A., Paerl, H. W., Ibelings, B. W., Verspagen, J. M. H., and Visser, P. M. (2018). Cyanobacterial blooms. *Nat. Rev. Microbiol*. **16**, 471–483. https://doi.org/10.1038/s41579-018-0040-1

Hyatt, D., Chen, G. L., LoCascio, P. F., Land, M. L., Larimer, F. W., and Hauser, L. J. (2010). Prodigal: Prokaryotic gene recognition and translation initiation site identification. *BMC Bioinformatics*. **11**, 119-119. https://doi.org/10.1186/1471-2105-11-119

Ibelings, B. W., and Maberly, S. C. (1998). Photoinhibition and the availability of inorganic carbon restrict photosynthesis by surface blooms of cyanobacteria. *Limnol. Oceanogr*. **43**, 408-419. https://doi.org/10.4319/lo.1998.43.3.0408

Ibelings, B. W., Mur, L. R., and Walsby, A. E. (1991). Diurnal changes in buoyancy and vertical distribution in populations of Microcystis in two shallow lakes. *J. Plankton Res*. **13**, 419-436. https://doi.org/10.1093/plankt/13.2.419

Ibrahim, A., Capo, E., Wessels, M., Martin, I., Meyer, A., Schleheck, D., et al. (2021). Anthropogenic impact on the historical phytoplankton community of Lake Constance reconstructed by multimarker analysis of sediment-core environmental DNA. in *Molecular Ecology*. **30**, 3040-3056. https://doi.org/10.1111/mec.15696

Irfan, S., and Alatawi, A. M. M. (2019). Aquatic Ecosystem and Biodiversity: A Review. *Open J. Ecol*. **9**, 1–13. https://doi.org/10.4236/oje.2019.91001

Ivanikova, N. V., Popels, L. C., McKay, R. M. L., and Bullerjahn, G. S. (2007). Lake superior supports novel clusters of cyanobacterial picoplankton. *Appl. Environ. Microbiol*. **73**, 4055–4065. https://doi.org/10.1128/AEM.00214-07

Jacquet, S., Briand, J. F., Leboulanger, C., Avois-Jacquet, C., Oberhaus, L., Tassin, B., et al. (2005). The proliferation of the toxic cyanobacterium Planktothrix rubescens following restoration of the largest natural French lake (Lac du Bourget). *Harmful Algae*. **170**, 125–132. https://doi.org/10.1016/j.hal.2003.12.006

Janse, I., Meima, M., Kardinaal, W. E. A., and Zwart, G. (2003). High-Resolution Differentiation of Cyanobacteria by Using rRNA-Internal Transcribed Spacer Denaturing Gradient Gel Electrophoresis. *Appl. Environ. Microbiol*. **69**, 6634–6643. https://doi.org/10.1128/AEM.69.11.6634-6643.2003

Jantzen, D., Brinker, U., Orschiedt, J., Heinemeier, J., Piek, J., Hauenstein, K., et al. (2011). A Bronze Age battlefield? Weapons and trauma in the Tollense Valley, north-eastern Germany. *Antiquity*. **85**, 417-433. https://doi.org/10.1017/S0003598X00067843

Jasser, I., Królicka, A., and Karnkowska-Ishikawa, A. (2011). A novel phylogenetic clade of picocyanobacteria from the Mazurian lakes (Poland) reflects the early ontogeny of glacial lakes. *FEMS Microbiol. Ecol*. **23**, 739-749. https://doi.org/10.1111/j.1574-6941.2010.00990.x

Jeppesen, E., Søndergaard, M., Jensen, J. P., Havens, K. E., Anneville, O., Carvalho, L., et al. (2005). Lake responses to reduced nutrient loading - An analysis of contemporary long-term data from 35 case studies. *Freshw. Biol*. **50**, 1747–1771. https://doi.org/10.1111/j.1365-2427.2005.01415.x

Jezberová, J., and Komárková, J. (2007). Morphological transformation in a freshwater *Cyanobium sp*. induced by grazers. *Environ. Microbiol*. **9**, 1858–1862. https://doi.org/10.1111/j.1462-2920.2007.01311.x

Jia, Y., Han, G., Wang, C., Guo, P., Jiang, W., Li, X., et al. (2010). The efficacy and mechanisms of fungal suppression of freshwater harmful algal bloom species. *J. Hazard. Mater*. **183**, 176-181. https://doi.org/10.1016/j.jhazmat.2010.07.009

Joint, I., Owens, N., and Pomeroy, A. (1986). Seasonal production of photosynthetic picoplankton and nanoplankton in the Celtic Sea. *Mar. Ecol. Prog. Ser*. **28**, 251–258. https://doi.org/10.3354/meps028251

Jüttner, F., and Watson, S. B. (2007). Biochemical and ecological control of geosmin and 2-methylisoborneol in source waters. *Appl. Environ. Microbiol*. **73**, 4395-4406. https://doi.org/10.1128/AEM.02250-06

Kahru, M., and Elmgren, R. (2014). Multidecadal time series of satellite-detected accumulations of cyanobacteria in the Baltic Sea. *Biogeosciences*. **11**, 3619–3633. https://doi.org/10.5194/bg-11-3619-2014

Kaiblinger, C., Greisberger, S., Teubner, K., and Dokulil, M. T. (2007). Photosynthetic efficiency as a function of thermal stratification and phytoplankton size structure in an oligotrophic alpine lake. in *Hydrobiologia*. **578**, 29–36. https://doi.org/10.1007/s10750-006-0430-7

Kaiser, J., Ön, B., Arz, H., and Akçer-Ön, S. (2016). Sedimentary lipid biomarkers in the magnesium rich and highly alkaline lake Salda (South-western anatolia). *J. Limnol*. **75**, n.pag. https://doi.org/10.4081/jlimnol.2016.1337

Kaiser, J., Wasmund, N., Kahru, M., Wittenborn, A. K., Hansen, R., Häusler, K., et al. (2020). Reconstructing N2-fixing cyanobacterial blooms in the Baltic Sea beyond observations using 6- And 7-methylheptadecane in sediments as specific biomarkers. *Biogeosciences*. **17**, 2579-2597. https://doi.org/10.5194/bg-17-25792020

Kaiser, K., Lorenz, S., Germer, S., Juschus, O., Küster, M., Libra, J., et al. (2012). Late Quaternary evolution of rivers, lakes and peatlands in northeast Germany reflecting past climatic and human impact – an overview. *E&G Quat. Sci. J*. **61**, 103–132. https://doi.org/10.3285/eg.61.2.01

Kaloudis, T., Triantis, T. M., and Hiskia, A. (2017). "Taste and Odour Compounds Produced by Cyanobacteria," in *Handbook of Cyanobacterial Monitoring and Cyanotoxin Analysis*. Newjersey, United States, John Wiley Sons, Ltd; 2016. pp 196-201. https://doi.org/10.1002/9781119068761.ch20

Kardinaal, W. E. A., Janse, I., Kamst-Van Agterveld, M., Meima, M., Snoek, J., Mur, L. R., et al. (2007). Microcystis genotype succession in relation to microcystin concentrations in freshwater lakes. *Aquat. Microb. Ecol.* **48**, 1-12. https://doi.org/10.3354/ame048001

Kemp, A. E. S. (1996). Laminated sediments as palaeo-indicators. *Geol. Soc. Spec. Publ*. **116**, vii-xii. https://doi.org/10.1144/GSL.SP.1996.116.01.01

Kienel, U., Dulski, P., Ott, F., Lorenz, S., and Brauer, A. (2013). Recently induced anoxia leading to the preservation of seasonal laminae in two NE-German lakes. *J. Paleolimnol*. **50**, 535–544. https://doi.org/10.1007/s10933-013-9745-3

Kienel, U., Kirillin, G., Brademann, B., Plessen, B., Lampe, R., and Brauer, A. (2017). Effects of spring warming and mixing duration on diatom deposition in deep Tiefer See, NE Germany. *J. Paleolimnol*. **57**, 37–49. https://doi.org/10.1007/s10933-016-9925-z

Kieser, S., Brown, J., Zdobnov, E. M., Trajkovski, M., and McCue, L. A. (2020). ATLAS: A Snakemake workflow for assembly, annotation, and genomic binning of metagenome sequence data. *BMC Bioinformatics.* **21**, 257. https://doi.org/10.1186/s12859-020-03585-4

Kisand, V., Talas, L., Kisand, A., Stivrins, N., Reitalu, T., Alliksaar, T., et al. (2018). From microbial eukaryotes to metazoan vertebrates: Wide spectrum paleo-diversity in sedimentary ancient DNA over the last ~14,500 years. *Geobiology*. **16**, 628-639. https://doi.org/10.1111/gbi.12307

Kleiven, H. F., Kissel, C., Laj, C., Ninnemann, U. S., Richter, T. O., and Cortijo, E. (2008). Reduced North Atlantic deep water coeval with the glacial lake agassiz freshwater outburst. *Science*. **319**, 60-64. https://doi.org/10.1126/science.1148924

Klemer, A. R., Feuillade, J., And Feuillade, M. (1982). Cyanobacterial Blooms: Carbon and Nitrogen Limitation Have Opposite Effects on the Buoyancy of Oscillatoria. *Science*. **215**, 1629-1631. https://doi.org/10.1126/science.215.4540.1629

Klindworth, A., Pruesse, E., Schweer, T., Peplies, J., Quast, C., Horn, M., et al. (2013). Evaluation of general 16S ribosomal RNA gene PCR primers for classical and next-generation sequencing-based diversity studies. *Nucleic Acids Res*. **41(1)**, e1, https://doi.org/10.1093/nar/gks808

Komárek, J., and Komárková-Legnerová, J. (1992). Variability of some planktic gomphosphaerioid cyanoprocaryotes in northern lakes. *Nord. J. Bot*. **12**, 513–524. https://doi.org/10.1111/j.1756-1051.1992.tb01830.x

Komárek, J., Santanna, C. L., Bohunická, M., Mareš, J., Hentschke, G. S., Rigonato, J., et al. (2013). Phenotype diversity and phylogeny of selected Scytonema-species (Cyanoprokaryota) from SE Brazil. *Fottea*. **13**, 173-200. https://doi.org/10.5507/fot.2013.015

Kong, P., Richardson, P., and Hong, C. (2019). Seasonal dynamics of cyanobacteria and eukaryotic phytoplankton in a multiple-reservoir recycling irrigation system. *Ecol. Process*. **8**, n. pag. https://doi.org/10.1186/s13717-019-0191-7

Konkel, R., Toruńska-Sitarz, A., Cegłowska, M., Ežerinskis, Ž., Šapolaitė, J., Mažeika, J., et al. (2020). Blooms of Toxic Cyanobacterium Nodularia spumigena in Norwegian Fjords during Holocene Warm Periods. *Toxins (Basel)*. **12**, n. pag. https://doi.org/10.3390/toxins12040257

Konopka, A. (1982). Physiological ecology of a metalimnetic Oscillatoria rubescens population. *Limnol. Oceanogr*. **23**, 10–25. https://doi.org/10.4319/lo.1982.27.6.1154

Kromkamp, J., Konopka, A., and Mur, L. R. (1986). Buoyancy regulation in a strain of *Aphanizomenon flos-aquae* (Cyanophycaea): The importance of carbohydrate accumulation and gas vesicle collapse. *J. Gen. Microbiol.* **132**, 2113–2121. https://doi.org/10.1099/00221287-132-8-2113

Kurmayer, R., and Jüttner, F. (1999). Strategies for the co-existence of zooplankton with the toxic cyanobacterium *Planktothrix rubescens* in Lake Zurich. *J. Plankton Res*. **21**, 659–683. https://doi.org/10.1093/plankt/21.4.659

Kurmayer, R., Sivonen, K., Wilmotte, A., and Salmaso, N. (2017). Molecular Tools for the Detection and Quantification of Toxigenic Cyanobacteria, First Edition. Hoboken, NJ: John Wiley & Sons Ltd.

Küster, M., Stöckmann, M., Fülling, A., and Weber, R. (2015). Kulturlandschaftselemente, Kolluvien und Flugsande als Archive der spätholozänen Landschaftsentwicklung im Bereich des Messtischblattes Thurow (Müritz-Nationalpark, Mecklenburg). – In: *Neue Beiträge zum Naturraum und zur Landschaftsgeschichte im Teilgebiet Forschung*., ed. M. (Hrsg. . Kaiser, K., Kobel, J., Küster, M. & Schwabe Berlin: Geozon Science Media.

Kuwae, M., Tamai, H., Doi, H., Sakata, M. K., Minamoto, T., and Suzuki, Y. (2020). Sedimentary DNA tracks decadal-centennial changes in fish abundance. *Commun. Biol*. **3**. https://doi.org/10.1038/s42003-020-01282-9

Kyle, M., Haande, S., Ostermaier, V., and Rohrlack, T. (2015). The red queen race between parasitic chytrids and their host, planktothrix: A test using a time series reconstructed from sediment DNA. *PLoS One.* **10(3)**. https://doi.org/10.1371/journal.pone.0118738

Kyle, M., Haande, S., Sønstebø, J., and Rohrlack, T. (2014). Amplification of DNA in sediment cores to detect historic Planktothrix occurrence in three Norwegian lakes. *J. Paleolimnol*. **53**, 61-72. https://doi.org/10.1007/s10933-014-9807-1

Lammers, Y., Heintzman, P. D., and Alsos, I. G. (2021). Environmental palaeogenomic reconstruction of an Ice Age algal population. *Commun. Biol*. **4(1)**, 220. https://doi.org/10.1038/s42003-021-01710-4

Langmead, B., and Salzberg, S. L. (2012). Fast gapped-read alignment with Bowtie 2. *Nat. Methods*. **9**, 357–359. https://doi.org/10.1038/nmeth.1923

Leavitt, P. R. (1993). A review of factors that regulate carotenoid and chlorophyll deposition and fossil pigment abundance. *J. Paleolimnol*. **9**, 109–127. https://doi.org/10.1007/BF00677513

Leavitt, P. R., Carpenter, S. R., and Kitchell, J. F. (1989). Whole???lake experiments: The annual record of fossil pigments and zooplankton. *Limnol. Oceanogr*. **34**, 700–717. https://doi.org/10.4319/lo.1989.34.4.0700

Leavitt, P. R., and Findlay, D. L. (1994). Comparison of fossil pigments with 20 years of phytoplankton data from eutrophic Lake 227, Experimental Lakes Area, Ontario. *Can. J. Fish. Aquat. Sci*. **51**, 2286–2299. https://doi.org/10.1139/f94-232

Lee, C. K., Herbold, C. W., Polson, S. W., Wommack, K. E., Williamson, S. J., McDonald, I. R., et al. (2012). Groundtruthing Next-Gen Sequencing for Microbial Ecology-Biases and Errors in Community Structure Estimates from PCR Amplicon Pyrosequencing. *PLoS One*. **7(9)**: e44224. https://doi.org/10.1371/journal.pone.0044224

Legendre, P., Borcard, D., and Peres-Neto, P. R. (2005). Analyzing beta diversity: Partitioning the spatial variation of community composition data. *Ecol. Monogr*. **75**, 435–450. https://doi.org/10.1890/05-0549

Legendre, P., and Gallagher, E. D. (2001). Ecologically meaningful transformations for ordination of species data. *Oecologia*. **129**, 271–280. https://doi.org/10.1007/s004420100716

Legnani, E., Copetti, D., Oggioni, A., Tartari, G., Palumbo, M. T., and Morabito, G. (2005). *Planktothrix rubescens*' seasonal dynamics and vertical distribution in Lake Pusiano (North Italy). *J. Limnol*. **47**, 1656–1663. https://doi.org/10.4081/jlimnol.2005.61

Lenschow, U. (2001). Bilanzen zum Moorverlust. Das Beispiel Mecklenburg-Vorpommern.

Letunic, I., and Bork, P. (2016). Interactive tree of life (iTOL) v3: an online tool for the display and annotation of phylogenetic and other trees. *Nucleic Acids Res*. **44**, 242–245. https://doi.org/10.1093/nar/gkw290

Litt, T., Schölzel, C., Kühl, N., and Brauer, A. (2009). Vegetation and climate history in the Westeifel Volcanic Field (Germany) during the past 11 000 years based on annually laminated lacustrine maar sediments. *Boreas*. **38**, 679-690. https://doi.org/10.1111/j.1502-3885.2009.00096.x

Liu, A., Zhu, T., Lu, X., and Song, L. (2013). Hydrocarbon profiles and phylogenetic analyses of diversified cyanobacterial species. *Appl. Energy*. **11**, 383–393. https://doi.org/10.1016/j.apenergy.2013.05.008

Liu, S., Li, K., Jia, W., Stoof-Leichsenring, K. R., Liu, X., Cao, X., et al. (2021). Vegetation Reconstruction From Siberia and the Tibetan Plateau Using Modern Analogue Technique–Comparing Sedimentary (Ancient) DNA and Pollen Data. *Front. Ecol. Evol*. **9**. https://doi.org/10.3389/fevo.2021.668611

Livingstone, D., and Jaworski, G. H. M. (1980). The viability of akinetes of blue-green algae recovered from the sediments of rostherne mere. *Br. Phycol. J*. **15**, 357–364. https://doi.org/10.1080/00071618000650361

Ljungqvist, F. C. (2010). A new reconstruction of temperature variability in the extra-tropical northern hemisphere during the last two millennia. Geogr. Ann. *Ser. A Phys. Geogr*. **92**, 339-351. https://doi.org/10.1111/j.1468-0459.2010.00399.x

Lotter, A. F., Sturm, M., Teranes, J. L., and Wehrli, B. (1997). Varve formation since 1885 and high-resolution varve analyses in hypertrophic Baldeggersee (Switzerland). *Aquat. Sci*. **59**, 304–325. https://doi.org/10.1007/BF02522361

Ludwig, W., Strunk, O., Westram, R., Richter, L., Meier, H., Yadhukumar, A., et al. (2004). ARB: A software environment for sequence data. *Nucleic Acids Res*. **32(4)**, 1363–1367. https://doi.org/10.1093/nar/gkh293

Magny, M., and Haas, J. N. (2004). A major widespread climatic change around 5300 cal. yr BP at the time of the Alpine Iceman. *J. Quat. Sci*. **19**, 423-430. https://doi.org/10.1002/jqs.850

Marcott, S. A., Shakun, J. D., Clark, P. U., and Mix, A. C. (2013). A reconstruction of regional and global temperature for the past 11,300 years. *Science*. **484**, 49-54. https://doi.org/10.1126/science.1228026

Martin, M. (2014). Cutadapt removes adapter sequences from high-throughput sequencing reads. *EMBnet.journal.* **17**, 10–12. https://doi.org/10.14806/ej.17.1.200

Martínez De La Escalera, G., Antoniades, D., Bonilla, S., and Piccini, C. (2014). Application of ancient DNA to the reconstruction of past microbial assemblages and for the detection of toxic cyanobacteria in subtropical freshwater ecosystems. *Mol. Ecol*. **23**, 5791-5802. https://doi.org/10.1111/mec.12979

Matthews, J. A., and Briffa, K. R. (2005). The "Little Ice Age": Re-evaluation of an evolving concept. *Geogr. Ann. Ser. A Phys. Geogr*. **87**, 17–36. https://doi.org/10.1111/j.0435-3676.2005.00242.x

Mazard, S., Penesyan, A., Ostrowski, M., Paulsen, I. T., and Egan, S. (2016). Tiny microbes with a big impact: The role of cyanobacteria and their metabolites in shaping our future. *Mar. Drugs.* **14**, 97. https://doi.org/10.3390/md14050097

McDonald, K. E., and Lehman, J. T. (2013). Dynamics of Aphanizomenon and microcystis (cyanobacteria) during experimental manipulation of an urban impoundment. *Lake Reserv. Manag*. **29**, 103-115. https://doi.org/10.1080/10402381.2013.800172

Meissner, S., Fastner, J., and Dittmann, E. (2013). Microcystin production revisited: Conjugate formation makes a major contribution. *Environ. Microbiol*. **15**, 1810-1820. https://doi.org/10.1111/1462-2920.12072

Mejbel, H. S., Dodsworth, W., Baud, A., Gregory-Eaves, I., and Pick, F. R. (2021). Comparing Quantitative Methods for Analyzing Sediment DNA Records of Cyanobacteria in Experimental and Reference Lakes. *Front. Microbiol*. **12**, n. pag. https://doi.org/10.3389/fmicb.2021.669910

Merel, S., Walker, D., Chicana, R., Snyder, S., Baurès, E., and Thomas, O. (2013). State of knowledge and concerns on cyanobacterial blooms and cyanotoxins. *Environ. Int*. **59**, 303-327. https://doi.org/10.1016/j.envint.2013.06.013

Mi, C., Shatwell, T., Ma, J., Wentzky, V. C., Boehrer, B., Xu, Y., et al. (2020). The formation of a metalimnetic oxygen minimum exemplifies how ecosystem dynamics shape biogeochemical processes: A modelling study. *Water Res*. **175**, 115701. https://doi.org/10.1016/j.watres.2020.115701

Monchamp, M.-E., Spaak, P., and Pomati, F. (2019a). Long Term Diversity and Distribution of Non-photosynthetic Cyanobacteria in Peri-Alpine Lakes. *Front. Microbiol*. **9**, 3344. https://doi.org/10.3389/fmicb.2018.03344

Monchamp, M. E., Enache, I., Turko, P., Pomati, F., Rîşnoveanu, G., and Spaak, P. (2017). Sedimentary and egg-bank DNA from 3 European lakes reveal concurrent changes in the composition and diversity of cyanobacterial and Daphnia communities. *Hydrobiologia*. **800**, 155-172. https://doi.org/10.1007/s10750-017-3247-7

Monchamp, M. E., Spaak, P., Domaizon, I., Dubois, N., Bouffard, D., and Pomati, F. (2018). Homogenization of lake cyanobacterial communities over a century of climate change and eutrophication. *Nat. Ecol. Evol*. **2**, 317–324. https://doi.org/10.1038/s41559-017-0407-0

Monchamp, M. E., Spaak, P., and Pomati, F. (2019b). High dispersal levels and lake warming are emergent drivers of cyanobacterial community assembly in peri-Alpine lakes. *Sci. Rep*. **9**, 7366. https://doi.org/10.1038/s41598-019-43814-2

Monchamp, M. E., Walser, J. C., Pomati, F., and Spaak, P. (2016). Sedimentary DNA reveals cyanobacterial community diversity over 200 years in two perialpine lakes. *Appl. Environ. Microbiol*. **82**, 6472–6482. https://doi.org/10.1128/AEM.02174-16

Moss, B. (2004). Tracking Environmental Change Using Lake Sediments. *Freshw. Biol*. **49**, 678-679. https://doi.org/10.1111/j.1365-2427.2004.01211.x

Niemeyer, B., Epp, L. S., Stoof-Leichsenring, K. R., Pestryakova, L. A., and Herzschuh, U. (2017). A comparison of sedimentary DNA and pollen from lake sediments in recording vegetation composition at the Siberian treeline. *Mol. Ecol. Resour*. **17**, e46-e62. https://doi.org/10.1111/1755-0998.12689

Nitin Parulekar, N., Kolekar, P., Jenkins, A., Kleiven, S., Utkilen, H., Johansen, A., et al. (2017). Characterization of bacterial community associated with phytoplankton bloom in a eutrophic lake in South Norway using 16S rRNA gene amplicon sequence analysis. *PLoS One*. **12**: e0173408. https://doi.org/10.1371/journal.pone.0173408

Nübel, U., Garcia-Pichel, F., and Muyzer, G. (1997). PCR primers to amplify 16S rRNA genes from cyanobacteria. *Appl. Environ. Microbiol*. **63**, 3327–3332

Nuhfer, E. B., Anderson, R. Y., Bradbury, J. P., and Dean, W. E. (1993). Modern sedimentation in Elk Lake, Clearwater County, Minnesota. *Spec. Pap. Geol. Soc. Am*. **276**, 1–6. https://doi.org/10.1130/SPE276-p75

Nwosu, E. C., Brauer, A., Kaiser, J., Horn, F., Wagner, D., and Liebner, S. (2021a). Evaluating sedimentary DNA for tracing changes in cyanobacteria dynamics from sediments spanning the last 350 years of Lake Tiefer See, NE Germany. *J. Paleolimno*l. **9**. https://doi.org/10.1007/s10933-021-00206-9

Nwosu, E. C., Roeser, P., Yang, S., Ganzert, L., Dellwig, O., Pinkerneil, S., et al. (2021b). From Water into Sediment—Tracing Freshwater Cyanobacteria via DNA Analyses. *Microorganisms*. 9081778 https://doi.org/10.3390/microorganisms9081778

Nwosu, E. C., Roeser, P., Yang, S., Pinkerneil, S., Ganzert, L., Dittmann, E., et al. (2021c). Species-Level Spatio-Temporal Dynamics of Cyanobacteria in a Hard-Water Temperate Lake in the Southern Baltics. *Front. Microbiol*. **12**, 761259. https://doi.org/10.3389/fmicb.2021.761259

Okazaki, Y., and Nakano, S. I. (2016). Vertical partitioning of freshwater bacterioplankton community in a deep mesotrophic lake with a fully oxygenated hypolimnion (Lake Biwa, Japan). *Environ. Microbiol*. Rep. **8**, 780–788. do https://doi.org/10.1111/1758-2229.12439

Oksanen, J., Blanchet, F. G., Friendly, M., Kindt, R., Legendre, P., McGlinn, D., et al. (2019). vegan: Community Ecology Package. R package version 2.5-2. *Cran* R.

Oren, A. (2015). Cyanobacteria in hypersaline environments: biodiversity and physiological properties. Biodivers. *Conserv*. **24**, 781–798. https://doi.org/10.1007/s10531-015-0882-z

Padisák, J., Barbosa, F., Koschel, R., and Krienitz, L. (2003). Deep layer cyanoprokaryota maxima in temperate and tropical lakes. *Adv. Limnol.* **24**, 1363–1366.

Paerl, H. W., and Huisman, J. (2008). Blooms like it hot. *Science* **320**, 57–58. https://doi.org/10.1126/science.1155398

Paerl, H. W., and Huisman, J. (2009). Climate change: A catalyst for global expansion of harmful cyanobacterial blooms. *Environ. Microbiol. Rep*. **1**, 27-37. https://doi.org/10.1111/j.1758-2229.2008.00004.x

Paerl, H. W., and Otten, T. G. (2013). Harmful Cyanobacterial Blooms: Causes, Consequences, and Controls. *Microb. Ecol*. **65**, 995-1010. https://doi.org/10.1007/s00248-012-0159-y

Paerl, H. W., and Paul, V. J. (2012). Climate change: Links to global expansion of harmful cyanobacteria. *Water Res*. **46**, 1349-1363. https://doi.org/10.1016/j.watres.2011.08.002

Pal, S., Gregory-Eaves, I., and Pick, F. R. (2015). Temporal trends in cyanobacteria revealed through DNA and pigment analyses of temperate lake sediment cores. *J. Paleolimnol*. **54**, 87–101. https://doi.org/10.1007/s10933-015-9839-1

Parducci, L., Bennett, K. D., Ficetola, G. F., Alsos, I. G., Suyama, Y., Wood, J. R., et al. (2017). Ancient plant DNA in lake sediments. *New Phytol*. **214**, 924-942. https://doi.org/10.1111/nph.14470

Pathak, J., Ahmed, H., Singh, P. R., Singh, S. P., Häder, D. P., and Sinha, R. P. (2018). "Mechanisms of Photoprotection in Cyanobacteria," in *Cyanobacteria: From Basic Science to Applications*. pp. 145-171. https://doi.org/10.1016/B978-0-12-814667-5.00007-6

Pearman, J. K., Biessy, L., Howarth, J. D., Vandergoes, M. J., Rees, A., and Wood, S. A. (2021a). Deciphering the molecular signal from past and alive bacterial communities in aquatic sedimentary archives. *Mol. Ecol. Resour*. **22**, 877890. https://doi.org/10.1111/1755-0998.13515

Pearman, J. K., Thomson-Laing, G., Howarth, J. D., Vandergoes, M. J., Thompson, L., Rees, A., et al. (2021b). Investigating variability in microbial community composition in replicate environmental DNA samples down lake sediment cores. *PLoS One*. **16**, n. pag. https://doi.org/10.1371/journal.pone.0250783

Pedersen, M. W., Ginolhac, A., Orlando, L., Olsen, J., Andersen, K., Holm, J., et al. (2013). A comparative study of ancient environmental DNA to pollen and macrofossils

from lake sediments reveals taxonomic overlap and additional plant taxa. *Quat. Sci. Rev*. **75**, 161-168. https://doi.org/10.1016/j.quascirev.2013.06.006

Pedersen, M. W., Overballe-Petersen, S., Ermini, L., Der Sarkissian, C., Haile, J., Hellstrom, M., et al. (2015). Ancient and modern environmental DNA. *Philos. Trans. R. Soc. B Biol. Sci*. **370**, 20130383. https://doi.org/10.1098/rstb.2013.0383

Pedersen, M. W., Ruter, A., Schweger, C., Friebe, H., Staff, R. A., Kjeldsen, K. K., et al. (2016). Postglacial viability and colonization in North America's ice-free corridor. *Nature*. **537**, 45–49. https://doi.org/10.1038/nature19085

Personnic, S., Domaizon, I., Sime-Ngando, T., and Jacquet, S. (2009). Seasonal variations of microbial abundances and virus- versus flagellate-induced mortality of picoplankton in three peri-alpine lakes. *J. Plankton Res*. **31**, 1161–1177. https://doi.org/10.1093/plankt/fbp057

Pfeifer, F. (2012). Distribution, formation and regulation of gas vesicles. *Nat. Rev. Microbiol*. **10**, 705–715. https://doi.org/10.1038/nrmicro2834

Picard, M.; Wood, S.A.; Pochon, X.; Vandergoes, M.J.; Reyes, L.; Howarth, J.D.; Hawes, I.; Puddick, J. (2022) Molecular and Pigment Analyses Provide Comparative Results When Reconstructing Historic Cyanobacterial Abundances from Lake Sediment Cores. *Microorganisms* **10**, 279. https://doi.org/10.3390/microorganisms10020279

Pick, F. R., and Agbeti, M. (1991). The Seasonal Dynamics and Composition of Photosynthetic Picoplankton Communities in Temperate Lakes in Ontario, Canada. *Int. Rev. der gesamten Hydrobiol. und Hydrogr*. **76**, 565–580. https://doi.org/10.1002/iroh.19910760409

Pilon, S., Zastepa, A., Taranu, Z. E., Gregory-Eaves, I., Racine, M., Blais, J. M., et al. (2019). Contrasting histories of microcystin-producing cyanobacteria in two temperate lakes as inferred from quantitative sediment DNA analyses. *Lake Reserv. Manag*. **35**, 102-117. https://doi.org/10.1080/10402381.2018.1549625

Planavsky, N. J., Asael, D., Hofmann, A., Reinhard, C. T., Lalonde, S. V., Knudsen, A., et al. (2014). Evidence for oxygenic photosynthesis half a billion years before the Great Oxidation Event. *Nat. Geosci*. **7**, 283-286. https://doi.org/10.1038/ngeo2122

Plunkett, G., and Swindles, G. T. (2008). Determining the Sun's influence on Lateglacial and Holocene climates: a focus on climate response to centennial-scale solar forcing at 2800 cal. BP. *Quat. Sci. Rev*. **27**, 175-184. https://doi.org/10.1016/j.quascirev.2007.01.015

Posch, T., Köster, O., Salcher, M. M., and Pernthaler, J. (2012). Harmful filamentous cyanobacteria favoured by reduced water turnover with lake warming. *Nat. Clim. Chang*. **2**, 809-813. https://doi.org/10.1038/nclimate1581

Postius, C., and Ernst, A. (1999). Mechanisms of dominance: Coexistence of picocyanobacterial genotypes in a freshwater ecosystem. *Arch. Microbiol*. **172**, 69-75. https://doi.org/10.1007/s002030050742

Preston, T., Stewart, W. D. P., and Reynolds, C. S. (1980). Bloom-forming cyanobacterium *Microcystis aeruginosa* overwinters on sediment surface. *Nature*. **288**, 365–367. https://doi.org/10.1038/288365a0

Preußel, K., Stüken, A., Wiedner, C., Chorus, I., and Fastner, J. (2006). First report on cylindrospermopsin producing Aphanizomenon flos-aquae (Cyanobacteria) isolated from two German lakes. *Toxicon*. **47**, 156-162. https://doi.org/10.1016/j.toxicon.2005.10.013

Price, G. D., Badger, M. R., Woodger, F. J., and Long, B. M. (2008). Advances in understanding the cyanobacterial CO2-concentrating- mechanism (CCM): Functional components, Ci transporters, diversity, genetic regulation and prospects

for engineering into plants. in *Journal of Experimental Botany*, **59**, 1441-1461. https://doi.org/10.1093/jxb/erm112

Qin, B., Zhou, J., Elser, J. J., Gardner, W. S., Deng, J., and Brookes, J. D. (2020). Water Depth Underpins the Relative Roles and Fates of Nitrogen and Phosphorus in Lakes. *Environ. Sci. Technol*. N. pag. https://doi.org/10.1021/acs.est.9b05858

Quast, C., Pruesse, E., Yilmaz, P., Gerken, J., Schweer, T., Yarza, P., et al. (2013). The SILVA ribosomal RNA gene database project: Improved data processing and web-based tools. *Nucleic Acids Res*. **41**, 590–596. https://doi.org/10.1093/nar/gks1219

Rabalais, N. N., Díaz, R. J., Levin, L. A., Turner, R. E., Gilbert, D., and Zhang, J. (2010). Dynamics and distribution of natural and human-caused hypoxia. *Biogeosciences*. **7**, 585–619. https://doi.org/10.5194/bg-7-585-2010

Rajaniemi-Wacklin, P., Rantala, A., Mugnai, M. A., Turicchia, S., Ventura, S., Komárková, J., et al. (2006). Correspondence between phylogeny and morphology of Snowella spp. and Woronichinia naegeliana, cyanobacteria commonly occurring in lakes. *J. Phycol*. **42**, 226–232. https://doi.org/10.1111/j.1529-8817.2006.00179.x

Ramette, A., and Tiedje, J. M. (2007). Multiscale responses of microbial life to spatial distance and environmental heterogeneity in a patchy ecosystem. *Proc. Natl. Acad. Sci. U. S. A.* **104**, 2761–2766. https://doi.org/10.1073/pnas.0610671104

Ramos, V., Morais, J., and Vasconcelos, V. M. (2017). A curated database of cyanobacterial strains relevant for modern taxonomy and phylogenetic studies. *Sci. Data*. **4**, 1–8. https://doi.org/10.1038/sdata.2017.54

Renssen, H., Goosse, H., Crosta, X., and Roche, D. M. (2010). Early Holocene laurentide ice sheet deglaciation causes cooling in the high-latitude southern hemisphere through oceanic teleconnection. *Paleoceanography*. **25**, PA3204. https://doi.org/10.1029/2009PA001854

Reynolds, C. S., Oliver, R. L., and Walsby, A. E. (1987). Cyanobacterial dominance: The role of buoyancy regulation in dynamic lake environments. *New Zeal. J. Mar. Freshw. Res*. **21,** 379–390, https://doi.org/10.1080/00288330.1987.9516234

Richardson, J., Miller, C., Maberly, S. C., Taylor, P., Globevnik, L., Hunter, P., et al. (2018). Effects of multiple stressors on cyanobacteria abundance vary with lake type. Glob. *Chang. Biol*. **24**, 5044-5055. https://doi.org/10.1111/gcb.14396

Rigosi, A., Carey, C. C., Ibelings, B. W., and Brookes, J. D. (2014). The interaction between climate warming and eutrophication to promote cyanobacteria is dependent on trophic state and varies among taxa. *Limnol. Oceanogr*. **59**, 99–114. https://doi.org/10.4319/lo.2014.59.01.0099

Roeser, P., Dräger, N., Brykała, D., Ott, F., Pinkerneil, S., Gierszewski, P., et al. (2021). Advances in understanding calcite varve formation: new insights from a dual lake monitoring approach in the southern Baltic lowlands. *Boreas*. 12506. https://doi.org/10.1111/bor.12506

Rohrlack, T., Edvardsen, B., Skulberg, R., Halstvedt, C. B., Utkilen, H. C., Ptacnik, R., et al. (2008). Oligopeptide chemotypes of the toxic freshwater cyanobacterium Planktothrix can form subpopulations with dissimilar ecological traits. *Limnol. Oceanogr*. **3**, 1279–1293. https://doi.org/10.4319/lo.2008.53.4.1279

Saary, P., Forslund, K., Bork, P., and Hildebrand, F. (2017). RTK: efficient rarefaction analysis of large datasets. *Bioinformatics*. **33**, 2594–2595. https://doi.org/10.1093/bioinformatics/btx206

Salmaso, N., Albanese, D., Capelli, C., Boscaini, A., Pindo, M., and Donati, C. (2018). Diversity and Cyclical Seasonal Transitions in the Bacterial Community in a Large and Deep Perialpine Lake. *Microb. Ecol.* **76**, 125–143. https://doi.org/10.1007/s00248-017-1120-x

Salmaso, N. et al. (2015). Historical colonization patterns of *Dolichospermum lemmermannii* (cyanobacteria) in a deep lake south of the Alps. Adv. *Oceanogr. Limnol.* **6**, 1–4. https://doi.org/10.4081/aiol.2015.5456

Salmaso, N., Capelli, C., Shams, S., and Cerasino, L. (2015b). Expansion of bloom-forming *Dolichospermum lemmermannii* (Nostocales, Cyanobacteria) to the deep lakes south of the Alps: Colonization patterns, driving forces and implications for water use. *Harmful Algae*. **50**, 76–87. https://doi.org/10.1016/j.hal.2015.09.008

Sanger, J. E. (1988). Fossil pigments in paleoecology and paleolimnology. *Palaeogeogr. Palaeoclimatol. Palaeoecol*. **62**, 343–359. https://doi.org/10.1016/00310182(88)90061-2

Saqrane, S., and Oudra, B. (2009). CyanoHAB occurrence and water irrigation cyanotoxin contamination: ecological impacts and potential health risks. *Toxins (Basel)*. **1**, 113-122. https://doi.org/10.3390/toxins1020113

Savichtcheva, O., Debroas, D., Kurmayer, R., Villar, C., Jenny, J. P., Arnaud, F., et al. (2011). Quantitative PCR enumeration of total/toxic Planktothrix rubescens and total cyanobacteria in preserved DNA isolated from lake sediments. *Appl. Environ. Microbiol*. **77**, 8744–8753. https://doi.org/10.1128/AEM.06106-11

Savichtcheva, O., Debroas, D., Perga, M. E., Arnaud, F., Villar, C., Lyautey, E., et al. (2015). Effects of nutrients and warming on Planktothrix dynamics and diversity: A palaeolimnological view based on sedimentary DNA and RNA. *Freshw. Biol*. **60**, pp.31-49. https://doi.org/10.1111/fwb.12465

Scheffer, M., Hosper, S. H., Meijer, M. L., Moss, B., and Jeppesen, E. (1993). Alternative equilibria in shallow lakes. *Trends Ecol. Evol*. **8**, 275-9. https://doi.org/10.1016/0169-5347(93)90254

Schertzer, W. M., and Sawchuk, A. M. (1990). Thermal Structure of the Lower Great Lakes in a Warm Year: Implications for the Occurrence of Hypolimnion Anoxia. *Trans. Am. Fish. Soc*. **119**, 195–209. https://doi.org/10.1577/15488659(1990)119<0195:tsotlg>2.3.co;2

Schirrmeister, B. E., Gugger, M., and Donoghue, P. C. J. (2015). Cyanobacteria and the Great Oxidation Event: Evidence from genes and fossils. *Paleontology*. **58**, 769-785. https://doi.org/10.1111/pala.12178

Schloss, P. D., Westcott, S. L., Ryabin, T., Hall, J. R., Hartmann, M., Hollister, E. B., et al. (2009). Introducing mothur: Open-source, platform-independent, community-supported software for describing and comparing microbial communities. *Appl. Environ. Microbiol*. **75**, 7537–7541. https://doi.org/10.1128/AEM.01541-09

Schmidt, J.-P. (2012). ders., Kein Ende in Sicht? - Neue Untersuchungen auf dem Feuerstellenplatz von Naschendorf, Lkr. Nordwestmecklenburg. Archäologische Berichte aus Mecklenburg-Vorpommern **19**, 26–46.

Schmidt, J.-P. (2016). Alte Funde und neue Forschungen zur Bronzezeit in Mecklenburg-Vorpommern. Vor 3000 J. , ed. W. R. Busch (Hrsg.) Geesthacht.

Schmidt, J.-P. (2017). Ein Fremdling im Nordischen Kreis Jungbronzezeitliche Funde aus dem Flachen See bei Sophienhof, Lkr. Mecklenburgische Seenplatte. Univ. zur Prähistorischen Archäologie **297**, 271–281.

Schmidt, J.-P. (2019). Ein bronzenes Hallstattschwert der Periode VI aus dem Flachen See bei Sophienhof, Lkr. Mecklenburgische Seenplatte. Archäologische Berichte aus Mecklenburg-Vorpommern **26**, 26–34.

Schmidt, J.-P. (2020). "Aller guten Dinge sind drei!" – Ein weiteres bronzezeitliches Schwert aus dem Flachen See bei Lütgendorf, Lkr. Mecklenburgische Seenplatte. Archäologische Berichte aus Mecklenburg-Vorpommern **27**, 49–55.

Schober, E., and Kurmayer, R. (2006). Evaluation of different DNA sampling techniques for the application of the real-time PCR method for the quantification of cyanobacteria in water. *Lett. Appl. Microbiol*. **42**, 412–417. https://doi.org/10.1111/j.1472-765X.2006.01857.x

Schulte, L., Bernhardt, N., Stoof-Leichsenring, K., Zimmermann, H. H., Pestryakova, L. A., Epp, L. S., et al. (2021). Hybridization capture of larch (Larix Mill.) chloroplast genomes from sedimentary ancient DNA reveals past changes of Siberian forest. *Mol. Ecol. Resour*. **21**, 801-815. https://doi.org/10.1111/1755-0998.13311

Schultz-Sternberg, R., Zeitz, J., Landgraf, L., Hoffmann, E., Lehrkamp, H., Luthardt, V., et al. (2000). Niedermoore in Brandenburg. Telma. 133-150

Schweitzer-Natan, O., Ofek-Lalzar, M., Sher, D., and Sukenik, A. (2019). Particle-Associated Microbial Community in a Subtropical Lake During Thermal Mixing and Phytoplankton Succession. *Front. Microbiol*. **10**, 2142. https://doi.org/10.3389/fmicb.2019.02142

Selmeczy, G. B., Tapolczai, K., Casper, P., Krienitz, L., and Padisák, J. (2016). Spatial-and niche segregation of DCM-forming cyanobacteria in Lake Stechlin (Germany). *Hydrobiologia*. **764**, 229–240. https://doi.org/10.1007/s10750-015-2282-5

Shen, W., and Ren, H. (2021). TaxonKit: A practical and efficient NCBI taxonomy toolkit. J. Genet. *Genomics*. **48**, 844-850. https://doi.org/10.1016/j.jgg.2021.03.006

Silva, A., and Palma, S. (2010). The Socio-Economical Impact of HABs : Portugal ' s Case Study (2005-2010). *J. Tour. Sustain*. **1**, 19-27.

Sinha, R., Pearson, L. A., Davis, T. W., Burford, M. A., Orr, P. T., and Neilan, B. A. (2012). Increased incidence of Cylindrospermopsis raciborskii in temperate zones - Is climate change responsible? *Water Res*. **46**, 1408–1419. https://doi.org/10.1016/j.watres.2011.12.019

Smilauer, P., and Leps, J. (2014). Multivariate analysis of ecological data using Canoco 5. Cambridge: Cambridge University Press. https://doi.org/10.1017/CBO9781139627061

Smol, J. (2009). Pollution of lakes and rivers: a paleoenvironmental perspective. *J Paleolimnol*. **42**, 301–302. https://doi.org/10.1002/aqc.571

Smol, J. P., Birks, H. J. B., and Last, W. M. (2002). Tracking Environmental Change Using Lake Sediments. Volume 4: Zoological Indicators, Developments in Paleoenvironmental Research. https://doi.org/10.1017/CBO9781107415324.004en

Sollai, M., Hopmans, E. C., Bale, N. J., Mets, A., Warden, L., Moros, M., et al. (2017). The Holocene sedimentary record of cyanobacterial glycolipids in the Baltic Sea: An evaluation of their application as tracers of past nitrogen fixation. *Biogeosciences*. **14**, 5789-5804. https://doi.org/10.5194/bg-14-5789-2017

Sønstebø, J. H., and Rohrlack, T. (2011). Possible implications of Chytrid parasitism for population subdivision in freshwater cyanobacteria of the genus Planktothrix. *Appl. Environ. Microbiol*. **77**, 1344-1351. https://doi.org/10.1128/AEM.02153-10

Soo, R. M., Hemp, J., Parks, D. H., Fischer, W. W., and Hugenholtz, P. (2017). On the origins of oxygenic photosynthesis and aerobic respiration in Cyanobacteria. *Science*. **355**, 1436–1440. https://doi.org/10.1126/science.aal3794

Soo, R. M., Skennerton, C. T., Sekiguchi, Y., Imelfort, M., Paech, S. J., Dennis, P. G., et al. (2014). An expanded genomic representation of the phylum yanobacteria. *Genome Biol. Evol*. **6**, 1031–1045. https://doi.org/10.1093/gbe/evu073

Soule, T., and Garcia-Pichel, F. (2019). "Cyanobacteria," in Encyclopedia of Microbiology 799–817. https://doi.org/10.1016/B978-0-12-809633-8.20886-8

Stal, L. J. (2009). Is the distribution of nitrogen-fixing cyanobacteria in the oceans related to temperature?: Minireview. *Environ. Microbiol*. **11**, 1632-1645. https://doi.org/10.1111/j.1758-2229.2009.00016.x

Starkel, L., Soja, R., and Michczyńska, D. J. (2006). Past hydrological events reflected in Holocene history of Polish rivers. *Catena*. **66**, 24-33. https://doi.org/10.1016/j.catena.2005.07.008

Steffen, W., Crutzen, P. J., and McNeill, J. R. (2007). The Anthropocene: Are Humans Now Overwhelming the Great Forces of Nature. *AMBIO A J. Hum. Environ*. **36**, 614–621. https://doi.org/10.1579/0044-7447(2007)36[614:TAAHNO]2.0.CO;2

Stockner, J., Callieri, C., and Cronberg, G. (2006). "Picoplankton and Other Non-Bloom-Forming Cyanobacteria in Lakes," in *The Ecology of Cyanobacteria* **42**, 1300–1311. https://doi.org/10.1007/0-306-46855-7_7

Stomp, M., Huisman, J., Vörös, L., Pick, F. R., Laamanen, M., Haverkamp, T., et al. (2007). Colourful coexistence of red and green picocyanobacteria in lakes and seas. *Ecol. Lett*. **10**, 290–298. https://doi.org/10.1111/j.1461-0248.2007.01026.x

Stoof-Leichsenring, K. R., Epp, L. S., Trauth, M. H., and Tiedemann, R. (2012). Hidden diversity in diatoms of Kenyan Lake Naivasha: A genetic approach detects temporal variation. *Mol. Ecol*. **21**, 1918-1930. https://doi.org/10.1111/j.1365294X.2011.05412.x

Sukenik, A., Hadas, O., Kaplan, A., and Quesada, A. (2012). Invasion of Nostocales (cyanobacteria) to subtropical and temperate freshwater lakes - physiological, regional, and global driving forces. *Front. Microbiol*. **3**. https://doi.org/10.3389/fmicb.2012.00086

Sukenik, A., Quesada, A., and Salmaso, N. (2015). Global expansion of toxic and non-toxic cyanobacteria: effect on ecosystem functioning. Biodivers. *Conserv*. **24**, 889–908. https://doi.org/10.1007/s10531-015-0905-9

Swain, E. B. (1985). Measurement and interpretation of sedimentary pigments. *Freshw. Biol*. **15**, 53–75. https://doi.org/10.1111/j.1365-2427.1985.tb00696.x

Taberlet, P., Bonin, A., Zinger, L., and Coissac, E. (2018). Environmental DNA: For biodiversity research and monitoring. https://doi.org/10.1093/oso/9780198767220.001.0001

Tallberg, P., and Heiskanen, A. S. (1998). Species-specific phytoplankton sedimentation in relation to primary production along an inshore-offshore gradient in the Baltic sea. *J. Plankton Res*. **20**, 2053–2070. https://doi.org/10.1093/plankt/20.11.2053

Tang, E. P. Y., Tremblay, R., and Vincent, W. F. (1997). Cyanobacterial dominance of polar freshwater ecosystems: Are high-latitude mat-formers adapted to low temperature? *J. Phycol.* **33**, 171-181. https://doi.org/10.1111/j.00223646.1997.00171.x

Taranu, Z. E., Gregory-Eaves, I., Leavitt, P. R., Bunting, L., Buchaca, T., Catalan, J., et al. (2015). Acceleration of cyanobacterial dominance in north temperate-subarctic lakes during the Anthropocene. *Ecol. Lett*. **18**, 375–384. https://doi.org/10.1111/ele.12420

Teubner, K., Tolotti, M., Greisberger, S., Morscheid, H., Dokulil, M. T., and Morscheid, H. (2003). Steady state phytoplankton in a deep pre-alpine lake: Species and pigments of epilimnetic versus metalimnetic assemblages. in *Hydrobiologia* **502**, 49-64. https://doi.org/10.1023/B:HYDR.0000004269.54705.cb

Theuerkauf, M., Blume, T., Brauer, A., Dräger, N., Feldens, P., Kaiser, K., et al. (2021). Holocene lake-level evolution of Lake Tiefer See, NE Germany, caused by climate and land cover changes. Boreas. https://doi.org/10.1111/bor.12561

Theuerkauf, M., Dräger, N., Kienel, U., Kuparinen, A., and Brauer, A. (2015). Effects of changes in land management practices on pollen productivity of open vegetation during the last century derived from varved lake sediments. *The Holocene*. **25**, 733–744. https://doi.org/10.1177/0959683614567881

Tse, T. J., Doig, L. E., Tang, S., Zhang, X., Sun, W., Wiseman, S. B., et al. (2018). Combining High-Throughput Sequencing of sedaDNA and Traditional Paleolimnological Techniques to Infer Historical Trends in Cyanobacterial Communities. *Environ. Sci. Technol*. **52**, 6842-6853. https://doi.org/10.1021/acs.est.7b06386

Ullah, H., Nagelkerken, I., Goldenberg, S. U. & Fordham, D. A. (2018). Climate change could drive marine food web collapse through altered trophic flows and cyanobacterial proliferation. *PLoS Biol*. **16,** e2003446. https://doi.org/1371/journal.pbio.2003446

Urrutia-Cordero, P., Ekvall, M. K., and Hansson, L. A. (2016). Controlling harmful cyanobacteria: Taxa-specific responses of cyanobacteria to grazing by large-bodied Daphnia in a biomanipulation scenario. *PLoS One*. **11**, e0153032. https://doi.org/10.1371/journal.pone.0153032

Väliranta, M., Salonen, J. S., Heikkilä, M., Amon, L., Helmens, K., Klimaschewski, A., et al. (2015). Plant macrofossil evidence for an early onset of the Holocene summer thermal maximum in northernmost Europe. *Nat. Commun*. **6**, 6809. https://doi.org/10.1038/ncomms7809

van Geel, B., Mur, L. R., Ralska-Jasiewiczowa, M., and Goslar, T. (1994). Fossil akinetes of *Aphanizomenon* and *Anabaena* as indicators for medieval phosphate-eutrophication of Lake Gosciaz (Central Poland). *Rev. Palaeobot. Palynol*. **83**, 97–105. https://doi.org/10.1016/0034-6667(94)90061-2

Verspagen, J. M. H., Van De Waal, D. B., Finke, J. F., Visser, P. M., Van Donk, E., and Huisman, J. (2014). Rising CO2 levels will intensify phytoplankton blooms in eutrophic and hypertrophic lakes. *PLoS One*. **9**, e104325. https://doi.org/10.1371/journal.pone.0104325

Větrovský, T., and Baldrian, P. (2013). The Variability of the 16S rRNA Gene in Bacterial Genomes and Its Consequences for Bacterial Community Analyses. *PLoS One*. **8**, e57923. https://doi.org/10.1371/journal.pone.0057923

Villareal, T. A., and Carpenter, E. J. (2003). Buoyancy regulation and the potential for vertical migration in the oceanic cyanobacterium Trichodesmium. *Microb. Ecol*. **45**, 1–10. https://doi.org/10.1007/s00248-002-1012-5

Visser, P. M., Ibelings, B. W., Bormans, M., and Huisman, J. (2016a). Artificial mixing to control cyanobacterial blooms: a review. *Aquat. Ecol*. **50**, 423-441. https://doi.org/10.1007/s10452-015-9537-0

Visser, P. M., Passarge, J., and Mur, L. R. (1997). Modelling vertical migration of the cyanobacterium *Microcystis*. Hydrobiologia. **349**, 99–109. https://doi.org/10.1023/A:1003001713560

Visser, P. M., Verspagen, J. M. H., Sandrini, G., Stal, L. J., Matthijs, H. C. P., Paerl, H. W., et al. (2016b). How rising CO2 and global warming may stimulate harmful cyanobacterial blooms. *Harmful Algae*. **54**, 145–159. https://doi.org/10.1016/j.hal.2015.12.006

Vitousek, P. M., Mooney, H. a, Lubchenco, J., and Melillo, J. M. (1997). Human Domination of Earth's Ecosystems. *Science*. **277**, 494–499. https://doi.org/10.1126/science.277.5325.494

Vonlanthen, P., Bittner, D., Hudson, A. G., Young, K. A., Müller, R., Lundsgaard-Hansen, B., et al. (2012). Eutrophication causes speciation reversal in whitefish adaptive radiations. *Nature* **482**, 357–362. https://doi.org/10.1038/nature10824

Vörös, L., Callieri, C., V-Balogh, K., and Bertoni, R. (1998). Freshwater picocyanobacteria along a trophic gradient and light quality range. in *Hydrobiologia* **369**, 117–125. https://doi.org/10.1007/978-94-017-2668-9_10

Vörös, L., Mózes, A., and Somogyi, B. (2009). A five-year study of autotrophic winter picoplankton in Lake Balaton, Hungary. *Aquat. Ecol*. **43**, 727–734. https://doi.org/10.1007/s10452-009-9272-5

Wagner, C., and Adrian, R. (2009). Cyanobacteria dominance: Quantifying the effects of climate change. *Limnol. Oceanogr*. **54**, 2460–2468. https://doi.org/10.4319/lo.2009.54.6_part_2.2460

Walker, M., Head, M. J., Berkelhammer, M., Björck, S., Cheng, H., Cwynar, L., et al. (2018). Formal ratification of the subdivision of the Holocene Series/ Epoch (Quaternary System/Period): Two new Global Boundary Stratotype Sections and Points (GSSPs) and three new stages/ subseries. *Episodes*. **41**, 213-223. https://doi.org/10.18814/epiiugs/2018/018016

Walsby, A. E. (2005). Stratification by cyanobacteria in lakes: A dynamic buoyancy model indicates size limitations met by Planktothrix rubescens filaments. *New Phytol*. **168**, 365–376. https://doi.org/10.1111/j.1469-8137.2005.01508.x

Walsby, A. E., Hayes, P. K., and Boje, R. (1995). The gas vesicles, buoyancy and vertical distribution of cyanobacteria in the Baltic Sea. *Eur. J. Phycol*. **30**, 87-94. https://doi.org/10.1080/09670269500650851

Walsby, A. E., Ng, G., Dunn, C., and Davis, P. A. (2004). Comparison of the depth where *Planktothrix rubescens* stratifies and the depth where the daily insolation supports its neutral buoyancy. *New Phytol*. **162**, 133–145. https://doi.org/10.1111/j.14698137.2004.01020.x

Walsby, A. E., and Schanz, F. (2002). Light-dependent growth rate determines changes in the population of *Planktothrix rubescens* over the annual cycle in lake Zürich, Switzerland. *New Phytol*. **154**, 671–687. https://doi.org/10.1046/j.14698137.2002.00401.x

Walsby, A. E., Schanz, F., and Schmid, M. (2006). The Burgundy-blood phenomenon: A model of buoyancy change explains autumnal waterblooms by *Planktothrix rubescens* in Lake Zürich. *New Phytol.* **169**, 109–122. https://doi.org/10.1111/j.1469-8137.2005.01567.x

Walsh, K., and Giguet-Covex, C. (2020). "A history of human exploitation of alpine regions," in *Encyclopedia of the World's Biomes* https://doi.org/10.1016/B978-0-12-409548-9.11908-6

Wanner, H., Wanner, H., Mercolli, L., Mercolli, L., Grosjean, M., Grosjean, M., et al. (2015). Holocene climate variability and change; a data-based review. *J. Geol. Soc. London*. **172**, 254–263. https://doi.org/10.1144/jgs2013-101

Waters, M. N. (2016). A 4700-Year History of Cyanobacteria Toxin Production in a Shallow Subtropical Lake. *Ecosystems*. **19**, 426–436. https://doi.org/10.1007/s10021-015- 9943-0

Weisbrod, B., Wood, S. A., Steiner, K., Whyte-Wilding, R., Puddick, J., Laroche, O., et al. (2020). Is a Central Sediment Sample Sufficient? Exploring Spatial and Temporal Microbial Diversity in a Small Lake. *Toxins (Basel)*. **12**, 580. https://doi.org/10.3390/toxins12090580

Weisse, T. (1993). "Dynamics of Autotrophic Picoplankton in Marine and Freshwater Ecosystems. Adv. *Microbial. Ecol*. **13**, 327–370. https://doi.org/10.1007/978-1-4615-2858-68

Wentzky, V. C., Frassl, M. A., Rinke, K., and Boehrer, B. (2019). Metalimnetic oxygen minimum and the presence of Planktothrix rubescens in a low-nutrient drinking water reservoir. *Water Res*. **148**, 208–218. https://doi.org/10.1016/j.watres.2018.10.047.

Whitton, B. A. (2012). Ecology of cyanobacteria II: *Their diversity in space and time*. https://doi.org/10.1007/978-94-007-3855-3

Willerslev, E., and Cooper, A. (2005). Ancient DNA. *Proc. R. Soc. B Biol. Sci*. **272**, 3-16. https://doi.org/10.1098/rspb.2004.2813.

Winder, M., Reuter, J. E., and Schladow, S. G. (2009). Lake warming favours small-sized planktonic diatom species. *Proc. R. Soc. B Biol. Sci*. **276**, 427–435. https://doi.org/10.1098/rspb.2008.1200

Wood, S. A., Pochon, X., Laroche, O., von Ammon, U., Adamson, J., and Zaiko, A. (2019). A comparison of droplet digital polymerase chain reaction (PCR), quantitative PCR and metabarcoding for species-specific detection in environmental DNA. *Mol. Ecol. Resour*. **19**, 1407-1419. https://doi.org/10.1111/1755-0998.13055

Wood, S. M., Kremp, A., Savela, H., Akter, S., Vartti, V. P., Saarni, S., et al. (2021). Cyanobacterial Akinete Distribution, Viability, and Cyanotoxin Records in Sediment Archives From the Northern Baltic Sea. Front. Microbiol. **12**, 681881. https://doi.org/10.3389/fmicb.2021.681881

Wrighton, K. C., Castelle, C. J., Wilkins, M. J., Hug, L. A., Sharon, I., Thomas, B. C., et al. (2014). Metabolic interdependencies between phylogenetically novel fermenters and respiratory organisms in an unconfined aquifer. *ISME J*. **8**, 1452-1463. https://doi.org/10.1038/ismej.2013.249

Wu, T., Hu, E., Xu, S., Chen, M., Guo, P., Dai, Z., et al. (2021). clusterProfiler 4.0: A universal enrichment tool for interpreting omics data. *Innov*. **2**, 100141. https://doi.org/10.1016/j.xinn.2021.100141

Wulf, S., Dräger, N., Ott, F., Serb, J., Appelt, O., Gudmundsdóttir, E., et al. (2016). Holocene tephrostratigraphy of varved sediment records from Lakes Tiefer See (NE Germany) and Czechowskie (N Poland). *Quat. Sci. Rev*. **132**, 1–14. https://doi.org/10.1016/j.quascirev.2015.11.007

Xu, Y., Jiao, N., and Chen, F. (2015). Novel psychrotolerant picocyanobacteria isolated from Chesapeake Bay in the winter. *J. Phycol*. **51**, 782-790. https://doi.org/10.1111/jpy.12318

Ye, W., Tan, J., Liu, X., Lin, S., Pan, J., Li, D., et al. (2011). Temporal variability of cyanobacterial populations in the water and sediment samples of Lake Taihu as determined by DGGE and real-time PCR. *Harmful Algae*. **10**, 472-479. https://doi.org/10.1016/j.hal.2011.03.002

Yilmaz, P., Parfrey, L. W., Yarza, P., Gerken, J., Pruesse, E., Quast, C., et al. (2014). The SILVA and "all-species Living Tree Project (LTP)" taxonomic frameworks. *Nucleic Acids Res*. **42**, 643-648. https://doi.org/10.1093/nar/gkt1209

Zastepa, A., Taranu, Z. E., Kimpe, L. E., Blais, J. M., Gregory-Eaves, I., Zurawell, R. W., et al. (2017). Reconstructing a long-term record of microcystins from the analysis of lake sediments. *Sci. Total Environ*. **579**, 893-901. https://doi.org/10.1016/j.scitotenv.2016.10.211

Zeeb, B. A., and Smol, J. P. (2005). Chrysophyte Scales and Cysts. In: Smol, J.P., Birks, H.J.B., Last, W.M., Bradley, R.S., Alverson, K. (eds) Tracking Environmental

Change Using Lake Sediments. Developments in *Paleoenvironmental Research*, vol 3. Springer, Dordrecht. https://doi.org/10.1007/0-306-47668-1_9

Zhang, H., Huo, S., Yeager, K. M., and Wu, F. (2021a). Sedimentary DNA record of eukaryotic algal and cyanobacterial communities in a shallow Lake driven by human activities and climate change. *Sci. Total Environ*. **753**, 141985. https://doi.org/10.1016/j.scitotenv.2020.141985

Zhang, J., Liu, J., Yuan, Y., Zhou, A., Chen, J., Shen, Z., et al. (2021b). Pre-industrial cyanobacterial dominance in Lake Moon (NE China) revealed by sedimentary ancient DNA. *Quat. Sci. Rev*. **261**, 106966. https://doi.org/10.1016/j.quascirev.2021.106966

Zimmermann, H. H., Raschke, E., Epp, L. S., Stoof-Leichsenring, K. R., Schirrmeister, L., Schwamborn, G., et al. (2017). The history of tree and shrub taxa on bol'shoy lyakhovsky Island (New Siberian Archipelago) since the last interglacial uncovered by sedimentary ancient DNA and pollen data. *Genes (Basel)*. **8**, 273. https://doi.org/10.3390/genes8100273

Appendix A Supplementary Material for Chapter 2

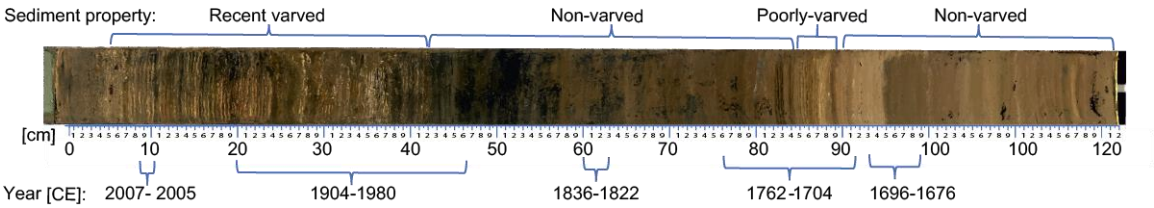

Figure A.1: Sediment core photograph showing oxidized sediments with recent-varved, non-varved, and subrecent-varved segments. The years indicate the depths at which study samples were collected from.

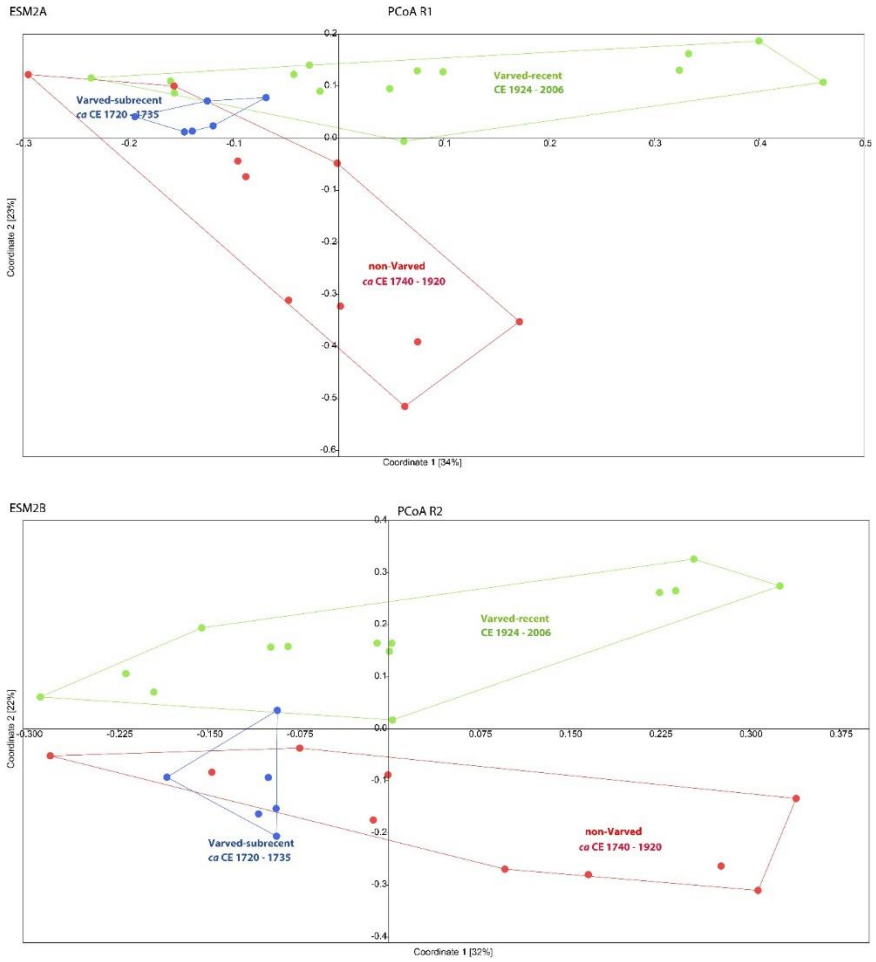

Figure A.2: Principal coordinate analysis (PCoA) based on Bray-Curtis distance matrix on the cyanobacteria abundance data from **(A)** read direction 1 R1, and **(B)** read direction 2 R2. The coordinates 1 and 2 together explain 56% and 54% of the observed variances in R1 and R2, respectively. The colors represent the sediment segments from which the OTUs originate; recent-varved in green, subrecent-varved in blue and non-varved in red.

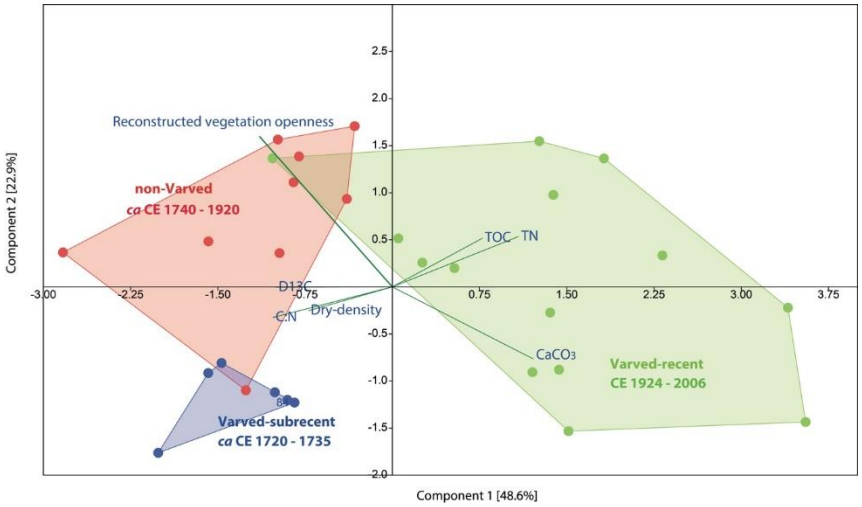

Figure A.3: Principal components analysis (PCA) of environmental data (Euclidean distance) from sediment samples with PC 1 explaining 48.6% and PC 2 explaining 22.9% of the variance between samples (both axes explain 71.5% in total). The clusters of the different sediment segments are represented by different colors: recent-varved in green, subrecent-varved in blue, and non-varved in red. The environmental variables are projected as green vectors.

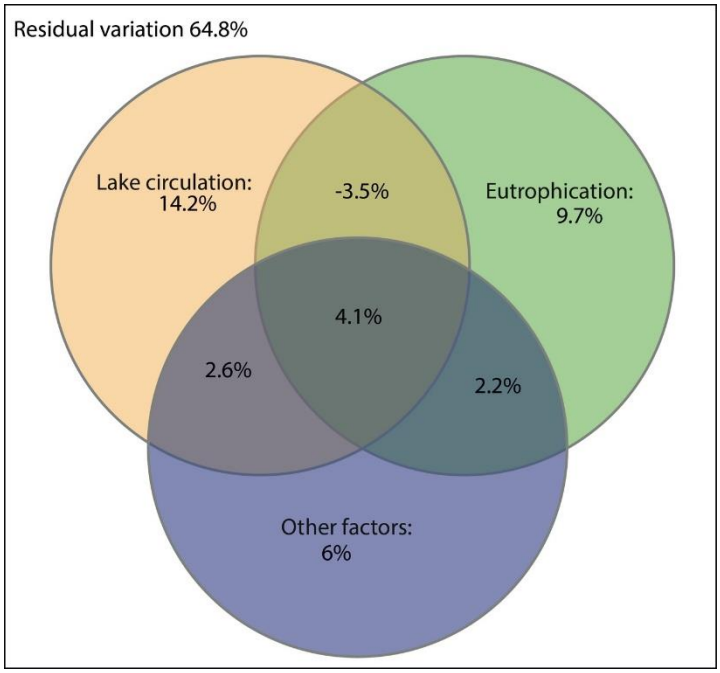

Figure A.4: Venn diagram displaying the results of variation partitioning analysis (VPA). The three explanatory matrices used contained variables pertaining to lake circulation, eutrophication, and other factors. Each circle represents the portion of variation accounted for by an explanatory matrix or a combination of explanatory matrices. The bounding rectangle represents the total variation in the response data showing the portion of residual variation not explained by the explanatory matrices.

Table A.1: Statistics of sequencing analysis and representative data providing an overview of sequencing reads before and after all filter steps. Alpha diversity indices without and with rarefaction, as well as the alpha diversity from the non-photosynthetic cyanobacteria sister clade.

Statistics of sequencing analysis and alpha diversity data										Alpha diversity for non-photosynthetic cyanobacteria sister clades		
Sediment type	Sample ID	Year (CE)	Raw reads	Quality filtered reads	Cyanobacteria Reads	Observed OTUs	Shannon (H)	Rarefied Observed OTUs	Rarefied Shannon (H)	non-photosynthetic cyanobacteria reads	Observed OTUs	Shannon (H)
Recent-varved segment	9	2006	221041	180593	143269	69	3.126	69	3.214			
	10	2002	374020	299735	185676	52	2.832	52	2.858			
	14	1990	233222	187981	153353	63	3.384	63	3.362	354	1	0
	15	1986	190462	152348	79613	43	3.021	43	3.051			
	20	1978	144388	118639	33265	29	2.742	29	2.749			
	21	1977	134219	101929	33732	39	2.984	39	2.949			
	22	1974	168159	132994	42389	26	2.641	26	2.613			
	23	1971	221549	180154	44700	36	3.024	36	3.012	240	1	0
	24	1969	135970	109729	19378	29	2.862	29	2.844			
	25	1965	111375	91677	27333	27	2.76	27	2.782			
	35	1937	113645	87232	11178	24	2.764	24	2.78	552	2	0.6927
	36	1933	144821	113541	21323	24	2.507	24	2.498	445	1	0
	37	1930	126396	107469	20034	21	2.544	21	2.556	220	1	0
	42	1919	136068	113455	3868	14	2.481	14	2.48	753	3	0.9764
Non-varved segment	43	1916	115165	95652	7726	21	2.682	21	2.679	1577	2	0.2675
	44	1913	101849	80539	3631	15	2.473	15	2.473	800	2	0.5731
	45	1907	116605	87604	14903	20	2.671	20	2.677	2457	2	0.3099
	46	1902	138274	112679	7355	11	2.035	11	2.035			
	60	1834	366434	307031	34978	18	2.334	18	2.339			
	61	1829	334838	284477	21915	10	1.99	10	1.999			
	62	1824	142980	121141	6706	13	2.218	13	2.209			
	76	1764	220467	195065	14614	15	2.285	15	2.296			
	80	1747	154408	127886	13824	19	2.709	19	2.694			
	81	1742	187526	155395	16370	20	2.707	20	2.681			
	82	1738	220587	188831	23796	20	2.743	20	2.734	439	1	0
Subrecent-varved segment	83	1735	141966	120212	15298	21	2.689	21	2.683	407	2	0.6925
	84	1732	186436	157004	26334	26	2.755	26	2.745			
	85	1729	170681	147726	28389	25	2.801	25	2.787			
	86	1726	139971	116781	20756	23	2.701	23	2.696			
	87	1722	268613	228275	58146	27	2.831	27	2.844	394	1	0
Non-varved segment	88	1717	394	388	118	27	2.897					
	89	1712	335	325	79	22	2.692					
	90	1709	353	343	50	28	3.155					
	93	1694	248	245	27	11	2.115					
	99	1678	215	214	20	14	2.484					

Table A.2: Overall test statistics of a one-way PerMANOVA using OTU data from the different sediment segments. Pairwise analysis of different sediment segments shows Bonferonni corrected p-values above the diagonal and the F-values below.

PERMANOVA Statistic		Bonferonni-corrected p values		
Permutation N:	9999		Recent-varved	Non-varved	Subrecent-varved
The total sum of squares:	2.352	Recent-varved		**0.0001**	**0.0125**
The within-group sum of squares:	1.708	Non-varved	6.784		**0.0253**
F:	5.089	Subrecent-varved	3.942	3.103	
p (same):	0.0001				

Table A.3: The overall significance of the distance-based redundancy analysis (dbRDA) (A) model, (B) its axes and (C) the marginal effect of each variable was tested by a 999 Monte Carlo permutation test. (D) The explanatory variables were forward selected based on a pseudo-*F* statistic using 999 permutations assessment of their significance. Adjusted R^2 for the significant explanatory variables = 0.38. AIC = Akaike information criterion.

The overall significance of the distance-based redundancy analysis (dbRDA) model, its axes and forward selection of each variable were tested by a 999 Monte Carlo permutation test

(A) By model: Partitioning of squared Bray distance:

	Inertia	Proportion
Total	3.229	1.0000
Constrained	1.564	0.4844
Unconstrained	1.665	0.5156

(B) By axes:

Axes	Df	Sum Of Squares	F	Pr(>F)
CAP1	1	0.76274	12.3686	0.001 ***
CAP2	1	0.36833	5.9729	0.001 ***
CAP3	1	0.19502	3.1625	0.028 *
CAP4	1	0.11537	1.8709	0.432
CAP5	1	0.05048	0.8186	0.978

Signif. codes: 0 '***' 0.001 '**' 0.01 '*' 0.05 '.' 0.1 ' ' 1

(C) Forward selection of explanatory variables

Explanatory variable	**AIC**	**Pseudo-*F***	***P***
TN	34.2	4.7	0.001
$\delta^{13}C$	32.1	3.6	0.002
Reconstructed Vegetation Openness	35.5	3.7	0.002
$CaCO_3$	37.1	3.1	0.005

Table A.4: Statistics results of two categories variation partitioning analysis (VPA) based on redundancy analyses (RDA) as implemented on two categories of environmental variables: eutrophication and lake circulation. The significance of their conditional effects on OTU variation was determined via 999 Monte Carlo permutations.

Explained variation

Fraction	**Variation (adj)**	**% of Explained**	**% of All**	**DF**	**Mean Square**
Eutrophication	0.11859	40.6	11.9	1	0.13482
Lake circulation	0.16804	57.5	16.8	2	0.10553
Eutrophication and lake circulation	0.0056358	1.9	0.6		
Total Explained	0.29226	100	29.2	3	0.12183
All Variation	1		100	29	

Significance tests

Tested Fraction	**F**	**P**
Eutrophication and lake circulation	5	0.0005
Eutrophication	5.5	0.0005
Lake circulation	4.3	0.0005

Group Members

Eutrophication	**Lake circulation**
TN	Reconstructed vegetation openness
	$\delta^{13}C$

Table A.5: Statistics results of three categories variation partitioning analysis (VPA) based on redundancy analysis (RDA) as implemented on three categories of environmental variables: lake circulation, eutrophication, and other factors. The significance of their conditional effects on OTU variation was determined via 999 Monte Carlo permutations.

Explained variation

Fraction	**Variation(adj)**	**% of Explained**	**% of All**	**DF**	**Mean Square**
Eutrophication	0.096945	27.5	9.7	1	0.10591
Lake circulation	0.14224	40.4	14.2	2	0.08609
Other factors	0.060097	17.1	6	2	0.04927
Lake circulation and eutrophication	-0.035134	-10	-3.5		
Eutrophication and other factors	0.025801	7.3	2.2		
Lake circulation and other factors	0.021645	6.1	2.6		
All groups	0.04077	11.6	4.1		
Total Explained	0.35236	100	35.2	5	0.0928
All Variation	1		100	29	

Significance tests

Tested Fraction	**F**	**P**
All groups	4.2	0.0005
Eutrophication	4.7	0.0005
Lake circulation	3.9	0.0005
Other factors	2.2	0.002
Lake circulation and eutrophication	3.1	0.0065
Eutrophication and other factors	4.3	0.0005
Lake circulation and other factors	2.5	0.0055

Group Members

Eutrophication	**Lake circulation**
TN	$\delta^{13}C$
	Reconstructed vegetation openness
Other factors	
Dry density	
$CaCO_3$	

Appendix B Supplementary Material for Chapter 3

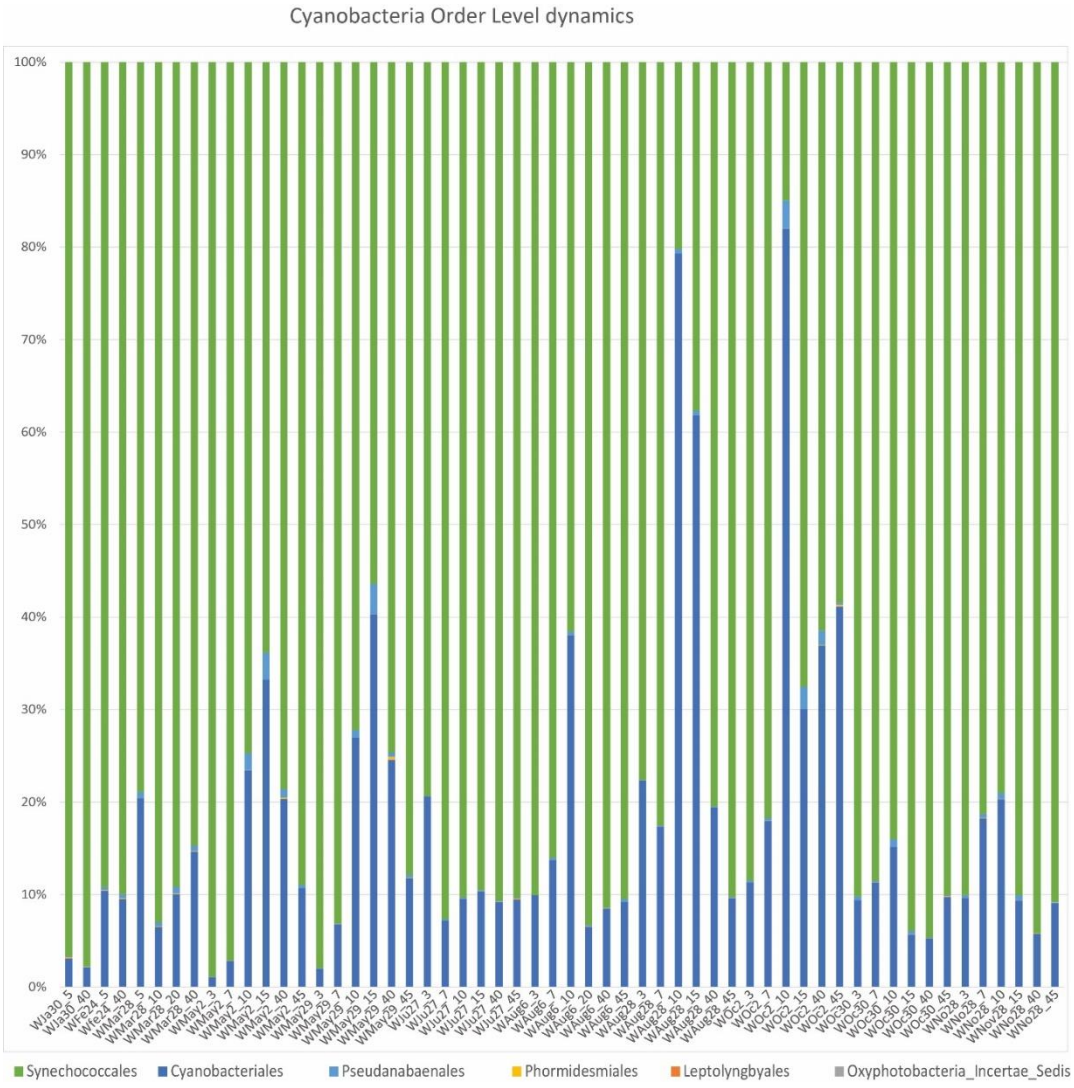

(A)

(B)

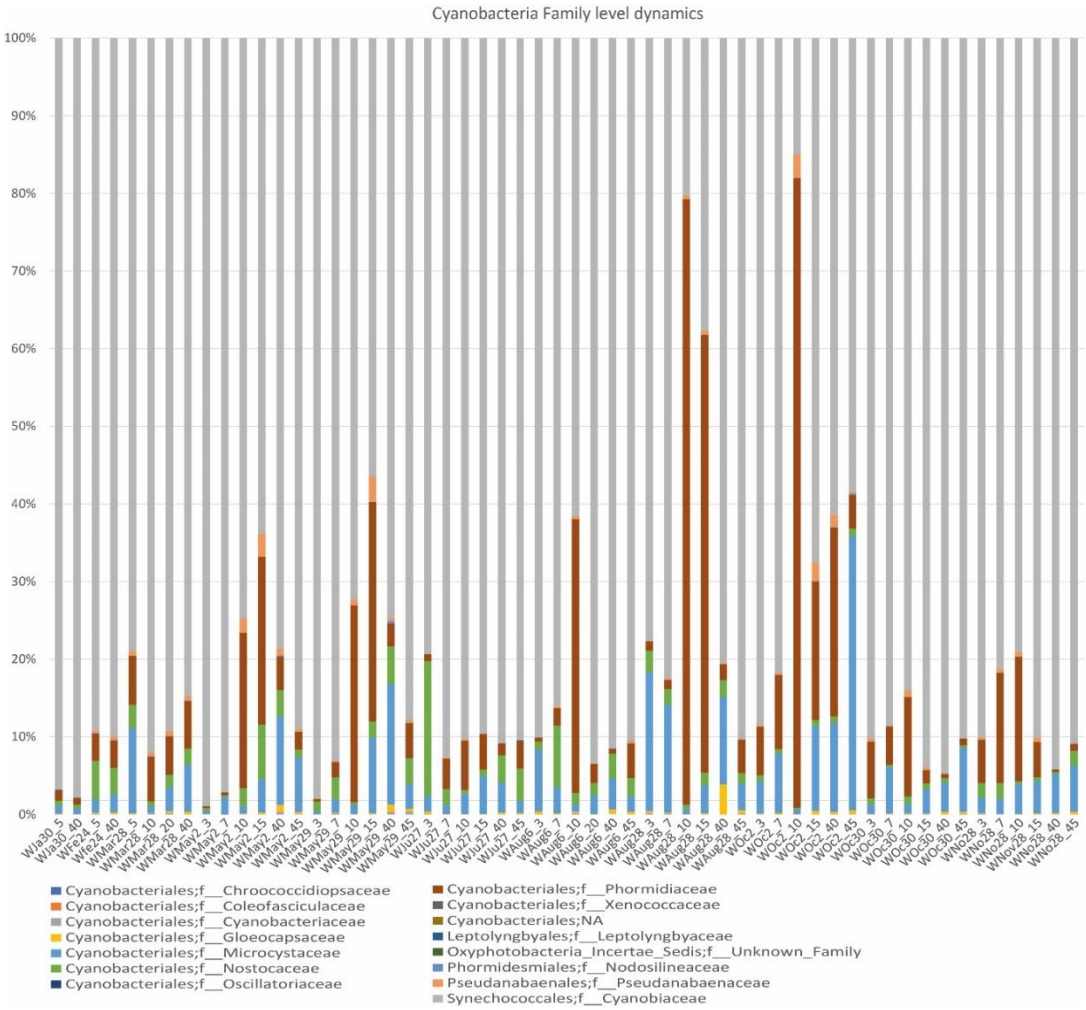
Cyanobacteria Family level dynamics
100%
90%
80%
70%
60%
50%
40%
30%
20%
10%
0%
Cyanobacteriales;f__Chroococcidiopsaceae
Cyanobacteriales;f__Coleofasciculaceae
Cyanobacteriales;f__Cyanobacteriaceae
Cyanobacteriales;f__Gloeocapsaceae
Cyanobacteriales;f__Microcystaceae
Cyanobacteriales;f__Nostocaceae
Cyanobacteriales;f__Oscillatoriaceae
Cyanobacteriales;f__Phormidiaceae
Cyanobacteriales;f__Xenococcaceae
Cyanobacteriales;NA
Leptolyngbyales;f__Leptolyngbyaceae
Oxyphotobacteria_Incertae_Sedis;f__Unknown_Family
Phormidesmiales;f__Nodosilineaceae
Pseudanabaenales;f__Pseudanabaenaceae
Synechococcales;f__Cyanobiaceae

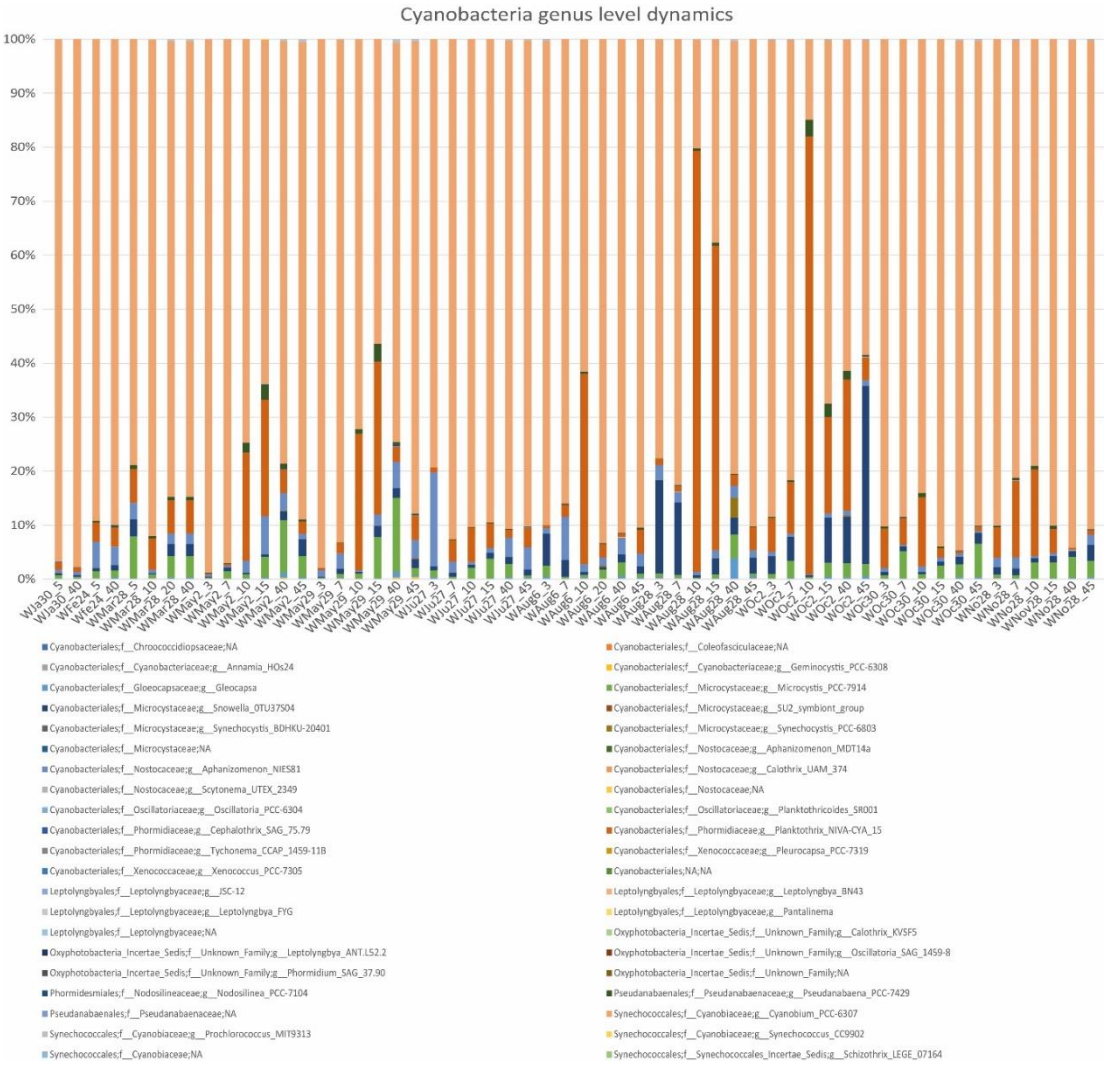

(C)

Figure B.1: Barplots showing sample-wise cyanobacteria taxonomic distribution at the (A) Order level, (B) Family level and (C) Genus level. Numbers beside months refer to sampling date while number after the underscore refers to water depth, e.g., May2_10 refers to a sample collected at 10 m water depth on 2nd May.

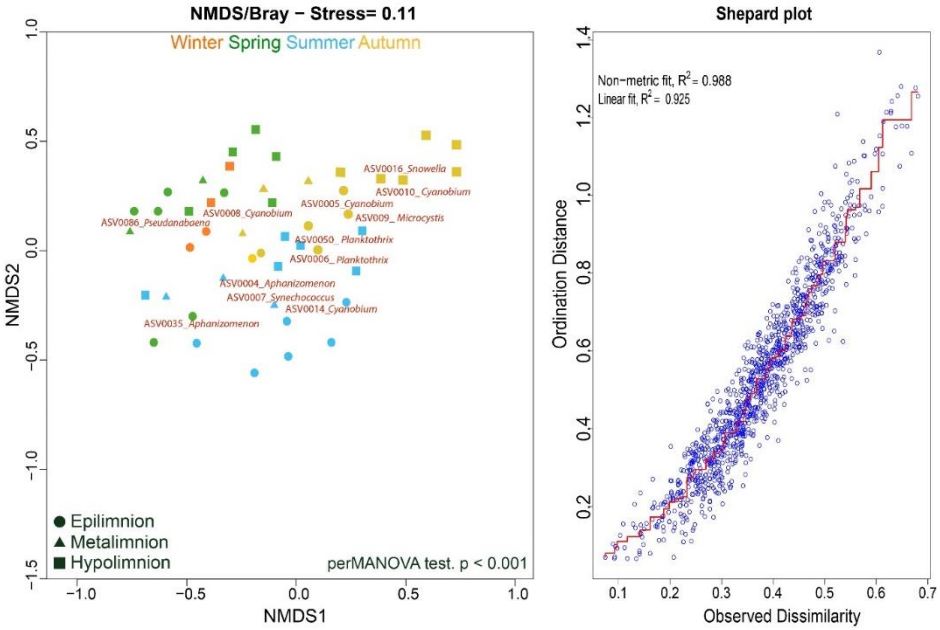

Figure B.2: Non-metric multidimensional scaling (NMDS) showing spatiotemporal clustering patterns of cyanobacteria amplicon sequence variants (ASVs ≥0.1%) from this study. Bray-Curtis distance was used. Stress = 0.11. A nonparametric PerMANOVA (Bray Curtis) was used to test the significance of the spatiotemporal clustering
Patterns. In the NMDS and PerMANOVA the sample seasons were predictors while Hellinger-transformed cyanobacteria absolute read counts were the response variables.

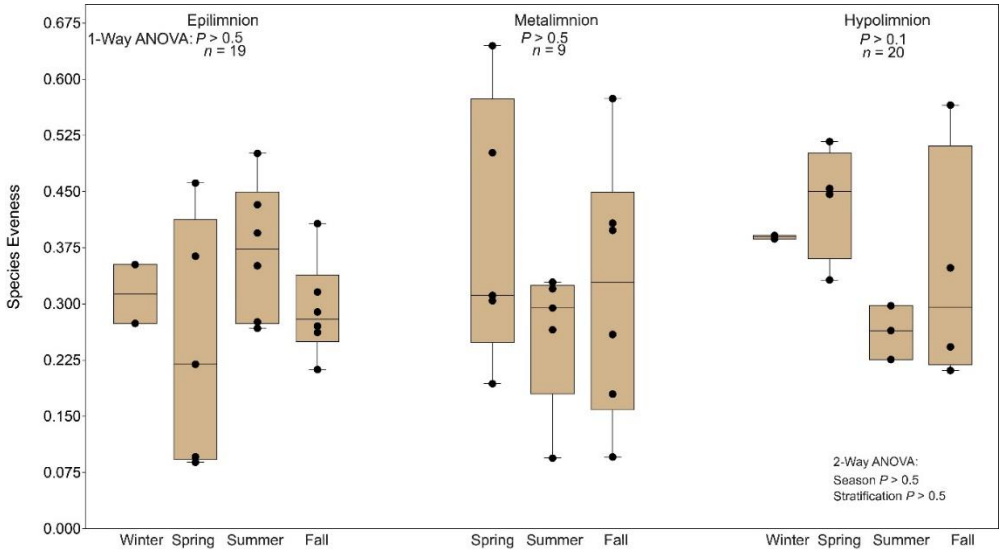

Figure B.3: Box plots showing the results of seasonal and stratification effects

on cyanobacteria species evenness in Lake Tiefer See via a two-way analysis of variance (ANOVA) analysis. Test for significant seasonal variation in cyanobacterial species evenness within the epi-, meta- and hypolimnion layers was tested via a one-way ANOVA.

Table B.1: Results of bioinformatical analyses of sequencing data for each sample, alpha diversity data for each sample and unique sample barcodes.

Sample Site	Sample ID	Raw read counts	Quality filtered read counts	Cyanobacteria read counts	Observed ASVs >1%	Shannon_H >1%	Pielou's Evenness >1%	Barcode sequence-F	Barcode sequence-R
Epilimnion water column	May2_3	175384	98630	81793	25	1,055	0,1149	CATCCAGT	CGTGATAC
	May29_3	222133	92445	72541	23	1,872	0,2827	CATCCAGT	CTTCTTCC
	Jun_3	149317	48309	45708	25	2,179	0,3534	CATCCAGT	TATCCTCC
	Aug6_3	150922	45764	42420	26	2,648	0,5435	CATCCAGT	AACACCGT
	Aug28_3	91961	31111	28751	26	2,378	0,4149	CATCCAGT	TTACCGCT
	Oc2_3	281533	114661	94889	26	2	0,2841	CATCCAGT	TGAGATGC
	Oc30_3	62337	26642	24724	27	2,139	0,3146	CATCCAGT	GTGCAACT
	No_3	143307	43009	33877	27	2,619	0,5081	CATCCAGT	TGAGCCTA
	Ja5	165673	84153	26826	27	2,307	0,3722	CAACCTCA	CGTGATAC
	Fe5	141976	66220	9396	25	2,38	0,4322	CAACCTCA	CTTCTTCC
	Mar_5	188223	116484	6880	25	2,594	0,5353	CAACCTCA	TATCCTCC
	May2_7	143438	76718	53025	26	1,21	0,1289	CAACCTCA	AACACCGT
	May29_7	87050	32700	19614	26	2,5	0,4684	CAACCTCA	TTACCGCT
	Jun_7	121635	45534	28964	26	2,284	0,3776	CAACCTCA	TGAGATGC
	Aug6_7	113860	41923	29158	27	2,694	0,5476	CAACCTCA	GTGCAACT
	Aug28_7	125613	38114	27369	27	2,685	0,5431	CAACCTCA	TGAGCCTA
	Oc2_7	165231	74945	42161	27	2,288	0,3652	CAACCTCA	ATGGAGGT
	Oc30_7	110619	44863	33462	27	2,169	0,3242	CAACCTCA	CTGAGTCT
	No_7	98597	30472	19070	26	2,605	0,5206	CAACCTCA	GAGGTGAA
Metalimnion water column	Mar_10	179609	90856	16944	25	1,761	0,2326	TGCTTGTC	CGTGATAC
	May2_10	130479	63282	12305	24	2,101	0,3405	TGCTTGTC	CTTCTTCC
	May29_10	156049	63943	38722	25	2,231	0,3723	TGCTTGTC	TATCCTCC
	Jun_10	142750	63870	32767	26	2,236	0,3598	TGCTTGTC	AACACCGT
	Aug6_10	123174	47865	32423	27	2,308	0,3723	TGCTTGTC	TTACCGCT
	Aug28_10	137861	66836	50276	26	1,21	0,129	TGCTTGTC	TGAGATGC
	Oc2_10	120789	70191	60084	27	1,149	0,1169	TGCTTGTC	GTGCAACT
	Oc30_10	133799	49913	37460	27	2,126	0,3105	TGCTTGTC	TGAGCCTA
	No_10	142473	51925	30701	27	2,597	0,497	TGCTTGTC	ATGGAGGT
	May2_15	81787	46493	2269	20	2,568	0,652	TCGTCGCTCG	CTTCTTCC
	May29_15	80368	40667	4737	22	2,47	0,5374	TCGTCGCTCG	TATCCTCC
	Jun_15	41918	18060	16238	24	2,209	0,3795	TCGTCGCTCG	AACACCGT
	Aug28_15	42116	18868	17440	27	2,311	0,3735	TCGTCGCTCG	TGAGATGC
	Oc2_15	51271	20196	11927	27	2,852	0,6417	TCGTCGCTCG	GTGCAACT
	Oc30_15	50931	24740	21906	27	1,738	0,2105	TCGTCGCTCG	TGAGCCTA
	No_15	48673	22522	14514	27	2,884	0,6626	TCGTCGCTCG	ATGGAGGT
Hypolimnion Water column	Mar_20	95758	46951	6179	22	2,047	0,352	TCGTCGCTCG	CGTGATAC
	Ja45	171550	91611	34366	26	2,457	0,4487	AGACGCACTC	CGTGATAC
	Fe45	114796	48626	9228	25	2,476	0,4756	AGACGCACTC	CTTCTTCC
	Mar_45	221091	101049	10111	26	2,639	0,5384	AGACGCACTC	TATCCTCC
	May2_45	153557	88720	13370	27	2,708	0,5553	AGACGCACTC	AACACCGT
	May29_45	156154	95642	15194	27	2,841	0,6345	AGACGCACTC	TTACCGCT
	Jun_45	177970	45534	37373	27	2,426	0,4188	AGACGCACTC	TGAGATGC
	Aug6_45	80692	36232	19745	27	2,084	0,2975	AGACGCACTC	GTGCAACT
	Aug28_45	129908	52656	39619	27	2,439	0,4245	AGACGCACTC	TGAGCCTA
	Oc2_45	202697	110256	56113	27	2,625	0,5114	AGACGCACTC	ATGGAGGT
	Oc30_45	109925	58519	42235	27	1,985	0,2696	AGACGCACTC	CTGAGTCT
	No_45	116083	58165	29652	27	2,126	0,3103	AGACGCACTC	GAGGTGAA

Table B.2: One-way PerMANOVA on cyanobacterial communities from the water column grouped into seasons. Summary presents overall test statistics. Pairwise analysis shows

Bonferroni corrected *P*-values above the diagonal and corresponding F-values below the diagonal.

PERMANOVA	Statistics	Pairwise	Spring	Summer	Fall	Winter
Permutation N:	9999	Spring		0.0001	0.0001	0.0166
Total sum of squares:	6.474	Summer	9.274		0.0001	0.0001
Within-group sum of squares:	4.531	Fall	18.61	10.46		0.0001
F:	10.72	Winter	2.815	6.178	12.75	
p (same):	0.0001					

Table B.3: A two-way ANOVA showing that cyanobacteria species richness was impacted by
seasonality and not by lake stratification (epi-, meta-, and hypolimnion) and/or an interaction
effect of both factors. A Tukey post-hoc test showing significant pairwise differences in cyanobacteria species richness in between seasons and between the epi- and hypolimnion layers. Significant *P*-values are in bold.

Summary statistics					
	Df	Sum	Sq Mean	Sq F-value	Pr(>F)
Season	3	501.0	167.01	8.046	**0.000238 *** **
Zone	2	133.0	66.49	3.203	0.050727 .
Residuals	42	871.8	20.76		

TukeyHSD (Tukey multiple comparisons of means 95% family-wise confidence level) Pairwise comparison of the seasons and stratification (epi-, meta-, and hypolimnion) predictors used in the ANOVA model. Underlined *p*-values show significant interactions.

Season				
	diff	**lwr**	**upr**	**p adj**
Spring-Autumn	**-8.009524**	**-12.538392**	**-3.480656**	**0.0001449**
Summer-Autumn	**-2.200000**	**-6.650099**	**2.250099**	**0.5541521**
Winter-Autumn	**-4.866667**	**-11.724730**	**1.991397**	**0.2442977**
Summer-Spring	**5.809524**	**1.280656**	**10.338392**	**0.0071634**
Winter-Spring	**3.142857**	**-3.766578**	**10.052293**	**0.6198716**
Winter-Summer	**-2.666667**	**-9.524730**	**4.191397**	**0.7270511**

Zone				
	diff	**lwr**	**upr**	**p adj**
Hypo-Epi	**-3.688947**	**-7.234956**	**-0.1429389**	**0.0398735**
Meta-Epi	**-2.051963**	**-6.530955**	**2.4270282**	**0.5115038**
Meta-Hypo	**1.636984**	**-2.805870**	**6.0798378**	**0.6463238**

Appendix C Supplementary Material for Chapter 4

Supplementary Information: Extended Materials and Methods

Study site. The hard water oligo-mesotrophic Lake Tiefer See (near Klocksin; 53°35.5′N, 12°31.8′E; 62 m a.s.l.) is part of the southern Baltic Lake District and was formed during the final stage of the last glacial period (~13,000 years ago) (Dräger et al., 2017; Fig. 1a, b). Lake Tiefer See is part of a subglacial gully system in a morainic terrain located in Nature Park 'Nossentiner/Schwinzer Heide.' Today, the lake is connected to Lake Hofsee in the south through a shallow sill, whereas the connection to Lake Flacher See in the north has been channelized into a tunnel after the construction of a railway dam between the two lakes (CE 1884–1886) and is currently largely interrupted. Lake Tiefer See has a surface area of approximately 0.75 km2, and the catchment area of approximately 5.5 km2 is dominated by glacial till. Although the catchment is mainly used for agriculture (Theuerkauf et al., 2015), the direct shore-line of the lake is covered by a fringe of trees, and there is no anthropogenic infrastructure, such as buildings or roads at the lakeshore. The lake has a maximum depth of 62 m and no major inflows or outflow. The
annual lake mixing is either mono- or dimictic, depending on the formation of a winter ice cover (Kienel et al., 2017). The study site is characterized by a warm-temperate climate during the transition from oceanic to continental conditions. Mean monthly temperatures range from 0°C in January to 17–18°C in July, with maxima up to 30°C and minima down to -5°C. Mean monthly precipitation varies between ~40 mm during winter and ~60 mm in summer, with a mean annual precipitation of 560–570 mm (Kienel et al., 2017). Lake Tiefer See has been the focus of an extensive and high-resolution climate monitoring program since the beginning of the last decade (Roeser et al., 2021). The lake is well-preserved and seasonally laminated sediments have aided climate reconstructions spanning the last 6,000 years (e.g., Dräger et al. 2019).

Collection of water, sediment trap material, and sediment cores

Water samples were collected monthly between January 30 and November 28, 2019, at the floating weather monitoring station, located at the maximum depth of the lake (62 m; Fig. 1b). The sampled water depths were 1, 3, 5, 7, 10, 15, 20, 40, 45, and 50 m. A sample volume of 250 mL of lake water was collected for the upper 1, 3, and 5 m water depths and pooled (750 mL), representing the epilimnion. Likewise, 375 mL volumes were collected for the lower 45 and 50 m water depths and pooled (750 mL), representing the bottom waters. For each of the other 7, 10, 15, 20, and 40 m water depths, 750-mL water samples were collected. The samples were collected in sterile glass bottles (Schott Duran®, Germany), filtered within 24 h after fieldwork using 0.2 µm cellulose filters (Sartorius AG, Germany), and the filters were stored at -20°C until nucleic acid extraction. The suspended particulate matter was trapped with four-cylinder traps (KC Denmark A/S total active area 0.0163 m2 for the four cylinders) at two depths in the water column (Fig. 1c). One trap was anchored in the metalimnion (12 m water depth), whereas the second trap was secured in the hypolimnion (55 m water depth). For both depths, the traps were emptied monthly between April and November 2019, i.e., the annual interval of increased lake productivity. The trapped material was transferred into 2 L plastic bottles, which were allowed to settle overnight at 4°C. An equal volume of water was discarded from the bottles, and the remaining suspension was transferred into sterile 50 mL Falcon tubes (Fischer Scientific GmbH,

Germany). The tubes containing suspended particulate matter were then centrifuged at 4000 g for 5 min. Subsequently, the supernatant was discarded, and the pellet was stored in Falcon tubes at -20°C until nucleic acid extraction. A surface sediment core (TSK19-SC6; 115 cm length) was collected on August 29, 2019, from the point of maximum water depth (62 m) using a 90 mm UWITEC piston corer. The temperature of the upright positioned core was maintained at 4 °C during transportation and short-term storage at the facilities of the GFZ Potsdam. To preserve the uppermost varves, the core was allowed to dry in a vertical position at 4 °C for approximately 2 weeks before longitudinal splitting. After splitting the core, one half was lithologically described. A triplicate 0–2 cm subsample of the other core half was stored in sterile 15 mL Falcon tubes at -20°C until nucleic acid extraction. All core handling was performed under clean conditions in a room where no molecular biological work had been previously conducted to avoid contamination.

Lake physicochemical properties

Measurements of the physicochemical parameters, such as temperature, pH, dissolved oxygen (DO), turbidity, and chlorophyll-a (Chla) in the water column were conducted automatically using a multi-parameter water quality probe (YSI 6600 V2, Yellow Springs USA), in 1-m steps and 12 h resolution. Owing to technical problems, in February, data were only collected on 2 d (1st and 28th), and in March, no data were recorded between the 2nd and 10th. Water temperature was additionally measured using 26 stationary data loggers (HOBO Water Temp Pro v2, Onset USA) in 1-m steps from 0 to 15 m and 5-m steps from 15 to 55 m water depth (Fig. 1c). Water samples for nitrate (NO3–) and total dissolved phosphorus (TDP) analyses were also collected monthly, in parallel with those for molecular analysis. Water samples for total sulfide were collected from the hypolimnion in October and November. Water samples for nitrate measurements were analyzed at the German Research Centre for Geosciences

(GFZ), whereas TDP and total sulfide were conducted at the Leibniz Institute for Baltic Sea Research Warnemünde (IOW). Nitrate was measured by suppressed ion chromatography using a SeQuant SAMS anion IC suppressor (EMD Millipore, Billerica, Massachusetts), an S5200 sample injector, a 3.0 × 250 mm LCA 14 column, and an S3115 conductivity detector (all Sykam, Fürstenfeldbruck, Germany). The eluent was 5 mM Na2CO3, 20 mg L-1 4–hydroxybenzonitrile and 0.2% methanol. The flow rate was set to 1 mL min-1, and the column oven temperature was to 50°C. The detection and quantification limits were calculated based on signal-to-noise (S/N) ratios of 3 and 10, respectively. All samples were measured in triplicate, and every 10 injections a standard was measured to check for drift. Reproducibility was always better than 5%, and the detection limit ranged between 1–4 µM. For TDP, the water samples were immediately filtered using 0.45 µm syringe filters and acidified with sub-boiled HNO3 to 2 vol%. The TDP was measured by inductively coupled plasma optical emission spectrometry (ICP-OES; iCAP 7400, Duo, Thermo Fisher Scientific) using external calibration and Sc as the internal standard. Precision and trueness were checked with the international reference material SLRS-6 (NRCC) spiked with 20 µg L-1 P, which were 9.6% and 5.7%, respectively. After fixation of 50 mL of an aliquot of the filtered water sample with 500 µL 20 vol% zinc acetate solution, total sulfide was determined spectrophotometrically according to the Cline method (Cline, 1969) with a precision of 3.2% (Dellwig et al., 2019).

The sediment fluxes (sediment flux: g m-2 d-1) were determined from the weighted and freeze-dried trapped sediment material. The samples were homogenized using an agate mortar. Prior to total organic carbon (TOC)

and total nitrogen (TN) determination, replicate aliquots (0.2 mg) were decalcified in situ in Ag capsules (20% HCl and dried at 75°C). The TOC and TN contents were measured using the elemental analyzers NC2500 and EA3000-CHS Eurovectors, respectively, and were used to calculate the atomic C:N ratio. CaCO3 content was estimated after obtaining the total inorganic carbon content (TIC = TC–TOC) and multiplying by a factor of 8.33, which is the percentage of molecular weight in inorganic carbon in the calcium carbonate structure.

Molecular analyses

All nucleic acid extractions were conducted in a clean laboratory where no polymerase chain reaction (PCR) was performed prior to the extraction, following established methods and precautions to limit contamination. Water sample DNA extraction was performed at different times than the sediment samples to avoid cross-contamination. Additionally, the sediment traps were processed independently from the surface sediment cores. Because of water column turnover in January and February, water samples for molecular analyses from 1, 3, 5, 7, and 10 m water depths were pooled and reported as the mean depth (5 m). Water depths of 40, 45, and 50 m were equally pooled and reported as the mean depth (45 m). In March, when temperatures began to increase, four depths in the water column were reported as follows: 5 (1, 3, 5, and 7 m pooled), 10, 20, and 45 m (40, 45, and 50 m pooled). Genomic DNA (gDNA) of water samples was extracted from the filters using the DNeasy PowerWater Kit (QIAGEN, Hilden, Germany) following the manufacturer's specifications. The gDNA from the homogenized sediment trap samples and surface sediment samples was extracted from approximately 0.75 g using the DNeasy PowerSoil Kit (QIAGEN, Hilden, Germany). The extracted gDNA from all samples was eluted in 100 µL elution buffer and stored at -20°C until downstream analysis.Cyanobacteria quantification Total cyanobacteria were quantified with a SYBR Green qPCR assay that amplified the cyanobacterial 16S rRNA-ITS (internal transcribed spacer) region using the primers CSIF (5′-GYCACGCCCGAAGTCRTTAC-3′) and 373R (5′-CTAACCACCTGAGCTAAT-3′) (Janse et al., 2003). The final volume of the qPCR reactions was 20 µL, which consisted 10 µL of KAPA HiFi 2x SensiFAST SYBR® FAST qPCR Master Mix (Sigma-Aldrich, Germany), 0.2 µL of each forward and reverse primer (100 µM, Biomers), 5.8 µL PCR water, and 4 µL of template DNA. The qPCR program consisted of an initial polymerase activation step (95°C for 15 min), followed by 40 cycles of denaturation at 94°C for 60 s, annealing at 60°C for 60 s, and extension at 72°C for 60 s. The qPCR program was followed by a melting curve step from 70°C to 95°C at a transition rate of 1°C per 5 s to determine the specificity of the amplification. The amplified products were confirmed using agarose gel electrophoresis. Tenfold dilution standards were prepared from gDNA of Synechocystis for each qPCR assay, which ranged from 4.7 × 107 to 4.7 × 103 copies ng-1 DNA, and was used to create the standard curves from which the quantification cycle (Cq) values were determined (Bustin et al. 2009). The copy numbers of the 16S rRNA-ITS region were calculated following Savichtcheva et al. (2011), and were the mean of triplicates of each sample expressed as cyanobacterial abundance normalized to extracted DNA (copies ng-1 DNA) with a minimum quantification efficiency of 91%. All qPCR assays were performed in triplicate on a CFX96 real-time thermal cycler (Bio-Rad Laboratories, Inc., USA).

Sequence library preparation All consumables and pipets used for PCR were sterilized in a laminar

flow hood under UVC light for at least 15 min prior to use. PCR for the Illumina high-throughput sequencing (HTS) libraries was conducted using the cyanobacteria-specific primers CYA359F (5′-CGGACGGGTGAGTAACGCGTG-3′) and CYA784R (5′-ACTACWGGGGTATCTAATCCC-3′) (Nübel et al. 1997). They amplify a >400-nt-long fragment of the V3–V4 regions of the 16S rRNA gene. The primers had unique tags (Supplemental Information SI 1) that served to differentiate the samples. The water and sediment samples, as well as the negative control (that is, a reaction with PCR water as a template) were amplified in a PCR reaction of 50 µL, containing 10x Pol Buffer C (Roboklon GmbH, Berlin, Germany), 25 mM MgCl2, 0.2 mM deoxynucleoside triphosphate (dNTP) mix (ThermoFisher Scientific), 0.5 mM each primer (TIB Molbiol, Berlin, Germany) and 1.25 U of Optitaq Polymerase (Roboklon). The volume of the template DNA used in each reaction varied between 1 and 4 µL, depending on the sedDNA concentration. The PCR program included an initial denaturation step at 95°C for 10 min, followed by 35 cycles at 95°C for 15 s, annealing at 60°C for 30 s, extension at 72°C for 45 s, and a final extension step at 72°C for 5 min. To avoid cross-contamination, the PCR reactions were performed monthly after each sampling, and the water samples were processed separately from the sediment samples. The tagged PCR products were then purified with the Agencourt AMPure XP kit (Beckman Coulter, Brea, CA, USA) and eluted in 30 µL DNA/RNA-free water. The purified product was quantified using a Qubit (2.0) fluorometer. Equimolar concentrations of all samples, including two negative purified PCR controls, were pooled into two multiplex libraries (n = 160 samples, including 78 samples and 2 controls per library). The two libraries contained technical replicates of the water samples and biological replicates of the sediment samples. The final libraries were paired-end sequenced (2 × 300 bp) on an Illumina MiSeq system (Eurofins Scientific (Constance, Germany)).

Bioinformatics. The obtained 14,649,824 sequence reads were quality checked on a raw FASTQ file with FastQC (Andrews et al. 2015). The reads were then demultiplexed using the make.contigs function in Mothur (v.1.39.5: pdiff=2, bdiff=1, and default settings for others) (Schloss et al. 2009). Based on the report files, the sequence identifiers were retrieved for those sequences with minimum overlap (length > 25), maximum mismatches (< 5), and the maximum number of ambiguous bases of zero (which means there was no base marked with N′). According to the sequence identifiers from the previous step, the sequences were then extracted with the filterbyname.sh function from BBtools (Bushnell et al. 2017) from the raw paired-end fastq files. This step was followed by checking and correcting the sequence orientation and removing sample unique barcodes using extract_barcodes.py in QIIME1 (Caporaso et al., 2010). Finally, primers were removed using Cutadapt (Martin 2014). The sequences were then fed to DADA2 (Callahan et al., 2016) for filtering, dereplication, chimera check, sequence merge, and amplicon sequence variant (ASV) calling. Then, QIIME2 (Bolyen et al. 2019) was used for taxonomic assignment against the SILVA138 database (Quast et al. 2013).

Data availability. Sequencing data and metadata are deposited in the European Nucleotide Archive (ENA) under BioProject accession number PRJEB40406 and sample accession numbers ERS5083533-ERS5083564 (trap material and surface sediment samples) and ERS5083566-ERS5083644 (water samples).

Sequence data processing. The 152 samples resulted in a total of 7,297,946 denoised and error-corrected sequences that DADA2 inferred in 2,538 ASVs. We filtered out all ASVs not assigned to cyanobacteria and

chloroplasts, and another 43 ASVs that occurred in fewer than three samples over the entire dataset to reduce bias from very rare taxa. The four negative controls that were included in the sequencing run each comprised less than 1% of the reads compared with the sample average and were therefore removed.

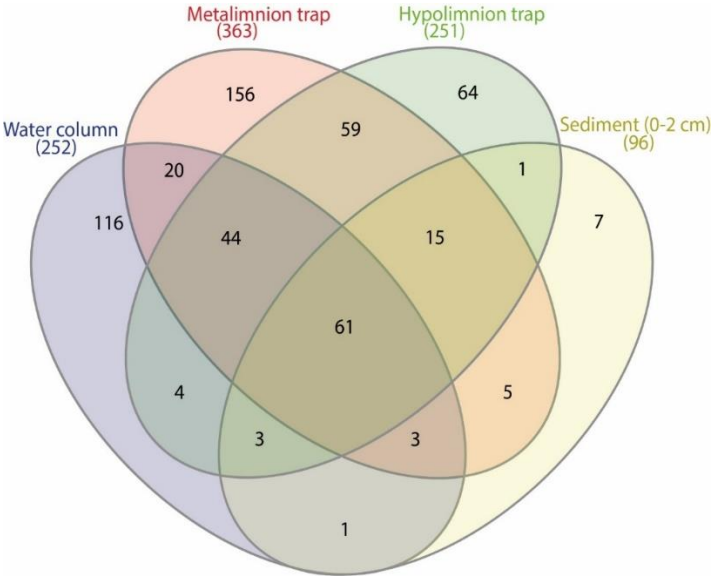

Figure C.1: Distribution of all cyanobacteria ASVs among sample types of Lake Tiefer See

Venn diagram shows distribution of the 559 cyanobacterial amplicon sequence variants (ASVs) among
the sample types.

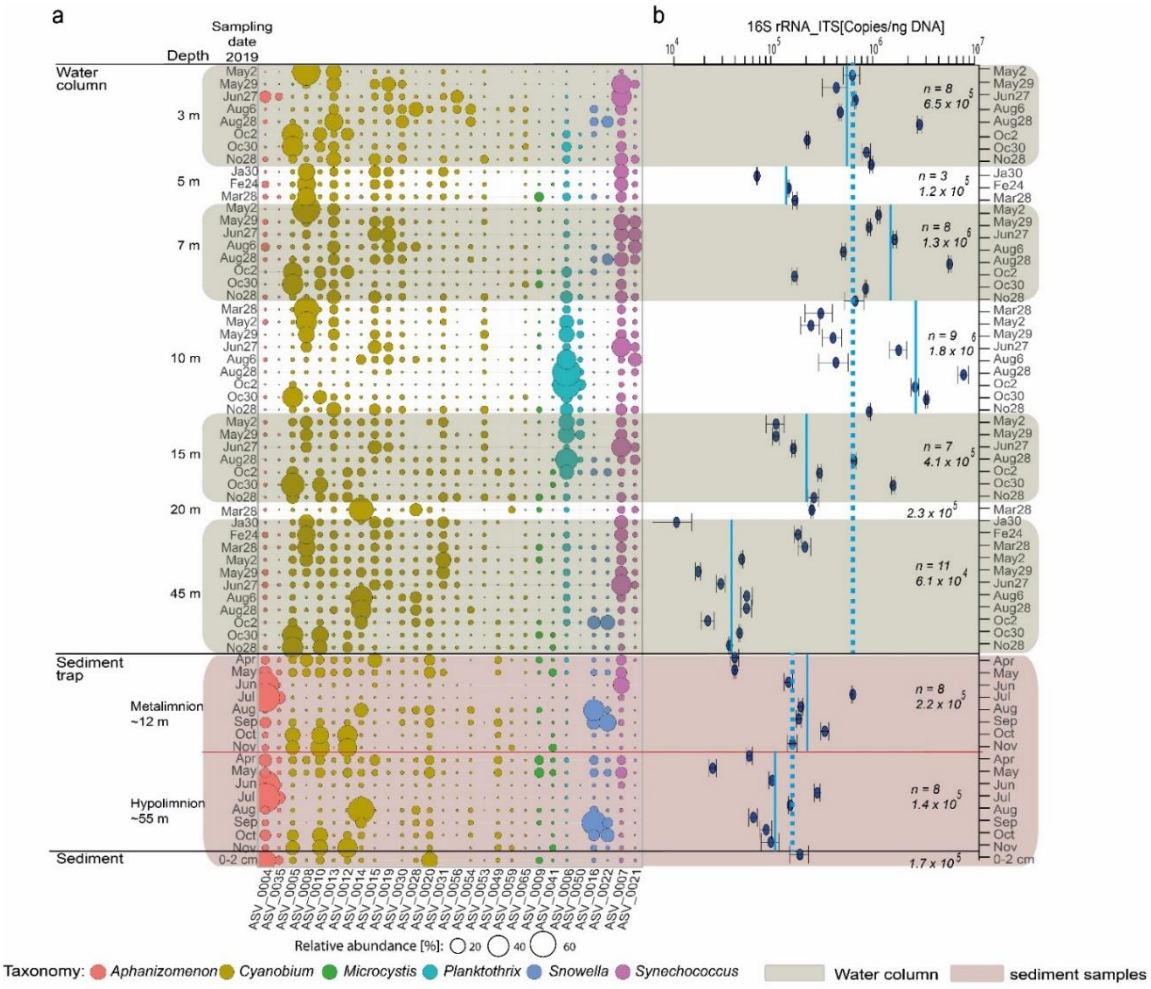

Figure C2: Cyanobacteria community distribution in Lake Tiefer See (a) Bubble plot showing spatial (depth) and temporal (monthly) variation of the most abundant cyanobacteria ASVs (> 1% reads) in 2019, and (b) Cyanobacterial abundance quantified via qPCR with primers that amplify part of the 16S rRNA internal transcriber spacer (ITS) region of cyanobacteria (data were normalized to ng DNA extracted). Blue vertical lines represent the average abundance in each depth while broken blue vertical line represents overall averages in water column and sediment traps, respectively.

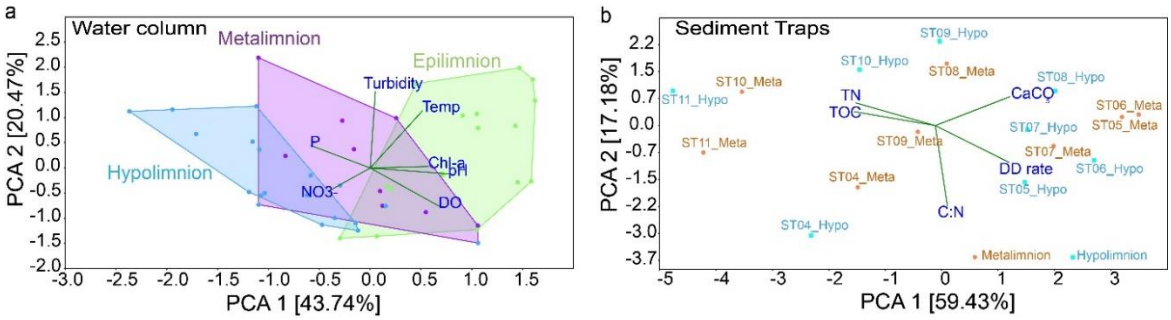

Figure C.3: Variation of environmental variables from water and sediment traps of Lake Tiefer See:

Principal components analyses (PCA) of environmental data based on Euclidean distance from (a) water column with percentage variation between samples from the thermal stratification zones indicated on the principal components PC1 and PC2 axes. Total variance explained by both axes = 64.14%. Epilimnion n = 19, metalimnion n = 16 and hypolimnion n = 12. (b) meta- (orange; n = 8) and

hypolimnion (cyan; n = 8) sediment trap samples. Both PC1 and PC2 together explain 76.61% of total

variance among the samples. In both plots the environmental variables are projected as green vectors.

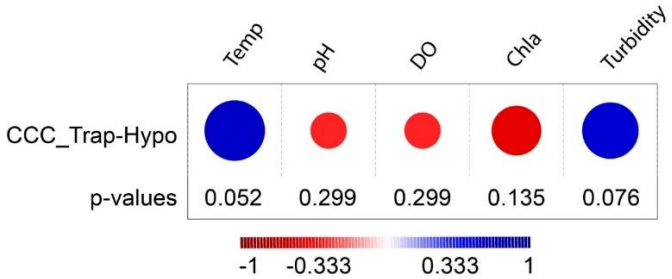

Figure C.4: Rank based spearman correlation of the total cyanobacteria community composition from the hypolimnion trap with internal physicochemical parameters in Lake Tiefer See. Blue bubbles show positive while red bubbles show negative correlation. The p values are shown below the figure.

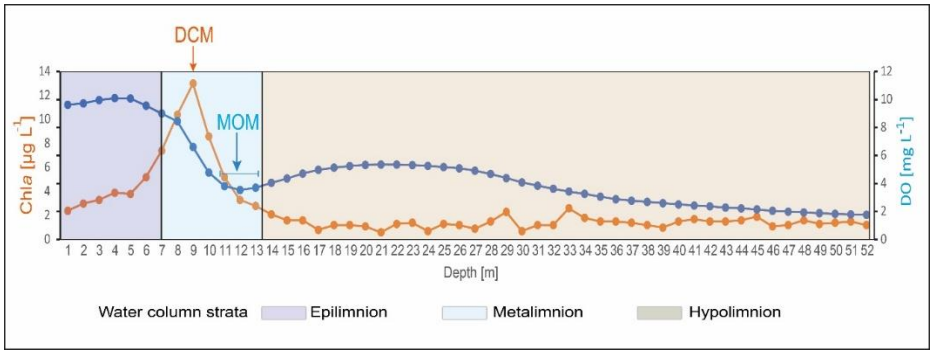

Figure C.5: Chlorophyll a and dissolved oxygen for the month of August 2019 throughout the water
column of Lake Tiefer See showing the formation of deep chlorophyll maximum (DCM) and the metalimnetic oxygen minimum (MOM) layers in the metalimnion.

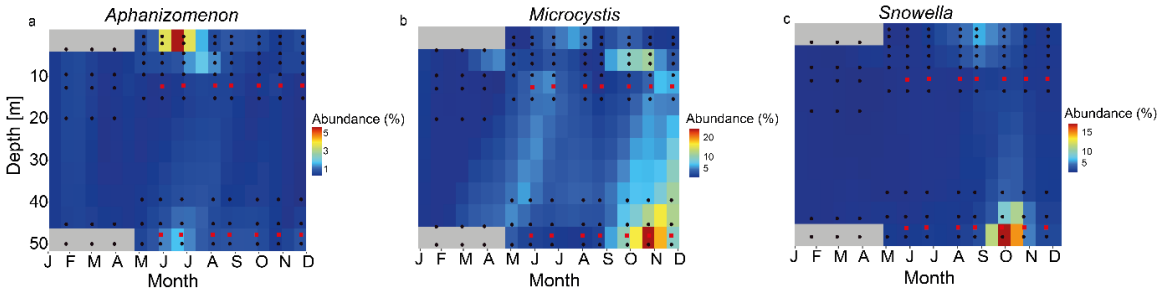

Figure C.6: Heatmaps of relative abundances of all amplicon sequence variants (ASVs) assigned to (a) Aphanizomenon, (b) Microcystis, and (c) Snowella. Data is interpolated for 15 days and 5 m water depth. Black circles and red squares represent the depths and timing of sampling of water and sediment traps, respectively

Table C.1: Statistical analyses of sequencing analysis and alpha diversity data.

Sample Site	Sample ID	Raw read counts	Quality filtered read counts	Cyanobacteria read counts	Observed ASVs >1%	Shannon_H >1%	Pielou's Evenness >1%	Barcode sequence-F	Barcode sequence-R
Epilimnion water column	May2_3	175384	98630	81793	25	1,055	0,1149	CATCCAGT	CGTGATAC
	May29_3	222133	92445	72541	23	1,872	0,2827	CATCCAGT	CTTCTTCC
	Jun_3	149317	48309	45708	25	2,179	0,3534	CATCCAGT	TATCCTCC
	Aug6_3	150922	45764	42420	26	2,648	0,5435	CATCCAGT	AACACCGT
	Aug28_3	91961	31111	28751	26	2,378	0,4149	CATCCAGT	TTACCGCT
	Oc2_3	281533	114661	94889	26	2	0,2841	CATCCAGT	TGAGATGC
	Oc30_3	62337	26642	24724	27	2,139	0,3146	CATCCAGT	GTGCAACT
	No_3	143307	43009	33877	27	2,619	0,5081	CATCCAGT	TGAGCCTA
	Ja5	165673	84153	26826	27	2,307	0,3722	CAACCTCA	CGTGATAC
	Fe5	141976	66220	9396	25	2,38	0,4322	CAACCTCA	CTTCTTCC
	Mar_5	188223	116484	6880	25	2,594	0,5353	CAACCTCA	TATCCTCC
	May2_7	143438	76718	53025	26	1,21	0,1289	CAACCTCA	AACACCGT
	May29_7	87050	32700	19614	26	2,5	0,4684	CAACCTCA	TTACCGCT
	Jun_7	121635	45534	28964	26	2,284	0,3776	CAACCTCA	TGAGATGC
	Aug6_7	113860	41923	29158	27	2,694	0,5476	CAACCTCA	GTGCAACT
	Aug28_7	125613	38114	27369	27	2,685	0,5431	CAACCTCA	TGAGCCTA
	Oc2_7	165231	74945	42161	27	2,288	0,3652	CAACCTCA	ATGGAGGT
	Oc30_7	110619	44863	33462	27	2,169	0,3242	CAACCTCA	CTGAGTCT
	No_7	98597	30472	19070	26	2,605	0,5206	CAACCTCA	GAGGTGAA
Metalimnion water column	Mar_10	179609	90856	16944	25	1,761	0,2326	TGCTTGTC	CGTGATAC
	May2_10	130479	63282	12305	24	2,101	0,3405	TGCTTGTC	CTTCTTCC
	May29_10	156049	63943	38722	25	2,231	0,3723	TGCTTGTC	TATCCTCC
	Jun_10	142750	63870	32767	26	2,236	0,3598	TGCTTGTC	AACACCGT
	Aug6_10	123174	47865	32423	27	2,308	0,3723	TGCTTGTC	TTACCGCT
	Aug28_10	137861	66836	50276	26	1,21	0,129	TGCTTGTC	TGAGATGC
	Oc2_10	120789	70191	60084	27	1,149	0,1169	TGCTTGTC	GTGCAACT
	Oc30_10	133799	49913	37460	27	2,126	0,3105	TGCTTGTC	TGAGCCTA
	No_10	142473	51925	30701	27	2,597	0,497	TGCTTGTC	ATGGAGGT
	May2_15	81787	46493	2269	20	2,568	0,652	TCGTCGCTCG	CTTCTTCC
	May29_15	80368	40667	4737	22	2,47	0,5374	TCGTCGCTCG	TATCCTCC
	Jun_15	41918	18060	16238	24	2,209	0,3795	TCGTCGCTCG	AACACCGT
	Aug28_15	42116	18868	17440	27	2,311	0,3735	TCGTCGCTCG	TGAGATGC
	Oc2_15	51271	20196	11927	27	2,852	0,6417	TCGTCGCTCG	GTGCAACT
	Oc30_15	50931	24740	21906	27	1,738	0,2105	TCGTCGCTCG	TGAGCCTA
	No_15	48673	22522	14514	27	2,884	0,6626	TCGTCGCTCG	ATGGAGGT
Hypolimnion Water column	Mar_20	95758	46951	6179	22	2,047	0,352	TCGTCGCTCG	CGTGATAC
	Ja45	171550	91611	34366	26	2,457	0,4487	AGACGCACTC	CGTGATAC
	Fe45	114796	48626	9228	25	2,476	0,4756	AGACGCACTC	CTTCTTCC
	Mar_45	221091	101049	10111	26	2,639	0,5384	AGACGCACTC	TATCCTCC
	May2_45	153557	88720	13370	27	2,708	0,5553	AGACGCACTC	AACACCGT
	May29_45	156154	95642	15194	27	2,841	0,6345	AGACGCACTC	TTACCGCT
	Jun_45	177970	45534	37373	27	2,426	0,4188	AGACGCACTC	TGAGATGC
	Aug6_45	80692	36232	19745	27	2,084	0,2975	AGACGCACTC	GTGCAACT
	Aug28_45	129908	52656	39619	27	2,439	0,4245	AGACGCACTC	TGAGCCTA
	Oc2_45	202697	110256	56113	27	2,625	0,5114	AGACGCACTC	ATGGAGGT
	Oc30_45	109925	58519	42235	27	1,985	0,2696	AGACGCACTC	CTGAGTCT
	No_45	116083	58165	29652	27	2,126	0,3103	AGACGCACTC	GAGGTGAA
Metalimnion Sediment Trap	ST04M	148116	96606	25447	24	2,669	0,6011	GGTAGTTCT	CTGAGTCT
	ST05M	103171	76608	6266	21	2,754	0,7477	GGTAGTTCT	GAGGTGAA
	ST06M	103612	62935	36315	21	1,095	0,1423	GGTAGTTCT	GGCATGTA
	ST07M	71344	54145	52049	24	0,9098	0,1035	CGTAAGTC	CTGAGTCT
	ST08M	87695	41455	22985	25	2,15	0,3435	CGTAAGTC	GAGGTGAA
	ST09M	121584	65137	52867	26	2,444	0,443	CGTAAGTC	GGCATGTA
	ST10M	83235	39122	29311	22	1,779	0,2692	AACTGTCC	GAGGTGAA
	ST11M	394735	157394	107948	26	1,768	0,2253	AACTGTCC	GGCATGTA
Hypolimnion Sediment Trap	ST04H	131181	104465	8796	25	2,868	0,704	TCACGTACTA	GAGGTGAA
	ST05H	117673	85782	16330	25	2,871	0,706	TCACGTACTA	GGCATGTA
	ST06H	70692	47525	26943	26	1,062	0,1112	CGCATAGA	GTGCAACT
	ST07H	141180	101235	76740	27	0,8603	0,08755	CGCATAGA	TGAGCCTA
	ST08H	62645	35007	25681	25	1,648	0,2079	CGCATAGA	ATGGAGGT
	ST09H	116154	63122	46134	25	1,87	0,2595	CGCATAGA	CTGAGTCT
	ST10H	77117	32037	29331	24	2,429	0,4727	CGCATAGA	GAGGTGAA
	ST11H	115038	49838	22808	21	1,996	0,3503	CGCATAGA	GGCATGTA
Sed	Sed	65357	35215	10585	23	2,046	0,3365	TCCTGGTA	GTGCAACT

Table C.2: Total sulphide measurements from water column samples.

Date	Water Depth [m]	Sample ID	Observation	H2S_µmolL-1
30.10.2019	54	54	filtered	2
30.10.2019	55	55a	filtered	7,9
30.10.2019	55	55b	filtered	5,2
30.10.2019	57	57	filtered	33,3
30.10.2019	59,5	59,5	filtered	44,8
30.10.2019	60,8	60,8	filtered	42,5
28.11.2019	53	53	filtered	11
28.11.2019	55	55	filtered	13,7
28.11.2019	57	57	filtered	9,7
28.11.2019	59	59	filtered	34

Table C.3: Nitrate measurements from water column samples. NA = not ascertained.

SampleID	NO_3^-
WMay2_3	0,57
WMay29_3	0,14
WJu27_3	0,19
WAug6_3	*NA*
WAug28_3	*NA*
WOc2_3	*NA*
WOc30_3	*NA*
WNo28_3	0,30
WJa30_5	2,02
WFe24_5	1,81
WMar28_5	1,40
WMay2_7	1,01
WMay29_7	1,04
WJu27_7	1,52
WAug6_7	*NA*
WAug28_7	*NA*
WOc2_7	*NA*
WOc30_7	*NA*
WNo28_7	0,19
WMar28_10	1,38
WMay2_10	1,26
WMay29_10	2,51
WJu27_10	1,94
WAug6_10	1,71

WAug28_10	1,08
WOc2_10	0,47
WOc30_10	*NA*
WNo28_10	0,20
WMay2_15	1,64
WMay29_15	1,85
WJu27_15	2,07
WAug28_15	2,04
WOc2_15	2,31
WOc30_15	2,24
WNov28_15	2,00
WMar28_20	2,16
WAug6_20	2,14
WJa30_45	1,96
WFe24_45	1,74
WMar28_45	1,71
WMay2_45	1,85
WMay29_45	2,02
WJu27_45	1,96
WAug6_45	2,11
WAug28_45	1,73
WOc2_45	2,04
WOc30_45	0,90
WNo28_45	0,75

Table C.4: ANOVA test for equal means on species richness from sediments and water column ($p < 0.05$; Figure 4). A subsequent Tukey's pairwise test showed hypolimnion sediment trap cyanobacteria communities to significantly differ to the communities from the epi-, meta and hypolimnion communities of the water column. Tukey's Q below the diagonal and P-values above the diagonal. Significant P-values are in bold. Shapiro Wilk: 0.9915, p_normal:0.9447. Where 'W' indicates water column samples from the from the epi-, meta- and hypolimnion, respectively. The 'ST' indicates sediment trap material from the meta- and hypolimnion, respectively. 'Sed' represents the surface sediment samples.

ANOVA Test for equal means across sample types					
	Sum of sqrs	df	Mean square	F	p (same)
Between groups:	1007.74	4	251.935	6,133	0.006964
Within groups:	3279.15	58	64.2957	Permutation p (n=99999)	
Total:	4736.69	62	0.00627		

Tukey's pairwise	W_Epi	W_Meta	W_Hypo	ST_Meta	ST_Hypo
W_Epi		0.9989	0.9982	0.2364	**0.03609**
W_Meta	0.3772		1	0.2609	**0.04405**
W_Hypo	0.4292	0.03314		0.1508	**0.01942**
ST_Meta	2.962	2.884	3.293		0.9518
ST_Hypo	4.165	3.927	4.496	1.014	

Table C.5: Similarity percentage (SIMPER) test on the cyanobacteria ASVs among the different sample types. Only ASVs with > 1% relative abundance in the sample types were used in the for the test.

Taxon	ASV_ID	Av. sim	Contrib. %	Cumulative %	Mean Water	Mean TrapM	Mean TrapH	Mean Sed
Aphanizomenon sp.	ASV_0004	4.427	9,34	9.34	1.01	3.64	4	5.04
Cyanobium sp.	ASV_0008	3.203	6.758	16.1	2.72	0.852	0.483	0.558
Planktothrix sp.	ASV_0006	2.526	5.328	21.43	2.51	0.586	0.752	0.541
Synechococcus sp.	ASV_0007	2.374	5.008	26.43	3.11	1.98	1.51	1.01
Cyanobium sp.	ASV_0005	2.258	4.765	31.2	2.37	2.02	1.89	1.61
Cyanobium sp.	ASV_0013	2.222	4.689	35.89	2.4	0.865	0.747	0.74
Snowella sp.	ASV_0016	2.219	4.681	40.57	0.906	1.88	2.5	1.02
Cyanobium sp.	ASV_0010	2.151	4.538	45.11	1.77	2.42	2.22	1.9
Cyanobium sp.	ASV_0012	1.969	4.154	49.26	1.42	2.27	1.92	1.65
Cyanobium sp.	ASV_0015	1.948	4.109	53.37	2.12	1.1	0.896	0.68
Cyanobium sp.	ASV_0014	1.898	4.004	57.37	1.4	1.3	2.41	1.12
Cyanobium sp.	ASV_0019	1.83	3.861	61.24	1.77	0.426	0.445	0
Synechococcus sp.	ASV_0021	1.662	3.507	64.74	1.66	0.323	0.456	0.599
Cyanobium sp.	ASV_0031	1.553	3.277	68.02	1.6	0.523	0.499	0
Snowella sp.	ASV_0022	1.553	3.276	71.3	0.786	1.35	1.64	0.476
Cyanobium sp.	ASV_0020	1.446	3.051	74.35	1.09	1.79	1.67	3.99
Aphanizomenon sp.	ASV_0035	1.433	3.024	77.37	0.478	1.29	1.39	2
Cyanobium sp.	ASV_0053	1.314	2.772	80.14	1.07	0.0541	0.0572	0.292
Cyanobium sp.	ASV_0049	1.258	2.653	82.8	0.434	1.12	1.23	0.987
Planktothrix sp.	ASV_0050	1.158	2.443	85.24	0.903	0	0.0651	0
Microcystis sp.	ASV_0009	1.077	2.272	87.51	0.724	0.644	1.02	1.59
Cyanobium sp.	ASV_0030	1.06	2.236	89.75	1.47	0.909	0.78	0.364
Cyanobium sp.	ASV_0028	1.049	2.213	91.96	1.04	0.863	1.26	1.15
Cyanobium sp.	ASV_0056	0.9107	1.921	93.88	0.941	0.236	0.379	0
Cyanobium sp.	ASV_0054	0.8186	1.727	95.61	0.699	0.64	0.811	0.466
Microcystis sp.	ASV_0041	0.7399	1.561	97.17	0.647	0.961	1.03	0.659

Table C.6: Rank-based Spearman correlation coefficients of the most abundant cyanobacteria ASVs, total cyanobacteria community composition, cyanobacteria 16S rRNA-ITS gene abundance with internal physicochemical parameters in Lake Tiefer See. Values in bold are significant at $p < 0.05$ with Bonferroni *p*-value correction. Spearman correlation coefficients (R_S) values highlighted red show a negative correlation, whereas RS values highlighted blue show a positive correlation.

	Shannon	CCC	16S rRNA	Turbidity	Temp	pH	Chl-a	DO	NO_3-	TDP
ASV0004_*Aphanizomenon*	0.24007	0.19907	0.049033	**0.39552**	0.12614	-0.044474	0.065278	-0.14404	-0.24663	0.17125
ASV0005_*Cyanobium*	0.1693	**0.42775**	0.047298	-0.10618	0.1036	**-0.35848**	**-0.63782**	**-0.63065**	-0.016639	0.31506
ASV0006_*Planktothrix*	0.022895	0.12569	0.21751	0.029515	0.12978	-0.26648	-0.23656	**-0.31275**	0.10059	0.041804
ASV0007_*Synechococcus*	0.047988	**0.53885**	0.17004	0.24482	**0.33239**	0.25416	-0.0045136	0.065279	-0.20578	-0.18739
ASV0008_*Cyanobium*	-0.16536	-0.049435	-0.059497	-0.064425	-0.11031	**0.46821**	**0.56957**	**0.68536**	-0.092004	-0.21856
ASV0009_*Microcystis*	0.21256	0.095783	-0.064783	-0.025959	-0.09784	-0.017674	0.063159	-0.010528	0.078191	-0.031918
ASV0014_*Cyanobium*	**0.37755**	0.20849	**-0.29517**	**0.30681**	-0.10762	**-0.51783**	**-0.55132**	**-0.64223**	0.30912	**0.49326**
ASV0016_*Snowella*	**0.37502**	**0.3778**	-0.010639	0.28227	0.21315	-0.11515	-0.23475	**-0.38262**	-0.0049261	0.10764
Shannon diversity		**-0.3262**	-0.2148	-0.20678	-0.14929	-0.088712	-0.19854	-0.072275	0.17765	0.2941
CCC	-0.3262		0.24856	**0.33644**	**0.49991**	0.09461	-0.07326	-0.24741	**-0.36219**	-0.15182
16S rRNA-ITS abundance	-0.2148	0.24856		0.085416	**0.74694**	**0.32438**	**0.32424**	0.031744	**-0.36927**	**-0.46901**

Table C.7: The significant explanatory parameters used in the Spearman correlation analysis. The significance of the environmental variables was tested by 999 Monte Carlo permutations and were selected by forward selection (Adjusted R^2 = 0.34). AIC = Akaike information criterion.

Explanatory variable	**AIC**	**Pseudo-*F***	***P***
DO	159.73	8.77	0.001
Turbidity	157.26	4.92	0.002
TDP	154.76	4.56	0.002
pH	153.98	4.42	0.005
NO_3-	152.98	3.56	0.004
Temperature	150.95	3.07	0.008

Appendix D Supplementary Material for Chapter 5

Supplementary Information – Methods. DNA extraction for shotgun sequencing.

The DNA for shotgun (metagenomic) sequencing was extracted using DNeasy PowerMax Soil DNA and the DNeasy Power Soil DNA 100 DNA isolation kits (Qiagen) from 12 sediment samples distributed from top to bottom of the long core (Supplementary Table 2, Supplementary Methods). For this, total DNA was extracted from the 12 samples weighing between 0.7 – 2.6 g wet sediment. Two DNA extraction kits were used in the paleogenetic laboratories at Alfred Wegener Institute (AWI) Potsdam inside a UV-cleaner box. To avoid contamination, the solutions C2, C3, and C4, which were only used on the second day of extraction, were prepared before working with the sediment samples. The extraction protocols were modified as previously described(Epp et al., 2019). Briefly, prior to adding the sediment sample, solution C1, 400 µL of proteinase K (2 mg ml^{-1}) and 100 µL of Dithiothreitol (DTT) (5M) were added and vortexed for 10 min. Afterwards, the tubes containing the samples and the control were placed into a rotating oven set to 56 °C overnight. The extracted DNA was eluted with 2 mL of provided elution buffer. Two extractions were performed for each depth and the extracts of the same sediment sample were pooled for the DNA concentration and purification steps. The elution of the extracts was done with 100 µL of the provided elution buffer. The DNA concentration was determined using a Qubit dsDNA broad range assay kit and the Qubit R 2.0 Fluorometer. Every sample was measured twice and the average was calculated. Such concentration analyses were conducted before concentrating and purifying the extracted DNA as well as afterwards. To concentrate and purify the sedaDNA extracts, the GeneJET PCR purification kit (ThermoFisher) was used following the manufacturer's instructions. The samples extracted from the same depth were pooled and concentrated together. The elution volume varied from 50 µL to 100 µL depending on the previously measured DNA concentration.

Supplementary Information – Results. Analysis of cyanobacterial and cyanopeptolin-producing *Planktothrix* DNA preservation

To assess potential post-depositional DNA fragmentation (see "Methods" section in Manuscript), we compared the cyanobacterial composition of the long (using long fragment primers ~1500 bp) amplicons with short to medium amplicons (qPCR amplification

products ~ 350 bp) from three sediment depths 210, 410 and 985 cm. The analysis of cyanobacterial DNA preservation resulted in successful short fragment amplicons for the sediment depths 210 (20 clones; 813 cal. a BP), 410 (19 clones; 2385 cal. a BP), and 985 cm (19 clones; 10,780 cal. a BP; Supplementary Table 3). The picocyanobacteria (*Synechococcus* and *Cyanobium*) made up the majority of the sequenced clones with mean sequence similarity ranging between 91 – 100%. Long fragment amplicons were only obtained from sediments dated to 813 cal. a BP (20 clones) and 2385 cal. a BP (19 clones). The composition of cyanobacterial assemblages was similar (*Synechococcus*) regardless of amplicon length in the sample dated to 813 cal. a BP. The long amplicon sequences from 2385 cal. a BP were dominated by *Leptolyngbya* and *Pseudanabaena*. These results confirmed that long and short cyanobacterial DNA fragments were well preserved along the entire sediment core (11 m).

To verify the preservation of cyanopeptolin-producing *Planktothrix* subpopulations in sediments, clone libraries from their qPCR amplification products from the sediment depths 210 and 1015 cm were sequenced. A total of 45 clone sequences were obtained from the cyanopeptolin targets (37-*oci*B161 and 8-*oci*B247). The sequences revealed a high similarity (>97%) to strains isolated from various Norwegian Lakes. Most of these sequences were retrieved from the sediment depth 210 cm (33 sequences; 840 cal. a BP), whereas only 12 sequences were retrieved from the sediment depth 1015 cm (11.058 cal. a BP). This is presumably due to low numbers of the *Planktothrix* chemotype and possible DNA degradation in this sample.

Table D.1: Sediment sample characteristics: Composite depth, SedaDNA concentration, chronology in calibrated age before present and common/before common era (BC/BCE), and total organic carbon (TOC), sediment quantity, sedaDNA normalized to gram sediment and TOC

Sample ID	Sediment composite depth (cm)	DNA conc. (ng/µl)	Age cal. a BP (= before 1950)	Age CE/BCE	TOC	Sed. Qty (g)	µg DNA/g Sed.	µg DNA/TOC
H1_1-2	1	37.1	-50	2000	11	1.1	3.4	0.33
H1_2-3	2	34.6	-45	1995	9	1.0	3.4	0.38
H1_3-4	3	32.5	-40	1990	9	0.7	4.4	0.34
H1_4-5	4	28.5	-36	1986	10	1.0	2.8	0.28
H1_5-6	5	33.2	-33	1983	8	1.1	3.0	0.41
H1_6-7	6	20.7	-30	1980	10	1.0	2.0	0.22
H1_7-8	7	22.8	-27	1977	8	1.0	2.2	0.28
H1_8-9	8	18.8	-24	1974	11	1.0	1.9	0.18
H1_9-10	9	21.8	-20	1970	9	1.2	1.9	0.23
H1_10-11	10	14.8	-15	1965	9	1.0	1.4	0.17
H1_11-12	11	20.6	-13	1963	8	1.1	1.9	0.27
H1_15-16	15	15.6	-2	1952	8	1.0	1.6	0.19
H1_20-21	20	16.1	10	1940	8	1.0	1.6	0.21
H1_25-26	25	12.5	26	1924	8	1.1	1.2	0.15
H1_30-31	30	8.54	30	1920	9	1.0	0.8	0.10
H1_35-36	35	7.4	60	1890	11	1.0	0.7	0.07
H1_40-41	40	3.7	80	1870	9	1.0	0.4	0.04
H1_45-46	45	8.48	95	1855	9	1.0	0.8	0.10
H1_50-51	50	7.13	111	1840	8	1.1	0.7	0.08
H1_55-56	55	5.97	121	1830	8	1.0	0.6	0.07
H1_60-61	60	8.98	141	1810	8	1.0	0.9	0.11
H1_65-66	65	4.9	156	1792	7	1.0	0.5	0.07
K1_28-29	128	9.83	534	1416	6	0.8	1.3	0.15
K1_38-39	138	8.53	565	1385	7	0.7	1.1	0.12
K1_48-49	148	8.43	595	1355	7	0.7	1.1	0.12
K1_58-59	158	11.2	626	1325	9	0.8	1.5	0.13
K1_68-69	168	14.8	656	1294	4	1.0	1.5	0.36
K1_78-79	178	17.2	686	1264	7	1.0	1.7	0.26
K1_88-89	188	14.4	717	1233	5	1.0	1.4	0.29
H2_10-11	210	29	813	1137	10	0.8	3.9	0.29
H2_15-16	215	15.7	847	1103	14	0.8	2.1	0.11
H2_20-21	220	12.1	880	1070	14	0.7	1.6	0.08
H2_40-41	240	10.9	1014	936	16	0.8	1.5	0.07
H2_60-61	260	10.9	1147	803	19	0.7	1.5	0.06
H2_80-81	280	15	1281	669	15	0.7	2.0	0.10
H2_95-96	295	16	1381	569	18	1.0	1.6	0.09
H2_105-106	305	14.5	1448	502	16	1.0	1.4	0.09

Sample ID	Sediment composite depth (cm)	DNA conc. (ng/µl)	Age cal. a BP (= before 1950)	Age CE/BCE	TOC	Sed. Qty (g)	µg DNA/g Sed.	µg DNA/TOC
H2_120-121	320	8.96	1548	402	17	1.0	0.9	0.05
H2_125-126	325	15.8	1582	368	16	1.0	1.6	0.10
H2_130-131	330	15.9	1615	335	17	1.0	1.6	0.09
H2_135-136	335	18.3	1649	301	16	1.0	1.8	0.12
H2_140-141	340	12.5	1682	268	15	1.0	1.3	0.08
H2_145-146	345	9.49	1716	235	16	1.0	0.9	0.06
H2_150-151	350	8.55	1749	201	14	1.0	0.9	0.06
H2_175-176	375	16.6	1897	54	19	1.0	1.7	0.09
H2_185-186	385	15	1960	-10	13	1.0	1.5	0.11
K2_108-109	408	13.9	2100	-150	17	1.0	1.4	0.08
H3_10-11	410	7.45	2385	-440	17	1.0	0.8	0.04
H3_35-36	435	4.61	2610	-660	15	1.0	0.5	0.03
H3_40-41	440	6.08	2662	-710	16	1.0	0.6	0.04
H3_55-56	455	4.74	2798	-850	11	1.0	0.5	0.04
H3_75-76	470	8.12	2976	-1050	15	1.0	0.8	0.05
H3_95-96	495	4.38	3194	-1260	15	1.0	0.4	0.03
H3_110-111	510	2.07	3358	-1420	6	1.1	0.2	0.04
H3_125-126	525	2.85	3522	-1580	6	0.9	0.3	0.05
H3_140-141	540	1.65	3685	-1750	4	1.0	0.2	0.04
H3_165-166	565	5.55	3958	-2020	17	1.0	0.5	0.03
H3_175-176	575	9.44	4067	-2120	15	0.9	1.0	0.06
H4_50-51	650	6.54	5070	-3120	18	1.1	0.6	0.04
H4_75-76	675	3.41	5260	-3310	14	1.0	0.3	0.03
H4_100-101	700	4.12	5450	-3500	14	1.0	0.4	0.03
H4_125-126	725	3.84	5690	-3740	20	1.0	0.4	0.02
H4_150-151	750	2.06	6183	-4080	16	1.0	0.2	0.01
H4_175-176	775	2.72	6582	-4400	22	1.0	0.3	0.01
H4_190-191	790	1.16	6840	-4590	19	1.0	0.1	0.01
H5_20-21	820	0.75	7531	-5450	20	0.9	0.1	0.00
H5_45-46	845	0.8	7997	-6060	19	1.0	0.1	0.00
H5_70-71	870	1	8471	-6550	15	1.0	0.1	0.01
H5_95-96	895	1.19	9016	-7110	11	1.0	0.1	0.01
H5_120-121	920	0.902	9385	-7520	16	1.0	0.1	0.01
H5_145-146	945	0.657	9824	-7980	11	1.0	0.1	0.01
H5_170-171	970	0.874	10431	-8530	12	1.0	0.1	0.01
H5_185-186	985	1.16	10824	-8830	12	1.0	0.1	0.01
H6_15-16	1015	0.903	11058	-9270	1	1.0	0.1	0.06

Table D.2: Total cyanobacteria, Planktothrix and cyanopeptolin-producing Planktothrix abundance determined via qPCR and shot gun metagenome sequencing data

Sample ID	Total Cyanobacteria	Total *Planktothrix*	Cyanopeptolin *Planktothrix* qPCR	
	16S rRNA-ITS	TNA qPCR	*oci*B161 bp	*oci*B247 bp
H1_1-2	8.26E+04		2.33E+00	1.57E+01
H1_2-3	2.09E+05		3.98E+00	1.24E+01
H1_3-4	1.45E+05	3.22E+01	4.41E+00	1.04E+01
H1_4-5	8.52E+04		3.51E+00	2.27E+01
H1_5-6	9.26E+04		2.36E+00	1.90E+01
H1_6-7	7.49E+04	1.36E+02	3.76E+00	2.31E+01
H1_7-8	7.71E+04	7.84E+01	4.07E+00	3.59E+00
H1_8-9	7.43E+04		4.71E+00	1.16E+01
H1_9-10	6.66E+04	2.99E+01	7.14E+00	7.33E+00
H1_10-11	7.78E+04		4.49E+00	6.97E+00
H1_11-12	6.19E+04		4.71E+00	8.68E+00
H1_15-16	9.42E+04		5.06E+00	1.04E+01
H1_20-21	4.82E+04		5.06E+00	1.30E+01
H1_25-26	6.47E+04		4.18E+00	8.38E-01
H1_30-31	2.40E+04		1.18E+01	1.44E+01
H1_35-36	1.44E+04		6.32E+00	1.20E+01
H1_40-41	1.85E+04		1.71E+01	7.14E+00
H1_45-46	2.32E+04		3.65E+00	2.21E+00
H1_50-51	2.14E+04	1.15E+02	5.38E+00	2.74E+00
H1_55-56	1.99E+04		3.68E+00	
H1_60-61	8.96E+03		7.14E+00	3.64E+00
H1_65-66	1.13E+04		4.43E+01	7.33E+00
K1_28-29	2.63E+04		3.93E+00	1.74E+01
K1_38-39	1.32E+04		6.01E+00	2.20E+01
K1_48-49	2.76E+04		7.90E+00	2.67E+01
K1_58-59	3.13E+04		4.27E+00	1.84E+01
K1_68-69	2.77E+04		9.40E+00	4.16E+01
K1_78-79	1.62E+04		2.00E+01	6.82E+01
K1_88-89	2.38E+04	5.79E+02	1.59E+01	8.16E+01
H2_10-11	8.37E+04		1.36E+02	1.03E+02
H2_15-16	3.13E+03		4.55E+00	2.47E+00
H2_20-21	6.14E+03		9.84E+00	3.01E+01
H2_40-41	9.14E+03		1.26E+01	2.99E+01
H2_60-61	1.20E+04	2.34E+02	2.65E+00	1.16E+01
H2_80-81	9.50E+03	7.28E+02	7.04E+00	1.77E+01
H2_95-96	1.69E+04		2.10E+00	7.29E+00
H2_105-106	9.87E+03		2.19E+00	9.89E+00
H2_120-121	8.25E+03	9.72E+02	5.63E+00	1.46E+01

Sample ID	Total Cyanobacteria	Total *Planktothrix*	Cyanopeptolin-producing *Planktothrix* qPCR	
	16S rRNA-ITS	**TNA qPCR**	***oci*B161 bp**	***oci*B247 bp**
H2_125-126	1.44E+03	9.82E+03	8.07E+02	6.71E+02
H2_130-131	5.80E+02	4.44E+03	6.50E+01	8.78E+01
H2_135-136	1.45E+05	5.82E+04	2.60E+03	8.33E+02
H2_140-141	5.82E+04	1.41E+04	1.05E+03	4.96E+02
H2_145-146	2.37E+03	2.73E+02	5.56E+00	1.03E+01
H2_150-151	2.18E+04	6.64E+02	8.23E+00	2.60E+01
H2_175-176	1.66E+04	3.81E+03	1.39E+02	1.13E+02
H2_185-186	1.59E+04	1.07E+03	5.47E+01	3.65E+01
K2_108-109	2.89E+04	3.49E+02	7.14E+00	3.80E+01
H3_10-11	1.33E+04		3.09E+00	1.80E+01
H3_35-36	6.50E+03		3.31E+00	1.64E+01
H3_40-41	7.85E+03		1.81E+00	9.84E+00
H3_55-56	3.70E+03		4.24E+00	1.02E+01
H3_75-76	2.59E+03		1.12E+00	5.83E+00
H3_95-96	1.57E+03		4.55E+00	9.58E+00
H3_110-111	1.40E+03		2.89E+00	1.27E+01
H3_125-126	3.18E+03		1.30E+00	8.19E+00
H3_140-141	2.21E+03		2.71E+00	
H3_165-166	5.42E+02		2.10E+00	
H3_175-176	1.23E+03			
H4_50-51	6.07E+02			
H4_75-76	3.70E+02		2.00E+00	2.87E+00
H4_100-101	3.55E+02		4.55E+00	2.78E+00
H4_125-126	7.16E+02			
H4_150-151			1.30E+00	
H4_175-176	8.73E+02			
H4_190-191				
H5_20-21	7.07E+02		1.35E+01	
H5_45-46	1.17E+02			4.50E+01
H5_70-71	1.37E+02		1.27E+00	1.23E+01
H5_95-96			1.12E+00	1.30E+01
H5_120-121	5.24E+02			
H5_145-146			1.30E+00	1.35E+01
H5_170-171				1.72E+01
H5_185-186	8.07E+02		2.07E+01	
H6_15-16	2.22E+02		6.47E+02	

Table D.2 cont.: Cyanobacteria amplicon sequence data, cyanobacteria ASV (taxonomic) richness and shotgun (metagenome) sequencing data.

Sample ID	Amplicon DADA2 Pipeline sequence data			Cyanobacteria ASV richness	Shotgun sequencing	
	Input	Processed	final reads		DNA conc. (µg)	Read counts
H1_1-2	190740	72119	50860	169		
H1_2-3	193995	76383	54106	149		
H1_3-4	177211	69737	49975	142		
H1_4-5	203517	75436	55116	129	3.5	29,652,699
H1_5-6	149892	52269	36940	122		
H1_6-7	210433	76204	55287	124		
H1_7-8	143140	50326	37929	105		
H1_8-9	161329	58610	43274	102		
H1_9-10	197884	60059	53853	113	6.7	32,992,166
H1_10-11	213174	81189	63998	99		
H1_11-12	113461	41063	30857	66		
H1_15-16	110832	41386	31665	76		
H1_20-21	167987	62149	50238	84	6.7	46,135,529
H1_25-26	178452	66129	49618	77		
H1_30-31	127694	44684	35867	53		
H1_35-36	146271	51423	41399	46		
H1_40-41	123983	41705	34808	42		
H1_45-46	145207	52076	41894	51		
H1_50-51	93337	34445	29000	45		
H1_55-56	96120	35334	29184	49		
H1_60-61	124951	48854	42838	54		
H1_65-66	126327	50682	45091	47		
K1_28-29	43546	17362	14639	38		43,159,479
K1_38-39	41772	17272	14542	31		
K1_48-49	57033	23457	20373	38		
K1_58-59	52654	22097	19064	37		
K1_68-69	269639	110322	95607	51		
K1_78-79	149955	63433	54722	41		
K1_88-89	181172	75516	64565	49		
H2_10-11	64246	26137	22181	49	17.1	35,268,604
H2_15-16	69454	29407	25348	33		
H2_20-21	119596	51931	45533	47		30,419,097
H2_40-41	131166	56482	49522	63		
H2_60-61	98812	41745	34714	76	2.8	36,115,008
H2_80-81	104427	42508	36288	75	4.5	33,803926
H2_95-96	118718	53821	46285	61		
H2_105-106	140183	67023	57810	46		
H2_120-121	133572	63326	58743	36		
H2_125-126	127681	58406	50711	65		

Sample ID	Amplicon DADA2 Pipeline sequence data			Cyanobacteria ASV richness	Shotgun sequencing	
	Input	Processed	final reads		DNA conc. (µg)	Raw read counts
H2_130-131	148675	65925	59513	63		
H2_135-136	173727	77744	69317	90		
H2_140-141	92200	40701	35855	66		
H2_145-146	40873	18993	17056	33		
H2_150-151	61687	28363	24760	51		
H2_175-176	83830	36093	31879	59	3.4	48,549,277
H2_185-186	50503	21905	18836	51		
K2_108-109	226915	99393	86999	64		
H3_10-11	59084	28927	26347	31		
H3_35-36	45463	21783	20040	16		
H3_40-41	71077	34379	30787	23		29,498,111
H3_55-56	127106	61546	56644	17		
H3_75-76	150072	71055	63173	22		
H3_95-96	166682	81369	75546	25		
H3_110-111	171428	82996	78000	22		
H3_125-126	93537	43937	39660	14	1.2	22,561,531
H3_140-141	88424	42003	38569	14		
H3_165-166	143820	66888	61894	21		
H3_175-176	184536	79270	73718	45		
H4_50-51	168242	71088	65951	40	2.6	7,737,446
H4_75-76	157310	71616	65368	25		
H4_100-101	136266	59377	53738	19		
H4_125-126	179962	78643	72998	19		
H4_150-151	119253	51744	47949	16		
H4_175-176	142164	60129	56130	22		
H4_190-191	144009	67404	64139	14		
H5_20-21	147074	67633	65105	22	8.6	2,087,930
H5_45-46	90106	41205	39805	7		
H5_70-71	84010	38887	36357	10		
H5_95-96	125798	57595	54945	18		
H5_120-121	122113	58852	56323	24		
H5_145-146	99336	47416	45707	18		
H5_170-171	38788	17195	16416	14		
H5_185-186	35024	14926	14542	13		
H6_15-16	36260	16571	15829	14	1.4	114,185

Table D.3: Test results for collinearity in the explanatory variables via variance inflation factor (VIF).

TOC	đ$^{13}C_{OM}$	RecVegOp	Varve Quality	Years/Sample
1.753536	2.262912	2.053130	2.161087	1.872460

Table D.4: To assess potential post-depositional DNA fragmentation (see "Methods" section in Manuscript). we compared the cyanobacterial composition of the long (~ 1500 bp) amplicons with short to medium amplicons (qPCR amplification products ~ 350 bp) from three depths: 210 (H2_10-11), 410 (H3_10-11), and 985 cm (H5_185-186).

Long fragments		Top BLASTn Hit	Perc. Iden.			Top BLASTn Hit	Perc. Iden.
Sample H2_10-11	H2_L_B1	*Synechococcus*	99%	**Sample H3_10-11**	H3_L_A7	No result	
	H2_L_C1	*Synechococcus*	96%		H3_L_A8	*Leptolyngbya*	75%
	H2_L_D1	*Synechococcus*	99%		H3_L_C8	*Leptolyngbya*	74%
	H2_L_G2	*Synechococcus*	95%		H3_L_G7	*Pseudanabaena*	80%
	H2_L_H2	*Synechococcus*	97%		H3_L_H7	*Leptolyngbya*	76%
	H2_L_B3	*Synechococcus*	98%		H3_L_H8	*Pseudanabaena*	78%
	H2_L_F3	*Synechococcus*	98%		H3_L_C9	*Pseudanabaena*	80%
	H2_L_C3	*Synechococcus*	96%		H3_L_D9	*Pseudanabaena*	77%
	H2_L_G3	*Synechococcus*	97%		H3_L_B10	*Spirulina*	74%
	H2_L_D3	*Synechococcus*	98%		H3_L_D10	*Leptolyngbya*	80%
	H2_L_A4	*Synechococcus*	96%		H3_L_E10	*Pseudanabaena*	79%
	H2_L_A5	*Synechococcus*	98%		H3_L_E11	*Pseudanabaena*	79%
	H2_L_B4	*Synechococcus*	98%		H3_L_G11	No result	
	H2_L_B5	*Synechococcus*	99%		H3_L_H11	*Pseudanabaena*	78%
	H2_L_C4	*Synechococcus*	98%		H3_L_A12	No result	
	H2_L_D4	*Synechococcus*	98%		H3_L_E12	No result	
	H2_L_E5	*Synechococcus*	99%		H3_L_F12	*Phormidium*	75%
	H2_L_G6	*Synechococcus*	99%		H3_L_G12	*Pseudanabaena*	77%
	H2_L_H6	*Synechococcus*	99%		H3_L_H12	No result	
		Average	**98%**			**Average**	**77%**

Short Fragments		**Top BLASTn Hit**	**Perc.Iden.**			Top BLASTn Hit	Perc.Iden.
Sample H2_10-11	H2_S_A1	*Synechococcus*	95%	**Sample H3_10-11**	H3_S_A1	*Cyanobium*	89%
	H2_S_A2	*Synechococcus*	94%		H3_S_A2	*Synechococcus*	96%
	H2_S_B1	*Synechococcus*	94%		H3_S_B1	*Synechococcus*	90%
	H2_S_B2	*Synechococcus*	96%		H3_S_B2	*Synechococcus*	88%
	H2_S_C1	*Synechococcus*	100%		H3_S_C1	*Cyanobium*	89%
	H2_S_C2	*Synechococcus*	94%		H3_S_C2	*Cyanobium*	89%
	H2_S_D1	*Synechococcus*	96%		H3_S_D2	*Synechococcus*	96%

	H2_S_D2	*Synechococcus*	96%		H3_S_E2	*Cyanobium*	90%
	H2_S_F1	*Synechococcus*	94%		H3_S_F1	*Cyanobium*	89%
	H2_S_F2	*Synechococcus*	96%		H3_S_F2	*Cyanobium*	89%
	H2_S_A3	*Synechococcus*	96%		H3_S_G1	*Synechococcus*	88%
	H2_S_E3	*Synechococcus*	96%		H3_S_G2	*Nodosilinea*	90%
	H2_S_C3	*Synechococcus*	95%		H3_S_H1	*Synechococcus*	89%
	H2_S_G3	*Synechococcus*	96%		H3_S_H2	*Synechococcus*	87%
	H2_S_D3	*Synechococcus*	94%		H3_S_E3	*Synechococcus*	94%
	H2_S_H3	*Synechococcus*	97%		H3_S_B3	*Synechococcus*	88%
	H2_S_A4	*Synechococcus*	95%		H3_S_F3	*Cyanobium*	89%
	H2_S_A5	*Synechococcus*	94%		H3_S_D3	*Cyanobium*	91%
	H2_S_B4	*Synechococcus*	94%		H3_S_H3	*Cyanobium*	100%
	H2_S_C4	*Cyanobium*	96%			**Average**	**91%**
		Average	**95%**				
		Top BLASTn Hit	**Perc.Iden.**				
Sample H5_185-186	H5_S_B8	*Synechococcus*	95%				
	H5_S_E7	*Synechococcus*	89%				
	H5_S_F7	*Synechococcus*	95%				
	H5_S_F8	*Cyanobium*	97%				
	H5_S_G7	*Cyanobium*	96%				
	H5_S_G8	*Synechococcus*	95%				
	H5_S_H7	*Synechococcus*	96%				
	H5_S_E9	*Synechococcus*	89%				
	H5_S_F9	*Synechococcus*	96%				
	H5_S_C9	*Synechococcus*	95%				
	H5_S_D9	*Synechococcus*	95%				
	H5_S_A10	*Cyanobium*	96%				
	H5_S_E11	*Synechococcus*	95%				
	H5_S_F11	*Synechococcus*	96%				
	H5_S_G10	*Synechococcus*	95%				
	H5_S_G11	*Synechococcus*	95%				
	H5_S_A12	*Synechococcus*	96%				
	H5_S_C12	*Cyanobium*	96%				
	H5_S_D12	*Synechococcus*	96%				
		Average	95%				

Table D.5: Rank-based Spearman correlation of cyanobacteria amplicon sequence variants from high throughput sequencing with lake environmental parameters in Lake Tiefer See. The permutation *p*-values are (values in bold are significant at *p*-values < 0.05) above the diagonal and the corresponding F-values below. Values in Blue show positive while red values show a negative correlation. TOC = Total organic carbon. RecVegOp = reconstructed vegetation openness. DNA concentration normalized to gram sediment (DNA g^{-1} sed.) and TOC (DNA TOC^{-1})

Spearman Correlation	ASV Richness	16S rRNA-ITS	TOC	$\delta^{13}C_{OM}$	RecVeg Op	Varve Quality	Years/Sample	DNA g^{-1} Sed.	DNA TOC^{-1}
ASV Richness		**0.003**	0.1	**0.003**	0.1	**0.003**	**0.003**	**0.003**	**0.003**
16S rRNA-ITS	0.73764		**0.003**	0.2	**0.003**	0.1	**0.003**	**0.003**	**0.003**
TOC	-0.17419	-0.46818		0.057	**0.003**	**0.02**	**0.003**	1	**0.003**
$\delta^{13}C_{OM}$	-0.45875	-0.20421	-0.26256		0.5	**0.003**	0.070634	0.007	0.3
RecVegOp	0.2604	0.49799	-0.59826	0.13629		**0.02**	**0.004**	**0.4**	**0.007**
Varve Quality	0.49581	0.2056	0.26969	-0.7097	-0.35345		0.16061	**0.003**	0.4
Years/Sample	-0.68766	-0.77357	0.48706	0.25032	-0.43326	-0.16479		**0.003**	**0.003**
DNA g^{-1} Sed.	0.86	0.65	-0.16	-0.54	0.39	0.49	-0.66		**0.003**
DNA TOC^{-1}	0.82	0.76	-0.53	-0.37	0.58	0.29	-0.7	0.89	

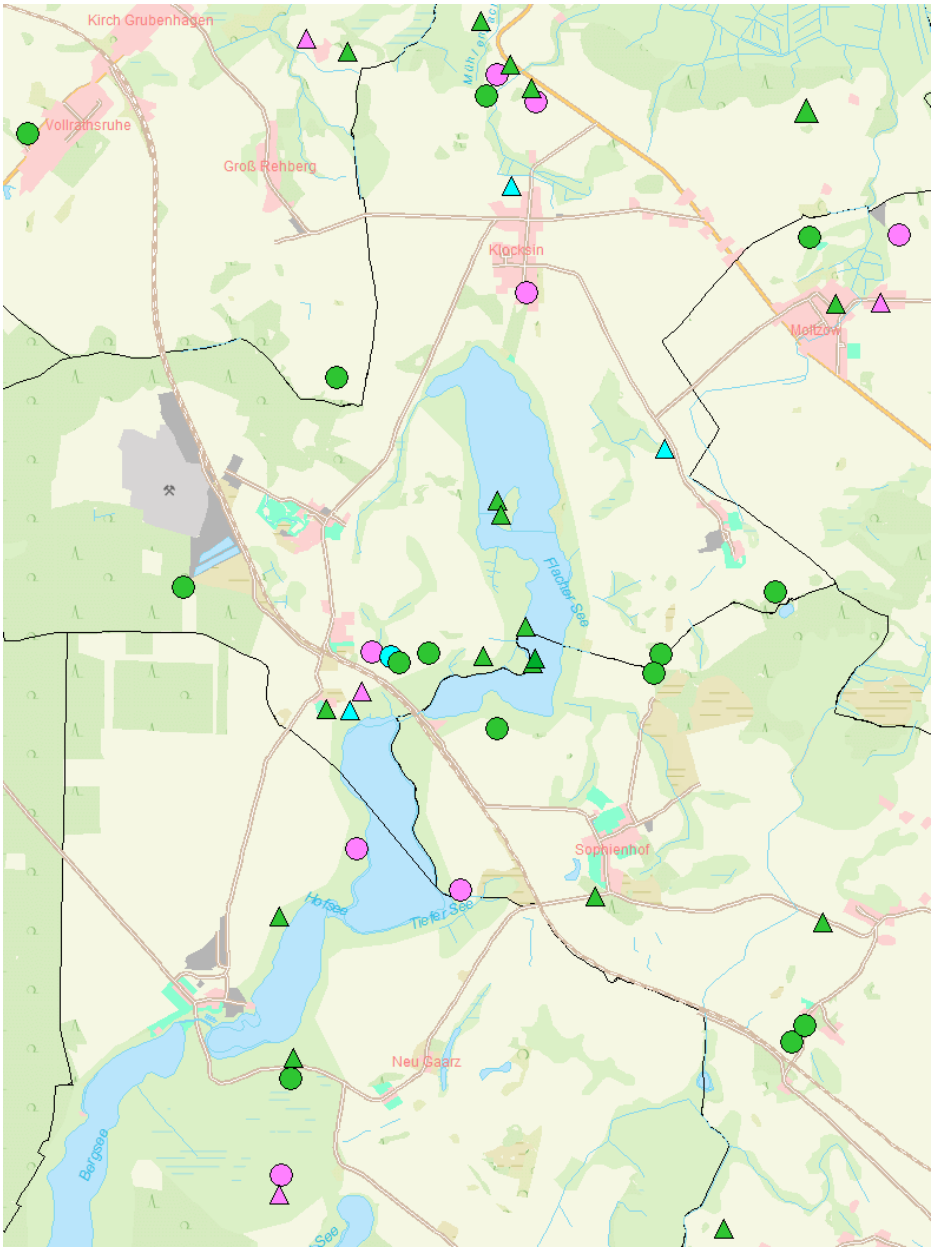

Figure D.1: Mapping of Bronze Age and Iron Age sites of archaeological finds in the vicinity of Lake Tiefer See. Green circles denote burial sites and settlements from the Bronze Age, blue and pink circles denote settlements from the pre-Roman Iron Age (ca. BCE 550 – 0) and the Roman Iron Age Period (ca. CE 0-400), respectively. Triangles represent scattered finds, individual finds, deposits (that is, victim graves) and bowl stones. (Figure source: Archeologist Jens-Peter Schmidt)

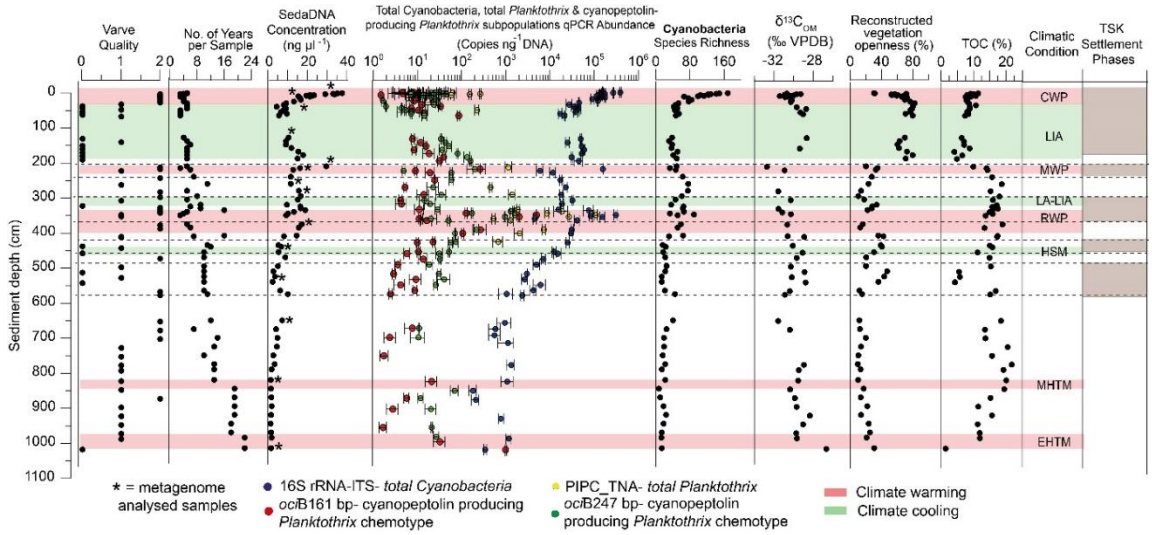

Figure D.2: composite profile (cm) with sedimentological parameters. sedaDNA. cyanobacteria data and. selected lake paleoenvironmental records. Sedimentological analysis: varve quality (VQ; 0 = non-varved, 1 = poorly-, and 2 = well-varved sediment samples) and the number of years in each analyzed sediment sample. Microbiological analysis: sedaDNA concentration. abundances of total cyanobacteria. *Planktothrix*. and cyanopeptolin-producing *Planktothrix* subpopulations (quantified via qPCR where error bars give the standard deviations for three independent amplifications). cyanobacteria species richness from metabarcoding sequencing. Geochemical analysis: TOC content and $\delta^{13}C_{OM}$ values. Pollen-based reconstructed vegetation openness data. Broken black lines demarcate the three significantly different temporal clusters identified by non-metric multidimensional scaling (see Fig. 5.4 in main manuscript). The climatic conditions (warmer periods; red. and cooler periods; light green) are based on Wanner et al. 2015. CWP = current warming period. LIA = Little Ice Age. MWP = Medieval Warm Period. LA-LIA = Lat antique Little Ice Age (Dark Ages). RWP = Roman Warm Period. HSM = Homeric Solar Minimum. MHTM = Mid-Holocene Temperature Maximum. and EHTM = Early Holocene Temperature Maximum

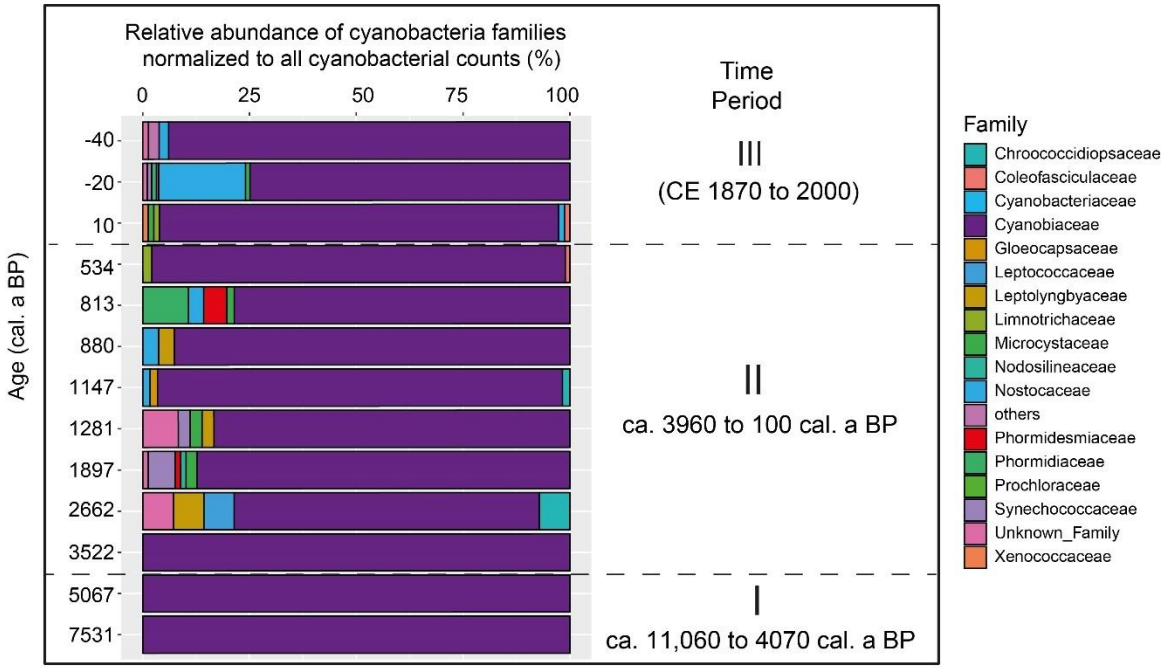

Figure D.3: Taxonomic composition of cyanobacteria communities at family level spanning the last 11,000 years. The relative abundance was normalized by the total read counts of the bacteria domain. All families with relative abundance below 1% were grouped into "others". Broken black lines demarcate the three significantly different temporal clusters identified by non-metric multidimensional scaling (see Fig. 5.4 in main manuscript).

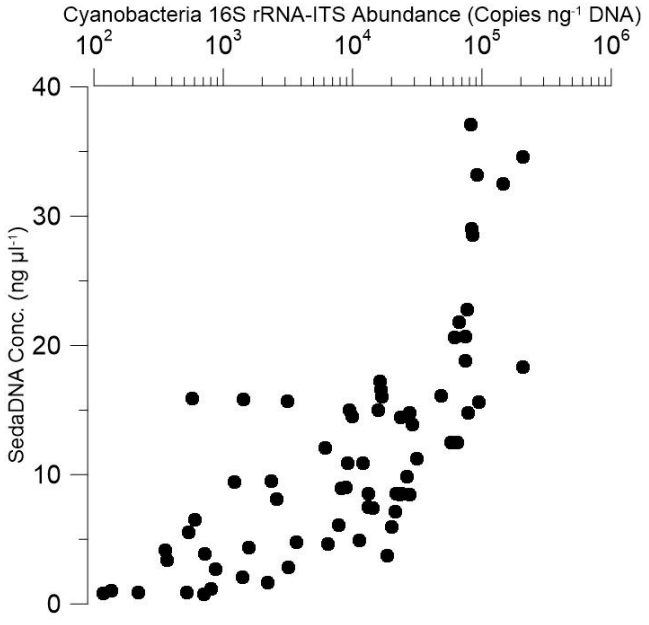

Figure D.4: Plot to test the relationship between DNA extracted from sediments and total cyanobacteria 16S rRNA-ITS copy numbers quantified via qPCR assay.

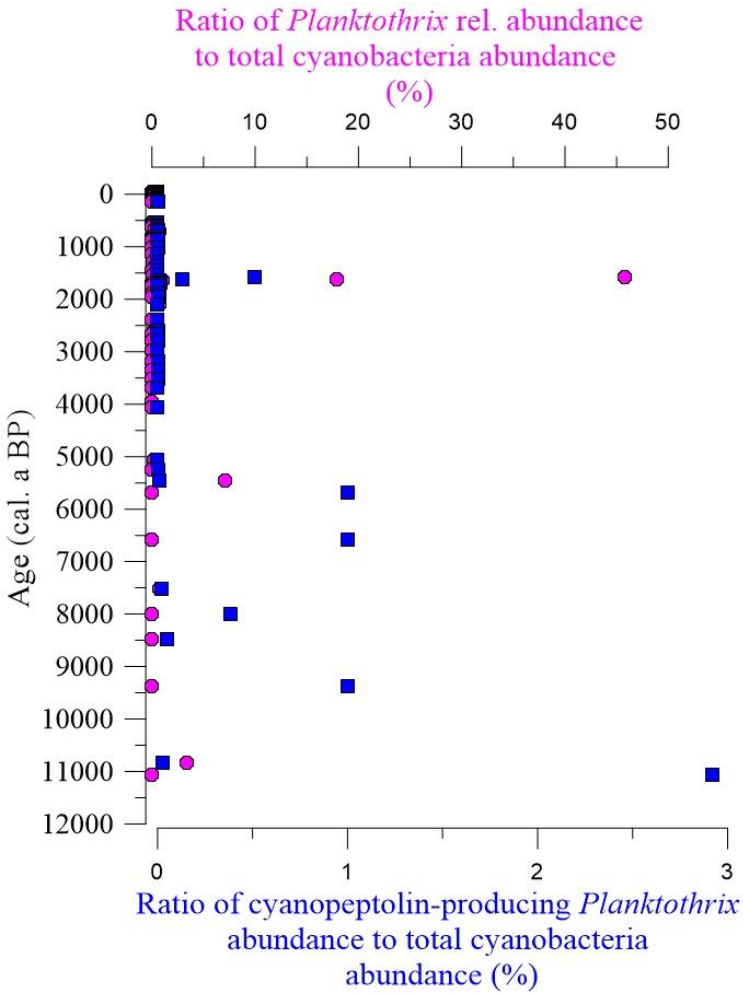

Figure D.5: Test for bias related to differential DNA preservation within sediment layers was done by calculating the ratio of relative abundance of *Planktothrix* read counts obtained from amplicon sequencing to the total cyanobacteria abundance estimated by qPCR (pink dots) and the ratio of cyanopeptolin-producing *Planktothrix* subpopulation from qPCR to the total cyanobacteria abundance also estimated by qPCR; (blue square).

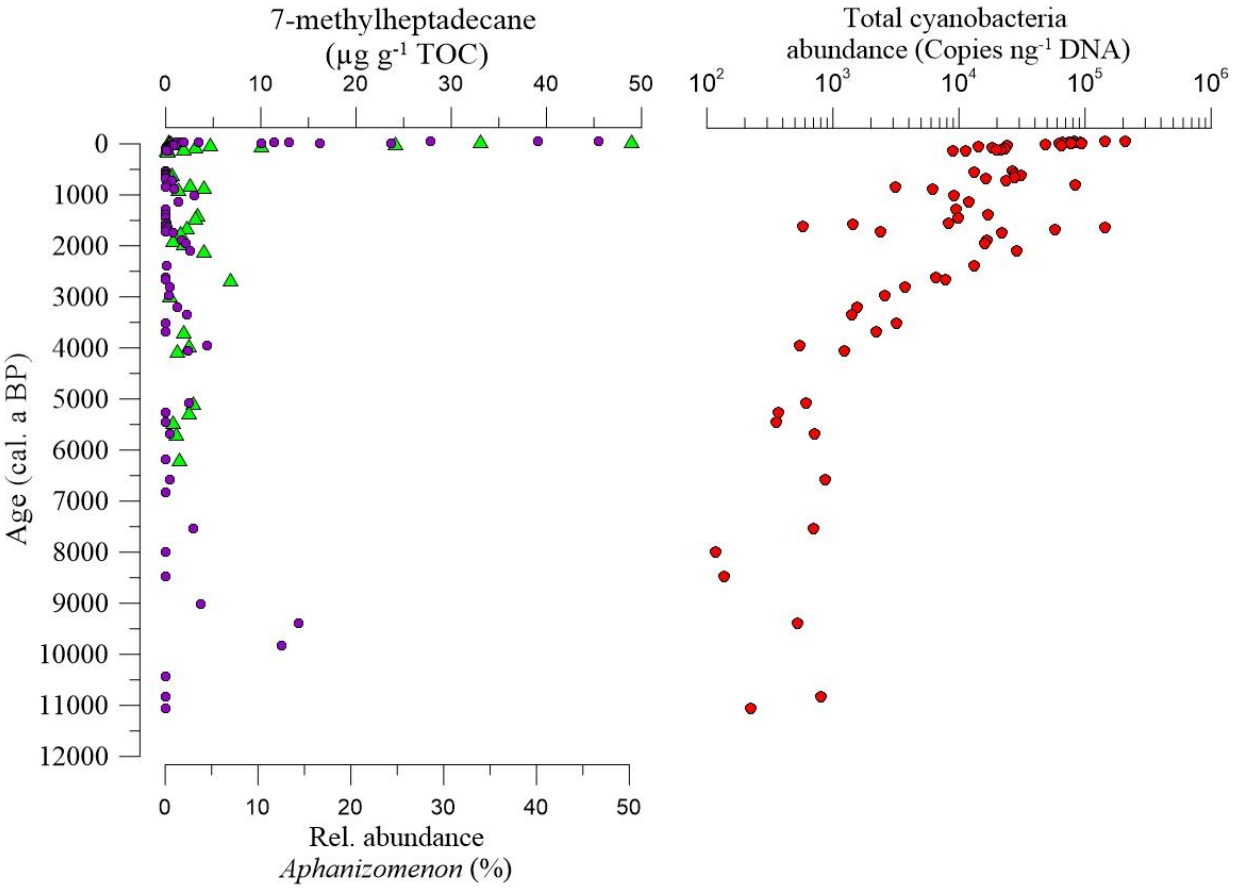

Figure D.6: Variability of Aphanizomenon relative abundance and cyanobacteria lipid biomarker over time. The abundance of ASVs assigned to *Aphanizomenon* relative to total cyanobacterial ASVs (in %) based on amplicon sequencing shown for the entire Holocene (purple dots) compared to 7-methylheptadecane normalized to total organic carbon lipid biomarker shown up to 6180 cal. a BP (green triangles µg g^{-1} TOC). Total cyanobacteria abundance (red dots) for the entire Holocene is shown beside for comparison.